Review

Complexes of silanethiolate ligands: Synthesis, structure, properties and application

Agnieszka Pladzyk [a], Daria Kowalkowska-Zedler [a], Anna Ciborska [a], Andreas Schnepf [b], Anna Dołęga [a],*

[a] Department of Inorganic Chemistry, Faculty of Chemistry, Gdańsk University of Technology, Narutowicza Str 11/12, 80-233 Gdańsk, Poland
[b] Institute of Inorganic Chemistry, University of Tübingen, Auf der Morgenstelle 18, D-72076 Tübingen, Germany

A R T I C L E I N F O

Dedicated to Professor Wiesław Wojnowski on the Occasion of His 88th Birthday and to Professor Barbara Becker on the Occasion of Her 75th Birthday.

A B S T R A C T

The purposeful syntheses of silanethiolate complexes started approximately in the mid-eighties of the 20th century but no summary of the synthetic efforts has been reported till now. The synthetic methods and the resulting complexes have some common features, which are emphasized throughout the review. Thereby specific difficulties during synthesis are outlined and the structures, properties and possible applications of the resulting complexes are presented. All groups of metals of the periodic table are included and associated with potential applications regarding the specific properties of the silicon-sulfur bond and the attached metals.

© 2020 The Authors. Published by Elsevier B.V. This is an open access article under the CC BY license (http://creativecommons.org/licenses/by/4.0/).

Contents

Abbreviations: Ad, adamantyl; 3-AMP, 3-(aminomethyl)pyridine; 4-AMP, 4-(aminomethyl)pyridine; 2-AP, 2-aminopyridine; 3-AP, 3-aminopyridine; 4-AP, 4-aminopyridine; api, 1-(3-aminopropyl)imidazole; azpy, 4,4′-azopyridine; bbi, 1,4-bis(imidazol-1-yl)butane; Bbt, 2,6-bis[bis(trimethylsilyl)methyl]-4-[tris(trimethylsilyl)methyl]phenyl; bda, 1,4-butanediamine; bdt, benzene-1,2- dithiolate; 2,2′-bipy, 2,2′-bipyridine; 4,4′-bipy, 4,4′-bipyridine; bpe, 1,2-bis(2-pyridyl)ethylene; bphen, 4,7-diphenyl-1,10-phenanthroline; Bu, butyl; nBu, n-butyl; *t*Bu, tert-butyl; bz, benzene; CAAC^Cy, CAAC 2-(2,6-diisopropylphenyl)-3,3-dimethyl-2-azaspiro[4.5]dec-1-ylidene; CN, coordination number; Cp*, pentamethylcyclopentadienyl; CP, CPs, coordination polymer(s); d_cov, the sum of covalent radii of the connected atoms; diglyme, bis(2-methoxyethyl)ether; dipp, 2,6-diisopropylphenyl; dippp, 1,3-bis(diisopropylphosphanyl)propane; DMAP, N,N-dimethylaminepyridine; Dmp, 2,6-dimesitylphenyl; dmpda, 3-(dimethylamino)-1-propylamine; 2,5-dMepy, 2,5-dimethylpyridine; 3,4-dMepy, 3,4-dimethylpyridine; 3,5-dMepy, 3,5-dimethylpyridine; E, any chalcogen – as described; Et, ethyl; 2-Etim, 2-ethylimidazole; GPLC, gel permeation liquid chromatography; hda, 1,6-hexanediamine; hpda, 1,7-heptanediamine; hypy, 2-(2′-hydroxyethyl)pyridine; him, histamine 2-(1H-imidazol-4-yl-)ethylamine; im, imidazole; *2-i*Prim, 2-isopropylimidazole; IMes, 1,3-bis(2,4,6-trimethylphenyl)imidazol-2-ylidene; IPR, 2,6-diisopropyl-phenyl)imidazolin-2-ylidene; IPR*, 1,3-bis(2,6-(diphenylmethyl)-4-methylphenyl)imidazol-2-ylidene; IPR2-bimy, 1,3-diisopropylbenzimidazolin-2-ylidene; Me, methyl; MeCp, methylcyclopentadienyl; 2-Meim, 2-methylimidazole; N-Meim, N-methylimidazole; 2-Mepy, 2-methylpyridine; 3-Mepy, 3-methylpyridine; 4-Mepy, 4-methylpyridine; Mes, mesityl; Me₃TACN, 1,4,7-trimethyl-1,4,7-triazacyclononane; mnt, 3-maleonitriledithiolate; morph, morpholine; NHC, 1,3-bis(2,6-diisopropylphenyl)-imidazol-2-ylidene; OAc, acetate; OTf, trifluoromethanesulfonate; pda, 1,5-pentanediamine; Ph, phenyl; 1,10-phen, 1,10-phenantroline; pmdeta, N,N,N',N'',N''-pentamethyldiethylene-triamine; Pr, propyl; *i*Pr, isopropyl; prda, 1,3, propanediamine; py, pyridine; pyridyl; pyH₂, 1,2-dihydropyridyl; pyr, pyrazine; pyrr, pyrrolidine; qx, quinoxaline; RT, room temperature; TBST, tri-*tert*-butoxysilanethiol; Tbt, 2,4,6-tris[bis(trimethylsilyl)methyl]phenyl; TDST, tris(2,6-diisopropylphenoxy)silanethiol; TFPB, tetrakis[3,5-bis(trifluoromethyl)phenyl]borate; THF, tetrahydrofurane; tht, tetrahydrothiophene; tmbiim, 2,2′-bis(4,5-dimethylimidazole); tmeda, N,N,N'N'-tetramethylethylenediamine; tol, toluene; triphos, 1,1,1-tris(diphenylphosphinomethyl)-ethane; WCC, wet column chromatography; X, any element, as described.

* Corresponding author.
   E-mail address: anna.dolega@pg.edu.pl (A. Dołęga).

1. Introduction

There are few reviews on the subject of silicon-sulfur compounds which is thus a chance but also a challenge in writing a new one. This is especially the case as nowadays the knowledge accumulates so rapidly and in such small pieces, that, if the starting point lies relatively far in the past, the collection of papers relevant to any subject is enormous. As far as we know, only three reviews close to the subject can be listed: first of which was authored by Haas and was published 55 years ago in 1965 [1]. The other related paper is a book chapter that summarizes the reactivity of silicon chalcogen bonds [2] and the third article is very loosely connected with the subject of this review and reports the selected silyl ligands in transition metal chemistry including rare silicon-sulfur examples bonded to metal ions *via* silicon atoms [3].

What are the important features that distinguish silanethiolate complexes from metal – thiolate compounds? As it is always the case by comparing silicon and carbon compounds - there are quite many differences. To begin with, the important distinction, responsible for the altered experimental attitude during the synthesis of silicon-sulfur compounds and their metal complexes, is the reactivity of the silicon – sulfur bond. Driven by both, the thermodynamics and kinetics, the silicon atom connected to the sulfur atom reacts with all oxygen nucleophiles, such as water or alcohol, to turn into the silanols or alkoxysilanes and finally into silicon dioxide. Consequently researchers in this field need to work in gloveboxes or under Schlenk line conditions while operating with most of the silicon-sulfur compounds. There are only few exceptions of compounds, in which the S–Si moiety is kinetically protected by large alkyl or aryl substituents and they are very prone to form crystalline products; hence, the process of complex formation and its isolation is faster than the decomposition *e.g.* [4,5] Thermodynamically the reactivity of the silicon – sulfur linkage stems from the fact that the Si–O bond has a higher bonding energy than the respective Si-S bond (by 183 kJ/mol if the comparison is made between the diatomic molecules [6]). The fast kinetics, on the other hand, comes from the longer and more polar S–Si bond,

$\Delta\chi_{CS}$ = 0.03, $\Delta\chi_{SiS}$ = 0.68; moreover the possibility of hypervalent states for third row elements allows different reaction mechanisms and gives access to transition states lower in energy. The reactivity of silicon-sulfur compounds has been often mentioned as an advantage – the cleavage of the S-Si bond is simple and allows to assemble metal-sulfide clusters of variable size *e.g.* [7–10] The ease with which the silyl substituents are detached from the sulfur atom was also utilized in the synthesis of silanethiolate complexes; apart from silanethiols or their salts also disilathianes or cyclic silathianes were applied as silanethiolate precursors – during the reaction one of the silyl substituents was detached and replaced by the metal ion as will be described in the following chapters *e.g.* [11,12].

The tendency of silanethiols to undergo oxidation resembles the tendency of organic thiols – at least at the first stage of disulfide bond formation, which was observed for silanethiols reacting with mild oxidizing agents such as iodine, Cu(II) [13] or simply atmospheric oxygen [14]. However, in the contact with *e.g.* water, this first stage may be followed by the decomposition of disulfide and formation of thiosulfate and the products of nucleophilic substitution at silicon *e.g.* [15].
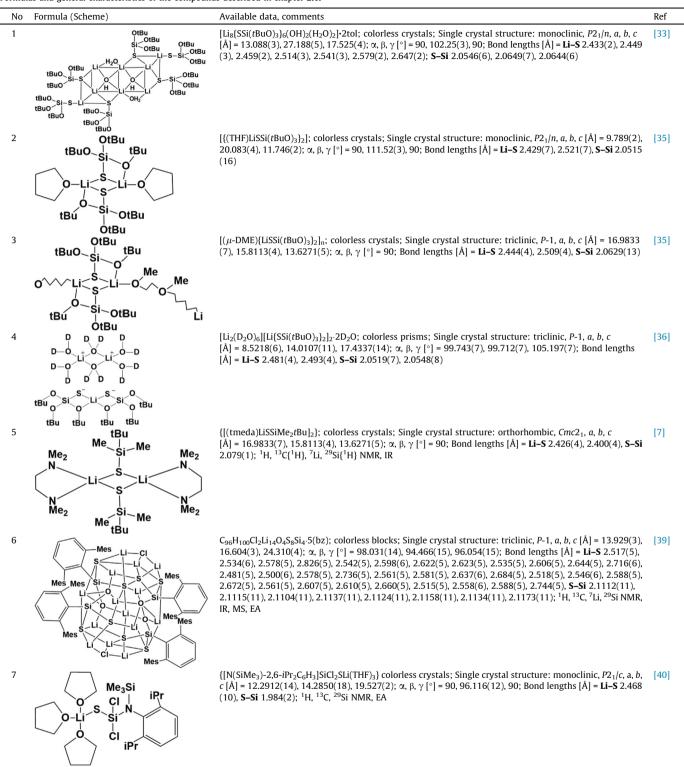
There are certainly differences in the acid-base properties between the silanethiols and organic thiols. In most cases the pK_a values of Si–S–H are lower than those of C–S–H. The lowest values of pK_a for silanethiols are equal to 4 [16], while most organic thiols display pK_a values well above 5 [17]. The exact values for the close analogs (*e.g.* *t*BuSH and $(CH_3)_3$SiSH) are difficult to find due to the low stability of the silicon analogs. However, pK_a values between 4 and 6 may be assigned to most of the studied silanethiols with alkyl, aryl and alkoxy/aryloxy substituents at silicon [16]. The exception among the silanethiols – TBST (pK_a of 8.0) is discussed within the paper of Chojnacki [18]. In the case of organic thiols the pK_a values are between 5.30 and 6.82 for mercaptophenol derivatives and 7.30 – 11 for alkylthiols [17]. The increased acidity of silanethiols is also partly responsible for the increased reactivity; it is possible to employ the methatesis between various salts

Table I
Formulas and general characteristics of the compounds described in chapter **2.1.**

No	Formula (Scheme)	Available data, comments	Ref
1		[Li$_8$\{SSi(tBuO)$_3$\}$_6$(OH)$_2$(H$_2$O)$_2$]·2tol; colorless crystals; Single crystal structure: monoclinic, $P2_1/n$, a, b, c [Å] = 13.088(3), 27.188(5), 17.525(4); α, β, γ [°] = 90, 102.25(3), 90; Bond lengths [Å] = **Li–S** 2.433(2), 2.449(3), 2.459(2), 2.514(3), 2.541(3), 2.579(2), 2.647(2); **S–Si** 2.0546(6), 2.0649(7), 2.0644(6)	[33]
2		[\{(THF)LiSSi(tBuO)$_3$\}$_2$]; colorless crystals; Single crystal structure: monoclinic, $P2_1/n$, a, b, c [Å] = 9.789(2), 20.083(4), 11.746(2); α, β, γ [°] = 90, 111.52(3), 90; Bond lengths [Å] = **Li–S** 2.429(7), 2.521(7), **S–Si** 2.0515(16)	[35]
3		[(μ-DME)\{LiSSi(tBuO)$_3$\}$_2$]$_n$; colorless crystals; Single crystal structure: triclinic, P-1, a, b, c [Å] = 16.9833(7), 15.8113(4), 13.6271(5); α, β, γ [°] = 90; Bond lengths [Å] = **Li–S** 2.444(4), 2.509(4), **S–Si** 2.0629(13)	[35]
4		[Li$_2$(D$_2$O)$_6$][Li\{SSi(tBuO)$_3$\}$_2$]$_2$·2D$_2$O; colorless prisms; Single crystal structure: triclinic, P-1, a, b, c [Å] = 8.5218(6), 14.0107(11), 17.4337(14); α, β, γ [°] = 99.743(7), 99.712(7), 105.197(7); Bond lengths [Å] = **Li–S** 2.481(4), 2.493(4), **S–Si** 2.0519(7), 2.0548(8)	[36]
5		\{[(tmeda)LiSSiMe$_2$$t$Bu]$_2$\}; colorless crystals; Single crystal structure: orthorhombic, $Cmc2_1$, a, b, c [Å] = 16.9833(7), 15.8113(4), 13.6271(5); α, β, γ [°] = 90; Bond lengths [Å] = **Li–S** 2.426(4), 2.400(4), **S–Si** 2.079(1); ^{1}H, ^{13}C\{^{1}H\}, ^{7}Li, ^{29}Si\{^{1}H\} NMR, IR	[7]
6		C$_{96}$H$_{100}$Cl$_2$Li$_{14}$O$_4$S$_8$Si$_4$·5(bz); colorless blocks; Single crystal structure: triclinic, P-1, a, b, c [Å] = 13.929(3), 16.604(3), 24.310(4); α, β, γ [°] = 98.031(14), 94.466(15), 96.054(15); Bond lengths [Å] = **Li–S** 2.517(5), 2.534(6), 2.578(5), 2.826(5), 2.542(5), 2.598(6), 2.622(5), 2.623(5), 2.535(5), 2.606(5), 2.644(5), 2.716(6), 2.481(5), 2.500(6), 2.578(5), 2.736(5), 2.561(5), 2.581(5), 2.637(6), 2.684(5), 2.518(5), 2.546(6), 2.588(5), 2.672(5), 2.561(5), 2.607(5), 2.610(5), 2.660(5), 2.515(5), 2.558(6), 2.588(5), 2.744(5), **S–Si** 2.1112(11), 2.1115(11), 2.1104(11), 2.1137(11), 2.1124(11), 2.1158(11), 2.1134(11), 2.1173(11); ^{1}H, ^{13}C, ^{7}Li, ^{29}Si NMR, IR, MS, EA	[39]
7		\{[N(SiMe$_3$)-2,6-iPr$_2$C$_6$H$_3$]SiCl$_2$SLi(THF)$_3$\} colorless crystals; Single crystal structure: monoclinic, $P2_1/c$, a, b, c [Å] = 12.2912(14), 14.2850(18), 19.527(2); α, β, γ [°] = 90, 96.116(12), 90; Bond lengths [Å] = **Li–S** 2.468(10), **S–Si** 1.984(2); ^{1}H, ^{13}C, ^{29}Si NMR, EA	[40]

Table 1 (*continued*)

No	Formula (Scheme)	Available data, comments	Ref
8		{[N(SiMe$_3$)-2,6-iPr$_2$C$_6$H$_3$Si][SLi(THF)](μ-S)$_2$Si[SLi(THF)$_2$][N(SiMe$_3$)-2,6-iPr$_2$C$_6$H$_3$]}; colorless crystals; Single crystal structure: monoclinic, $P2_1/n$, a, b, c [Å] = 14.035(3), 20.367(4), 18.446(4); α, β, γ [°] = 90, 90.00(3), 90; Bond lengths [Å] = **Li–S** 2.436(10), 2.458(10), 2.491(10), 2.515(10), 2.554(10), **S–Si** 2.0492(19), 2.171(2), 2.198(2), 2.049(2), 2.174(2), 2.196(2); ^{1}H NMR	[40]
9		[{N(SiMe$_3$)-2,6-iPr2C6H$_3$}Si[SLi(THF)]$_3$}$_2$]; colorless crystals; Single crystal structure: monoclinic, $P2_1/n$, a, b, c [Å] = 11.2887(4), 12.5105(5), 24.5874(10); α, β, γ [°] = 90, 97.663(4), 90; Bond lengths [Å] = **Li–S** 2.446(5), 2.422(5), 2.496(5), 2.427(5), 2.515(5), 2.398(5), 2.528(5), 2.425(5), 2.440(5), **S–Si** 2.1276(10), 2.1098(10), 2.1383(10); ^{1}H, ^{13}C, ^{29}Si NMR, EA	[40]
10		[{(THF)$_2$LiSSi(SiMe$_3$)$_3$}$_2$]; colorless crystals; Single crystal structure: monoclinic, $P2_1/n$, a, b, c [Å] = 14.035(3), 20.367(4), 18.446(4); α, β, γ [°] = 90, 90.00(3), 90; Bond lengths [Å] = **Li–S** 2.424(5), 2.430(5), **S–Si** 2.1015(11), 2.3417(11); ^{1}H, ^{13}C{^{1}H}, ^{29}Si NMR	[42]
11		NaSSiPh$_3$·3H$_2$O; colorless crystals; Single crystal structure: monoclinic, $P2_1/n$, a, b, c [Å] = 31.950(12), 15.479(7), 7.976(4); α, β, γ [°] = 90, 91.64(4), 90; Bond lengths [Å] = **Na···S** 2.429(7), 2.521(7), **S–Si** 2.079(1)	[44]
12		[(NaSSiPh$_3$)$_6$(tol)$_2$]; colorless plates; Single crystal structure: triclinic, $P–1$, a, b, c [Å] = 16.1995(2), 16.3657(2), 16.3680(2); α, β, γ [°] = 73.765(1), 63.484(1), 62.160(1); Bond lengths [Å] = **Na–S** 2.892(1), 2.777(1), 2.728(1), 2.817(1), 2.751(1), 2.803(1), 2.981(1), 2. 182(2), 2.782(1), 2.826(1) **S–Si** 2.088(1), 2.081(1); ^{1}H, ^{13}C{1H} NMR, IR	[45]
13		[(THF)NaSSiPhtBu$_2$]$_4$ colorless plates; Single crystal structure: monoclinic, $P2_1/n$, a, b, c [Å] = 21.3211(14), 14.6608(9), 29.3513(18); α, β, γ [°] = 90, 90.022(5), 90; Bond lengths [Å] = **Na–S** 2.892(1), 2.777(1), 2.728(1), 2.817(1), 2.751(1), 2.803(1), 2.981(1), 2. 182(2), 2.782(1), 2.826(1) **S–Si** 2.088(1), 2.081(1); ^{1}H, ^{13}C, ^{29}Si NMR	[14]
14		[(THF)$_2$NaSSitBu$_3$]$_2$; colorless needles; Single crystal structure: monoclinic, $P2_1/n$, a, b, c [Å] = 18.9536(18), 15.6396(10), 18.9675(19); α, β, γ [°] = 90, 118.517(7), 90; Bond lengths [Å] = **Na–S** 2.738(3), 2.747(3), **S–Si** 2.086(2)	[48]

Table I (*continued*)

No	Formula (Scheme)	Available data, comments	Ref
15		[(THF)NaSSi*t*Bu₃]₄, colorless crystals; Single crystal structure: monoclinic, $P2_1$, a, b, c [Å] = 13.3756(6), 15.3886(4), 19.9654(8); α, β, γ [°] = 90, 90.623(3), 90; Bond lengths [Å] = **Na–S** 2.800(3), 2.806(3), 2.812(3), 2.770(3), 2.783(3), 2.860(3), 2.782(3), 2.834(3), 2.859(3), 2.795(3), 2.842(3), 2.851(3), **S–Si** 2.1130(18), 2.101(2), 2.115(2), 2.102(2)	[48]
16		[Na₂(MeOH)₆][Na{SSi(O*t*Bu)₃}₂]₂, colorless plates; Single crystal structure: triclinic, P–1, a, b, c [Å] = 8.298(2), 14.988(3), 17.932(4); α, β, γ [°] = 101.90(3), 99.64(3), 103.38(3); Bond lengths [Å] = **Na–S** 2.7386(15), 2.7632(13), 2.8542(13), **S–Si** 2.0559(10), 2.0434(13)	[49]
17		[(DME)₂Na][Na{SSi(O*t*Bu)₃}₂], colorless crystals; Single crystal structure: monoclinic, $P2_1/c$, a, b, c [Å] = 15.5007(9), 17.4385(9), 17.2438(12); α, β, γ [°] = 90, 91.003(5), 90; Bond lengths [Å] = **Na–S** 2.7172(9), 2.7765(9), **Na···S** 2.9431(8), 2.9281(8), **S–Si** 2.0532(6), 2.0543(6)	[50]
18		[(H₂O)NaSSi(Odipp)₃}₂], colorless crystals; Single crystal structure: triclinic, P-1, a, b, c [Å] = 10.7839(5), 12.1344(6), 16.0385(8); α, β, γ [°] = 86.689(4), 72.849(4), 66.292(5); Bond lengths [Å] = **Na–S** 2.7582(9), 2.7631(8), **S–Si** 2.0248(7); IR	[20]
19		[{NaSSi(Odipp)₃}₂]·hex, colorless crystals; Single crystal structure: orthorhombic, $P2_12_12$, a, b, c [Å] = 12.6124(7), 24.0235(9), 12.7530(4); α, β, γ [°] = 90; Bond lengths [Å] = **Na–S** 2.7474(13), 2.7830(14), **S–Si** 2.0289(9)	
20		[(diglyme)(H₂O)NaSSi(Odipp)₃]; colorless crystals; Single crystal structure: monoclinic, $P2_1/c$, a, b, c [Å] = 14.4754(5), 17.0472(5), 22.9059(10); α, β, γ [°] = 90, 124.100(3), 90; Bond lengths [Å] = **Na–S** 2.7518(14), **S–Si** 2.0392(9); IR, EA	[51]
21		[{(MeCN)NaSSi(Odipp)₃}₂]·tol; colorless crystals; Single crystal structure: monoclinic, $P2_1/c$, a, b, c [Å] = 12.6823(4), 19.4498(5), 20.2522(6); α, β, γ [°] = 90, 124.157(2), 90; Bond lengths [Å] = **Na–S** 2.7361(12), **S–Si** 2.0311(9); EA	[52]

5

Table I (*continued*)

No	Formula (Scheme)	Available data, comments	Ref
22		[(THF)$_2${KSSi(OtBu)$_3$}$_6$]·2THF, colorless crystals; Single crystal structure: monoclinic, $P2_1/c$; *a, b, c* [Å] = 15.227(4), 14.650(5), 32.067(9); α, β, γ [°] = 90, 117.001(18), 90; Bond lengths [Å] = **K–S** 3.166(2), 3.186(2), 3.255(2), 3.120(2), 3.503(3), 3.277(2), 3.213(2), **S–Si** 2.058(2), 2.069(2), 2.054(2)	[53]
23		[{KSSi(OtBu)$_3$}$_2$]$_n$, colorless crystals; Single crystal structure: triclinic, *P*-1, *a, b, c* [Å] = 11.6305(14), 13.348(3), 13.531(4); α, β, γ [°] = 67.27(2), 76.064(16), 88.706(14); Bond lengths [Å] = **K–S** 3.1046(19), 3.119(2), 3.1435(19), 3.310(2), 3.117(2), 3.094(2) 3.277(2), 3.213(2), **S–Si** 2.047(2), 2.047(2); EA	[53]
24		[{(H$_2$O)KSSi(OtBu)$_3$}$_4$]·bz, colorless crystals; Single crystal structure: orthorhombic, *P*-4*b*2, *a, b, c* [Å] = 20.854(3), 20.854(3), 9.283(2); α, β, γ [°] = 90, 90, 90; Bond lengths [Å] = **K–S** 3.2177(17), 3.1345(19), 3.3849(19), **S–Si** 2.0592(18); EA	[53]
25		[{PhC(NtBu)$_2$Si(S)$_2$}K(THF)$_2$]$_2$; colorless crystals; Single crystal structure: triclinic, *P*-1, *a, b, c* [Å] = 11.1594(8), 11.4396(8), 12.4599(9); α, β, γ [°] = 87.130(3), 72.379(4), 74.688(3) ; Bond lengths [Å] = **K–S** 3.2648(5), 3.3046(5), 3.3449(5), 3.2783(5), **S–Si** 2.0302(5), 2.0243(5); ^{1}H, ^{13}C{^{1}H}, ^{29}Si{^{1}H} NMR, EA	[54,55]
26		{(18-crown-6)KSSi(SiMe$_3$)$_3$}, colorless crystals, Single crystal structure: triclinic, *P*-1; *a, b, c* [Å] = 9.8800(19), 11.562(2), 15.130(3); α, β, γ [°] = 94.589(3), 93.784(3), 100.611(3); Bond lengths [Å] = **K–S** 3.1109(12), **S–Si** 2.0925(12); ^{1}H, ^{13}C{^{1}H}, ^{29}Si{^{1}H} NMR	[42]
27		[(18-crown-6)KSSiPh$_3$], pale blue crystals; Single crystal structure: triclinic, *P*-1, *a, b, c* [Å] = 9.188(8), 10.473(9), 17.685(14); α, β, γ [°] = 95.930(9), 93.438(9), 94.815(9); Bond lengths [Å] = **K–S** 3.143(2), **S–Si** 2.039(2); ^{1}H, ^{13}C{^{1}H}, ^{29}Si{^{1}H} NMR, IR (KBr), UV–Vis (THF), EA	[56]

of weaker acids (*e.g.* amides, acetylacetonates) and silanethiols to prepare silanethiolate complexes [*e.g.* [19]] or the reaction of silanethiol with the metal – not only reactive alkali metals [*e.g.* [20]] but also metals of moderate activity such as zinc [*e.g.* [4]].

The reasons behind the synthetic efforts to prepare silanethiolate complexes of metal ions are different for different metals, however some common motives are most often named by the researchers:

- Silanethiolate complexes provide a convenient source of the M−S fragment during the synthesis of homo- and heterometallic sulfido clusters with formation of a silane byproduct [*e.g.* 7–10]
- Similarly, some of the silanethiolato complexes were considered as single-source precursors to semiconducting metal chalcogenides [12,21]

- Transition metal-sulfur clusters and thiolate complexes have relevance to active sites of metalloproteins and attempts to develop rational synthetic methods of assembling (hetero) metal-sulfur fragments have often employed silanethiolate ligands [*e.g.* [22–24]].
- Basic studies on structural diversity and properties (spectroscopic, magnetic) of metal ions complexed by S-donor ligands [*e.g.* [24–28]]

The results of these studies for all metals of the periodic table are collected and if possible summarized in the following; If there are no known representatives, the group is omitted.

All covalent radii used through the manuscript are taken from works of Pyykkö and co-workers [29–31] The simplified structural formulas of the silanethiolate complexes are shown in the Tables
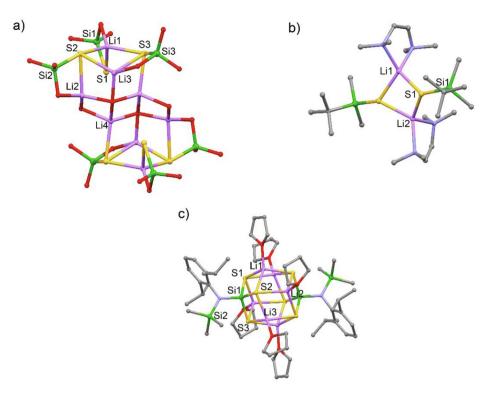
Fig. 1. Selected molecular structures of lithium silanethiolate complexes; solvent molecules and H atoms are omitted for clarity: a) $[(H_2O)_2Li_8\{SSi(tBuO)_3\}_6(OH)_2]\cdot2tol$, C atoms omitted for clarity [33]; b) $[\{(tmeda)LiSSiMe_2tBu\}_2]$ [7]; c) $[\{N(SiMe_3)-2,6-iPr2C6H3\}Si[SLi(THF)]_3\}_2]$ [40].

accompanying each chapter; the formal charges are indicated only for ionic compounds.

2. Complexes of the main group metals

2.1. Group 1 elements

Alkali metal silanethiolates were usually synthesized and described as precursors for the development of transition metal complexes and clusters. The number of complexes is quite large, but they are usually highly reactive and decompose at atmospheric conditions and their sensitivity increases with the number of sulfur atoms attached to the silicon atom. Therefore, the characterization of this group of compounds was usually confined to structural studies and all the syntheses were conducted under inert gas, with the use of standard Schlenk technique. In case of these reactive metals the reaction of the element with the silanethiol is a common method of synthesis – if the silanethiol is available. Due to the low affinity of alkali metal cations (hard Pearson acids [32]) for sulfur (soft base), the usual structural features of alkali metal silanethiolates include long metal-sulfur bonds that substantially exceed the sum of covalent radii and very short S–Si bond lengths that confirm the ionic character of these compounds. The ionic character of the alkali metal - sulfur bond allows to increase the coordination number of the metal ions. Moreover, it enables the formation of extended interactions and complicated aggregates simultaneously; these complexes are often characterized by a solvated (*e.g.* hydrated) inner core in the form of a cluster or a polymer, which is coated by the hydrophobic silanethiolate ligands from the outside. Below we discuss each group 1 metal separately, starting from the lightest lithium.

The structural chemistry of lithium silanethiolates started in 2002 when $[Li_8\{SSi(tBuO)_3\}_6(OH)_2(H_2O)_2]\cdot2tol$ was obtained by the direct reaction of tri-*tert*-butoxysilanethiol (TBST) with lithium powder in diethyl ether (Table I-1) [33]. The complicated cluster

structure was described as a hydrated adduct of lithium silanethiolate and lithium hydroxide. The compound contains four μ_3-bridging silanethiolate residues and two terminal ones (Fig. 1a). There are very short Li···Li contacts within the structure (2.5 Å), which is a unique feature among lithium silanethiolates. The Li–S bonds are longer, whereas the S–Si bond is shorter than the sum of the covalent radii (2.36 and 2.19 Å, respectively) [29–31,33]. Later, the same reaction was carried out without a solvent (TBST, which was first described in 1962, is liquid in a wide range of temperatures [34]) and recrystallization of the obtained white powder from THF or DME allowed the isolation of dimeric $[\{(THF)LiSSi(tBuO)_3\}_2]$ as well as polymeric $[(\mu\text{-}DME)\{LiSSi(tBuO)_3\}_2]_n$ (Table I-2,3) [35]. The dimeric compound contains a planar Li_2S_2 ring with Li ions distanced at 2.888 Å and adopting a LiO_2S_2 distorted tetrahedral geometry, while the chain polymer $[(\mu\text{-}DME)\{LiSSi(tBuO)_3\}_2]_n$ is composed of dimeric units of $[\{LiSSi(tBuO)_3\}_2]$ inteconnected *via* DME molecules. In both complexes the Li–S bonds are longer than the sum of the covalent radii of Li and S atoms whereas the S–Si bond lengths are short, indicating the ionic character of the sulfur metal linkage. Yet another form of lithium tri-*tert*-butoxysilanethiolate $[Li_2(D_2O)_6][Li\{SSi(tBuO)_3\}_2]_2\cdot2D_2O$ was obtained by Kloskowska and co-workers [36] in the reaction of metallic Li with the solution of $[SnCl\{SSi(tBuO)_3\}_3]$ in THF, followed by the addition of heavy water. This is the only example of a lithium complex, where the metal ion is included in the dimeric cation $[Li_2(D_2O)_6]^{2+}$ and the lithate anion $[Li\{SSi(OtBu)_3\}_2]^-$ interconnected *via* intermolecular O–D···O and O–D···S hydrogen bond interactions (Table I-4). The Li atom in the anionic part of the complex is coordinated by two silanethiolate residues acting as O,S-donor chelating ligands resulting in significantly distorted tetrahedral geometry around the Li atom [36].

A different synthetic approach was described by Komuro and co-workers, where $LiSSiMe_3$ and $LiSSiMe_2tBu$ were obtained in the reaction of cyclotrisilathiane $(Me_2SiS)_3$ with MeLi or *t*BuLi [7]. The precursor of the silanethiolate ligand - $(Me_2SiS)_3$ - was synthesized
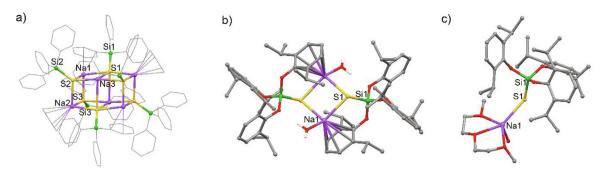
Fig. 2. Molecular structure of selected silanethiolate complexes of Na(I); solvent molecules and H atoms are omitted for clarity: a) [(NaSSiPh₃)₆(tol)₂] [45]; b) {[{(H₂O)NaSSi(Odipp)₃}₂] [20]; c) [(diglyme)(H₂O)NaSSi(Odipp)₃] [51].

according to an earlier procedure [37] The reaction of LiSSiMe₂tBu with tmeda gave crystalline [{(tmeda)LiSSiMe₂tBu}₂] which crystallized as a dimer with a bent Li₂S₂ ring (Table I-5, Fig. 1b). The Li–S bond distances are slightly elongated in comparison with the sum of the covalent radii, however they are similar to those observed in lithium thiolates [38], whereas the S–Si bonds are short. The lithium silanethiolates were further used in synthesis of Fe, Co, Ni and Cu silanethiolates which will be described in the following chapters [7].

Unusual multinuclear Li silanedithiolate/silanethiolate was described by Pietschnig and co-workers [39]. The complex was obtained in the reaction of DmpSiCl₃ with Li₂S, freshly prepared from n-BuLi and gaseous H₂S at 193 K. The synthesis was conducted in dry and neutral atmosphere, however, the authors didn't avoid the contamination with water, which seemed to be necessary to obtain the complex in its final structure. Structural analysis revealed the presence of a tetramer built of four DmpSi(SLi)₂(OLi) and two additional LiCl units; altogether it was described as a 32 vertex polyhedral cluster stabilized by large 2,6-dimesitylphenyl substituents (Table I-6). The S–Si distances are similar ranging from 2.1104(11)-2.1173(11) Å, whereas the Li–S distances (range 2.481(5)-2.826(5) Å) were significantly elongated probably due to the high stress present inside the structure [39].

Li and co-workers showed that reactions of Li₂S with N(SiMe₃)-2,6-iPr₂C₆H₃SiCl₃ led to the formation of mononuclear RSiCl₂SLi (THF)₃, bimetallic RSi[SLi(THF)](μ-S)₂Si[SLi(THF)₂]R and cluster [RSi{SLi(THF)}₃]₂ exhibiting six lithium atoms (R = N(SiMe₃)-2,6-iPr₂C₆H₃) (Table I-7–9, respectively, Fig. 1c) [40]. The type of the final product was determined by the ratio of the precursors, time and temperature of synthesis. Mononuclear RSiCl₂SLi(THF)₃ was isolated from the synthesis carried out at low temperature, while the increase of temperature resulted in the mixture of RSiCl₂SLi (THF)₃ and RSi[SLi(THF)](μ-S)₂Si[SLi(THF)₂]R. The excess of Li₂S and extended time of the reaction generated the third compound [RSi{SLi(THF)}₃]₂ with the Si₂S₆Li₆ core. The protonation of [RSi{SLi(THF)}₃]₂ with acetic acid gives the very reactive aminesilanetrithiol {N(SiMe₃)-2,6-iPr₂C₆H₃}Si(SH)₃ [40].

The insertion of sulfur into the Li–Si bond was employed by Schnepf and co-workers to prepare lithium and potassium silanethiolates, which were later utilized as precursors of nanoscale clusters of coinage metals [42]. The synthesis of tris(trimethylsilyl)silyllithium in hydrocarbon solvents was originally described in 1982 [41]. The reaction of [(THF)₃LiSi(SiMe₃)₃] with elemental sulfur led to a dimer [{(THF)₂LiSSi(SiMe₃)₃}₂] with two molecules of THF coordinated to each Li ion (Table I-10) [42]. The compound has an average Si–Si bond distance of 2.35 Å, typical for Si–Si single bonds in silanides [43].

The structural chemistry of alkali metals silanethiolates started in our department in 1987 with the synthesis of sodium triphenylsilanethiolate trihydrate NaSSiPh₃·3H₂O, which was obtained in the reaction of Ph₃SiSH with Na in THF [44]. NaSSiPh₃·3H₂O is a polymeric compound, in which a zig-zag chain of hydrated sodium cations is shielded by strongly oriented silanethiolate anions (Table I-11) [44]. A different example of sodium triphenylsilanethiolate was described 10 years later; it was obtained by the metalation of Ph₃SiSH with sodium hydride NaH [45]. This anhydrous hexameric complex [(NaSSiPh₃)₆(tol)₂] is built of face-fused cubes (Fig. 2a, Table I-12). Two of the Na atoms at a corner position exhibit additional η^6-arene interactions with toluene, while two others showed η^6-arene interactions with proximal phenyl groups of silanethiolate residues. The Na atoms that build-up the internal Na₂S₂ ring between the cubes are coordinated by four thiolate residues with no π contacts. Na–S bonds are considerably elongated in comparison to the sum of covalent radii of Na and S (2.58 Å [29–31]), but they are similar to average distances found in other hexameric Na thiolates [46].

The reaction of S₈ with sodium silanide NaSiRtBu₂ (R = Ph, tBu) originally described by Arnold and co-workers in 1993 [47] was employed to prepare sodium silanethiolates: [{(THF)NaSSiPhtBu₂}₄] [14], [{(THF)₂NaSSitBu₃}₂] and [{(THF)NaSSitBu₃}₄] [48] (Table I-13–15, respectively). Dimer [{(THF)₂NaSSitBu₃}₂] crystallized from the THF solution of NaSSitBu₃ whereas the tetrameric [{(THF)NaSSitBu₃}₄] was obtained via recrystallization of [{(THF)₂NaSSitBu₃}₂] from a non-coordinating solvent. These airsensitive compounds easily underwent oxidation to the corresponding disilyldisulfides, which could be isolated in pure form. Their protonolysis with an excess of trifluoroacetic acid in C₆D₆ gave the corresponding organosilanethiols tBu₂RSiSH (R = Ph, tBu). Similar reactions were observed for selenides and tellurides [14]. The tetrameric compounds form Na₄S₄ cubanes whereas the dimer forms a characteristic Na₂S₂ ring with Na atoms adopting tetrahedral geometry. The coordination spheres of the Na atoms are completed with the appropriate number of THF molecules. The comparison of the structures shows that the Na–S bond distances in the dimeric compound are slightly shorter than those found in the cubanes. In contrast, the S–Si bond lengths are comparable in [{(THF)₂NaSSitBu₃}₂] and [{(THF)NaSSiPhtBu₂}₄], whereas the same bonds are longer in [{(THF)NaSSitBu₃}₄] [14,48].

The alkali metal complexes in which the metal may be found both in the cationic and the anionic part (for lithium complex see [36]) have been obtained exclusively in our Department. Hence, the reaction of a toluene solution of [SnBr{SSi(OtBu)₃}₃] with MeONa in methanol gives [Na₂(MeOH)₆][Na{SSi(OtBu)₃}₂]₂ (Table I-16) [49], composed of two Na{SSi(OtBu)₃}₂⁻ and one [Na₂(MeOH)₆]²⁺ unit. The Na ions within the cationic unit are coordinated by molecules of water and methanol which are engaged in hydrogen bonding interactions that link the counter-ions. Another ionic complex [(DME)₂Na][Na{SSi(OtBu)₃}₂] with the same type of anion was obtained in the reaction of TBST with metallic Na in
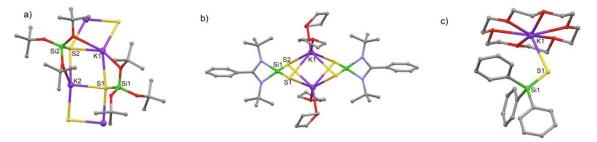
Fig. 3. Molecular structure of the selected silanethiolate complexes of potassium; solvent molecules and H atoms are omitted for clarity: a) [{KSSi(O*t*Bu)$_3$}$_2$]$_n$ [53]; b) [{(THF)$_2$K(S)$_2$Si(C(NBut)$_2$Ph)}$_2$] [54]; c) [(18-crown-6)KSSiPh$_3$] [56].
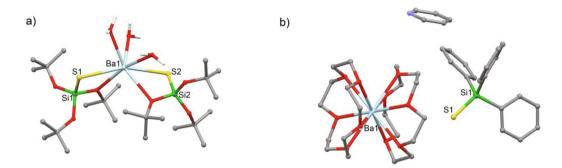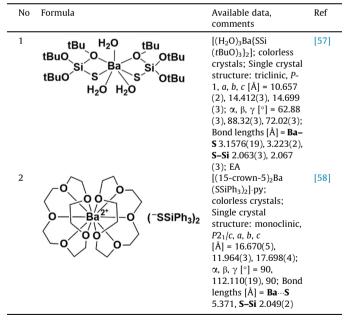

Fig. 4. Molecular structure of Ba silanethiolate complexes without H atoms: a) [(H$_2$O)$_3$Ba{SSi(*t*BuO)$_3$}$_2$] [57]; b) [(15-crown-5)$_2$Ba(SSiPh$_3$)$_2$]·py (only one of the silanethiolate anions is shown) [58].

Table II
Formulas and general characteristics of the compounds described in chapter **2.2.**

No	Formula	Available data, comments	Ref
1		[(H$_2$O)$_3$Ba{SSi (*t*BuO)$_3$}$_2$]; colorless crystals; Single crystal structure: triclinic, *P*-1, *a*, *b*, *c* [Å] = 10.657 (2), 14.412(3), 14.699 (3); α, β, γ [°] = 62.88 (3), 88.32(3), 72.02(3); Bond lengths [Å] = **Ba–S** 3.1576(19), 3.223(2), **S–Si** 2.063(3), 2.067 (3); EA	[57]
2		[(15-crown-5)$_2$Ba (SSiPh$_3$)$_2$]·py; colorless crystals; Single crystal structure: monoclinic, *P*2$_1$/*c*, *a*, *b*, *c* [Å] = 16.670(5), 11.964(3), 17.698(4); α, β, γ [°] = 90, 112.110(19), 90; Bond lengths [Å] = **Ba···S** 5.371, **S–Si** 2.049(2)	[58]

DME (Table I-17). In this case the ions are not coupled through hydrogen bonding, but instead there is a direct Na···S interaction between them [50].

The reactions between metallic sodium and tris(2,6-diisopropyl phenoxy)silanethiol (TDST) resulted in the formation of typical dimers: aqua complex [(H$_2$O)NaSSi(Odipp)$_3$}$_2$] (Fig. 2b) and less common, asymmetric complex with no metal-solvent interactions [{NaSSi(Odipp)$_3$}$_2$]·hex (Table I-18,19) [20]. In both complexes sodium ions interact with phenyl rings of TDST. In the anhydrous form [{NaSSi(Odipp)$_3$}$_2$], the water molecules are replaced by two O atoms from two aryloxysilanethiolate anions that coordinate to one of the sodium ions, while the second Na is surrounded by two S atoms of the silanethiolate ligands and their aryl rings [20]. The use of a similar synthetic procedure with the addition of diglyme allowed the isolation of the unique mononuclear sodium silanethiolate [(diglyme)(H$_2$O)NaSSi(Odipp)$_3$] (Fig. 2c, Table I-20) [51]. Another dimer [{(MeCN)NaSSi(Odipp)$_3$}$_2$]·tol (Table I-21) was obtained in the reaction of sodium borohydride with TDST in acetonitrile [52].

Three of the eight characterized potassium silanethiolates are obtained *via* the treatment of TBST with metallic potassium in various solvents, which in fact occurred to be crucial for the final structures of the products. Depending on the solvent, isolated compounds were either hexameric [(THF)$_2${KSSi(O*t*Bu)$_3$}$_6$]·2THF, polymeric [{KSSi(O*t*Bu)$_3$}$_2$]$_n$ or tetrameric (cubane) [{(H$_2$O)KSSi (O*t*Bu)$_3$}$_4$]·bz derivatives (Fig. 3a, Table I-22–24) [53]. The hexameric form resembles the double cubane [(NaSSiPh$_3$)$_6$(tol)$_2$] described by Ruhlandt-Senge and co-workers [45] which is shown in Fig. 2a; it is however stabilized by two THF molecules and the interactions between sodium cations and O atoms of the alkoxy substituents at silicon. In the single cubane [{(H$_2$O)KSSi(O*t*Bu)$_3$}$_4$]·bz each potassium ion is bonded to a single molecule of water, while the polymeric derivative does not contain any solvent molecules and K and S atoms occupy alternate position in an infinite ladder structure (Fig. 3a) [53].

The coordination properties of the reactive siladithiocarboxylates were investigated by Zhang and co-workers [54]. Potassium siladithiocarboxylate [{PhC(NBut)$_2$Si(S)$_2$K(THF)$_2$}$_2$] was synthesized in the reaction of PhC(NBut)$_2$SiCl (the procedure of synthesis of chlorosilylene was described earlier [55]), with KC$_8$ and S$_8$ in THF at RT. The complex crystallizes as a dimer with each K$^+$ ion coordinated by PhC(NBut)$_2$SiS$_2^-$ in a chelating/bridging manner as well as two molecules of THF (Fig. 3b, Table I-25). The potassium salt was reacted with GeCl$_2$ to yield the germanium(II) siladithiocarboxylate [{PhC(NBut)$_2$Si(S)$_2$}$_2$Ge] (see chapter 2.4) [54].

Table III

Formulas and general characteristics of Group 13 compounds described in chapter **2.3.**

No	Formula	Available data, comments	Ref.
1		[{TlSSi(tBuO)$_3$}$_2$]; colorless crystals; Single crystal structure: triclinic, $P1$, a, b, c [Å] = 9.275(3), 13.951(4), 8.821(3); α, β, γ [°] = 108.43(2), 116.77(2), 90.98(2); Bond lengths [Å] = **Tl–S** 2.880(2), 2.903(2), **S–Si** 2.078(2); ^{13}C, ^{29}Si NMR, MS	[59]
2		[{Me$_2$Al(μ-SSiPh$_3$)}$_2$]; colorless crystals;Single crystal structure: triclinic, $P1$, a, b, c [Å] = 9.077(2), 13.847(3), 16.724(4), α, β, γ [°] = 101.08(2), 95.34(2), 103.38(2); Bond lengths [Å] = **Al–S** 2.372(2), 2.237(2), 2.368(2), 2.355(2), **S–Si** 2.148(2), 2.161(2); ^{1}H, ^{13}C, ^{29}Si NMR	[60]
3		[HC{C(Me)N(2,6-iPr$_2$C$_6$H$_3$)}$_2$Al(SSiMe$_2$)$_2$O]; colorless crystals; Single crystal structure: monoclinic, $P2_1/n$, a, b, c [Å] = 12.749(3), 18.857(4), 15.726(3); α, β, γ [°] = 90, 104.29(3), 90; Bond lengths [Å]: **Al–S** 2.234(1), 2.223(1), **S–Si** 2.128(1), 2.138(1); ^{1}H, ^{13}C NMR, MS	[61]
4		[{Mes$_2$In(μ-SSiPh$_3$)}$_2$]; colorless crystals; Single crystal structure: triclinic, $P1$, a, b, c [Å] = 12.423(3), 13.019(3), 14.126(2); α, β, γ [°] = 91.50(1), 113.23(1), 117.72(2); Bond lengths [Å] = **In–S** 2.697(2), 2.598(2), **S–Si** 2.148(2), 2.148(2); ^{1}H, ^{13}C NMR, MS	[67]
5		[(Me$_2$InSSiPh$_3$)$_3$]; colorless crystals; Single crystal structure: triclinic, $P1$, a, b, c [Å] = 15.012(5), 17.784(5), 24.838(8); α, β, γ [°] = 76.23(2), 83.03(3), 69.84(2); Bond lengths [Å] = **In–S** 2.589(3), 2.587(3), 2.636(4), 2.602(3), 2.597(3), 2.614(3), 2.644(3), 2.617(3), 2.628(2), 2.603(3), 2.604(3), 2.605(3), **S–Si** 2.131(4), 2.1118(4), 2.136(4), 2.144(3), 2.135(4), 2.111(5); ^{1}H, ^{13}C NMR, MS	[67]
6		[{Et$_2$GaSSiPh$_3$}$_2$]; colorless crystals; Single crystal structure: triclinic, $P1$, a, b, c [Å] = 9.2715(15), 9.5413(13), 14.1872(22); α, β, γ [°] = 71.135(11), 89.409(13), 65.247(10); Bond lengths [Å] = **Ga–S** 2.450(2), 2.396(2), **S–Si** 2.148(3); ^{1}H NMR	[62]
7		[(H$_2$O)Ga{SSi(tBuO)$_3$}$_3$]; colorless crystals; Single crystal structure: monoclinic, $P2_1/c$, a, b, c [Å] = 21.697(1), 14.023(1), 17.791(1); α, β, γ [°] = 90, 90.667(7), 90; Bond lengths [Å] = **Ga–S** 2.2446(5), 2.2326(5), 2.2518(5), **S–Si** 2.1076(7), 2.1152(7), 2.1117(8)	[63]
8		[Ga{SSi(tBuO)$_3$}$_2$Li{μ-SSi(OtBu)$_3$}$_2$]; colorless crystals; Single crystal structure: monoclinic, $P2_1/c$, a, b, c [Å] = 25.071(5), 23.872(5), 26.189(5); α, β, γ [°] = 90, 113.16(3), 90; Bond lengths [Å] = **Ga–S** 2.2261(9), 2.2234(11), 2.3353(8), 2.3363(7), 2.2280(9), 2.2285(9), 2.3231(10), 2.3302(8), **Li–S** 2.502(4), 2.534(4), **S–Si** 2.0994(10), 2.1065(12), 2.1086(11), 2.1049(10); MS	[64]
9		[(Me$_2$In)$_6$S(SSiMe$_3$)$_4$]; colorless crystals; Single crystal structure: Monoclinic, $C2/c$; a, b, c [Å] = 18.3377(15), 16.0154(15), 18.0037(16); α, β, γ [°] = 90, 93.703(7), 90; Bond lengths [Å] = **In–S** 2.592(8), 2.5904(8), 2.589(7), 2.5933(7), 2.589(2), 2.589(4), **S–Si** 2.171(2), 2.166(1)	[68]
10		[(Me$_2$Ga)$_6$S(SSiMe$_3$)$_4$]; colorless crystals; Single crystal structure: monoclinic, $C2/c$, a, b, c [Å] = 18.0496(12), 15.5519(11), 17.5417(12); α, β, γ [°] = 90, 91.053(6), 90; Bond lengths [Å] = **Ga–S** 2.416(1), 2.3891(7), 2.3980, 2.3932(7), 2.4134, 2.3925, **S–Si** 2.172(1), 2.1681(9)	[68]
11		[(bis-NHC)Si(S)S→GaCl$_3$]; colorless crystals; Single crystal structure: monoclinic, Cm, a, b, c [Å] = 25.071(5), 23.872(5), 26.189(5); α, β, γ [°] = 90, 113.16(3), 90; Bond lengths [Å] = **Ga–S** 2.262(2), **S–Si** 2.106(2), 2.006(2); ^{13}C, ^{29}Si NMR, IR, CP/MAS, HR-MS, DFT	[65]

Table III (*continued*)

No	Formula	Available data, comments	Ref.
12		DMPyr[Ga(SSiMe$_3$)$_4$] colorless crystals; ^{1}H, ^{13}C, ^{29}Si, TGA-DSC, EA	[66]
13		Ph$_4$P[In(SSiMe$_3$)$_4$]; colorless crystals; Single crystal structure: orthorhombic, *Pna*2$_1$, *a*, *b*, *c* [Å] = 21.588(4), 23.872(5), 26.189(5); α, β, γ [°] = 90, 90, 90; Bond lengths [Å] = **In–S** 2.452(1), 2.447(1), 2.453(8), 2.4577(9), **S–Si** 2.146(1), 2.124(1), 2.121(1), 2.131(1); ^{1}H, ^{13}C, ^{29}Si, TGA-DSC, EA	[66]

Fig. 5. Molecular structure of tri-*tert*-butoxysilanethiolate complexes of Ga(III); the H atoms are omitted for clarity: a) [(H$_2$O)Ga{SSi(*t*BuO)$_3$}$_3$] [63]; b) [Ga{SSi(*t*BuO)$_3$}$_2$Li{μ-SSi(O*t*Bu)$_3$}$_2$] [64].

Three similar, molecular potassium silanethiolates were synthesized with the use of 18-crown-6 [42,56]. [(18-crown-6)KSSi(SiMe$_3$)$_3$] was isolated from the reaction mixture consisting of the silanide KSi(SiMe$_3$)$_3$, elemental sulfur and 18-crown-6 (Table I-26) [42], whereas [(18-crown-6)KSSiPh$_3$] (Fig. 3c, Table I-27) and [(18-crown-6)KSSiPh$_2$tBu] were obtained in the reactions of elemental sulfur with previously prepared crown ether potassium silanides [56]. All complexes adopt a similar structure with the coordination sphere of K$^+$ ions "saturated" by the crown ether; short S–Si distances confirm the ionic character of the compounds (Table I-26,27).

2.2. Group 2 elements

Only two silanethiolates of the group 2 elements are known so far and both are barium salts, thus, no trends among their molecular structures can be pursued. The complex [(H$_2$O)$_3$Ba{SSi(*t*BuO)$_3$}$_2$] is the product of the treatment of TBST with metallic barium [57]. Although the reaction was conducted under an inert and dry gas atmosphere, trace amounts of water entered the reaction mixture being probably crucial for the formation of the crystalline product (Fig. 4a Table II-1). In this simple, molecular complex Ba^{2+} ions are coordinated by two tri-*tert*-butoxysilane-anions as O,S-chelating ligands and three molecules of water which complete the coordination sphere of the barium atom.

The second compound, published only as an entry in CSD, has the form of an ionic pair: Ba^{2+} cation sandwiched between two crown ether molecules is accompanied by triphenylsilanethiolate residues which interact with the cation through weak intermolecular C$_{crown}$–H···S interactions (Fig. 4b, Table II-2) [58]. These almost purely ionic interactions between counterions result in a shortening of the S–Si bond (2.049(2) Å) indicating a significant transfer of charge within the sulfur–silicon bond, characteristic for ionic silanethiolates.

2.3. Group 13 elements

The earliest work for group 13 elements describes the only known tallium(I) complex, obtained as colorless crystals in the reaction between the two phases: TlNO$_3$ dissolved in water with the ammonium salt of TBST dissolved in toluene (Table III-1) [59]. Similar to some silanethiolate salts of alkali metals, [{TlSSi(*t*BuO)$_3$}$_2$] is a dimer with a significantly shortened S–Si bond (2.078(2) Å) and elongated Tl–S bond distances (d$_{cov}$ = 2.46 Å, Tl–S, [29–31]). This similarity of thallium and potassium compounds is expected due to comparable charges and ionic radii of Tl$^+$ and K$^+$.

Merely two aluminum silanethiolates: binuclear, organometallic [{Me$_2$Al(μ-SSiPh$_3$)}$_2$] [60] and mononuclear [HC{C(Me)N(2,6-*i*Pr$_2$C$_6$H$_3$)}$_2$Al(SSiMe$_2$)$_2$O] [61] have been obtained so far and both are extremely moisture sensitive, which is not suprising for compounds with aluminum–sulfur bonds, in which the hard Pearson acid (Al^{3+}) is linked to the soft Pearson base (RS$^-$) (Table III-2,3). The dimer [{Me$_2$Al(μ-SSiPh$_3$)}$_2$] was obtained in the reaction of AlMe$_3$ with Ph$_3$SiSH in pentane at RT and recrystallized from a
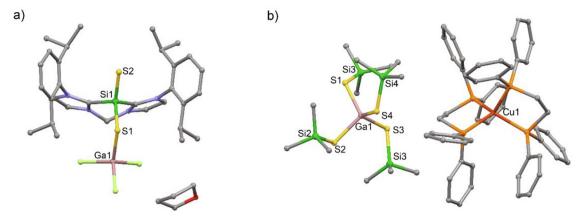
Fig. 6. Molecular structures of silanethiolate complexes of Ga(III) without H atoms: a) (bis-NHC)Si(S)S→GaCl$_3$ [65]; b) [(dppe)$_2$Cu][Ga(SSiMe$_3$)$_4$] [66].
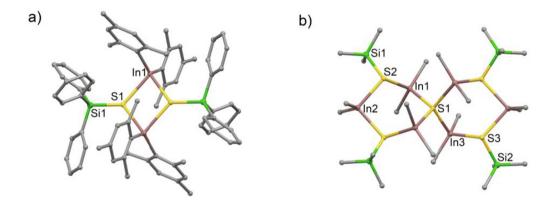

Fig. 7. Molecular structures of selected silanethiolate complexes of In(III) without H atoms: a) [{Mes$_2$In(μ-SSiPh$_3$)}$_2$] [67]; b) [(Me$_2$In)$_6$(μ_4-S)(SSiMe$_3$)$_4$] [68].

pentane/toluene mixture. It features a four-membered, almost planar Al$_2$S$_2$ ring [60]. The synthesis of mononuclear [HC{C(Me) N(2,6-iPr$_2$C$_6$H$_3$)}$_2$Al(SSiMe$_2$)$_2$O] was achieved by the double deprotonation of [HC[C(Me)N(2,6-iPr$_2$C$_6$H$_3$)]$_2$Al(SH)$_2$] with 2 equiv of N,N'-bismesitylimidazol-2-ylidene and further reaction with O(Me$_2$SiCl)$_2$; N,N'-bis-mesitylimidazolium chloride was easily separated as the other product [61]. In both complexes the S–Si bond lengths are close to the value of the sum of r_{cov} of elements (2.19 Å). The Al–S bond distances in the binuclear complex are elongated (2.355(2)-2.368(2) Å) in comparison with d_{cov} (2.29 Å) and within the mononuclear complex shorter Al–S bond distances of 2.223(1) and 2.234(1) Å are realized.

The first gallium silanethiolate, organometallic [{Et$_2$GaSSiPh$_3$}$_2$] was obtained in high yield *via* the elimination of cyclopentadiene from Et$_2$Ga(C$_5$H$_5$) by the reaction with Ph$_3$SiSH in benzene at RT. The ^{1}H NMR spectrum of the complex in benzene showed only one set for the protons of the ethyl groups, consistent with the presence of the *trans* isomer of the complex in solution (Table III-6) [62]. Two more Ga(III) silanethiolates were synthesized in the Wojnowski group: homometallic [(H$_2$O)Ga{SSi(tBuO)$_3$}$_3$] [63] and heterometallic [Ga{SSi(tBuO)$_3$}$_2$Li{μ-SSi(OtBu)$_3$}$_2$] [64] (Table III-7,8, Fig. 5a,b). Both compounds were obtained in the reaction of metastable GaBr with LiSSi(OtBu)$_3$ in toluene/THF solution and in both of them Ga(III) adopts a tetrahedral geometry with GaS$_3$O and GaS$_4$ cores, respectively. The conformation of the homometallic complex is stabilized by a water molecule, which forms two intramolecular hydrogen bonds (Fig. 5a, Table III-7). The heterometallic complex [Ga{SSi(tBuO)$_3$}$_2$Li{μ-SSi(OtBu)$_3$}$_2$] is a minor product of the reaction; two of its silanethiolate residues are engaged in the twofold coordination of the lithium cation by

two *tert*-butoxy O atoms creating a kind of zwitterionic structure (Fig. 5b, Table III-8) [64].

Unusual Lewis acid-base adduct [(bis-NHC)Si(S)S→GaCl$_3$] (NHC=H$_2$C[{NC(H)C(H)N-(dipp)}C:]$_2$) – was described by Matthias Driess (Fig. 6a, Table III-11) [65]. The compound was synthesized by the reaction of (bis-NHC)SiS$_2$ with GaCl$_3$ in acetonitrile at RT and recrystallized from THF at 243 K with good yield. Additionally, the authors described the alternative way to prepare the adduct, which was the reaction of silylone-GaCl$_3$ [(bis-NHC)Si → GaCl$_3$] with elemental sulfur. Two S–Si bonds are shorter than d_{cov} and differ in length: one has the typical length of a S=Si double bond, whereas the other one is elongated indicating a moderate multiple bonding character [65].

In search of metastable precursors for the synthesis of chalcogenide heterometallic clusters, new gallium and indium silanethiolates have been described recently. The compounds are organic and organometallic salts of anionic [M(ESiMe$_3$)$_4$]$^-$ (M = Ga or In and E = S or Se) with a choice of cations: (DMPyr$^+$), Ph$_4$P$^+$, (dppe)$_2$-Cu$^+$, (dmpe)$_2$Cu$^+$. Complex [(dppe)$_2$Cu][Ga(SSiMe$_3$)$_4$] is shown in Fig. 6b. Hence, the reaction of GaCl$_3$ with 1 equiv of ionic liquid DMPyr[ESiMe$_3$] (E = S, Se) and 3 equiv of LiSSiMe$_3$ in THF at 193 K gives, after extraction with diethyl ether, two complexes: DMPyr[Ga(SSiMe$_3$)$_4$] (Table III-12) and DMPyr[Ga(SeSiMe$_3$)$_4$]. A similar indium salt: Ph$_4$P[In(SSiMe$_3$)$_4$] (Table III-13), was obtained in the reaction of LiSSiMe$_3$ (from S(SiMe$_3$)$_2$ and *n*-BuLi) with [Ph$_4$P (InCl$_4$)]. Heterometallic [Cu(dppe)$_2$][In(SSiMe$_3$)$_4$] and [(η^2-dmpe) Cu(μ_2-dmpe)$_2$]$_2$[Ga(SSiMe$_3$)$_4$]$_2$ described in the same paper served as precursors to CuInS$_2$ and CuGaS$_2$ – generated by their thermal decomposition [66].
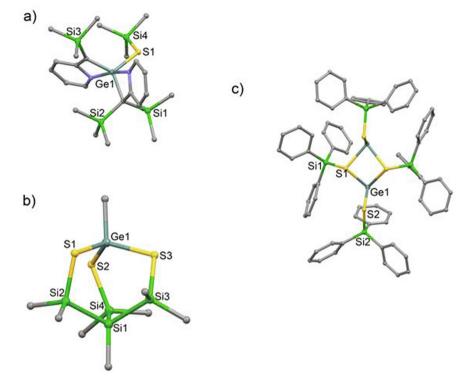
Fig. 8. Molecular structures of Ge silanethiolates without H atoms: a) [Ge{κ-*C,N*-C(SiMe$_3$)$_2$(2-py)}{κ-*C,N*-C(SiMe$_3$)$_2$(2-pyH$_2$)}SSiMe$_3$] [69]; b) [GeMe(SSiMe$_2$)$_3$SiMe] [72]; c) [{Ge(μ-SSiPh$_3$)(SSiPh$_3$)}$_2$] [74].

Before the work of Sundermeyer and co-workers [66] indium silanethiolates were represented by only three air sensitive and easily hydrolyzing compounds. Two of them: dimer [{Mes$_2$In(μ-SSiPh$_3$)}$_2$] and trimer [(Me$_2$InSSiPh$_3$)$_3$] were obtained in the reaction of triphenylsilanethiol with Mes$_3$In and Me$_3$In respectively (Table III-4,5) [67]. The dimeric complex contained a planar In$_2$S$_2$ ring with the organothiolate ligands in a transoid orientation (Fig. 7a), whereas the trimeric derivative featured an (InS)$_3$ ring in a skew-boat conformation and crystallized with two individual molecules in the unit cell. The third indium complex [(Me$_2$In)$_6$(μ_4-S)(SSiMe$_3$)$_4$] and its isostructural Ga(III) derivative were obtained in the reaction of InMe$_3$ (or GaMe$_3$) with S(SiMe$_3$)$_2$ in dichloromethane and recrystallized from toluene (Fig. 7b, Table III-9,10) [68]. The indium complex is built of two mutually twisted In$_3$S$_3$ rings connected through one central sulfide. The organization of the complex is interesting as the S atom and the two peripheral In atoms lie in one plane (Fig. 7b). The S–Si bond lengths in both complexes are almost identical and insignificantly elongated in comparison with the average value. In–S and Ga–S bond lengths are longer than d$_{cov}$ values (2.45 and 2.27 Å, respectively), which seems to be an evident consequence of the bridging role of sulfur atoms in the structure [68].

2.4. Group 14 elements

Among few silanethiolates of the group 14 elements there is a majority of Ge complexes. The first attempts, in which Ge silanethiolates were produced, were undertaken at the end of 20th century by Ossig et al. [69] *via* a multi-step reaction. Thereby within the first step the labile Ge(II) substrate [Ge{κ-*C,N*-C(SiMe$_3$)$_2$(2-py)}$_2$] was obtained by the reaction of the lithiated 2-[bis(trimethylsilyl)methyl]pyridine and GeCl$_2$-dioxane in ether at 195 K. Afterwards, elemental sulfur was added to the obtained solution at RT resulting in the formation of the corresponding thione. Further increase of the temperature to 333 K triggered the

1,3-trimethylsilyl shift from one of the methyl bridges to the sulfur atoms and formation of deep red crystals of the dihydropyridinato/silanethiolato Ge(IV) compounds [Ge{κ-*C,N*-C(SiMe$_3$)$_2$(2-py)}{κ-*C,N*-C(SiMe$_3$)$_2$(2-pyH$_2$)}SSiMe$_3$] (Fig. 8a, Table IV-1). A similar reaction was described for selenium [69].

Several papers on the subject were published by Herzog and co-workers, who initially focused on the attempts of defining the reactivity of 2,4,6,8-tetrachalcogena-bicyclo[3.3.0]octanes as starting materials for the synthesis of heterobimetallic compounds with unsupported M−M' bonds [70,71]. For this purpose, equal amounts of Me$_2$MCl$_2$ (M = Ge, Sn) or Ph$_2$SnCl$_2$ were reacted with Cl$_2$-MeSi−SiMeCl$_2$ and the solution was subsequently saturated with a stream of dry H$_2$S in the presence of NEt$_3$. Out of the obtained complexes, the molecular structure was determined only for the Ge complex [Me$_2$Ge(S)$_2$Si$_2$Me$_2$(S)$_2$GeMe$_2$] (Table IV-2) [71]. The continuation of the studies was dedicated to the bicyclo[2.2.2]octanes. The bicyclic [GeMe(SSiMe$_2$)$_3$SiMe] was obtained from MeSi(SiMe$_2$Cl)$_3$, MeGeCl$_3$ and Li$_2$S and the product was recrystallized from hexane (Fig. 8b, Table IV-3) [72]. The series was completed with a silicon–germanium chalcogenide [Me$_2$Si$_2$(MeGe)$_2$S$_5$] exhibiting a noradamantane-like structure; it was obtained in the reaction of 1,2-Me$_2$Si$_2$Cl$_4$ and MeGeCl$_3$ with H$_2$S/NEt$_3$ (Table IV-4). A similar reaction was also carried out for MeSnCl$_3$ but no product was isolated, while the treatment of a mixture of 1,2-Me$_2$Si$_2$Cl$_4$ and PhSnCl$_3$ with Li$_2$Se resulted in the formation of the first silicon- and tin-containing noradamantane [Me$_2$Si$_2$(PhSn)$_2$Se$_5$] [73].

At the beginning of the 21st century the search for precursors of Ge nanodots and nanowires as a promising replacement of silicon in electronic devices and detection systems became the subject of increased interest. As part of this research two Ge(II) thiolate complexes were synthesized by a reaction with two different thiols: Ph$_3$SiSH and benzenethiol [74]. The methatesis reaction of Ge[N(SiMe$_3$)$_2$]$_2$ and Ph$_3$SiSH leads to colorless crystals of dimeric [{Ge(μ-SSiPh$_3$)(SSiPh$_3$)}$_2$], where the Ge(II) ions are tetrahedrally

Table IV
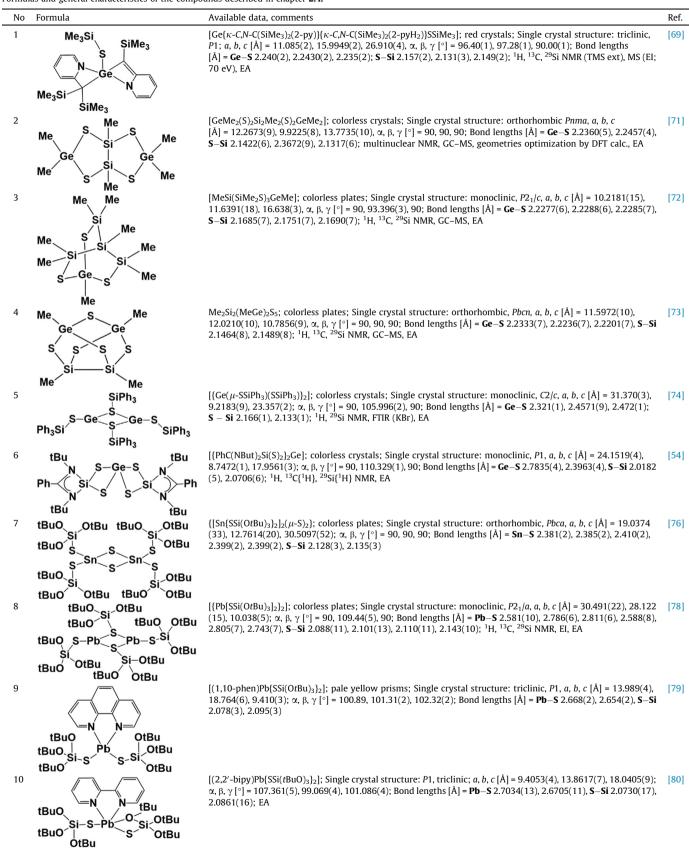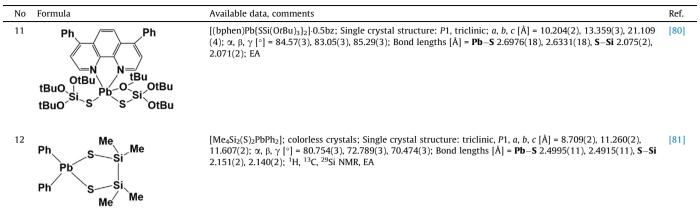Formulas and general characteristics of the compounds described in chapter **2.4.**

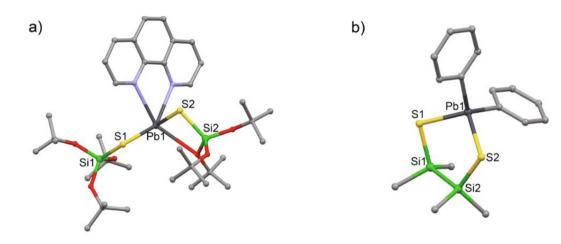| No	Formula	Available data, comments	Ref.
1	[structure]	[Ge{κ-C,N-C(SiMe₃)₂(2-py)}{κ-C,N-C(SiMe₃)₂(2-pyH₂)}SSiMe₃]; red crystals; Single crystal structure: triclinic, $P1$; a, b, c [Å] = 11.085(2), 15.9949(2), 26.910(4), α, β, γ [°] = 96.40(1), 97.28(1), 90.00(1); Bond lengths [Å] = **Ge**−**S** 2.240(2), 2.2430(2), 2.235(2); **S**−**Si** 2.157(2), 2.131(3), 2.149(2); ¹H, ¹³C, ²⁹Si NMR (TMS ext), MS (EI; 70 eV), EA	[69]
2	[structure]	[GeMe₂(S)₂Si₂Me₂(S)₂GeMe₂]; colorless crystals; Single crystal structure: orthorhombic *Pnma*, a, b, c [Å] = 12.2673(9), 9.9225(8), 13.7735(10), α, β, γ [°] = 90, 90, 90; Bond lengths [Å] = **Ge**−**S** 2.2360(5), 2.2457(4), **S**−**Si** 2.1422(6), 2.3672(9), 2.1317(6); multinuclear NMR, GC−MS, geometries optimization by DFT calc., EA	[71]
3	[structure]	[MeSi(SiMe₂S)₃GeMe]; colorless plates; Single crystal structure: monoclinic, $P2_1/c$, a, b, c [Å] = 10.2181(15), 11.6391(18), 16.638(3), α, β, γ [°] = 90, 93.396(3), 90; Bond lengths [Å] = **Ge**−**S** 2.2277(6), 2.2288(6), 2.2285(7), **S**−**Si** 2.1685(7), 2.1751(7), 2.1690(7); ¹H, ¹³C, ²⁹Si NMR, GC−MS, EA	[72]
4	[structure]	Me₂Si₂(MeGe)₂S₅; colorless plates; Single crystal structure: orthorhombic, *Pbcn*, a, b, c [Å] = 11.5972(10), 12.0210(10), 10.7856(9), α, β, γ [°] = 90, 90, 90; Bond lengths [Å] = **Ge**−**S** 2.2333(7), 2.2236(7), 2.2201(7), **S**−**Si** 2.1464(8), 2.1489(8); ¹H, ¹³C, ²⁹Si NMR, GC−MS, EA	[73]
5	[structure]	[{Ge(μ-SSiPh₃)(SSiPh₃)}₂]; colorless crystals; Single crystal structure: monoclinic, $C2/c$, a, b, c [Å] = 31.370(3), 9.2183(9), 23.357(2); α, β, γ [°] = 90, 105.996(2), 90; Bond lengths [Å] = **Ge**−**S** 2.321(1), 2.4571(9), 2.472(1); **S** − **Si** 2.166(1), 2.133(1); ¹H, ²⁹Si NMR, FTIR (KBr), EA	[74]
6	[structure]	[{PhC(NBut)₂Si(S)₂}₂Ge]; colorless crystals; Single crystal structure: monoclinic, $P1$, a, b, c [Å] = 24.1519(4), 8.7472(1), 17.9561(3); α, β, γ [°] = 90, 110.329(1), 90; Bond lengths [Å] = **Ge**−**S** 2.7835(4), 2.3963(4), **S**−**Si** 2.0182(5), 2.0706(6); ¹H, ¹³C{¹H}, ²⁹Si{¹H} NMR, EA	[54]
7	[structure]	{[Sn{SSi(OtBu)₃}₂]₂(μ-S)}; colorless plates; Single crystal structure: orthorhombic, *Pbca*, a, b, c [Å] = 19.0374(33), 12.7614(20), 30.5097(52); α, β, γ [°] = 90, 90, 90; Bond lengths [Å] = **Sn**−**S** 2.381(2), 2.385(2), 2.410(2), 2.399(2), 2.399(2), **S**−**Si** 2.128(3), 2.135(3)	[76]
8	[structure]	[{Pb[SSi(OtBu)₃]₂}₂]; colorless plates; Single crystal structure: monoclinic, $P2_1/a$, a, b, c [Å] = 30.491(22), 28.122(15), 10.038(5); α, β, γ [°] = 90, 109.44(5), 90; Bond lengths [Å] = **Pb**−**S** 2.581(10), 2.786(6), 2.811(6), 2.588(8), 2.805(7), 2.743(7), **S**−**Si** 2.088(11), 2.101(13), 2.110(11), 2.143(10); ¹H, ¹³C, ²⁹Si NMR, EI, EA	[78]
9	[structure]	[(1,10-phen)Pb{SSi(OtBu)₃}₂]; pale yellow prisms; Single crystal structure: triclinic, $P1$, a, b, c [Å] = 13.989(4), 18.764(6), 9.410(3); α, β, γ [°] = 100.89, 101.31(2), 102.32(2); Bond lengths [Å] = **Pb**−**S** 2.668(2), 2.654(2), **S**−**Si** 2.078(3), 2.095(3)	[79]
10	[structure]	[(2,2′-bipy)Pb{SSi(tBuO)₃}₂]; Single crystal structure: $P1$, triclinic; a, b, c [Å] = 9.4053(4), 13.8617(7), 18.0405(9); α, β, γ [°] = 107.361(5), 99.069(4), 101.086(4); Bond lengths [Å] = **Pb**−**S** 2.7034(13), 2.6705(11), **S**−**Si** 2.0730(17), 2.0861(16); EA	[80]

Table IV (*continued*)

No	Formula	Available data, comments	Ref.
11		[(bphen)Pb{SSi(O*t*Bu)₃}₂]·0.5bz; Single crystal structure: *P*1, triclinic; *a*, *b*, *c* [Å] = 10.204(2), 13.359(3), 21.109(4); α, β, γ [°] = 84.57(3), 83.05(3), 85.29(3); Bond lengths [Å] = **Pb–S** 2.6976(18), 2.6331(18), **S–Si** 2.075(2), 2.071(2); EA	[80]
12		[Me₄Si₂(S)₂PbPh₂]; colorless crystals; Single crystal structure: triclinic, *P*1, *a*, *b*, *c* [Å] = 8.709(2), 11.260(2), 11.607(2); α, β, γ [°] = 80.754(3), 72.789(3), 70.474(3); Bond lengths [Å] = **Pb–S** 2.4995(11), 2.4915(11), **S–Si** 2.151(2), 2.140(2); ¹H, ¹³C, ²⁹Si NMR, EA	[81]

Fig. 9. Molecular structure of the selected Pb silanethiolates without H atoms: a) [(1,10-phen)Pb{SSi(O*t*Bu)₃}₂] [79]; b) [Me₄Si₂(S)₂PbPh₂] [81]

Fig. 10. Molecular structure of selected silanethiolates of Group 15 elements; H atoms are omitted for clarity: a) [As{SSi(O*t*Bu)₃}₃] [82]; b) [Tbt(Mes)Si(μ-S)₂SbBbt] [86].

coordinated by two silanethiolate residues acting as terminal and chelating ligands (Fig. 8c, Table IV-5). The structural analysis of dimer shows that both Ge–S bonds are elongated, whereas the S–Si bond lengths are comparable with the value of d_{cov} (2.24 and 2.19 Å, respectively). The complex was further investigated for the generation of Ge-based nanomaterials but TEM and EDS techniques proved the formation of amorphous Ge$_x$S$_y$ material and it was concluded that [{Ge(μ-SSiPh₃)(SSiPh₃)}₂] could not be a satisfying precursor for Ge(0) nanomaterials [74].

The coordination properties of siladithiocarboxylates towards germanium were investigated by Zhang and co-workers [54]. Using standard Schlenk techniques they obtained [{PhC(NBut)₂Si(S)₂}K(THF)₂]₂ (see chapter 2.1) and the potassium salt was further reacted with GeCl₂·dioxane in THF at 273 K to give germanium(II) siladithiocarboxylate [{PhC(NBut)₂Si(S)₂}₂Ge] with good yield [54]. The siladithiocarboxylate anions chelate the Ge atom in an asymmetric way with one of the Ge–S bonds strongly elongated, accompanied by the simultaneous shrinkage of one of the S–Si bonds

Table V
Formulas and general characteristics of the compounds described in chapter **2.5.**

No	Formula	Available data, comments	Ref.
1	M = As, Sb, Bi	[As{SSi(OtBu)₃}₃]; pale brown prisms; Single crystal structure: orthorhombic, $P2_12_12_1$, a, b, c [Å] = 15.364(6), 24.61(1), 14.591(6); α, β, γ [°] = 90, 90, 90; Bond lengths [Å] = **As−S** 2.260 (4), 2.245(4), 2.257(3), **S−Si** 2.115(5), 2.132(5), 2.097(6); EA	[82]
2		[Sb{SSi(OtBu)₃}₃]; colorless lump; Single crystal structure: $P2_13$; cubic; a, b, c [Å] = 17.802 (6); α, β, γ [°] = 90, 90, 90; Bond lengths [Å] = **Sb−S** 2.406(4), 2. 406(5), **S−Si** 2.122(6), 2.122(7); EA	[83]
3		[Bi{SSi(OtBu)₃}₃]; pale yellow prisms; Single crystal structure: $P2_13$; Cubic; a, b, c [Å] = 17.793(2); α, β, γ [°] = 90, 90, 90; Bond lengths [Å] = **Bi−S** 2.535 (3), 2.535(4), **S−Si** 2.111 (4), 2.111(5); EA	[84]
4		[Tbt(Mes)Si (μ-S)₂SbBbt]; pale yellow crystals; Single crystal structure: monoclinic, $P2_1/c$, a, b, c [Å] = 12.43510(10), 19.5286(2), 36.7653(4); α, β, γ [°] = 90, 91.1935 (5), 90; Bond lengths [Å] = **Sb−S** 2.4515(9), 2.4577(8), **S−Si** 2.1510 (10), 2.1744(12); ^{1}H, ^{13}C {^{1}H}, ^{29}Si NMR, EA, LRMS (FAB⁺) m/z, HRMS (FAB⁺) m/z	[86]

which becomes close to the S=Si double bond length (average 1.95 Å) pointing at its zwitterionic Si⁺–S⁻ bonding character (Table IV-6) [75].

The only structurally characterized representative of Sn silanethiolates is 2,2,4,4-tetrakis(tri-*tert*-butoxysilanethiolato)-1,3,2,4-dithiadistannetane [(Sn(μ–S){SSi(OtBu)₃}₂)₂] obtained initially from TBST, sulfur and Et₃N with SnCl₂ in toluene solution at 343 K [76]. The same compound was isolated in the reaction of TBST and Et₃N with SnCl₂ or SnCl₄ without the addition of sulfur and two different polymorphs were obtained [77]. Structural analysis showed that the Sn–S bonds within the planar Sn₂S₂ ring are slightly elongated with respect to the Sn–S bonds to the terminal TBST residues (Table IV-7). Nevertheless, the S–Si bonds distances are comparable with d_{cov} [29–31]. The existence and reactivity of [SnCl{SSi(tBuO)₃}₃] and [SnBr{SSi(OtBu)₃}₃] were mentioned in two papers [36,49].

The first synthesized lead silanethiolate is the homoleptic [(Pb {SSi(tBuO)₃}₂)₂], obtained in the exothermic reaction of TBST with PbO in benzene (Table IV-8) [78]. It is a binuclear complex with the characteristic, central four-membered puckered Pb₂S₂ ring. Pb–S bond lengths are significantly elongated in comparison to d_{cov} (2.47 Å), whereas one of the S–Si bonds is noticeably shorter than the sum of the covalent radii. The homoleptic compound was

reacted with 1,10-phenantroline to give a mononuclear [(1,10-phen)Pb{SSi(tBuO)₃}₂] complex, where the Pb atoms are octahedrally coordinated by two O,S-chelating silanethiolate residues and a chelating 1,10-phenanthroline (Fig. 9a, Table IV-9) [79].

The reaction of [{Pb[SSi(tBuO)₃}₂}₂] with nitrogen nucleophiles was further investigated in 2007. Two Pb(II) silanethiolate complexes [(bpy)Pb{SSi(OtBu)₃}₂] and [(bphen)Pb{SSi (OtBu)₃}₂]·0.5bz were obtained in reactions with 2,2′-bipyridine and 4,7-diphenyl-1,10-phenanthroline, respectively (Table IV-10,11) [80]. Both complexes exhibited a distorted square-pyramidal coordination of the Pb atoms with S atoms in the apical position and O,S coordination mode of the silanethiolate residues.

In 2002 organometallic plumbolanes were described, obtained in the reaction between Ph₂PbCl₂ and ClSiMe₂–SiMe₂Cl in the presence of H₂S/NEt₃ [81]. Two compounds were obtained: [Me₄-Si₂(S)₂PbPh₂] and [Ph₂Pb(S)₂Si₂Me₂(S)₂PbPh₂]; the crystal structure measured for [Me₄Si₂(S)₂PbPh] revealed the presence of a five membered Si₂S₂Pb ring (Fig. 9b, Table IV-12). The structure of the other one, bicyclic [Ph₂Pb(S)₂Si₂Me₂(S)₂PbPh₂], was established with the use of NMR spectroscopy [81].

2.5. Group 15 elements

Three out of four known silanethiolate complexes of the group 15 elements were synthesized by the group of Wojnowski with the use of TBST and salts of the respective elements: AsCl₃, SbCl₃, Bi₂(SO₄)₃ [82–84] (Fig. 10a, Table V-1–3). All three complexes [M{SSi(OtBu)₃}₃], where M = As, Sb, Bi, are mononuclear and form molecular crystals. The molecular structures of the complexes exhibit a noticeable correlation between the lengths of M−S and S–Si bonds, whereby longer M−S bonds are correlated with shorter S–Si bond. However, they are still close to the value of their d_{cov}: As–S 2.24 Å, Sb–S 2.43 Å, Bi–S 2.54 Å [29–31].

Final example of group 15 silanethiolates was described by Tanabe and co-workers and obtained with the use of overcrowded silanedichalcogenol (for the synthesis of the precursor of silanedichalcogenol see [85]) [86]. Antimony(III) compound – 1,3,2,4-dithiastibasiletane [Tbt(Mes)Si(μ-S)SbBbt] (Fig. 10b, Table V-4) - was obtained by the reaction of the lithium salt of Tbtμ(Mes)Si(SH)₂ and Bbt-substituted dibromostibine BbtSbBr₂. The product was isolated with the use of GPLC and WCC chromatography and recrystallized from hexane at 253 K. The complex consists of an almost planar four-membered ring; the Sb–S and S–Si bond lengths are slightly elongated in comparison with those found in other related complexes [83,87]. Crystals of the isostructural Bi derivative were also obtained in a similar reaction, but severe disorders did not allow the detailed X-ray structure analysis [86].
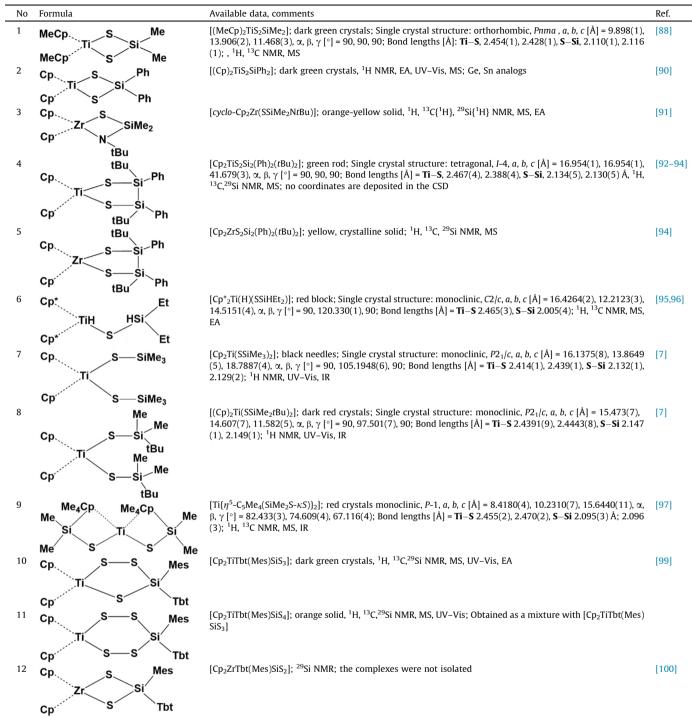
3. Transition and post-transition elements

3.1. Group 4 elements

The silanethiolate complexes of group 4 elements are rare as both M−S and S–Si bonds are very reactive [88]. Due to this reactivity the complexes are unstable, whereby the reactivity of the M−S bond exceeds the one of the S–Si bond, which is rather unusual among silanethiolate complexes of transition metals. Most of the compounds described in the literature are Ti(IV) complexes. Interestingly no Ti(III) compounds were reported in spite of known, reducing properties of the thiolate compounds and hard–soft character of the Ti(IV)–S system. Two major types of molecular Ti/Zr silanethiolates were observed – either mononuclear compounds with monodentate ligands or small M−Sₙ−Si rings with chelating

Table VI
Formulas and general characteristics of the Ti/Zr compounds described in chapter **3.1.**

No	Formula	Available data, comments	Ref.
1	MeCp, Ti, S, Si, Me / MeCp, S, Me	[(MeCp)$_2$TiS$_2$SiMe$_2$]; dark green crystals; Single crystal structure: orthorhombic, *Pnma*, *a, b, c* [Å] = 9.898(1), 13.906(2), 11.468(3), α, β, γ [°] = 90, 90, 90; Bond lengths [Å]: **Ti–S**, 2.454(1), 2.428(1), **S–Si**, 2.110(1), 2.116 (1); , ^{1}H, ^{13}C NMR, MS	[88]
2	Cp, Ti, S, Si, Ph / Cp, S, Ph	[(Cp)$_2$TiS$_2$SiPh$_2$]; dark green crystals, ^{1}H NMR, EA, UV–Vis, MS; Ge, Sn analogs	[90]
3	Cp, Zr, S, SiMe$_2$, N, tBu / Cp	[*cyclo*-Cp$_2$Zr(SSiMe$_2$N*t*Bu)]; orange-yellow solid, ^{1}H, ^{13}C{^{1}H}, ^{29}Si{^{1}H} NMR, MS, EA	[91]
4	tBu, Cp, S, Si, Ph, Ti, S, Si, Cp, tBu, Ph	[Cp$_2$TiS$_2$Si$_2$(Ph)$_2$(*t*Bu)$_2$]; green rod; Single crystal structure: tetragonal, *I-4*, *a, b, c* [Å] = 16.954(1), 16.954(1), 41.679(3), α, β, γ [°] = 90, 90, 90; Bond lengths [Å] = **Ti–S**, 2.467(4), 2.388(4), **S–Si**, 2.134(5), 2.130(5) Å, ^{1}H, ^{13}C,^{29}Si NMR, MS; no coordinates are deposited in the CSD	[92–94]
5	tBu, Cp, S, Si, Ph, Zr, S, Si, Cp, tBu, Ph	[Cp$_2$ZrS$_2$Si$_2$(Ph)$_2$(*t*Bu)$_2$]; yellow, crystalline solid; ^{1}H, ^{13}C, ^{29}Si NMR, MS	[94]
6	Cp*, Et, TiH, HSi, Cp*, S, Et	[Cp*$_2$Ti(H)(SSiHEt$_2$)]; red block; Single crystal structure: monoclinic, *C2/c*, *a, b, c* [Å] = 16.4264(2), 12.2123(3), 14.5151(4), α, β, γ [°] = 90, 120.330(1), 90; Bond lengths [Å] = **Ti–S** 2.465(3), **S–Si** 2.005(4); ^{1}H, ^{13}C NMR, MS, EA	[95,96]
7	Cp, S, SiMe$_3$, Ti, Cp, S, SiMe$_3$	[Cp$_2$Ti(SSiMe$_3$)$_2$]; black needles; Single crystal structure: monoclinic, *P2$_1$/c*, *a, b, c* [Å] = 16.1375(8), 13.8649(5), 18.7887(4), α, β, γ [°] = 90, 105.1948(6), 90; Bond lengths [Å] = **Ti–S** 2.414(1), 2.439(1), **S–Si** 2.132(1), 2.129(2); ^{1}H NMR, UV–Vis, IR	[7]
8	Me, Me, Cp, S, Si, tBu, Ti, Me, Me, Cp, S, Si, tBu	[(Cp)$_2$Ti(SSiMe$_2$*t*Bu)$_2$]; dark red crystals; Single crystal structure: monoclinic, *P2$_1$/c*, *a, b, c* [Å] = 15.473(7), 14.607(7), 11.582(5), α, β, γ [°] = 90, 97.501(7), 90; Bond lengths [Å] = **Ti–S** 2.4391(9), 2.4443(8), **S–Si** 2.147 (1), 2.149(1); ^{1}H NMR, UV–Vis, IR	[7]
9	Me$_4$Cp, Me$_4$Cp, Me, Si, Ti, Si, Me, Me, S, S, Me	[Ti{η^5-C$_5$Me$_4$(SiMe$_2$S-κS)}$_2$]; red crystals monoclinic, *P-1*, *a, b, c* [Å] = 8.4180(4), 10.2310(7), 15.6440(11), α, β, γ [°] = 82.433(3), 74.609(4), 67.116(4); Bond lengths [Å] = **Ti–S** 2.455(2), 2.470(2), **S–Si** 2.095(3) Å; 2.096 (3); ^{1}H, ^{13}C NMR, MS, IR	[97]
10	Cp, S, S, Mes, Ti, Si, Cp, S, Tbt	[Cp$_2$TiTbt(Mes)SiS$_3$]; dark green crystals, ^{1}H, ^{13}C,^{29}Si NMR, MS, UV–Vis, EA	[99]
11	Cp, S, S, Mes, Ti, Si, Cp, S, S, Tbt	[Cp$_2$TiTbt(Mes)SiS$_4$]; orange solid, ^{1}H, ^{13}C,^{29}Si NMR, MS, UV–Vis; Obtained as a mixture with [Cp$_2$TiTbt(Mes) SiS$_3$]	
12	Cp, S, Mes, Zr, Si, Cp, S, Tbt	[Cp$_2$ZrTbt(Mes)SiS$_2$]; ^{29}Si NMR; the complexes were not isolated	[100]

dithiolate ligands. All of them are characterized by the presence of a metallocene unit and tetrahedral coordination of the M(IV) centre.

The first example - the titanocene [(MeCp)$_2$TiS$_2$SiMe$_2$] – was prepared by treating a THF solution of Me$_2$SiCl$_2$ with Li$_2$S and subsequent addition of (MeCp)$_2$TiCl$_2$. Alternatively, the probable intermediate of the first synthetic way (Me$_2$SiS)$_3$ can be used as the thiolate source during the reaction. The complex [(MeCp)$_2$TiS$_2$SiMe$_2$] features two tetrahedral centers: Ti and Si, linked by two bridging sulfur atoms (Table VI-1, Fig. 11a).

The resulting TiSiS$_2$ ring is planar. The bond orders were not predicted but the established bond lengths within the complex: S–Si 2.110 Å (d$_{cov}$ 2.19 Å [29–31]) and Ti–S 2.454 Å (d$_{cov}$ 2.39 Å) hint to a weak stabilizing interaction between Ti(IV) and sulfur. The studies on the reactivity of the complex indeed revealed that the Ti–S bonds in [(MeCp)$_2$TiS$_2$SiMe$_2$] are more labile than the S–Si bonds and that the S atoms are readily exchanged for O atoms without electron transfer [88], as also observed recently for titanium(IV) complexes with other soft ligands [89].
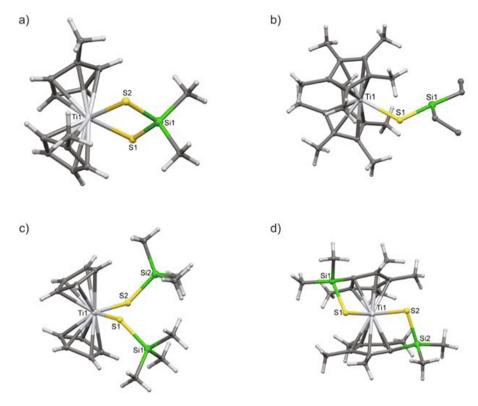
Fig. 11. Molecular structures of selected silanethiolate complexes of Ti(IV): a) [(MeCp)$_2$TiS$_2$SiMe$_2$] [88]; b) [Cp*$_2$Ti(H)(SSiHEt$_2$)] [95]; c) [Cp$_2$Ti(SSiMe$_3$)$_2$] [7]; d) [Ti{η^5-C$_5$Me$_4$(SiMe$_2$S-κS)}$_2$] [97].

The reactions of the halides Ph$_2$SiCl$_2$, Ph$_2$GeBr$_2$, and Ph$_2$SnCl$_2$ with Li$_2$S and (RCp)$_2$TiCl$_2$ (R = H, CH$_3$) were further studied by Albertsen and Steudel [90]. The reactions were carried out in dry THF to give the four-membered titanacyles [(RCp)$_2$TiS$_2$XPh$_2$] X = Si, Ge, Sn characterized by ^{1}H NMR, UV spectroscopy and mass spectrometry (Table VI-2). The green crystals reacted with sulfur chlorides with the formation of sulfur-rich heterocycles of Group 14 elements and precipitation of (RCp)$_2$TiCl$_2$ [90].

In 1993 the first compound with Zr–S–Si bonds was reported as the result of the reaction between the silanimine Zr complex and carbon disulfide. The orange-yellow solid, which was the major product of the insertion of sulfur into the Zr–Si bond, was identified from spectroscopic data and elemental analysis as [*cyclo*-Cp$_2$Zr(SSiMe$_2$N*t*Bu)] (Table VI-3) [91].

The straightforward reaction between the lithium salt of the chelating disilanedithiolate ligand and Cp$_2$TiCl$_2$ allowed the isola-

tion of five-membered metallocycle [Cp$_2$TiS$_2$Si$_2$(Ph)$_2$(*t*Bu)$_2$] adopting a half-chair conformation (Table VI-4). The formation of the zirconium analog [Cp$_2$ZrS$_2$Si$_2$(Ph)$_2$(*t*Bu)$_2$] was also achieved under argon (Table VI-5). The titanocene/zirconocene unit could be readily displaced from the heterocycle by some of the tested electrophilic reagents *e.g.* SCl$_2$, however it was also isolated unchanged even after prolonged heating with others such as Ph$_2$-SiCl$_2$ [92,93]. In 1996 the research on zirconium metallacycles was continued. Though the reaction between disilanediitiolate ligand and Cp$_2$ZrCl$_2$ proceeded with a yield of 90%, the zirconocycle ZrS$_2$Si$_2$ was a reactive compound, unstable towards water and oxygen and its structure or chemistry were not investigated [94].

Formation of the mononuclear, tetrahedral decamethylti-tanocene silanethiolate complexes [Cp*$_2$Ti(H)(SSiR$_3$)] was observed in the reaction of tetrahedral [Cp*$_2$Ti=S(py)] with trialkyl-silanes. Three compounds were obtained in the form of yellow
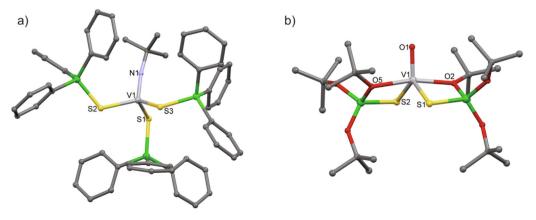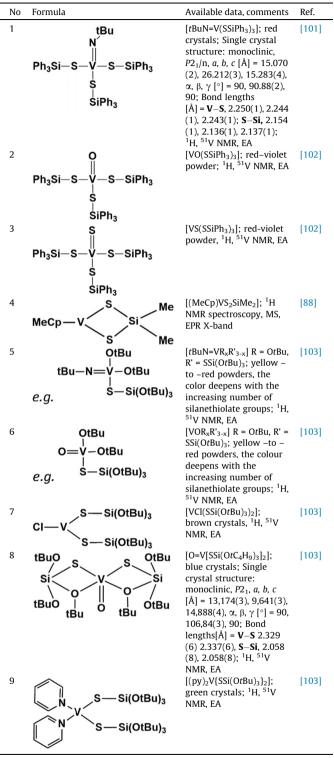
Fig. 12. Known molecular structures of the silanethiolate complexes of V(V) and V(IV) without H atoms: a) *t*BuN=V(SSiPh$_3$)$_3$ [101]; b) [VO{SSi(O*t*Bu)$_3$}$_2$] [103].

Table VII

Formulas and general characteristics of the vanadium compounds described in chapter **3.2.**

No	Formula	Available data, comments	Ref.
1	[*t*BuN=V(SSiPh$_3$)$_3$]; structure	[*t*BuN=V(SSiPh$_3$)$_3$]; red crystals; Single crystal structure: monoclinic, $P2_1/n$, a, b, c [Å] = 15.070 (2), 26.212(3), 15.283(4), α, β, γ [°] = 90, 90.88(2), 90; Bond lengths [Å] = **V**–**S**, 2.250(1), 2.244 (1), 2.243(1); **S**–**Si**, 2.154 (1), 2.136(1), 2.137(1); ^{1}H, ^{51}V NMR, EA	[101]
2	[VO(SSiPh$_3$)$_3$]; structure	[VO(SSiPh$_3$)$_3$]; red–violet powder; ^{1}H, ^{51}V NMR, EA	[102]
3	[VS(SSiPh$_3$)$_3$]; structure	[VS(SSiPh$_3$)$_3$]; red–violet powder, ^{1}H, ^{51}V NMR, EA	[102]
4	[(MeCp)VS$_2$SiMe$_2$]; structure	[(MeCp)VS$_2$SiMe$_2$]; ^{1}H NMR spectroscopy, MS, EPR X-band	[88]
5	[*t*BuN=VR$_x$R'$_{3-x}$]; structure	[*t*BuN=VR$_x$R'$_{3-x}$] R = O*t*Bu, R' = SSi(O*t*Bu)$_3$; yellow – to –red powders, the color deepens with the increasing number of silanethiolate groups; ^{1}H, ^{51}V NMR, EA	[103]
6	[VOR$_x$R'$_{3-x}$]; structure	[VOR$_x$R'$_{3-x}$] R = O*t*Bu, R' = SSi(O*t*Bu)$_3$; yellow –to – red powders, the colour deepens with the increasing number of silanethiolate groups; ^{1}H, ^{51}V NMR, EA	[103]
7	[VCl(SSi(O*t*Bu)$_3$)$_2$]; structure	[VCl(SSi(O*t*Bu)$_3$)$_2$]; brown crystals, ^{1}H, ^{51}V NMR, EA	[103]
8	[O=V[SSi(O*t*C$_4$H$_9$)$_3$]$_2$]; structure	[O=V[SSi(O*t*C$_4$H$_9$)$_3$]$_2$]; blue crystals; Single crystal structure: monoclinic, $P2_1$, a, b, c [Å] = 13,174(3), 9,641(3), 14,888(4), α, β, γ [°] = 90, 106,84(3), 90; Bond lengths[Å] = **V**–**S** 2.329 (6) 2.337(6), **S**–**Si**, 2.058 (8), 2.058(8); ^{1}H, ^{51}V NMR, EA	[103]
9	[(py)$_2$V{SSi(O*t*Bu)$_3$}$_2$]; structure	[(py)$_2$V{SSi(O*t*Bu)$_3$}$_2$]; green crystals; ^{1}H, ^{51}V NMR, EA	[103]

solids and for one of the derivatives, namely [Cp*$_2$Ti(H)(SSiHEt$_2$)] the molecular structure was confirmed by single-crystal X-ray diffraction (Table VI-6, Fig. 11b) [95]. The immediate reaction of [Cp*$_2$Ti=S(py)] with silanes is accompanied by a color change from red to orange and gives the pure products in nearly quantitative yield. The silane addition to the Ti=S bond is reversible and the silanes can be removed from the product by thermolysis at moderate temperatures [96].

Three tetrahedral Ti silanethiolate complexes: [Cp$_2$Ti(SSiMe$_3$)$_2$], [(Cp)$_2$Ti(SSiMe$_2$*t*Bu)$_2$] and [Ti{η^5-C$_5$Me$_4$(SiMe$_2$S-κS)}$_2$] were reported in 2004 [7,97]. The first of them was obtained by the reaction of (Me$_2$SiS)$_3$ in Et$_2$O with MeLi in Et$_2$O followed by the transfer of the resulting solution to the suspension of Cp$_2$TiCl$_2$ in toluene. In the first stage of this reaction probably the lithium salt of the trimethylsilanethiol formed in the (Me$_2$SiS)$_3$/MeLi system. Low temperature is required during the synthesis. No reactivity studies were performed for this complex (Table VI-7, Fig. 11c) [7]. Dark, red crystals of [(Cp)$_2$Ti(SSiMe$_2$*t*Bu)$_2$] (Table VI-8) were obtained by the reaction of Cp$_2$TiCl$_2$ with [Li(tmeda)SSiMe$_2$*t*Bu]$_2$. The third complex - red crystalline [Ti{η^5-C$_5$Me$_4$(SiMe$_2$S-κS)}$_2$] is obtained after the addition of an excess of gaseous hydrogen sulfide to the toluene solution of the silanide [TiCl$_2${η^5-C$_5$Me$_4$(SiMe$_2$NMe$_2$)}$_2$]. After gentle warming of the reaction mixture, initially prepared at liquid nitrogen temperature, Si–N and Ti–Cl bonds were cleaved yielding sulfido-tethered titanocene and dimethylamine hydrochloride (Table VI-9, Fig. 11d). [Ti{η^5-C$_5$Me$_4$(SiMe$_2$S-κS)}$_2$] decomposes in contact with water [97]. A structurally similar Zr thiolate [Zr({η^5-C$_5$Me$_4$)CH$_2$CH$_2$S-κS)$_2$] was earlier reported [98].

Novel silacyclic compounds containing titanium and chalcogen atoms were prepared by the reactions of the titanocene pentachalcogenides [Cp$_2$TiX$_5$], X = S, Se with the reactive disilene Tbt (Mes)Si=Si(Mes)Tbt. The structures of these silacyclic compounds were determined by spectroscopic methods and elemental analysis. Five- and six-membered rings [Cp$_2$TiTbt(Mes)SiS$_3$] and [Cp$_2$-TiTbt(Mes)SiS$_4$] (Table VI-10,11) were reported with a variable number of sulfur (also selenium) atoms. The number of chalcogene atoms that constituted the ring depended on the polarity of the solvent applied for the synthesis [99]. The compounds could be desulfurized with triphenylphosphane to the four-membered titanocene [Cp$_2$TiS$_2$Si(Mes)(Tbt)] similar to those reported earlier both by Giolando and by Choi [88,94]. Zirconium analogs [Cp$_2$ZrS$_2$Si-(Mes)(Tbt)] were mentioned to form in the reactions of Tbt(Mes)-Si=Si(Mes)Tbt with [Cp$_2$ZrS$_5$]. The compounds were not isolated but instead served as one-pot precursors to bulky silanedithiols and silanediselenols (Table VI-12) [100]. Their formation was confirmed later by observation of relevant ^{29}Si NMR signals [86].
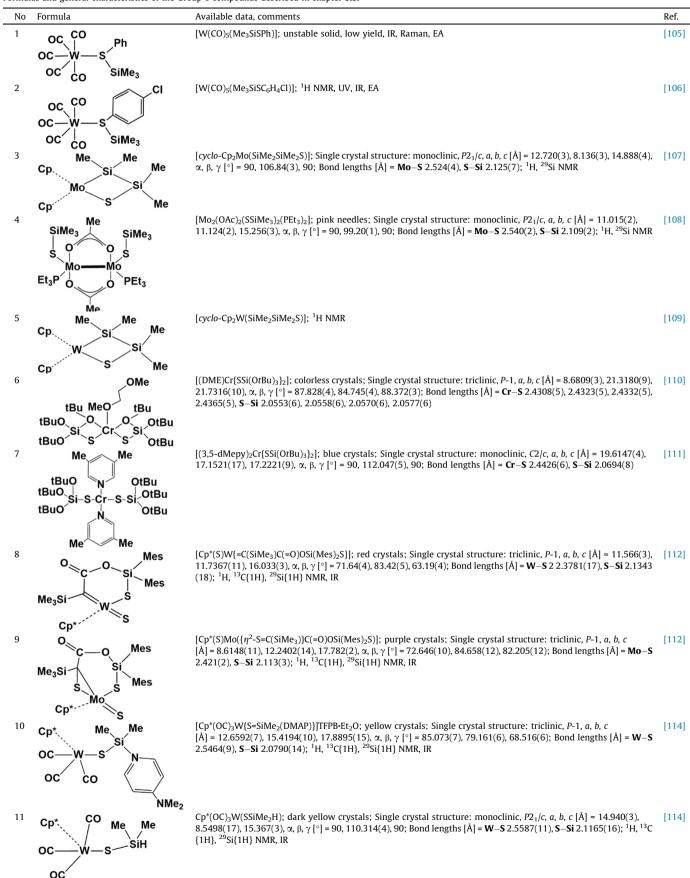
3.2. Group 5 elements

The silanethiolates of group 5 elements are even less common than those of group 4. They were described in a few papers between 1986 and 1990. Both thiolates and silanethiolate of vanadium(V) were prepared by reaction of iminovanadium(V) chlorides with LiSR at low as well as room temperature. X-ray diffraction analyses revealed a distorted tetrahedral arrangement of the ligands in the thiolate and silanethiolate complexes of vanadium (V). The molecular thiolates were crystalline solids soluble in organic solvents and stable at RT, whose orange color deepened with increasing number of thiolate ligands to red violet [101]. In the structure of vanadium(V) silanethiolate: *t*BuN=V(SSiPh$_3$)$_3$ (Fig. 12a, Table VII-1) the shortening of the metal-sulfur bond and elongation of the silicon-sulfur bond is observed in comparison to known Ti silanethiolates; this in our opinion indicates a more covalent character of the vanadium sulfur bond in V(V) silanethiolates. The V–S bond lengths are shorter than the sum of respective van der Waals radii, which is 2.37 Å [29–31]. One year later the research on oxovanadium(V) and thiovanadium(V) silanethiolates followed. The VO(SSiPh$_3$)$_3$ was obtained in the reaction of oxovanadium(V) trichloride with LiSSiPh$_3$ whereas VS(SSiPh$_3$)$_3$

Table VIII
Formulas and general characteristics of the Group 6 compounds described in chapter **3.3.**

No	Formula	Available data, comments	Ref.
1		[W(CO)$_5$(Me$_3$SiSPh)]; unstable solid, low yield, IR, Raman, EA	[105]
2		[W(CO)$_5$(Me$_3$SiSC$_6$H$_4$Cl)]; ^{1}H NMR, UV, IR, EA	[106]
3		[cyclo-Cp$_2$Mo(SiMe$_2$SiMe$_2$S)]; Single crystal structure: monoclinic, P2$_1$/c, a, b, c [Å] = 12.720(3), 8.136(3), 14.888(4), α, β, γ [°] = 90, 106.84(3), 90; Bond lengths [Å] = **Mo**—**S** 2.524(4), **S**—**Si** 2.125(7); ^{1}H, ^{29}Si NMR	[107]
4		[Mo$_2$(OAc)$_2$(SSiMe$_3$)$_2$(PEt$_3$)$_2$]; pink needles; Single crystal structure: monoclinic, P2$_1$/c, a, b, c [Å] = 11.015(2), 11.124(2), 15.256(3), α, β, γ [°] = 90, 99.20(1), 90; Bond lengths [Å] = **Mo**—**S** 2.540(2), **S**—**Si** 2.109(2); ^{1}H, ^{29}Si NMR	[108]
5		[cyclo-Cp$_2$W(SiMe$_2$SiMe$_2$S)]; ^{1}H NMR	[109]
6		[(DME)Cr{SSi(OtBu)$_3$}$_2$]; colorless crystals; Single crystal structure: triclinic, P-1, a, b, c [Å] = 8.6809(3), 21.3180(9), 21.7316(10), α, β, γ [°] = 87.828(4), 84.745(4), 88.372(3); Bond lengths [Å] = **Cr**—**S** 2.4308(5), 2.4323(5), 2.4332(5), 2.4365(5), **S**—**Si** 2.0553(6), 2.0558(6), 2.0570(6), 2.0577(6)	[110]
7		[(3,5-dMepy)$_2$Cr{SSi(OtBu)$_3$}$_2$]; blue crystals; Single crystal structure: monoclinic, C2/c, a, b, c [Å] = 19.6147(4), 17.1521(17), 17.2221(9), α, β, γ [°] = 90, 112.047(5), 90; Bond lengths [Å] = **Cr**—**S** 2.4426(6), **S**—**Si** 2.0694(8)	[111]
8		[Cp*(S)W{=C(SiMe$_3$)C(=O)OSi(Mes)$_2$S}]; red crystals; Single crystal structure: triclinic, P-1, a, b, c [Å] = 11.566(3), 11.7367(11), 16.033(3), α, β, γ [°] = 71.64(4), 83.42(5), 63.19(4); Bond lengths [Å] = **W**—**S** 2 2.3781(17), **S**—**Si** 2.1343 (18); ^{1}H, ^{13}C{1H}, ^{29}Si{1H} NMR, IR	[112]
9		[Cp*(S)Mo({η^2-S=C(SiMe$_3$)}C(=O)OSi(Mes)$_2$S}]; purple crystals; Single crystal structure: triclinic, P-1, a, b, c [Å] = 8.6148(11), 12.2402(14), 17.782(2), α, β, γ [°] = 72.646(10), 84.658(12), 82.205(12); Bond lengths [Å] = **Mo**—**S** 2.421(2), **S**—**Si** 2.113(3); ^{1}H, ^{13}C{1H}, ^{29}Si{1H} NMR, IR	[112]
10		[Cp*(OC)$_3$W{S=SiMe$_2$(DMAP)}]TFPB·Et$_2$O; yellow crystals; Single crystal structure: triclinic, P-1, a, b, c [Å] = 12.6592(7), 15.4194(10), 17.8895(15), α, β, γ [°] = 85.073(7), 79.161(6), 68.516(6); Bond lengths [Å] = **W**—**S** 2.5464(9), **S**—**Si** 2.0790(14); ^{1}H, ^{13}C{1H}, ^{29}Si{1H} NMR, IR	[114]
11		Cp*(OC)$_3$W(SSiMe$_2$H); dark yellow crystals; Single crystal structure: monoclinic, P2$_1$/c, a, b, c [Å] = 14.940(3), 8.5498(17), 15.367(3), α, β, γ [°] = 90, 110.314(4), 90; Bond lengths [Å] = **W**—**S** 2.5587(11), **S**—**Si** 2.1165(16); ^{1}H, ^{13}C {1H}, ^{29}Si{1H} NMR, IR	[114]

Fig. 13. Molecular structures of the silanethiolate complexes of low valent Mo and Cr(II); except a) H atoms are omitted for clarity: a) [*cyclo*-Cp$_2$Mo(SiMe$_2$SiMe$_2$S)] [107]; b) [Mo$_2$(OAc)$_2$(SSiMe$_3$)$_2$(PEt$_3$)$_2$] [108]; c) [(DME)Cr{SSi(O*t*Bu)$_3$}$_2$] [110]; d) [(3,5-dMepy)$_2$Cr{SSi(O*t*Bu)$_3$}$_2$] [111].

was isolated in the reaction between VCl$_4$ and LiSSiPh$_3$. The latter vanadium(V) complex is intrinsically unstable and slowly decomposed at RT. Both compounds were identified on the basis of NMR spectroscopy and EA (Table VII-2,3) [102]. During the reactions of the V(V) salts with thiolates apart from the formation of the V(V) thiolates, the reduction of vanadium with the formation of relevant disulfides was observed [101,102].

Vanadocene [(MeCp)VS$_2$SiMe$_2$] was synthesized from [(MeCp)$_2$-TiS$_2$SiMe$_2$] during the investigation of the reactivity of the latter. The authors commented that it was possible to prepare the same V(IV) complex by the direct reaction of Li$_2$S$_2$SiMe$_2$ and vanadocene dichloride (Table VII-4) [88].

In 1990 a series of vanadium tri-*tert*-butoxysilanethiolate complexes was prepared by the reaction of chlorovanadium compounds with LiSSi(O*t*Bu)$_3$. All of the complexes, which included one V(III), two V(IV) and six V(V) compounds, were characterized by ^{1}H, ^{51}V NMR and EPR spectroscopy (Table VII-5–8) [103]. Silanethiolate complexes of vanadium(V) were obtained with the use of iminovanadium(V) and oxovanadium(V) *tert*-butanolates and LiSSi-(O*t*Bu)$_3$. The reaction of vanadium(IV) tetrachloride with silanethiols in the presence of triethylammine did not yield V(IV) silanethiolates but instead allowed the isolation of certain amounts of the V(III) silanethiolate [VCl{SSi(O*t*Bu)$_3$}$_2$], which was also directly obtainable from VCl$_3$ and LiSSi(O*t*Bu)$_3$. Silanethiolates of V(IV) were finally achieved with the use of pyridine solvates of oxovanadium dichloride (V=O)Cl$_2$·2Py. Out of nine reported complexes [VO{SSi(O*t*Bu)$_3$}$_2$] was the only one studied by X-ray diffraction. Within the complex the tri-*tert*-butoxysilanethiolate ligand featured its characteristic bidentate mode of coordination and the geometry of the complex was described as trigonal bipyramidal (Fig. 12b). Compared to V(V) silanethiolates the elongation of the V—S bonds together with the substantial shortening of the

S—Si, indicate a more ionic character of the metal-sulfur bond [103,104].

3.3. Group 6 elements

The first described complexes of thiosilyl ligands and group 6 elements are very rare examples of molecular complexes of silathioether ligand. The series of tungsten compounds with the general formula (R$_3$XSPh)W(CO)$_5$ (R = Me, Ph; X = Si. Ge, Sn, Table VIII-1) was synthesized by the irradiation of tungsten hexacarbonyl in THF with a UV lamp and subsequent addition of an appropriate ligand. The crude products were purified on an Al$_2$O$_3$, column and characterized by Raman and IR spectroscopy. The changes in the carbonyl stretching area reflected changes in electron density on sulfur and allowed to establish that among the studied compounds Me$_3$SiSPh is a better π-acid and a better σ-donor than its carbon analogue Me$_3$CSPh. A complicated mechanism involving pπ→dπ S→Si donation as well as contraction of sulfur d-orbitals was suggested, to explain the more effective overlap of silyl sulfide with tungsten *d* orbitals [105]. The research was continued and broadened to include other sulfides *e.g.* Me$_3$SiSPhCl or Me$_3$SiSPhOMe (Table VIII-2). The effects of M—S multiple bonding in organometallic thioethers could be detected by both IR and UV spectroscopy. Such bonding diminished in magnitude from Si through Ge to Sn and had structural significance only for silyl compounds, however even then the M—S bond was easily cleaved [106].

As a part of the reactivity studies on the transition metal complexes with unsaturated silicon ligands the reactions of disilene complex of molybdenum: [Cp$_2$Mo(η^2-Me$_2$Si=SiMe$_2$)] with elemental sulfur and triphenylphosphane sulfide were studied. Whereas the reaction with S$_8$ led to the rapid formation of symmetrical silicide:
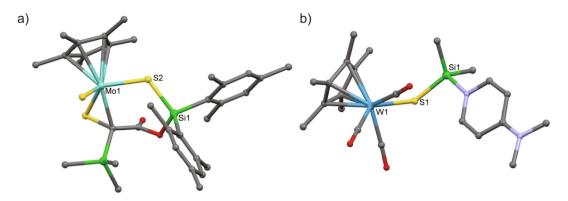
Fig. 14. Molecular structures of the silanethiolate complex of Mo(IV) and silanethione complex of W(II) without hydrogen atoms: a) Cp*(S)Mo[{η^2-S=C(SiMe$_3$)}C(=O)OSi (Mes)$_2$S] [112]; b) [Cp*(OC)$_3$W{S=SiMe$_2$(DMAP)}]TFPB·Et$_2$O - the voluminous TFPB anion and solvating Et$_2$O are omitted [114].

cyclo-Cp$_2$Mo(SiMe$_2$SSiMe$_2$), the reaction with Ph$_3$P=S yielded both the silicide and the unsymmetrical product of insertion of sulfur into the Mo–Si bond: [*cyclo*-Cp$_2$Mo(SiMe$_2$SiMe$_2$S)], which may be considered as silanethiolate complex (Table VIII-3, Fig. 13a). Both products: silicide and silicide/silanethiolate were isolated as crystalline solids [107].

The first "genuine" molybdenum complex with silanethiolate ligands was prepared and characterized structurally by Yu [108]. The author isolated the complex while searching for the possible routes to Mo–S clusters; instead he obtained the first example of a Mo–SSiMe$_3$, ligation. Although excess (Me$_3$Si)$_2$S and phosphane were used to force the full exchange of acetates in the Mo$_2$(OAc)$_4$ substrate, only the partial substitution product was isolated (Table VIII-4, Fig. 13b), which indicates the equilibrium character of the reaction. The obtained complex is binuclear with each metal centre tetrahedrally coordinated by two bridging acetates, triethylphosphane and trimethylsilanothiolate (Fig. 13b) [108].

The studies on the reactivity of a disilene complexes of group 6 metals had a continuation in 1993, in which Berry and co-workers described the reactions of the tungsten analog of the previously described [Cp$_2$Mo(η^2-Me$_2$Si=SiMe$_2$)] [107,109]. Thereby [Cp$_2$W-(η^2-Me$_2$Si=SiMe$_2$)] reacted with chalcogens yielding products of symmetrical insertion of chalcogene into the Si=Si double bond, whereas with phosphane chalcogenides a mixture of symmetrical tungsten silanides and unsymmetrical silanols or silanethiols was produced. The formation of unsymmetrical silanethiols was slightly favoured with smaller phosphane sulfides. The products were not isolated and were identified in the reaction mixtures on the basis of their ^{1}H NMR spectra. (Table VIII-5) [109].

Several chromium silanethiolates were described by our group in 2007–2009 *e.g.* [110,111]. All four compounds are chromium (II) tri-*tert*-butoxysilanethiolates obtained from CrCl$_2$ and NaSSi-(O*t*Bu)$_3$. No complexes were isolated with the use of chromium (III) salts, however, in one case the formation of a mixed-valent Cr(II)/Cr(III) polynuclear complex was observed (unpublished data). The complexes displayed C.N. = 5 with two chelating O,S-alkoxysilanethiolates and one additional O-donor ligand *e.g.* 1,2-dimethoxyethane, which was used as solvent (Fig. 13c, Table VIII-6) [110]. If additional N-ligands were introduced to the solution, weak Cr(II)–O bonds were replaced by Cr(II)–N and complexes with C.N. = 4 were obtained *e.g.* [(3,5-dMepy)$_2$Cr{SSi-(O*t*Bu)$_3$}$_2$] (Fig. 13d, Table VIII-7) [111]. Complexes with C.N. = 5 were described as square pyramidal (though distorted) and complexes with C.N. = 4 were square planar. Long Cr–S distances in the range 2.4080(7) − 2.4426(6) Å largely exceed the sum of the covalent radii (2.25 Å) and are accompanied by short Si–S distances, indicating a more ionic character of the chromium(II) silanethiolates compared to Mo or W derivatives (Table VIII-6,7).

The reactions of the unique (silyl)(silylene) complexes [Cp*-(OC)$_2$M(SiMe$_3$)(=SiMes$_2$)] (M = Mo, W, Fe; R = alkyl, aryl) with sulfur reagents were investigated in 2010 [112]. The reactions led to cyclic carbene complexes and their sulfur adducts in which the silylene fragment remains in the metallacycle core. The conversions start by the addition of a sulfur atom to the M=Si bond to give a M–Si–S three-membered ring complex. At the end the reactions lead to a carbene complex of tungsten and an (η^2-S=C) complex of molybdenum; both complexes exhibit silanethiolate bonds within a cyclic system, in which the silicon atom is bonded to two large, mesityl substituents (Table VIII-8,9, Fig. 14a). The reaction utilized different sulfur sources – elemental sulfur in the case of tungsten, and thiirane for the molybdenum complex, which did not react with sulfur towards any isolable products [112].

The reactions of (silyl)(silylene)tungsten and molybdenum complexes were further studied by DFT calculations. It was concluded that the reactions proceed *via* the formation of the η^2-silanethione-coordinated complexes. Subsequently the C=O bond is gradually weakened and cleaved by the nucleophilic attack of oxygen to the π^* orbital of the silanethione R$_2$Si=S followed by migration of SiH$_3$ to carbon. The metal − ligand interactions were found to be stronger in the tungsten complex than in the molybdenum complex and the insertion of a sulfur atom into the metal − ligand bond takes place more easily in the molybdenum complex in comparison to that in the tungsten one [113]. This explains the different final products described in the experimental paper [112]. The recent paper of the same group of researchers brought the description of the second and third known metal silanethione complexes *i.e.* [Cp*(OC)$_3$W{S=SiR$_2$(DMAP)}]TFPB (R = Me or Ph) [114]. These rare species were obtained in high yields (up to 80%) *via* H$^-$ abstraction from SSiR$_2$H ligand in the silanethiolate complexes: Cp*(OC)$_3$WSSiR$_2$H (R = Me, Ph) by Ph$_3$C$^+$, followed by the coordination of DMAP to the silicon center of the resultant R$_2$Si=S ligand. The starting silanethiolate complexes were prepared by the reactions of Li[Cp*(OC)$_3$WS] with chlorosilanes R$_2$SiHCl. Both silanethiolate and silanothione complexes of tungsten were structurally characterized and showed η^1 coordination of the sulfur ligand as indicated by wide W−S−Si angles (Fig. 14b). The S−Si bond lengths presented in Table VIII in entries 10 and 11 suggested at least partial double bond character in the silanethione complex, while the W−S bonds in the silanethiolato and silanethione complexes are of comparable lengths indicating similar metal − sulfur interactions. Methanolysis of silanethione complex produced another tungsten silanethiolate: [Cp*(OC)$_3$W(SSiPh$_2$OMe)] [114].

3.4. Group 7 elements

Out of the group 7 elements only manganese silyl sulfides have been prepared so far and the research was initiated in our Department.
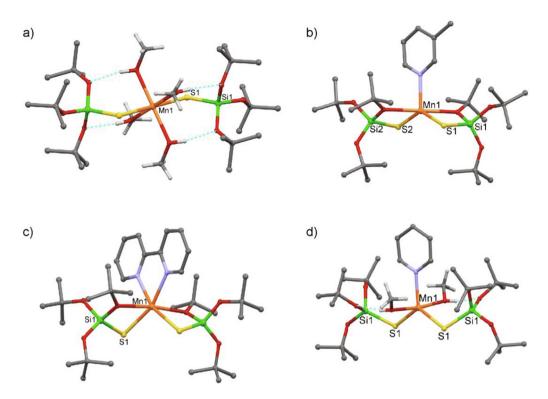
Fig. 15. Molecular structures of the heteroleptic tri-*tert*-butoxysilanethiolate complexes of Mn(II) H atoms of the *t*Bu groups and pyridine ligands are omitted for clarity: a) [(MeOH)₄Mn{SSi(O*t*Bu)₃}₂] [115]; b) [(3-Mepy)Mn{SSi(O*t*Bu)₃}₂] [117]; c) [(2,2′-bipy)Mn{SSi(O*t*Bu)₃}₂] [116]; d) [(MeOH)₂(py)Mn{SSi(O*t*Bu)₃}₂] [117].

Undoubtedly, one of the major applications of silanethiolate ligands in metal complexes is the creation of the metal environments mimicking the binding of metal ions by proteins, which very often contain metal-sulfur linkage. A lot of Zn, Co, and Mn tri-*tert*-butylsilanethiolate complexes were synthesized in search of the system mimicking the structural and spectroscopic properties of the active site of alcohol dehydrogenase and the research on the tri-*tert*-butoxysilanethiolates of manganese(II) was an important part of these studies [22]. Over 10 complexes with different coordination numbers of manganese(II) from 4 up to 6 and different numbers of methanol molecules bonded to manganese – 1, 2 or 4 – were obtained. The selected examples representing different coordination patterns are shown in Fig. 15a-d and Table IX-1–6 [115–119].

A common substrate for the syntheses of all heteroleptic Mn(II) complexes is bis(tri-*tert*-butoxysilanethiolato)tetra(methanol)manganese(II) (Fig. 15a, Table IX-1) prepared by reacting manganese(II) chloride, tri-*tert*-butoxysilanethiol and triethylamine in boiling methanol. Cooling of the reaction mixture led to the formation of the crystalline product in nearly quantitative yield [115]. The coordination of methanol to Mn(II) is stabilized by intramolecular hydrogen bonds between the hydroxyl group of methanol and the alkoxy substituents at silicon (Fig. 15a, Table IX-1). The complex is stable in an inert atmosphere and the stepwise substitution of methanol provided a route to other Mn silanethiolates. These were usually heteroleptic complexes with one or two N-donor ligands, derivatives of imidazole and pyridine. It could be observed that small differences in the structure of the pyridine ligand decided whether methanol remained within the complex or was replaced by the chelating alkoxy groups (Fig. 15b-d, Table IX-2–4) [116,117]. The same was observed for the high-spin Mn(II) silanethiolates with imidazole-based co-ligands as illustrated with the molecular structure of co-crystallizing complexes [(2-MeIm)-(MeOH)Mn{SSi(O*t*Bu)₃}₂] and [(2-MeIm)Mn{SSi(O*t*Bu)₃}₂] in

Fig. 16a and Table IX-5. With imidazole co-ligand tetrahedral [(N-MeIm)₂Mn{SSi(O*t*Bu)₃}₂] was also obtained (Fig. 16b, Table IX-6) [118]. In all structurally characterized alkoxysilanethiolate complexes the Mn–S bonds are very long, while the S–Si bonds are very short, displaying a partially double bond character, which, as mentioned before may indicate the ionic character of the M−S interaction. Apart from structural characterization, thermal properties of manganese tri-*tert*-butoxysilanethiolates were investigated and revealed unusual thermal stability of these complexes [119].

Low-valent manganese carbonyl thiolates were prepared from [(THF)₂NaSS*it*Bu₃] and [Mn(CO)₅Br], which reacted in different molar ratios, different solvents and over different reaction times to yield four different products (Table IX-7–10) [120]. When [Mn-(CO)₅Br] was treated with 1 or 2 equiv of [(THF)₂NaSS*it*Bu₃], the 1:2 substitution product [(OC)₄Mn(μ-SS*it*Bu₃)₂Na(THF)₂] was quickly formed (Fig. 17a, Table IX-7). With an additional 1 equiv of [Mn(CO)₅Br], the dinuclear Mn(I)Mn(II) complex [(OC)₄Mn(μ-SS*it*Bu₃)₂Mn(THF)Br] could be isolated, which in turn became a precursor to the mixed-valent dinuclear manganese silanethiolate complex [(OC)₄Mn(μ-SS*it*Bu₃)₂Mn(THF)SS*it*Bu₃] (Table IX-8, 9). Finally the complex anion [(OC)₃Mn(μ-SS*it*Bu₃)₃MnSS*it*Bu₃]⁻ was synthesized by the reaction of the latter with one additional equivalent of NaSS*it*Bu₃ (Fig. 17b, Table IX-10). This final complex contained a terminal thiolate ligand with a unique linear Mn−S−Si unit, which results from a unique six-electron $\pi_{(p\rightarrow d)}$ donation of supersilyl SS*it*Bu₃⁻ chalcogenolates – in addition to "usual" σ-bonding. The increase in the metal–ligand bond order is certainly accompanied by the significant, by ~ 0.2 Å, shortening of the Mn–S bond (Table IX-10). The authors observed that the formation of such a linear unit could be only effective in the case of sterically hindered residues [120].

The ability of trimethylsilylchalcogenolates to serve as molecular precursors to clusters was utilized in the synthesis of a set of polynuclear manganese (also cobalt) trimethylsilylchalcogenolates

Table IX

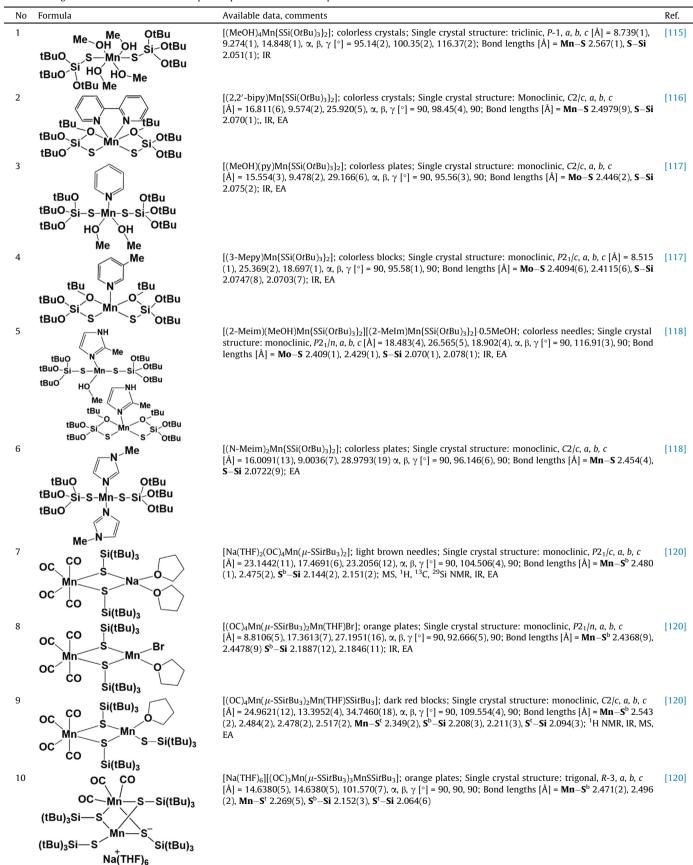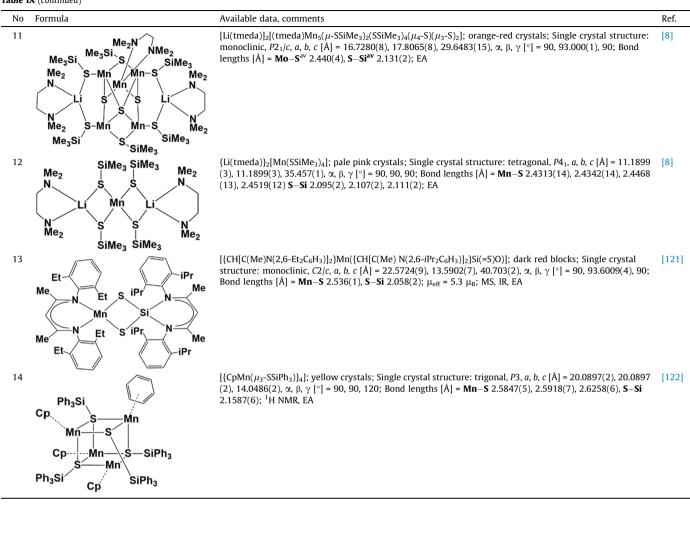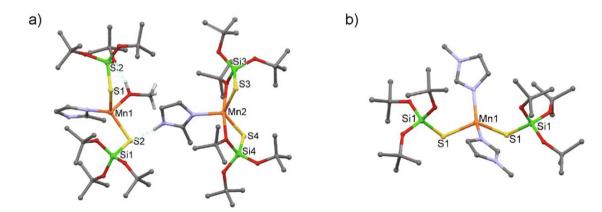Formulas and general characteristics of the Group 7 compounds described in chapter 3.4.

No	Formula	Available data, comments	Ref.
1		[(MeOH)$_4$Mn{SSi(OtBu)$_3$}$_2$]; colorless crystals; Single crystal structure: triclinic, P-1, a, b, c [Å] = 8.739(1), 9.274(1), 14.848(1), α, β, γ [°] = 95.14(2), 100.35(2), 116.37(2); Bond lengths [Å] = **Mn–S** 2.567(1), **S–Si** 2.051(1); IR	[115]
2		[(2,2′-bipy)Mn{SSi(OtBu)$_3$}$_2$]; colorless crystals; Single crystal structure: Monoclinic, $C2/c$, a, b, c [Å] = 16.811(6), 9.574(2), 25.920(5), α, β, γ [°] = 90, 98.45(4), 90; Bond lengths [Å] = **Mn–S** 2.4979(9), **S–Si** 2.070(1);, IR, EA	[116]
3		[(MeOH)(py)Mn{SSi(OtBu)$_3$}$_2$]; colorless plates; Single crystal structure: monoclinic, $C2/c$, a, b, c [Å] = 15.554(3), 9.478(2), 29.166(6), α, β, γ [°] = 90, 95.56(3), 90; Bond lengths [Å] = **Mo–S** 2.446(2), **S–Si** 2.075(2); IR, EA	[117]
4		[(3-Mepy)Mn{SSi(OtBu)$_3$}$_2$]; colorless blocks; Single crystal structure: monoclinic, $P2_1/c$, a, b, c [Å] = 8.515(1), 25.369(2), 18.697(1), α, β, γ [°] = 90, 95.58(1), 90; Bond lengths [Å] = **Mo–S** 2.4094(6), 2.4115(6), **S–Si** 2.0747(8), 2.0703(7); IR, EA	[117]
5		[(2-Meim)(MeOH)Mn{SSi(OtBu)$_3$}$_2$][(2-MeIm)Mn{SSi(OtBu)$_3$}$_2$]·0.5MeOH; colorless needles; Single crystal structure: monoclinic, $P2_1/n$, a, b, c [Å] = 18.483(4), 26.565(5), 18.902(4), α, β, γ [°] = 90, 116.91(3), 90; Bond lengths [Å] = **Mo–S** 2.409(1), 2.429(1), **S–Si** 2.070(1), 2.078(1); IR, EA	[118]
6		[(N-Meim)$_2$Mn{SSi(OtBu)$_3$}$_2$]; colorless plates; Single crystal structure: monoclinic, $C2/c$, a, b, c [Å] = 16.0091(13), 9.0036(7), 28.9793(19) α, β, γ [°] = 90, 96.146(6), 90; Bond lengths [Å] = **Mn–S** 2.454(4), **S–Si** 2.0722(9); EA	[118]
7		[Na(THF)$_2$(OC)$_4$Mn(μ-SSitBu$_3$)$_2$]; light brown needles; Single crystal structure: monoclinic, $P2_1/c$, a, b, c [Å] = 23.1442(11), 17.4691(6), 23.2056(12), α, β, γ [°] = 90, 104.506(4), 90; Bond lengths [Å] = **Mn–S**^{b} 2.480(1), 2.475(2), **S**^{b}**–Si** 2.144(2), 2.151(2); MS, ^{1}H, ^{13}C, ^{29}Si NMR, IR, EA	[120]
8		[(OC)$_4$Mn(μ-SSitBu$_3$)$_2$Mn(THF)Br]; orange plates; Single crystal structure: monoclinic, $P2_1/n$, a, b, c [Å] = 8.8106(5), 17.3613(7), 27.1951(16), α, β, γ [°] = 90, 92.666(5), 90; Bond lengths [Å] = **Mn–S**^{b} 2.4368(9), 2.4478(9) **S**^{b}**–Si** 2.1887(12), 2.1846(11); IR, EA	[120]
9		[(OC)$_4$Mn(μ-SSitBu$_3$)$_2$Mn(THF)SSitBu$_3$]; dark red blocks; Single crystal structure: monoclinic, $C2/c$, a, b, c [Å] = 24.9621(12), 13.3952(4), 34.7460(18), α, β, γ [°] = 90, 109.554(4), 90; Bond lengths [Å] = **Mn–S**^{b} 2.543(2), 2.484(2), 2.478(2), 2.517(2), **Mn–S**^{t} 2.349(2), **S**^{b}**–Si** 2.208(3), 2.211(3), **S**^{t}**–Si** 2.094(3); ^{1}H NMR, IR, MS, EA	[120]
10		[Na(THF)$_6$][(OC)$_3$Mn(μ-SSitBu$_3$)$_3$MnSSitBu$_3$]; orange plates; Single crystal structure: trigonal, R-3, a, b, c [Å] = 14.6380(5), 14.6380(5), 101.570(7), α, β, γ [°] = 90, 90, 90; Bond lengths [Å] = **Mn–S**^{b} 2.471(2), 2.496(2), **Mn–S**^{t} 2.269(5), **S**^{b}**–Si** 2.152(3), **S**^{t}**–Si** 2.064(6)	[120]

Table IX (*continued*)

No	Formula	Available data, comments	Ref.
11		[Li(tmeda)]$_2$[(tmeda)Mn$_5$(μ-SSiMe$_3$)$_2$(SSiMe$_3$)$_4$(μ_4-S)(μ_3-S)$_2$]; orange-red crystals; Single crystal structure: monoclinic, $P2_1/c$, a, b, c [Å] = 16.7280(8), 17.8065(8), 29.6483(15), α, β, γ [°] = 90, 93.000(1), 90; Bond lengths [Å] = **Mo–S**^{av} 2.440(4), **S–Si**^{av} 2.131(2); EA	[8]
12		{Li(tmeda)}$_2$[Mn(SSiMe$_3$)$_4$]; pale pink crystals; Single crystal structure: tetragonal, $P4_1$, a, b, c [Å] = 11.1899 (3), 11.1899(3), 35.457(1), α, β, γ [°] = 90, 90, 90; Bond lengths [Å] = **Mn–S** 2.4313(14), 2.4342(14), 2.4468 (13), 2.4519(12) **S–Si** 2.095(2), 2.107(2), 2.111(2); EA	[8]
13		[{CH[C(Me)N(2,6-Et$_2$C$_6$H$_3$)]$_2$}Mn({CH[C(Me) N(2,6-iPr$_2$C$_6$H$_3$-S)]$_2$}Si(=S)O)]; dark red blocks; Single crystal structure: monoclinic, C2/c, a, b, c [Å] = 22.5724(9), 13.5902(7), 40.703(2), α, β, γ [°] = 90, 93.6009(4), 90; Bond lengths [Å] = **Mn–S** 2.536(1), **S–Si** 2.058(2); μ_{eff} = 5.3 μ_B; MS, IR, EA	[121]
14		[{CpMn(μ_3-SSiPh$_3$)}$_4$]; yellow crystals; Single crystal structure: trigonal, $P3$, a, b, c [Å] = 20.0897(2), 20.0897 (2), 14.0486(2), α, β, γ [°] = 90, 90, 120; Bond lengths [Å] = **Mn–S** 2.5847(5), 2.5918(7), 2.6258(6), **S–Si** 2.1587(6); ^{1}H NMR, EA	[122]

Fig. 16. Molecular structures of the heteroleptic tri-*tert*-butoxysilanethiolate complexes of Mn(II); H atoms of the *t*Bu groups and the imidazole ligands are omitted: a) [(2-Meim)(MeOH)Mn{SSi(O*t*Bu)$_3$}$_2$] [(2-MeIm)Mn{SSi(O*t*Bu)$_3$}$_2$]·0.5MeOH [118]; b) [(N-Meim)$_2$Mn{SSi(O*t*Bu)$_3$}$_2$] [118].

stabilized with 3,5-lutidine and tmeda ligands. The reaction of tetrameric (tmeda)MnCl$_2$ with two equivalents of LiESiMe$_3$ led to the isolation of two pentanuclear manganese chalcogenolate complexes [Li(tmeda)]$_2$[(tmeda)Mn$_5$(μ-ESiMe$_3$)$_2$-(ESiMe$_3$)$_4$(μ_4-E)(μ_3-E)$_2$] (E = S, Se). Both complexes exhibit an Mn$_5$E$_3$ core, with five

manganese atoms linked *via* bridging chalcogenide ligands (for E = S, Fig. 18a, Table IX-11). The addition of four equivalents of LiSSiMe$_3$, resulted in the formation of the mononuclear, tetrahedral complex [Li(tmeda)]$_2$[Mn(SSiMe$_3$)$_4$] as the sole product (Fig. 18b, Table IX-12). The studies on the magnetic properties of the Mn
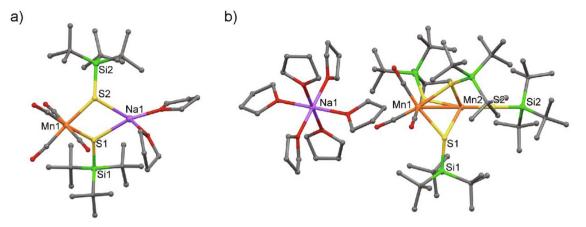
Fig. 17. Molecular structures of the heteroleptic tri-*tert*-butylsilanethiolate complexes of Mn(I)/(II) without hydrogen atoms: a) [Na(THF)$_2$(OC)$_4$Mn(μ-SSitBu$_3$)$_2$] [120]; b) [Na(THF)$_6$][(OC)$_3$Mn(μ-SSitBu$_3$)$_3$MnSSitBu$_3$] [120].
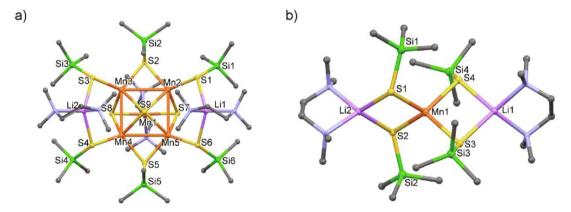
Fig. 18. Molecular structures of the trimethylsilanethiolate/sulfide cluster of Mn(II) and anionic trimethylsilanethiolate complex of Mn(II); H atoms are omitted: a) [Li(tmeda)]$_2$[(tmeda)Mn$_5$(μ-SSiMe$_3$)$_2$(SSiMe$_3$)$_4$(μ_4-S)(μ_3-S)$_2$] [8]; b) {Li(tmeda)}$_2$[Mn(SSiMe$_3$)$_4$] [8].
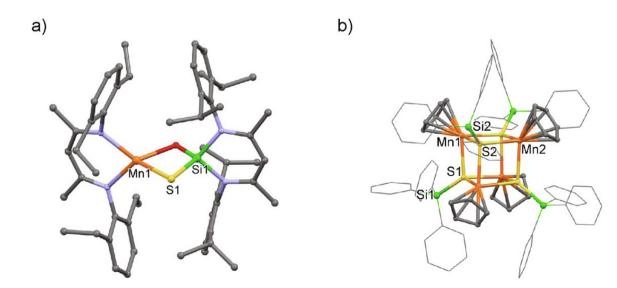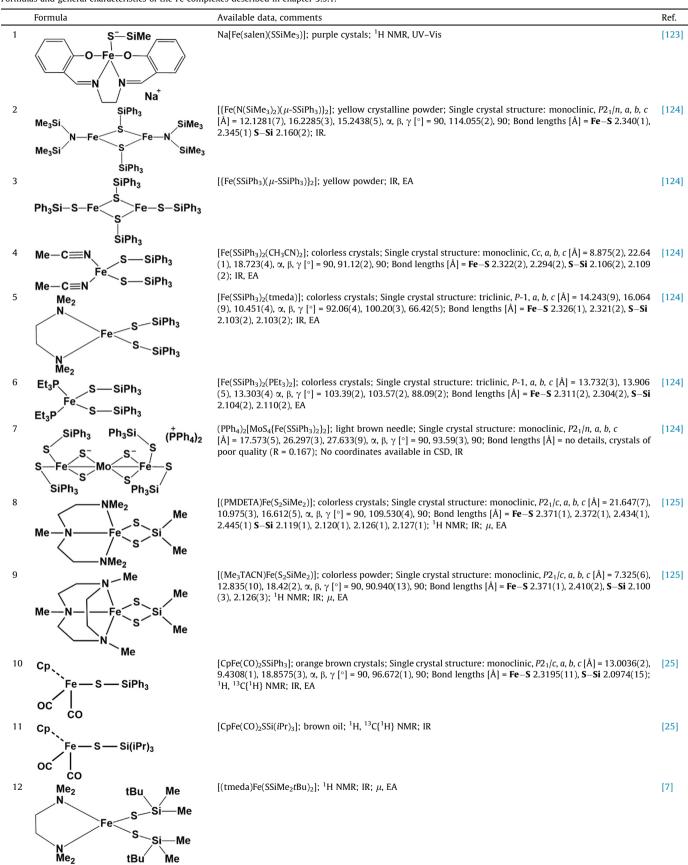
Fig. 19. Molecular structures of the first manganese(II) silathiocarboxylate and triphenylsilanethiolato/Cp supported Mn(II) cubane; H atoms are omitted for clarity: a) [{CH[C(Me)N(2,6-Et$_2$C$_6$H$_3$)]$_2$}Mn({CH[C(Me)N(2,6-^{i}Pr$_2$C$_6$H$_3$)]$_2$}Si(=S)O)] [121]; b) [{CpMn(μ_3-SSiPh$_3$)}$_4$] [122].

Table X

Formulas and general characteristics of the Fe complexes described in chapter 3.5.1.

	Formula	Available data, comments	Ref.
1		Na[Fe(salen)(SSiMe₃)]; purple cystals; ^{1}H NMR, UV–Vis	[123]
2		[{Fe(N(SiMe₃)₂)(μ-SSiPh₃)}₂]; yellow crystalline powder; Single crystal structure: monoclinic, $P2_1/n$, a, b, c [Å] = 12.1281(7), 16.2285(3), 15.2438(5), α, β, γ [°] = 90, 114.055(2), 90; Bond lengths [Å] = **Fe**−**S** 2.340(1), 2.345(1) **S**−**Si** 2.160(2); IR.	[124]
3		[{Fe(SSiPh₃)(μ-SSiPh₃)}₂]; yellow powder; IR, EA	[124]
4		[Fe(SSiPh₃)₂(CH₃CN)₂]; colorless crystals; Single crystal structure: monoclinic, Cc, a, b, c [Å] = 8.875(2), 22.64 (1), 18.723(4), α, β, γ [°] = 90, 91.12(2), 90; Bond lengths [Å] = **Fe**−**S** 2.322(2), 2.294(2), **S**−**Si** 2.106(2), 2.109 (2); IR, EA	[124]
5		[Fe(SSiPh₃)₂(tmeda)]; colorless crystals; Single crystal structure: triclinic, P-1, a, b, c [Å] = 14.243(9), 16.064 (9), 10.451(4), α, β, γ [°] = 92.06(4), 100.20(3), 66.42(5); Bond lengths [Å] = **Fe**−**S** 2.326(1), 2.321(2), **S**−**Si** 2.103(2), 2.103(2); IR, EA	[124]
6		[Fe(SSiPh₃)₂(PEt₃)₂]; colorless crystals; Single crystal structure: triclinic, P-1, a, b, c [Å] = 13.732(3), 13.906 (5), 13.303(4) α, β, γ [°] = 103.39(2), 103.57(2), 88.09(2); Bond lengths [Å] = **Fe**−**S** 2.311(2), 2.304(2), **S**−**Si** 2.104(2), 2.110(2), EA	[124]
7		(PPh₄)₂[MoS₄{Fe(SSiPh₃)₂}₂]; light brown needle; Single crystal structure: monoclinic, $P2_1/n$, a, b, c [Å] = 17.573(5), 26.297(3), 27.633(9), α, β, γ [°] = 90, 93.59(3), 90; Bond lengths [Å] = no details, crystals of poor quality (R = 0.167); No coordinates available in CSD, IR	[124]
8		[(PMDETA)Fe(S₂SiMe₂)]; colorless crystals; Single crystal structure: monoclinic, $P2_1/c$, a, b, c [Å] = 21.647(7), 10.975(3), 16.612(5), α, β, γ [°] = 90, 109.530(4), 90; Bond lengths [Å] = **Fe**−**S** 2.371(1), 2.372(1), 2.434(1), 2.445(1) **S**−**Si** 2.119(1), 2.120(1), 2.126(1), 2.127(1); ^{1}H NMR; IR; μ, EA	[125]
9		[(Me₃TACN)Fe(S₂SiMe₂)]; colorless powder; Single crystal structure: monoclinic, $P2_1/c$, a, b, c [Å] = 7.325(6), 12.835(10), 18.42(2), α, β, γ [°] = 90, 90.940(13), 90; Bond lengths [Å] = **Fe**−**S** 2.371(1), 2.410(2), **S**−**Si** 2.100 (3), 2.126(3); ^{1}H NMR; IR; μ, EA	[125]
10		[CpFe(CO)₂SSiPh₃]; orange brown crystals; Single crystal structure: monoclinic, $P2_1/c$, a, b, c [Å] = 13.0036(2), 9.4308(1), 18.8557(3), α, β, γ [°] = 90, 96.672(1), 90; Bond lengths [Å] = **Fe**−**S** 2.3195(11), **S**−**Si** 2.0974(15); ^{1}H, ^{13}C{^{1}H} NMR; IR, EA	[25]
11		[CpFe(CO)₂SSi(iPr)₃]; brown oil; ^{1}H, ^{13}C{^{1}H} NMR; IR	[25]
12		[(tmeda)Fe(SSiMe₂tBu)₂]; ^{1}H NMR; IR; μ, EA	[7]

(continued on next page)

Table X (*continued*)

	Formula	Available data, comments	Ref.
13		[{CH[C(Me)N(2,6-tBu$_2$C$_6$H$_3$)]$_2$}FeSSiMe$_3$]; dark red block; Single crystal structure: monoclinic, $P2_1/n$, a, b, c [Å] = 15.4030(8), 26.3684(15), 19.7988(11), α, β, γ [°] = 90, 97,3040(10), 90; Bond lengths [Å] = **Fe − S** 2.2487 (12), 2.2460(12) **S−Si** 2.1100(16), 2.0991(16); ^{1}H NMR, μ	[128]
14		[Fe(SSitBu$_3$)(μ-SSitBu$_3$)]$_2$; orange blocks; Single crystal structure: orthorhombic, $Pbcn$, a, b, c [Å] = 19.382(4), 17.872(4), 17.842(4), α, β, γ [°] = 90, 90, 90; Bond lengths [Å] = **Fe−S^b** 2.323(2), 2.333(2), **Fe−S^t** 2.218(2), **S^b−Si** 2.186(3), **S^t−Si** 2.137(2) ^{1}H NMR, EA	[129]
15		[(THF)$_2$Fe(SSitBu$_3$)$_2$]; Single crystal structure: triclinic, P-1, a, b, c [Å] = 12.897(2), 13.2170(10), 13.2200(10), α, β, γ [°] = 98.100(10), 104.320(10), 109.860(10); Bond lengths [Å] = **Fe−S** 2.271(2), 2.289(2), **S−Si** 2.124(2), 2.129(2); ^{1}H NMR, EA	[129]
16		[Br$_2$Fe(μ-SSitBu$_3$)$_2$FeBr(THF)][Na(THF)$_4$]; yellow solid; Single crystal structure: monoclinic, $P2_1/c$, a, b, c [Å] = 24.363(2), 13.3296(10), 17.8294(10), α, β, γ [°] = 90, 90.000(2), 90; Bond lengths [Å] = **Fe−S** 2.346(3), 2.348(3), 2.381(3), 2.387(3), **S−Si** 2.141(4), 2.143(4); μ; ^{1}H NMR; IR, EA	[129]
17		[{(THF)FeI(μ-SSitBu$_3$)}$_2$]; yellow solid; Single crystal structure: orthorhombic, $Pna2_1$, a, b, c [Å] = 31.884(6), 9.0048(16), 15.318(3), α, β, γ [°] = 90, 90, 90; Bond lengths [Å] = **Fe−S** 2.351(3), 2.356(3), 2.359(3), 2.374(3), **S−Si** 2.162(4), 2.167(4); μ; ^{1}H NMR; IR, EA	[129]
18	[(THF)Fe(SSitBu$_3$)$_3$]	[(THF)Fe(SSitBu$_3$)$_3$]; purple crystals; ^{1}H NMR	[129]
19		[Cp(CO)$_2$FeSSitBu$_3$]; orange plates; Single crystal structure: triclinic, P–1, a, b, c [Å] = 8.671(1), 8.707(1), 16.215(2), α, β, γ [°] = 86.25(1), 88.78(1), 62.36(1); Bond lengths [Å] = **Fe−S** 2.345(2), **S−Si** 2.147(2); ^{1}H, ^{13}C {1H}, ^{29}Si{^{1}H} NMR, IR	[130]
20		[{Fe(CO)$_3$(μ-SSitBu$_3$)}$_2$]; dark red needles; Single crystal structure: monoclinic, $P2_1/n$, a, b, c [Å] = 8.9399(6), 27.2788(14), 15.4510(9), α, β, γ [°] = 90, 90.427(5), 90; Bond lengths [Å] = **Fe−S** 2.303(2), 2.317(2), 2.318(2), 2.322(2), **S−Si** 2.210(2), 2.231(2); ^{1}H, ^{13}C{^{1}H}, ^{29}Si{1H} NMR, IR	[48]
21		[Cp(CO)Fe(CHNMe$_2$)(SSiPh$_3$)]; dark red powder; Single crystal structure: monoclinic, $P2_1/c$, a, b, c [Å] = 16.037(2), 9.3525(11), 16.402(3), α, β, γ [°] = 90, 101.572(3), 90; Bond lengths [Å] = **Fe−S** 2.3371(3), **S−Si** 2.1016(5); ^{1}H, ^{13}C{^{1}H}, ^{29}Si NMR, IR	[131]
22		[Fe(SSiiPr$_3$)(TPP)]; dark red powder; Single crystal structure: triclinic, P-1, a, b, c [Å] = 11.113(3), 12.600(3) 16.927(4), α, β, γ [°] = 80.693(11), 85.049(12), 77.332(11); Bond lengths [Å] = **Fe−S** 2.269(1), **S−Si** 2.152(1); ^{1}H NMR, IR, EPR, EA	[24]
23		[(μ-O$_2$){(Me$_3$TACN)Fe(S$_2$SiMe$_2$)}$_2$]; Mössbauer; ^{1}H NMR; IR; Raman; UV–Vis; X-ray absorption	[126]

Table X (continued)

Formula	Available data, comments	Ref.
24	[Fe(=O)(Me$_3$TACN)(S$_2$SiMe$_2$)]; Mössbauer; ^{1}H NMR; IR; Raman; UV–Vis; X-ray absorption	[126]

Fig. 20. Molecular structures of the iron(II) silanothiolates (Part I) without hydrogen atoms: a) [{Fe(N(SiMe$_3$)$_2$)(μ-SSiPh$_3$)}$_2$] [124]; b) [(4-tBuC$_5$H$_4$N)$_2$Fe(SSiPh$_3$)$_2$] [124]; c) [(Me$_3$TACN)Fe(S$_2$SiMe$_2$)] [125].

clusters suggested that the compounds could be precursors for the synthesis of ternary clusters manifesting magnetic as well as semiconducting properties [8].

Divalent manganese complex [{CH[C(Me)N(2,6-Et$_2$C$_6$H$_3$)]$_2$}Mn ({CH[C(Me)N(2,6-iPr$_2$C$_6$H$_3$)]$_2$}Si(=S)O)] (Fig. 19a) supported by silathiocarboxylate (also germathiocarboxylate) was obtained in high yield from the reaction of the DMAP adduct of silathiocarboxylic acid {CH[C(Me)N(2,6-iPr$_2$C$_6$H$_3$)]$_2$}Si(=S)OH with *nacnac* manganese hydride: {CH[C(Me)N(2,6-Et$_2$C$_6$H$_3$)]$_2$}MnH. The synthesis of the latter was also reported from the corresponding manganese bromide. The S=Si bonds within the Mn(II) complex are stabilized by S→Mn and N→Si dative interaction as well as p-electron delocalization of the X(=S)O moieties (X = Si, Ge). The bond lengths clearly indicated the double bond character of the S=Si bond (Table IX-13) [121].

Although many transition metal compounds containing [M$_4$S$_4$] structural units have been studied in detail, crystallographically characterized examples of manganese–sulfur cubanes remain exceptionally rare. The singular example of thiolate-bridged Mn (II) cubane [{CpMn(μ_3-SSiPh$_3$)}$_4$] was prepared *via* two different routes: either by deprotonation of Ph$_3$SiSH with manganocene Cp$_2$-Mn, or by transmetallation of manganocene with LiSSiPh$_3$. The Mn (II) centres in the compound were reported to be antiferromagnetically coupled, with $J = -3.0$ cm^{-1} (Fig. 19b, Table IX-14) [122].

3.5. Group 8 elements

Since the number of known transition metal complexes for a given group of the periodic table reflects the Irving-Williams series of their stabilities, in other words is constantly growing towards the late transition metals, we decided to split the description of group 8 silanethiolates into several subsections. Thus we will separately describe:

- mononuclear/binuclear silanethiolates of iron,
- cubanes and less typical supramolecular iron species and finally

- ruthenium silanethiolates.

3.5.1. Iron silanethiolates of low nuclearity

The first silanethiolate of Fe(II) was mentioned in 1988 as one of a series of [Fe(II)(N,N'-bis(salicylideneamino)ethanato)L]$^-$ or [Fe-(salen)L]$^-$ complexes. The heterogeneous reaction of the insoluble, oligomeric Fe(II) complex [Fe(salen)] with a variety of ligands L$^-$, including SSiMe$_3^-$, in acetonitrile, afforded the purplish complexes [Fe(salen)L]$^-$, obtained as sodium or Et$_4$N$^+$ salts (see Table X-1 for L$^-$ = SSiMe$_3^-$). All complexes contained high-spin Fe(II) in a square-pyramidal coordination mode with an axial ligand L, exhibit isotropically shifted ^{1}H NMR spectra of good resolution and can be reversibly oxidized electrochemically to [Fe(salen)L]. It was established that the iron(III) thiolate complexes – including silanethiolate - autoreduced with the formation of [Fe(salen)] along with the respective disulfide and were too unstable to be isolated with the exception of the Fe(III) complex [Fe(salen)(SPh)] [123].

Several years passed before further, systematic studies on iron silanethiolates were undertaken. Dinuclear iron(II) silanethiolates [{Fe(N(SiMe$_3$)$_2$)(μ-SSiPh$_3$)}$_2$] and [{Fe(SSiPh$_3$)(μ-SSiPh$_3$)}$_2$] were obtained as, insoluble, yellow, air-sensitive powders in the reactions of iron(II) bis(trimetylsilyl)amide [{Fe(N(SiMe$_3$)$_2$)(μ-N-(SiMe$_3$)$_2$}$_2$] with 1 or 2 equivalents of bulky silanethiol Ph$_3$SiSH in hexane (Table X-2,3). Each of the two Fe(II) centers in [{Fe(N-(SiMe$_3$)$_2$)(μ-SSiPh$_3$)}$_2$] was bridged by two silanethiolate ligands, and bonded to one terminal amide ligand; in this way the Fe atoms gain a trigonal planar geometry, where the sum of the angles at the Fe atom is 360.0° (Fig. 20a). The average Fe−S bond distance amounts to 2.343 Å (Table X-2). The authors did not manage to grow single crystals of [{Fe(SSiPh$_3$)(μ-SSiPh$_3$)}$_2$] suitable for X-ray study, however, the homoleptic complex reacts with various Lewis bases to yield mononuclear adducts [Fe(SSiPh$_3$)$_2$(L)$_2$] L = MeCN, 4-tBuC$_5$H$_4$N, PEt$_3$, (L)$_2$ = tmeda, which could be purified and characterized. The mononuclear complexes had a common, slightly distorted tetrahedral geometry at the Fe atom, which was coordinated by two silanethiolate sulfur atoms and two N or P atoms
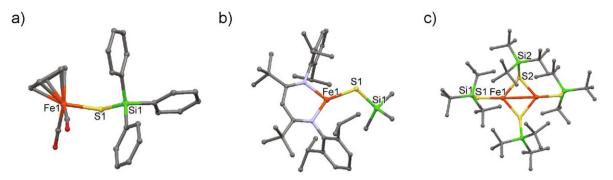
Fig. 21. Molecular structures of the iron(II) silanothiolates (Part II) without hydrogen atoms: a) [CpFe(CO)$_2$SSiPh$_3$] [25]; b) [{CH[C(Me)N(2,6-tBu$_2$C$_6$H$_3$)]$_2$}FeSSiMe$_3$] [128]; c) [{Fe(SSitBu$_3$)(μ-SSitBu$_3$)}$_2$] [129].

of the basic co-ligand. Selected examples are presented in Fig. 20b and in Table X-4–6. The tetrahedral complexes were unstable in solution and degraded to unidentified products, which prompted the authors to investigate their reactivity with (PPh$_4$)$_2$[MoS$_4$], (NEt$_4$)$_2$[FeCl$_4$], and [Cu(CH$_3$CN)$_4$](PF$_6$). In the reaction of [Fe(SSiPh$_3$)$_2$(MeCN)$_2$] with (PPh$_4$)$_2$[MoS$_4$] the trinuclear complex (PPh$_4$)$_2$[MoS$_4${Fe(SSiPh$_3$)$_2$}$_2$] was isolated, featuring a linear Fe—Mo—Fe unit where the two iron atoms are tetrahedrally coordinated by two triphenylsilanethiolato ligands and two sulfur atoms of the MoS$_4$ unit (Table X-7). The reaction with (NEt$_4$)$_2$-[FeCl$_4$] resulted in the redistribution of ligands and formation of colorless dinuclear chlorido/triphenylsilanethiolato complex, (NEt$_4$)$_2$[Fe$_2$(SSiPh$_3$)$_2$Cl$_4$]. Finally the reaction of [(MeCN)$_2$Fe-(SSiPh$_3$)$_2$] with [Cu(MeCN)$_4$](PF$_6$) led to the transfer of ligands and formation of a cyclic, tetranuclear copper(I) complex [{Cu(μ-SSiPh$_3$)}$_4$] [124].

The research on iron silanethiolates was continued in 2003 with the use of a different precursor of the silanethiolate ligand [125]. Treatment of Fe(OAc)$_2$ with cyclo-trisilathiane (SSiMe$_2$)$_3$ in the presence of multidonor Lewis bases resulted in the formation of [(PMDETA)Fe(S$_2$SiMe$_2$)] and [(Me$_3$TACN)Fe(S$_2$SiMe$_2$)] (Me$_3$TACN = 1,4,7-trimethyl-1,4,7-triazacyclononane). The yields are reproducible on condition that the metal acetates are treated with triamines before the addition of the hexane solution of cyclotrisilathiane. These iron(II) silanedithiolato complexes were air- and moisture-sensitive, but thermally stable. Magnetic moment measurements yielded a value of 5.2 μB for both of the compounds, typical for high-spin d^6 iron(II) and greater than the spin-only value for four unpaired electrons (4.90 μB). The complexes featured C.N. = 5 and the geometry imposed by the steric requirements of the multidentate ligands (Fig. 20c, Table X-8,9) [125]. The same group of researchers described one more mononuclear, tetrahedral Fe(II) silanethiolate [(tmeda)Fe(SSiMe$_2$$t$Bu)$_2$] (Table X-12) obtained in high yield as a result of the reaction of [(MeCN)$_2$Fe(CF$_3$SO$_3$)$_2$] with [(tmeda)LiSSiMe$_2$$t$Bu]$_2$ in acetonitrile.

Interestingly, the analogous reactions with LiSSiMe$_3$ in the presence of tmeda were not straightforward. Attempts to isolate the trimethylsilanethiolato congener of [(tmeda)Fe(SSiMe$_2$$t$Bu)$_2$] were not successful [7]. In 2019 one of these complexes - [(Me$_3$TACN)Fe-(S$_2$SiMe$_2$)] - was reacted with O$_2$ to generate a peroxo(diiron(III)) species [(μ-O$_2$){(Me$_3$TACN)Fe(S$_2$SiMe$_2$)}$_2$] - a unique example of a thiolate ligated Fe/O$_2$ adduct, which was characterized by UV−Vis, Mössbauer, Resonance Raman, and X-ray absorption spectroscopy (Table X-23) [126]. The O−O bond in [Fe$_2$(O$_2$)(Me$_3$TACN)$_2$(S$_2$-SiMe$_2$)$_2$] can be cleaved either photochemically or thermally to give the Fe(IV)=O species [Fe(=O)(Me$_3$TACN)(S$_2$SiMe$_2$)] (Table X-24). The study showed that mechanisms of O−O bond homolysis producing high-valent metal−oxo complexes could be feasible for O$_2$ activation by nonheme iron centers. It also proved that metal-bound, reactive oxygen species could be supported by thiolate ligation, and the Fe/O$_2$ intermediates did not trigger the immediate oxidation of sulfur [126].

Alkali metal salts of silanethiols: LiSSiPh$_3$ and NaSSiiPr$_3$ were utilized to prepare mononuclear iron silanethiolato complexes of the type [Cp(CO)$_2$FeSSiR$_3$] (R = Ph, iPr) (Table X-10,11). Complex [CpFe(CO)$_2$SSiPh$_3$] (Fig. 21a, Table X-10) was prone to hydrolysis of the S−Si bond with the probable formation of [CpFe(CO)$_2$SH] before further degradation [25]. It was suggested that the reaction route is similar to that of [CpRu(PPh$_3$)$_2$SSiPh$_3$] which yielded [CpRu-(PPh$_3$)$_2$SH] as will be also mentioned later in chapter 3.5.3 [25,127]. Since the intention of the authors was to investigate the insertion of SO$_2$ into the S−Si bond, the reaction of [CpFe(CO)$_2$SSiPh$_3$] with sulfur dioxide was investigated in details. Contrary to ruthenium silanethiolato complexes which instantly and quantitatively gave the corresponding O-silyl thiosulfito complexes [127] the solution of [CpFe(CO)$_2$SSiPh$_3$] in benzene d_6 reacted slowly with SO$_2$ with the complete and irreversible conversion into a single product, CpFe(CO)$_2$SS(O)OSiPh$_3$. The product was identified by a comparison of its spectroscopic features with the relevant Ru complex [25].
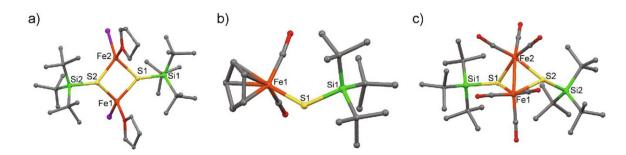
Fig. 22. Molecular structures of the iron(II) silanothiolates (Part III) without hydrogen atoms: a) [{(THF)FeI(μ-SSitBu$_3$)}$_2$] [129]; b) [Cp(CO)$_2$FeSSitBu$_3$] [130]; c) [{Fe(CO)$_3$(μ-SSitBu$_3$)}$_2$] [48].
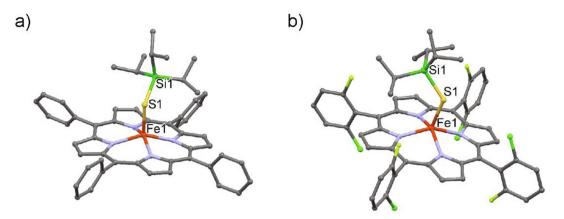
Fig. 23. Molecular structures of iron(III) silanethiolates without hydrogen atoms: a) [Fe(SS*ii*Pr$_3$)(TPP)] [24]; b) [Fe(SS*ii*Pr$_3$)(2,6-F,Cl-TPP)] [133].

Unprecedented mononuclear, three-coordinate iron(II) silanethiolate was reported as a part of a research on the equally exceptional three- and four-coordinate iron(II) fluorides that were isolated with the use of bulky β-diketiminate ligands. The Fe−F bond in these fluoride complexes was short, and they were thermally stable, however, with appropriate fluoride acceptors these compounds became reactive. Silyl compounds Me$_3$SiSSiMe$_3$, Me$_3$-SiCCSiMe$_3$, and Et$_3$SiH, which belong to "very appropriate" fluoride acceptors, reacted with the fluoride complexes of Fe(II) to yield new silanethiolate, acetylide and hydride complexes. In this way the trimethylsilanethiolate complex [{CH[C(Me)N(2,6-*t*Bu$_2$C$_6$H$_3$)]$_2$}-FeSSiMe$_3$] was isolated in 86% yield (Table X-13, Fig. 21b). Within the complex and exceptionally short iron-sulfur bond is realized (Table X-13) [128].
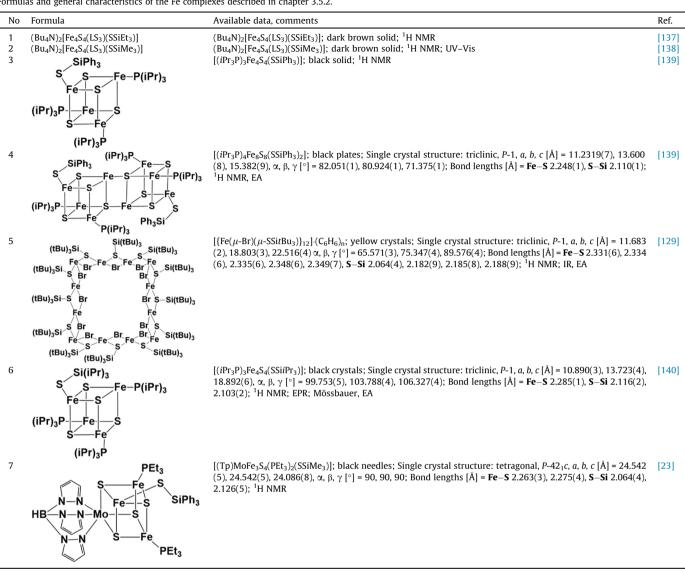
The X-ray molecular structure of the homoleptic silanethiolato iron(II) dimer that had not been previously achieved by Komuro and his co-workers [124] was successfully established for the iron(II) complex of the *t*Bu$_3$SiS$^-$ ligand [{Fe(SS*t*Bu$_3$)(μ-SS*t*Bu$_3$)}$_2$] (Fig. 21c, Table X-14) [129]. The dimer formed as an orange crystalline solid in the reaction of [{((Me$_3$Si)$_2$)N)Fe(μ-N(SiMe$_3$)$_2$)}$_2$] (as in [124]) and the tri-*tert*-butylsilanethiol in benzene. The dissolution of the dimer in THF allowed the formation of the mononuclear iron(II) complex [(THF)$_2$Fe(SS*t*Bu$_3$)$_2$] (Table X-15). In both: homoligand dimer and heteroligand mononuclear complex very short terminal Fe−S^t bonds were observed as indicated in Table X-14,15 [129].

The same authors described the use of iron(II) halides and sodium tri-*tert*-butylsilanethiolate in the synthesis of several heteroligand iron(II) dimers. The examples of dimeric complexes, which consisted of two or three tri-*tert*-butylsilanethiolate ligands and three or two coordinated halide anions, are illustrated in Fig. 22a and in Table X-16,17. These dimers were used to assemble supramolecular wheels, which will be described in chapter 3.5.2 [129]. Finally the unique, entirely unstable Fe(III) tri-*tert*-butylsilanethiolate was mentioned to be produced in the form of red crystals in the reaction of Fe(III) chloride and *t*Bu$_3$SiSNa in THF (Table X-18) [129].

In 2007 the experimental and theoretical study of the properties of two series of isoelectronic ligands including PPh$_2$Me, PPh$_2$-BH$_3^-$, SiPh$_2$Me$^-$, SP*t*Bu$_3$, SP*t*Bu$_2$BH$_3^-$, and SS*t*Bu$_3^-$ was undertaken. The X-ray crystal structure determinations of Fe−CO and C−O bond lengths within the relevant iron(II) complexes as well as NMR and IR investigations of the corresponding [CpFe(CO)$_2$]$^+$ led to the conclusion that, with respect to electron donor strength, silyl ligands proved to be the strongest donors. Complex [Cp(CO)$_2$FeSS*t*Bu$_3$] investigated as one of the seventeen compounds of this systematic study was synthesized by reacting [(THF)$_2$NaSS*t*Bu$_3$] with [Cp-

(CO)$_2$(THF)Fe]BF$_4$ in dichloromethane with over 90% yield (Fig. 22b, Table X-19) [130]. The structurally comparable, carbene complex [Cp(CO)Fe(CHNMe$_2$)(SSiPh$_3$)] was isolated and characterized as an intermediate of the desulfurization of N,N-dimethylthioformamide (Me$_2$NCHS) by hydrosilane. The reaction was achieved under photoirradiation in the presence of a methyl iron complex [Cp(CO)$_2$FeMe] and the reaction sequence anticipated the migration of silyl from Fe to S of thioformamide. Within this intermediate, the silyl group is transiently bonded to sulfur before the evolution of (R$_3$Si)$_2$S (Table X-21) [131,132].

The research on carbonyliron silanethiolates was continued in 2010 [48], however the method of synthesis had been developed earlier as a synthetic recipe for a tricarbonyliron tellurolate [14]. It was then established that the photochemical oxidative addition of silyl dichalcogenides to low-oxidation-state metals allowed the quantitative formation of chalcogenolato iron(I) complexes. In the same way the tricarbonyliron silanethiolate and silaneselenolate complexes [{Fe(CO)$_3$(μ-ES*t*Bu$_3$)}$_2$] (E = S, Se) were obtained in the photochemical reaction of pentacarbonyliron with the relevant dichalcogenide *t*Bu$_3$Si−E$_2$−Si*t*Bu$_3$ (E = S, Se). The cyclic voltammograms of the complexes – including the silanetellurolate - resembled each other and could be characterized by two redox processes. The dinuclear complexes adopted a butterfly-type structure in which each of the iron atoms was coordinated by three carbonyl ligands and two bridging chalcogenolates. The distorted octahedral coordination spheres were completed by an iron–iron bond (Fig. 22c, Table X-20). The extremely long S–Si distances within this complexes, which exceeded 2.2 Å, were not commented by the authors, but in our opinion indicate that the compounds undergo desilylation very easily [48].

With regard to late transition and post transition metals, the silanethiolate complexes would sometimes provide (relatively) easily accessible models for examining the chemistry of sulfur-bound metal ions. In 2013 the synthesis and chemical behaviour of several iron(III) porphyrinates derived from *meso*-tetraphenylporphyrine with silanethiolate co-ligands were described. The complexes were prepared by the direct reactions of silanethiols with the iron(III) porphyrinates in toluene and were fully characterized in solution and the solid state (*e.g.* Fig. 23a, Table X-22) [24]. The presence of the silyl group on sulfur generated differences in the structure and chemistry of these species compared with iron(III) porphyrinates containing thiolate ligands. The silanethiolate species were all high-spin and displayed five-coordinate geometries in the solid state with short Fe−S distances. Electrochemical measurements demonstrated quasi-reversible initial oxidation contrary to the entirely irreversible event observed for a related benzenethiolate complex. The reaction pathways of

Table XI
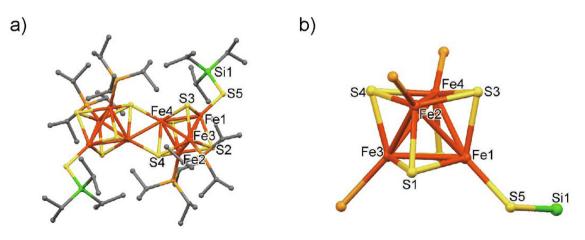Formulas and general characteristics of the Fe complexes described in chapter 3.5.2.

No	Formula	Available data, comments	Ref.
1	$(Bu_4N)_2[Fe_4S_4(LS_3)(SSiEt_3)]$	$(Bu_4N)_2[Fe_4S_4(LS_3)(SSiEt_3)]$; dark brown solid; ^{1}H NMR	[137]
2	$(Bu_4N)_2[Fe_4S_4(LS_3)(SSiMe_3)]$	$(Bu_4N)_2[Fe_4S_4(LS_3)(SSiMe_3)]$; dark brown solid; ^{1}H NMR; UV–Vis	[138]
3		$[(iPr_3P)_3Fe_4S_4(SSiPh_3)]$; black solid; ^{1}H NMR	[139]
4		$[(iPr_3P)_4Fe_8S_8(SSiPh_3)_2]$; black plates; Single crystal structure: triclinic, P-1, a, b, c [Å] = 11.2319(7), 13.600 (8), 15.382(9), α, β, γ [°] = 82.051(1), 80.924(1), 71.375(1); Bond lengths [Å] = **Fe–S** 2.248(1), **S–Si** 2.110(1); ^{1}H NMR, EA	[139]
5		$[\{Fe(\mu\text{-Br})(\mu\text{-SSi}tBu_3)\}_{12}]\cdot(C_6H_6)_n$; yellow crystals; Single crystal structure: triclinic, P-1, a, b, c [Å] = 11.683 (2), 18.803(3), 22.516(4) α, β, γ [°] = 65.571(3), 75.347(4), 89.576(4); Bond lengths [Å] = **Fe–S** 2.331(6), 2.334 (6), 2.335(6), 2.348(6), 2.349(7), **S–Si** 2.064(4), 2.182(9), 2.185(8), 2.188(9); ^{1}H NMR; IR, EA	[129]
6		$[(iPr_3P)_3Fe_4S_4(SSiiPr_3)]$; black crystals; Single crystal structure: triclinic, P-1, a, b, c [Å] = 10.890(3), 13.723(4), 18.892(6), α, β, γ [°] = 99.753(5), 103.788(4), 106.327(4); Bond lengths [Å] = **Fe–S** 2.285(1), **S–Si** 2.116(2), 2.103(2); ^{1}H NMR; EPR; Mössbauer, EA	[140]
7		$[(Tp)MoFe_3S_4(PEt_3)_2(SSiMe_3)]$; black needles; Single crystal structure: tetragonal, P-42$_1c$, a, b, c [Å] = 24.542 (5), 24.542(5), 24.086(8), α, β, γ [°] = 90, 90, 90; Bond lengths [Å] = **Fe–S** 2.263(3), 2.275(4), **S–Si** 2.064(4), 2.126(5); ^{1}H NMR	[23]

Fig. 24. Molecular structures of the supramolecular iron(II) silanothiolates (Part I); H atoms are omitted: a) $[(iPr_3P)_4Fe_8S_8(SSiPh_3)_2]$ [139]; b) $[(iPr_3P)_3Fe_4S_4(SSiiPr_3)]$ – isopropyl substituents at P and SiiPr_3 groups are omitted for clarity [140].

a)   b)
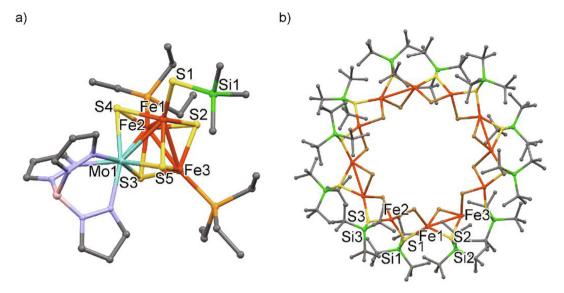
Fig. 25. Molecular structures of the supramolecular iron(II) silanothiolates (Part II). Hydrogen atoms are omitted: a) [(Tp)MoFe$_3$S$_4$(PEt$_3$)$_2$(SSiMe$_3$)] [23]; b) [Fe(μ-Br)(μ-SSitBu$_3$)}$_{12}$]·(C$_6$H$_6$)$_n$ [129].

the silanethiolate complexes with biologically relevant small molecules such as H$_2$S, NO, and 1-methylimidazole usually resulted in the reduction to iron(II) species [24]. Similar silanethiolate 5,10,15,20-tetrakis(2-chloro-6-fluorophenyl)porphinate complex of iron(III) was described two years later by the same authors (*e.g.* Fig. 23b) [133].

3.5.2. Supramolecular Fe—S—Si systems

Iron-sulfur clusters are ubiquitous motives and versatile cofactors involved in a wide variety of biological roles, such as ensuring structural stability or performing catalysis. The first instances of Fe—S—Si linkage within the biomimetic cubane type cluster were described in 1991 [134]. These silanethiolate derivatives were obtained as a result of substitution reactions of the clusters [Fe$_4$S$_4$-(LS$_3$)Cl]$^{2-}$ and [Fe$_4$S$_4$(LS$_3$)(OC$_6$H$_4$-p-Br)]$^{2-}$ with the silanethiolate anions - LiSSiMe$_3$ - or trimethylsilyl reagent (Me$_3$Si)$_2$S, respectively. The formation of the products was followed exclusively by ^{1}H NMR [134]. The reaction of similar cubane [Fe$_4$S$_4$(LS$_3$)-(SSiEt$_3$)]$^{2-}$ with the fluoride of iron(III) porphyrinate was used as one of the synthetic pathways to achieve the coupling of Fe(II) in the form of a cubane with heme Fe(III). The research was aimed at the reconstruction of the catalytic site of bacterial sulfite reductase, which is known to consist of both: cubane-type Fe$_4$S$_4$ cluster and heme component bridged by a sulfur atom [135]. Though rather slow, the reaction proceeded, driven by the high energy of the Si—F bond (Si—F and Si—S differ in energy by about 270 kJ/-mol). The identity of coupling products was established by ^{1}H NMR [136–138]. The cubane [Fe$_4$S$_4$(LS$_3$)(SSiEt$_3$)]$^{2-}$ (Table XI-1) utilized in these coupling reactions was obtained in the reaction of an acetonitrile solution of a mixture of CF$_3$SO$_3$SiEt$_3$/NaSH with an acetonitrile solution of (Bu$_4$N)$_2$[Fe$_4$S$_4$(LS$_3$)(SEt)] [137]. Two years later the isolation of another cubane (Bu$_4$N)$_2$[Fe$_4$S$_4$(LS$_3$)-(SSiMe$_3$)] (Table XI-2) was reported as a result of the reaction of [Fe$_4$S$_4$(LS$_3$)(OC$_6$H$_4$-p-Br)]$^{2-}$ with (Me$_3$Si)$_2$S in acetonitrile (in the studies previously described the product was not isolated [134]) [138]. A similar coupling procedure was applied to link this cubane to porphyrinato-Fe(III); the only difference is that instead of the fluoride complex the chloride –Fe(III)-porphyrynate complex was used for the coupling. The reactions were followed by ^{1}H NMR and UV–Vis spectroscopies [138].

The first determination of an X-ray molecular structure of a [Fe$_4$S$_4$] cubane featuring silanehiolato ligands came several years

later [139]. [Fe$_8$S$_8$(PiPr$_3$)$_4$(SSiPh$_3$)$_2$] (Fig. 24a, Table XI-4) formed as a result of recrystallization of a "simple" cubane [Fe$_4$S$_4$(PiPr$_3$)$_3$-(SSiPh$_3$)] from THF/Et$_2$O. The monosubstituted cluster [Fe$_4$S$_4$-(PiPr$_3$)$_3$(SSiPh$_3$)] is thereby obtained by the reaction: [Fe$_4$S$_4$(P^{i}Pr$_3$)$_4$]-(BPh$_4$) + (Ph$_4$P)SSiPh$_3$ → [Fe$_4$S$_4$(P^{i}Pr$_3$)$_3$(SSiPh$_3$)] + (Ph$_4$P)(BPh$_4$) + P^{i}Pr$_3$, driven by the insolubility of (Ph$_4$P)(BPh$_4$) in toluene, in which the neutral clusters are freely soluble. [[(iPr$_3$P)$_3$Fe$_4$S$_4$(SSiPh$_3$)] was identified by its ^{1}H NMR spectrum (Table XI-3) and though not obtained in pure form, it served as a useful precursor of the dicubane [Fe$_8$S$_8$(PiPr$_3$)$_4$(SSiPh$_3$)$_2$]. The formation of dicubane was reversible - addition of excess phosphane to a solution of dicubane in dichloromethane resulted in formation of monocubane; it was also readily cleaved with thiolates. When monitored by cyclic voltammetry in dichloromethane, the dicubane exhibited one reduction and one oxidation step at E$_{1/2}$ = −0.94 and −0.09 V respectively. The centrosymmetric dicubane with the [Fe$_8$S$_8$]$^{2+}$ core is illustrated in Fig. 24a. The Fe–S intercubane bond is significantly shorter than the Fe–S intracubane bond within the rhomb (Table XI-4). The three types of iron atoms were not resolved in the Mössbauer spectrum [139]. Another few years had passed before the structure of monocubane [Fe$_4$S$_4$] with silanethiolate terminal ligand was established [140]. The cluster [(iPr$_3$P)$_3$Fe$_4$S$_4$(SSiiPr$_3$)] (also [(iPr$_3$P)$_3$Fe$_4$-S$_4$(SSiPh$_3$)]) was obtained by ligand substitution from (BPh$_4$)-[(iPr$_3$P)$_4$Fe$_4$S$_4$] and NaSSiiPr$_3$ in THF/acetonitrile (Table XI-3, 6, Fig. 24b). Ground state properties of [Fe$_4$S$_4$]$^+$ clusters were investigated. EPR spectra of both clusters were consistent with S = 1/2 and the isomer shifts registered in Mössbauer spectra of polycrystalline [(iPr$_3$P)$_3$Fe$_4$S$_4$(SSiiPr$_3$)] were in agreement with the [Fe$_4$S$_4$]$^+$ state [140].

A popular synthetic goal in the field of biomimetic chemistry is the synthesis of iron-molybdenum sulfide clusters which are present in the active site of the versatile reducing enzyme nitrogenase, which is capable of multielectron reductions of a variety of substrates including unreactive dinitrogen [141]. In 2011 [(Tp)MoFe$_3$-S$_4$(PEt$_3$)$_3$]$^+$ containing the cubane-type [MoFe$_3$(μ_3-S)$_4$]$^{2+}$ core was demonstrated to undergo facile ligand substitution reactions at the iron sites leading to a variety of species including silanethiolato derivatives: [(Tp)MoFe$_3$S$_4$(PEt$_3$)$_2$(SSiMe$_3$)], [(Tp)MoFe$_3$S$_4$(PEt$_3$)$_2$-(SSiiPr$_3$)] and [(Tp)MoFe$_3$S$_4$(PEt$_3$)$_2$(SSiPh$_3$)] [23]. Cubane [(Tp)-MoFe$_3$S$_4$(PEt$_3$)$_2$(SSiMe$_3$)] is shown in Fig. 25a and Table XI-7. Xi & Holm emphasized not only relatively rare, low oxidation state of [MoFe$_3$(μ_3-S)$_4$]$^{2+}$ compared to the abundance of clusters in the

Table XII
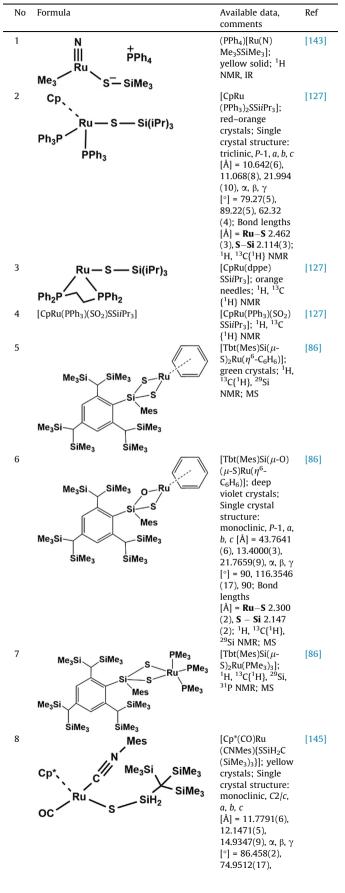Formulas and general characteristics of the Ru complexes described in chapter 3.5.3.

No	Formula	Available data, comments	Ref
1		(PPh$_4$)[Ru(N)Me$_3$SSiMe$_3$]; yellow solid; ^{1}H NMR, IR	[143]
2		[CpRu(PPh$_3$)$_2$SSiiPr$_3$]; red–orange crystals; Single crystal structure: triclinic, P-1, a, b, c [Å] = 10.642(6), 11.068(8), 21.994(10), α, β, γ [°] = 79.27(5), 89.22(5), 62.32(4); Bond lengths [Å] = **Ru**−**S** 2.462(3), **S**−**Si** 2.114(3); ^{1}H, ^{13}C{^{1}H} NMR	[127]
3		[CpRu(dppe)SSiiPr$_3$]; orange needles; ^{1}H, ^{13}C{^{1}H} NMR	[127]
4	[CpRu(PPh$_3$)(SO$_2$)SSiiPr$_3$]	[CpRu(PPh$_3$)(SO$_2$)SSiiPr$_3$]; ^{1}H, ^{13}C{^{1}H} NMR	[127]
5		[Tbt(Mes)Si(μ-S)$_2$Ru(η^6-C$_6$H$_6$)]; green crystals; ^{1}H, ^{13}C{^{1}H}, ^{29}Si NMR; MS	[86]
6		[Tbt(Mes)Si(μ-O)(μ-S)Ru(η^6-C$_6$H$_6$)]; deep violet crystals; Single crystal structure: monoclinic, P-1, a, b, c [Å] = 43.7641(6), 13.4000(3), 21.7659(9), α, β, γ [°] = 90, 116.3546(17), 90; Bond lengths [Å] = **Ru**−**S** 2.300(2), **S** − **Si** 2.147(2); ^{1}H, ^{13}C{^{1}H}, ^{29}Si NMR; MS	[86]
7		[Tbt(Mes)Si(μ-S)$_2$Ru(PMe$_3$)$_3$]; ^{1}H, ^{13}C{^{1}H}, ^{29}Si, ^{31}P NMR; MS	[86]
8		[Cp*(CO)Ru(CNMes){SSiH$_2$C(SiMe$_3$)$_3$}]; yellow crystals; Single crystal structure: monoclinic, C2/c, a, b, c [Å] = 11.7791(6), 12.1471(5), 14.9347(9), α, β, γ [°] = 86.458(2), 74.9512(17),	[145]

Table XII (continued)

No	Formula	Available data, comments	Ref
		63.014(4); Bond lengths [Å] = **Ru**−**S** 2.442(2), **S**−**Si** 2.092(2); ^{1}H, ^{13}C{^{1}H}, ^{29}Si {^{1}H} NMR	

oxidized [MoFe$_3$S$_4$]$^{3+}$ state but also its ability to bind hard and soft σ-donors as well as strong and weak π-acid ligands. Moreover the equimolar reaction of [(Tp)MoFe$_3$S$_4$(PEt$_3$)$_3$]$^+$ and NaSSiMe$_3$ in THF afforded the unusual cluster {[(Tp)-MoFe$_3$S$_4$(PEt$_3$)$_2$]$_3$S}$^+$ in which three cubane units were bridged by a central μ_3-S atom. Monocubane [(Tp)MoFe$_3$S$_4$(PEt$_3$)$_2$(SSiMe$_3$)], which was obtained by the reaction of [(Tp)MoFe$_3$S$_4$(PEt$_3$)$_2$Cl] with (Me$_3$Si)$_2$S was indicated as a likely intermediate in the formation of the tricluster compound [23].

Entirely different supramolecular systems were described in two papers by Sydora and co-workers [129,142]. The use of the bulky tBu$_3$SiS$^-$ ligand enabled the synthesis of unusual ferrous wheels, a unique ellipse, and an uncommon ferrous cube based on tetrahedral coordination. The structures were initially communicated [142] and then systematically studied [129]. Thermal desolvations of complexes mentioned in chapter 3.5.1: [X$_2$Fe(μ-SSitBu$_3$)$_2$FeBr-(THF)][Na(THF)$_4$] (X = Cl, Br) and [{(THF)FeI(μ-SSitBu$_3$)}$_2$] afforded molecular wheels [{Fe(μ-X)(μ-SSitBu$_3$)}$_{12}$]·(C$_6$H$_6$)$_n$ (X = Cl, Br) and the ellipse [{Fe(μ-I)(μ-SSitBu$_3$)}$_{14}$]·(C$_6$H$_6$)$_n$. One of the wheels: [{Fe(μ-Br)-(μ-SSitBu$_3$)}$_{12}$]·(C$_6$H$_6$)$_n$ is presented in Fig. 25b and Table XI-5. Variable-temperature magnetic susceptibility measurements revealed weakly antiferromagnetic coupling for the majority of wheel structures [129].

3.5.3. Silanethiolates of ruthenium

The first reported ruthenium silanethiolate (PPh$_4$)[Ru(N)Me$_3$-SSiMe$_3$] was reported in 1996 [143]. It was prepared by the reaction of (PPh$_4$)[Ru(N)Me$_3$Br] with NaSSiMe$_3$ at room temperature (Table XII-1). Complex (PPh$_4$)[Ru(N)Me$_3$SSiMe$_3$] reacted readily with a variety of halide sources such as CsF or PPh$_4$Cl with the formation of the hydrosulfide species (PPh$_4$)[Ru(N)Me$_3$(SH)] characterized by X-ray crystallography [143]. A similar approach to cleave a S–Si bond had been utilized earlier by Cai and Holm as described in 3.5.2 [137].

Ruthenium silanethiolato complexes and their reactions with sulfur dioxide served as models for the activation of SO$_2$ in the Claus process [127]. Five new heteroligand Ru complexes of the general formula [CpRu(PPh$_3$)(L)SSiiPr$_3$] and [CpRu(dppe)SSiiPr$_3$] (L = PPh$_3$, CO, PMe$_3$, P(OMe)$_3$) were synthesized from Ru precursors: CpRu(PPh$_3$)$_2$Cl or CpRu(PPh$_3$)(CO)Cl and NaSSiiPr$_3$. The examples are presented in Table XII-2,3 and in Fig. 26a. The complexes react instantly with SO$_2$ to give mainly the O-silyl esters of the hydrothiosulfito complexes CpRu(PPh$_3$)(L)SS(O)OSiiPr$_3$] (L = CO, PMe$_3$, P(OMe)$_3$) as a result of 1,2-insertion of SO$_2$ into the S–Si bond. The authors suggested that similar intermediates may form in the reaction of [cis-(Ph$_3$P)$_2$Pt(SH)$_2$] with SO$_2$ during the Claus process catalyzed by the ruthenium complex [127]. The research on the reactivity of silanethiolate and Ru complexes was continued in 2001 [144]. It was then established that [CpRu(PPh$_3$)$_2$SSiiPr$_3$] and [CpRu(PPh$_3$)$_2$SH] reacted with aryloisothiocyanates to give the corresponding $\kappa^2 S,S$-dithiocarbamato complexes as the result of insertion of the isothiocyanates into the S—Si and S–H bonds, respectively. The reactions proceeded *via* precoordination of the isothiocyanates to the ruthenium atom, followed by the formation of N-silyl $\kappa^2 S,S$-dithiocarbamates [144].
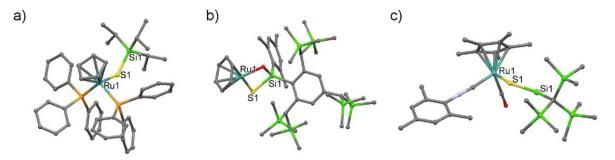
Fig. 26. Molecular structures of the ruthenium(II) silanethiolates without hydrogen atoms: a) [CpRu(PPh$_3$)$_2$SSiiPr$_3$] [127]; b) [Tbt(Mes)Si(μ-O)(μ-S)Ru(η^6-C$_6$H$_6$)] [86]; c) [Cp*(CO)Ru(CNMes){SSiH$_2$C(SiMe$_3$)$_3$}] [145].
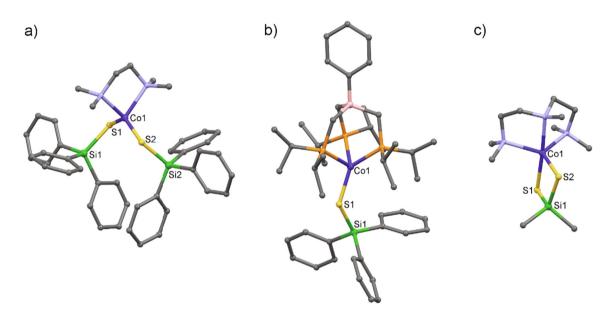
Fig. 27. Molecular structures of the selected silanethiolate complexes of Co(II) without hydrogen atoms: a) [(tmeda)Co(SSiPh$_3$)$_2$]·2CH$_2$Cl$_2$ [124]; b) [{PhB(CH$_2$PiPr$_2$)$_3$}-CoSSiPh$_3$] [152]; c) [(pmdeta)Co(S$_2$SiMe$_2$)] [125].

Overcrowded silanedithiol Tbt(Mes)Si(SH)$_2$, as well as hydroxysilanethiol and hydroxysilaneselenol Tbt(Mes)Si(OH)(EH) (E = S, Se), which were synthesized and isolated as air- and moisture-stable crystals, were utilized to prepare a series of Ru complexes. The initial [Tbt(Mes)Si(μ-S)$_2$Ru(η^6-C$_6$H$_6$)] and [Tbt(Mes)Si(μ-O)-(μ-S)Ru(η^6-C$_6$H$_6$)] compounds (also selenolate) were obtained by the deprotonation of the dithiol and thiol/silanol with BuLi/NaH in THF followed by the addition of [{(C$_6$H$_6$)RuCl$_2$}$_2$]. (Table XII-5,6). These monomeric complexes featured four-membered-ring cores with an almost planar geometry (*e.g.* Fig. 26b). Their UV–Vis spectra in hexane show characteristic absorptions of coordinatively unsaturated ruthenium complexes. The remaining compounds in the series resulted from the double replacement reactions of the initial (η^6-benzene) coordinated Ru complexes with trimethylphosphane (for example see Table XII-7) [86].

In 2012 the reaction of the neutral silylene ruthenium complex [Cp*(CO)(H)Ru=Si(H){C(SiMe$_3$)$_3$}] with an isothiocyanate MesNCS was communicated. In this reaction the C=S bond of MesNCS was cleaved and converted into an isocyanide ligand (CNMes) and a silanethiolato ligand {SSiH$_2$C(SiMe$_3$)$_3$} within the ruthenium complex [Cp*(CO)Ru(CNMes){SSiH$_2$C(SiMe$_3$)$_3$}]. The Ru silanethiolate was obtained quantitatively, as observed by NMR spectroscopy and its molecular structure was confirmed by X-ray crystallography (Fig. 26c, Table XII-8) [145]. The detailed reaction mechanisms of the C=S bond cleavage of isothiocyanate mediated by the neutral

ruthenium silylene hydride complex was later investigated with the use of DFT calculations [146].

The C–F bond, which is one of the thermodynamically strongest, covalent single bonds, can be heterolytically activated by exceptionally potent, cationic or neutral main group element Lewis acids. Sulfur-stabilized silylium (also carbenium) ions were indicated as transient products that formed at ruthenium thiolate hydride complexes [(R$_3$P)Ru(2,6-di-MesPh)H] (R = Me, Et, Ph, Ph$_2$-Me) during a heterolytic C(sp^3)–F bond cleavage of activated CF$_3$ groups using a catalytically generated silicon electrophile [147]. The mechanism was further supported by DFT calculations [148] and the [(R$_3$P)Ru(2,6-di-MesPh)H] complexes were additionally applied to enantioselective imine reduction [149] and 1,4-selective reduction of pyridine with hydrosilanes [150].

3.6. Group 9 elements
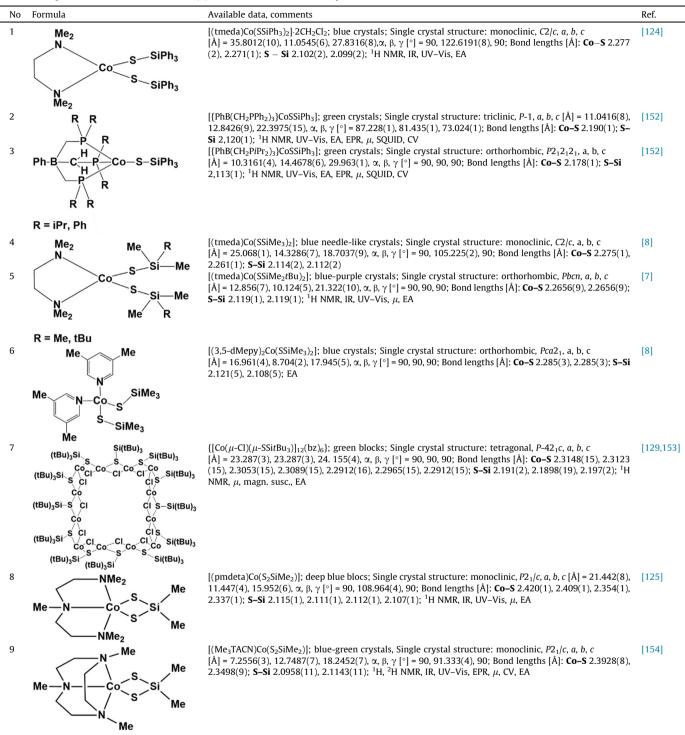
The silanethiolate complexes of group 9 elements are numerous and in vast majority they are cobalt complexes, which were a subject to detailed magnetic studies, while for rhodium and iridium only one silanethiolate is described so far.

3.6.1. Co complexes

All of the described Co compounds can be divided into groups depending on the type of silanethiolate substituents bonded to

A. Pladzyk, D. Kowalkowska-Zedler, A. Ciborska et al.

Table XIII
Formulas and general characteristics of the cobalt(II) silanethiolates described in chapter **3.6.1.1.**

No	Formula	Available data, comments	Ref.
1	Me₂N–(CH₂)–NMe₂ chelate Co with two S–SiPh₃	[(tmeda)Co(SSiPh₃)₂]·2CH₂Cl₂; blue crystals; Single crystal structure: monoclinic, $C2/c$, a, b, c [Å] = 35.8012(10), 11.0545(6), 27.8316(8), α, β, γ [°] = 90, 122.6191(8), 90; Bond lengths [Å]: **Co–S** 2.277(2), 2.271(1); **S–Si** 2.102(2), 2.099(2); ^{1}H NMR, IR, UV–Vis, EA	[124]
2	R R P P Co–SSiPh₃ (R = iPr, Ph)	[{PhB(CH₂PPh₂)₃}CoSSiPh₃]; green crystals; Single crystal structure: triclinic, P-1, a, b, c [Å] = 11.0416(8), 12.8426(9), 22.3975(15), α, β, γ [°] = 87.228(1), 81.435(1), 73.024(1); Bond lengths [Å]: **Co–S** 2.190(1); **S–Si** 2,120(1); ^{1}H NMR, UV–Vis, EA, EPR, μ, SQUID, CV	[152]
3	Ph–B–C P P Co–S–SiPh₃ (R = iPr, Ph)	[{PhB(CH₂PiPr₂)₃}CoSSiPh₃]; green crystals; Single crystal structure: orthorhombic, $P2_12_12_1$, a, b, c [Å] = 10.3161(4), 14.4678(6), 29.963(1), α, β, γ [°] = 90, 90, 90; Bond lengths [Å]: **Co–S** 2.178(1); **S–Si** 2,113(1); ^{1}H NMR, UV–Vis, EA, EPR, μ, SQUID, CV	[152]
4	Me₂N–(CH₂)–NMe₂ chelate Co with two S–SiMe₂R (R = Me, tBu)	[(tmeda)Co(SSiMe₃)₂]; blue needle-like crystals; Single crystal structure: monoclinic, $C2/c$, a, b, c [Å] = 25.068(1), 14.3286(7), 18.7037(9), α, β, γ [°] = 90, 105.225(2), 90; Bond lengths [Å]: **Co–S** 2.275(1), 2.261(1); **S–Si** 2.114(2), 2.112(2)	[8]
5	(same chelate, R = Me, tBu)	[(tmeda)Co(SSiMe₂tBu)₂]; blue-purple crystals; Single crystal structure: orthorhombic, $Pbcn$, a, b, c [Å] = 12.856(7), 10.124(5), 21.322(10), α, β, γ [°] = 90, 90, 90; Bond lengths [Å]: **Co–S** 2.2656(9), 2.2656(9); **S–Si** 2.119(1), 2.119(1); ^{1}H NMR, IR, UV–Vis, μ, EA	[7]
6	(3,5-dMepy)₂Co with two S–SiMe₃	[(3,5-dMepy)₂Co(SSiMe₃)₂]; blue crystals; Single crystal structure: orthorhombic, $Pca2_1$, a, b, c [Å] = 16.961(4), 8.704(2), 17.945(5), α, β, γ [°] = 90, 90, 90; Bond lengths [Å]: **Co–S** 2.285(3), 2.285(3); **S–Si** 2.121(5), 2.108(5); EA	[8]
7	{[Co(μ-Cl)(μ-SSitBu₃)]₁₂(bz)₆} cluster structure	{[Co(μ-Cl)(μ-SSitBu₃)]₁₂(bz)₆}; green blocks; Single crystal structure: tetragonal, P-42₁c, a, b, c [Å] = 23.287(3), 23.287(3), 24.155(4), α, β, γ [°] = 90, 90, 90; Bond lengths [Å]: **Co–S** 2.3148(15), 2.3123(15), 2.3053(15), 2.3089(15), 2.2912(16), 2.2965(15), 2.2912(15); **S–Si** 2.191(2), 2.1898(19), 2.197(2); ^{1}H NMR, μ, magn. susc., EA	[129,153]
8	NMe₂ pmdeta chelate Co with S₂SiMe₂	[(pmdeta)Co(S₂SiMe₂)]; deep blue blocs; Single crystal structure: monoclinic, $P2_1/c$, a, b, c [Å] = 21.442(8), 11.447(4), 15.952(6), α, β, γ [°] = 90, 108.964(4), 90; Bond lengths [Å]: **Co–S** 2.420(1), 2.409(1), 2.354(1), 2.337(1); **S–Si** 2.115(1), 2.111(1), 2.112(1), 2.107(1); ^{1}H NMR, IR, UV–Vis, μ, EA	[125]
9	Me₃TACN chelate Co with S₂SiMe₂	[(Me₃TACN)Co(S₂SiMe₂)]; blue-green crystals, Single crystal structure: monoclinic, $P2_1/c$, a, b, c [Å] = 7.2556(3), 12.7487(7), 18.2452(7), α, β, γ [°] = 90, 91.333(4), 90; Bond lengths [Å]: **Co–S** 2.3928(8), 2.3498(9); **S–Si** 2.0958(11), 2.1143(11); ^{1}H, ^{2}H NMR, IR, UV–Vis, EPR, μ, CV, EA	[154]

the silicon atom. A significant number of cobalt derivatives has been obtained in our department with the use of the tri-*tert*-butoxysyilanethiolate residue. Therefore, the Co complexes are divided into two groups for clarity:

- triaryl- and trialkylsilanethiolates
- trialkoxy- and triaryloxysilanethiolate cobalt complexes.

3.6.1.1. Triaryl- and trialkylsilanethiolates of cobalt. The first Co(II) triphenylsilanethiolate [(tmeda)Co(SSiPh₃)₂]·2CH₂Cl₂ was obtained in 2002 with the use of triphenysilanethiol and Co[N(SiMe₃)₂]₂ in the presence of tmeda [124]. Blue crystals of the mononuclear complex contain Co(II) ions adopting a distorted tetrahedral geometry *via* coordination of a tmeda molecule in chelating manner and two triphenylsilanethiolate residues acting as S-terminal ligands (Fig. 27a, Table XIII-1). The reactivity of the resulted compound
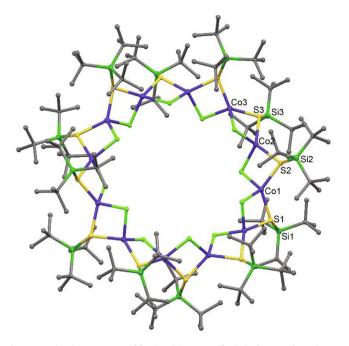
Fig. 28. Molecular structure of $[Co(\mu\text{-Cl})(\mu\text{-SSi}t\text{Bu}_3)]_{12}(\text{bz})_6$ [129,153]. Hydrogen atoms and bz molecules are omitted for clarity.

was examined with the use of $(\text{NBu}_4)\text{F/PPh}_3$ to induce S–Si cleavage to give the hexanuclear cobalt-sulfido cluster $\text{Co}_6(\mu_3\text{-S})_8(\text{PPh}_3)_6$ initially described by Cecconi and co-workers [151], but the yield was low. Two other mononuclear pseudotetrahedral triphenylsilanethiolato complexes $[\{\text{PhB}(\text{CH}_2\text{PPh}_2)_3\}\text{CoSSiPh}_3]$ and $[\{\text{PhB}(\text{CH}_2\text{P}i\text{Pr}_2)_3\}\text{CoSSiPh}_3]$ were obtained in the purpose of investigating the magnetic properties of pseudotetrahedral d^7 Co(II) complexes braced by tripodal tris(phosphane)borates [152]. The complexes were obtained by the reaction of TlSSiPh_3 with $[\text{PhB}(\text{CH}_2\text{PPh}_2)_3]\text{CoI}$ and $[\text{PhB}(\text{CH}_2\text{P}i\text{Pr}_2)_3]\text{CoI}$, respectively (Fig. 27b; Table XIII-2,3). The electronic properties of the obtained complexes were supported by DFT calculations [152].

Further examples of tetrahedral Co(II) silanethiolates are heteroligand complexes with tmeda or 3,5-dimethylpyridine: $[(\text{tmeda})\text{Co}(\text{SSiMe}_2t\text{Bu})_2]$ [7], $[(\text{tmeda})\text{Co}(\text{SSiMe}_3)_2]$ and $[(3,5\text{-Me}_2\text{C}_5\text{H}_3\text{N})_2\text{Co}(\text{SSiMe}_3)_2]$ [8] (Table XIII-4–6). Blue crystals of $[(\text{tmeda})\text{Co}(\text{SSiMe}_3)_2]$ and $[(3,5\text{-Me}_2\text{C}_5\text{H}_3\text{N})_2\text{Co}(\text{SSiMe}_3)_2]$ were obtained from the reaction of CoCl_2 with tmeda or 3,5-dMepy and freshly prepared lithium trimethylsilanethiolate LiSSiMe_3 obtained in the reaction of $(\text{Me}_2\text{SiS})_3$ with $t\text{BuLi}$ and tmeda. The third complex $[(\text{tmeda})\text{Co}(\text{SSiMe}_2t\text{Bu})_2]$ was obtained in the reaction of $[(\text{tmeda})\text{LiSSiMe}_2t\text{Bu}]_2$ and CoCl_2. Complexes were synthesized as potential precursors for ternary nanoclusters, but they appeared to be too reactive for this purpose [7,8].

The aggregation of $(t\text{Bu}_3\text{SiS})\text{CoCl}$ to the cyclic oligomer $\{[\text{Co}(\mu\text{-Cl})(\mu\text{-SSi}t\text{Bu}_3)]_{12}(\text{bz})_6\}$ was reported in 2004 and 2006 (Fig. 28) [129,153]. A mixture of anhydrous CoCl_2 and $t\text{Bu}_3\text{SiSNa(THF)}_x$ in THF yielded a blue solid which, recrystallized from benzene, resulted in green crystalline blocks of the twelve-membered cobaltous wheel based on edge-shared tetrahedra (Fig. 28, Table XIII-7). The measurements of magnetic properties revealed weak anferromagnetic properties with μ_{eff} = 15 μ_B at 298 K.

The Co–S bond distances in the majority of trialkyl- and as triphenylsilanethiolate Co(II) complexes described above are longer than the average Co–S bond length (2.14 Å) and they are about 2.26–2.31 Å, while the S–Si bond lengths are close to the value of average S–Si bond distance (2.19 Å) [29–31].

The synthesis of the first silanedithiolate Co(II) complex was described in 2003 [125]. Deep blue crystals of $[(\text{pmdeta})\text{Co}(\text{S}_2\text{-SiMe}_2)]$ were obtained with high yield in the reaction of Co(OAc)$_2$ with cyclotrisilathiane in the presence of pmdeta (Fig. 27c, Table XIII-8). The complex is mononuclear with a non-planar four-membered CoS_2Si ring. Both, the silanedithiolate residue and the pmdeta coordinate to the Co(II) in a chelating mode, therefore, the metallic center adopts distorted trigonal-bipyramidal geometry. The compound is air- and moisture sensitive, but thermally stable [125]. The same synthetic route was applied for the synthesis of another Co(II) silanedithiolate complex reported in 2019 [154]. Blue-green crystals of $[(\text{Me}_3\text{TACN})\text{Co}(\text{S}_2\text{-SiMe}_2)]$ were obtained with good yield by reacting Co(OAc)$_2$ with Me_3TACN, followed by the addition of hexamethylcyclotrisilathiane $(\text{Me}_2\text{SiS})_3$. The resulted compound is a five-coordinated Co(II) complex with a square-pyramidal geometry at the cobalt atom (Table XIII-9). The reaction of the obtained Co(II) compound with O_2 gives access to the thiolate-ligated cobalt-superoxo complex $[(\text{Me}_3\text{TACN})\text{Co}(\text{O}_2)\text{S}_2\text{SiMe}_2]$, which is able to oxidize the O–H bonds of 2,2,6,6-tetramethylpiperidin-1-ol derivatives via abstraction of a hydrogen atom [154]. Two silanedithiolate Co(II) complexes described in this paragraph have Co–S bond lengths significantly longer than the sum of the covalent radii of Co and S atoms, whereas the S–Si bond distances are shorter than the average S–Si bond length. (Table XIII-8,9)

3.6.1.2. Co tri-tert-butoxy- and tris(2,6-diisopropylphenoxy)silanethiolates. The majority of Co(II) silanethiolates belongs to the group of the tri-*tert*-butoxysilanethiolate derivatives. Among them are heteroleptic mononuclear, dinuclear as well as polynuclear complexes with diverse structures and geometries at the Co ion. Their syntheses were conducted at atmospheric conditions, often in water as the reaction medium due to the noticeable resistance of TBST towards the hydrolysis of the S–Si bond. The first aim of these syntheses was the need of finding Co(II) complexes that would imitate the active sites of Zn-enzymes as their spectral models. The different research direction was based on several reports which described low-coordinate Co(II) complexes as precursors for materials with interesting magnetic properties. Therefore the recent papers on Co(II) silanethiolates were focused on the relation between their molecular structure and magnetic character. For all compounds belonging to this group, the Co–S bond lengths range from 2.24 Å to 2.36 Å and are thus longer than the average Co–S single bond length (2.14 Å), while the S–Si bond lengths are slightly shorter than the average S–Si bond distance (2.19 Å) with the values varying from 2.06 Å to 2.12 Å.

The first Co(II) tri-*tert*-butoxysilanethiolate was reported in 1995 by Becker and co-workers [155]. Dark blue crystals of $[(\text{MeCN})\text{Co}\{\text{SSi}(\text{O}t\text{Bu})_3\}_2]$ were obtained from the mixture of CoCl_2, TBST and trimethylamine in acetonitrile. The complex is mononuclear with Co(II) coordinated by two bidentate TBST residues as O, S-chelating ligand and one molecule of acetonitrile (Table XIV-1). Thus, the metallic center adopts a distorted trigonal bipyramidal geometry [155]. In 2006, Kropidłowska and co-workers reported the cocrystalization of $[(\text{MeCN})\text{Co}\{\text{SSi}(\text{O}t\text{Bu})_3\}_2]$ with its isomorphous Zn analogue, leading to a solid mixture with a Co:Zn ratio of 0.81(5):0.19(5) ((Table XIV-2) [156].

A series of Co tri-*tert*-butoxysilanethiolates with ammonia as co-ligand(s) was initiated in 2001 [157]. It started with a dinuclear compound obtained by the reaction of a cobalt(II) ammino complex generated in situ with TBST; the reaction was carried out in water. Green crystals of the dimer $[\{(\text{NH}_3)\text{Co}(\mu\text{-SSi}(\text{O}t\text{Bu})_3)(\text{SSi}(\text{O}t\text{Bu})_3)\}_2]$ were isolated after the recrystallization of the product from hexane. Both Co(II) atoms within the dimer adopt a distorted tetrahedral geometry (Table XIV-3, Fig. 29a), forming a non-planar four-membered Co_2S_2 ring with a Co-Co distance of 3.083 Å and
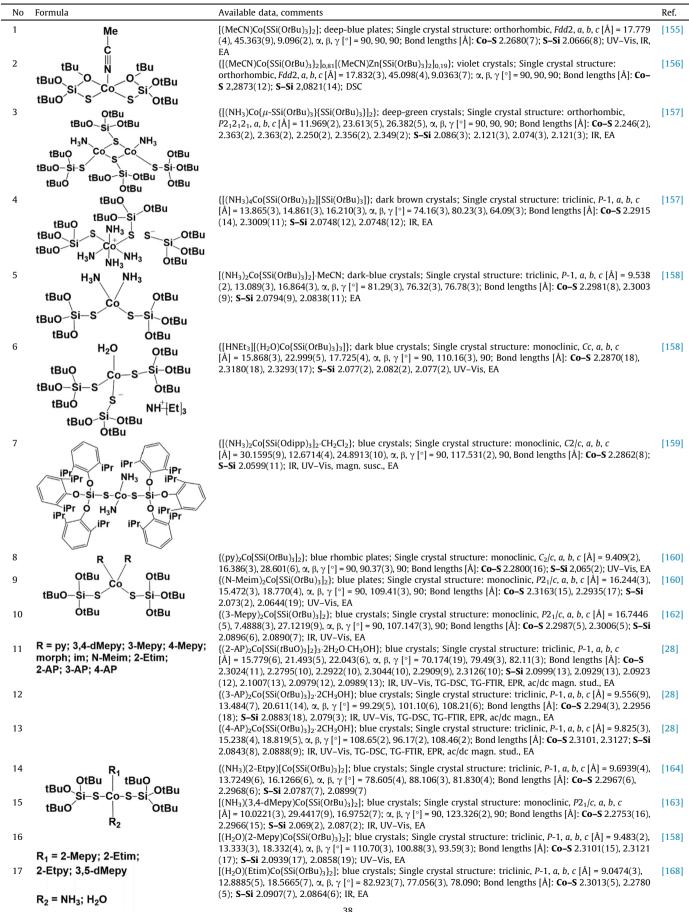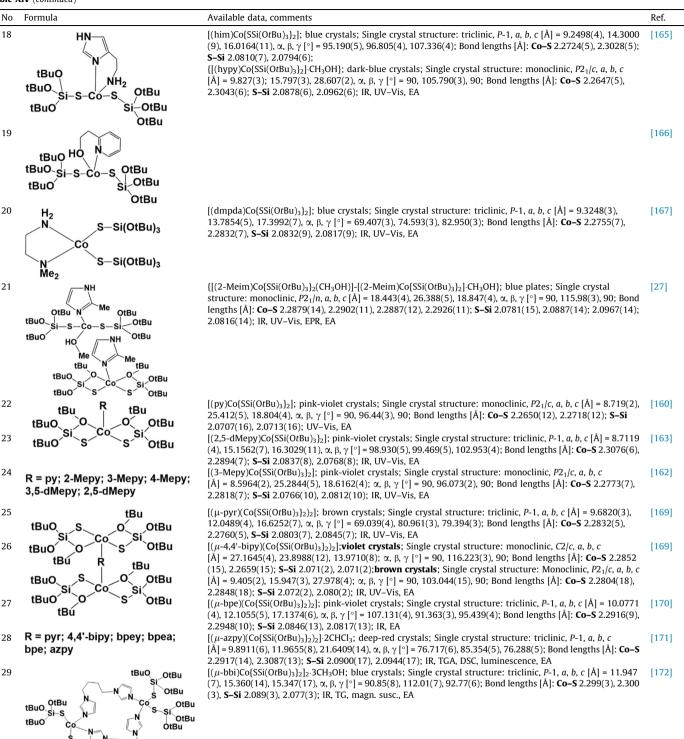
Table XIV
Formulas and general characteristics of the Group 9 elements described in chapter **3.6.1.2.**

No	Formula	Available data, comments	Ref.
1		[(MeCN)Co{SSi(OtBu)₃}₂]; deep-blue plates; Single crystal structure: orthorhombic, *Fdd*2, *a, b, c* [Å] = 17.779 (4), 45.363(9), 9.096(2), α, β, γ [°] = 90, 90, 90; Bond lengths [Å]: **Co–S** 2.2680(7); **S–Si** 2.0666(8); UV–Vis, IR, EA	[155]
2		{[(MeCN)Co{SSi(OtBu)₃}₂]₀,₈₁[(MeCN)Zn{SSi(OtBu)₃}₂]₀,₁₉}; violet crystals; Single crystal structure: orthorhombic, *Fdd*2, *a, b, c* [Å] = 17.832(3), 45.098(4), 9.0363(7); α, β, γ [°] = 90, 90, 90; Bond lengths [Å]: **Co–S** 2,2873(12); **S–Si** 2,0821(14); DSC	[156]
3		{[(NH₃)Co{μ-SSi(OtBu)₃}{SSi(OtBu)₃}]₂}; deep-green crystals; Single crystal structure: orthorhombic, *P*2₁2₁2₁, *a, b, c* [Å] = 11.969(2), 23.613(5), 26.382(5), α, β, γ [°] = 90, 90, 90; Bond lengths [Å]: **Co–S** 2.246(2), 2.363(2), 2.363(2), 2.250(2), 2.356(2), 2.349(2); **S–Si** 2.086(3); 2.121(3), 2.074(3), 2.121(3); IR, EA	[157]
4		{[(NH₃)₄Co{SSi(OtBu)₃}₂][SSi(OtBu)₃]}; dark brown crystals; Single crystal structure: triclinic, *P*-1, *a, b, c* [Å] = 13.865(3), 14.861(3), 16.210(3), α, β, γ [°] = 74.16(3), 80.23(3), 64.09(3); Bond lengths [Å]: **Co–S** 2.2915 (14), 2.3009(11); **S–Si** 2.0748(12), 2.0748(12); IR, EA	[157]
5		[(NH₃)₂Co{SSi(OtBu)₃}₂]·MeCN; dark-blue crystals; Single crystal structure: triclinic, *P*-1, *a, b, c* [Å] = 9.538 (2), 13.089(3), 16.864(3), α, β, γ [°] = 81.29(3), 76.32(3), 76.78(3); Bond lengths [Å]: **Co–S** 2.2981(8), 2.3003 (9); **S–Si** 2.0794(9), 2.0838(11); EA	[158]
6		{[HNEt₃][(H₂O)Co{SSi(OtBu)₃}₃]}; dark blue crystals; Single crystal structure: monoclinic, *Cc*, *a, b, c* [Å] = 15.868(3), 22.999(5), 17.725(4), α, β, γ [°] = 90, 110.16(3), 90; Bond lengths [Å]: **Co–S** 2.2870(18), 2.3180(18), 2.3293(17); **S–Si** 2.077(2), 2.082(2), 2.077(2), UV–Vis, EA	[158]
7		{[(NH₃)₂Co[SSi(Odipp)₃]₂·CH₂Cl₂}; blue crystals; Single crystal structure: monoclinic, *C*2/*c*, *a, b, c* [Å] = 30.1595(9), 12.6714(4), 24.8913(10), α, β, γ [°] = 90, 117.531(2), 90, Bond lengths [Å]: **Co–S** 2.2862(8); **S–Si** 2.0599(11); IR, UV–Vis, magn. susc., EA	[159]
8	R = py; 3,4-dMepy; 3-Mepy; 4-Mepy; morph; im; N-Meim; 2-Etim; 2-AP; 3-AP; 4-AP	{(py)₂Co[SSi(OtBu)₃]₂}; blue rhombic plates; Single crystal structure: monoclinic, *C*₂/*c*, *a, b, c* [Å] = 9.409(2), 16.386(3), 28.601(6), α, β, γ [°] = 90, 90.37(3), 90; Bond lengths [Å]: **Co–S** 2.2800(16); **S–Si** 2,065(2); UV–Vis, EA	[160]
9		{(N-Meim)₂Co[SSi(OtBu)₃]₂}; blue plates; Single crystal structure: monoclinic, *P*2₁/*c*, *a, b, c* [Å] = 16.244(3), 15.472(3), 18.770(4), α, β, γ [°] = 90, 109.41(3), 90; Bond lengths [Å]: **Co–S** 2.3163(15), 2.2935(17); **S–Si** 2.073(2), 2.0644(19); UV–Vis, EA	[160]
10		{(3-Mepy)₂Co[SSi(OtBu)₃]₂}; blue crystals; Single crystal structure: monoclinic, *P*2₁/*c*, *a, b, c* [Å] = 16.7446 (5), 7.4888(3), 27.1219(9), α, β, γ [°] = 90, 107.147(3), 90; Bond lengths [Å]: **Co–S** 2.2987(5), 2.3006(5); **S–Si** 2.0896(6), 2.0890(7); IR, UV–Vis, EA	[162]
11		{(2-AP)₂Co[SSi(tBuO)₃]₂}₃·2H₂O·CH₃OH}; blue crystals; Single crystal structure: triclinic, *P*-1, *a, b, c* [Å] = 15.779(6), 21.493(5), 22.043(6), α, β, γ [°] = 70.174(19), 79.49(3), 82.11(3); Bond lengths [Å]: **Co–S** 2.3024(11), 2.2795(10), 2.2922(10), 2.3044(10), 2.2909(9), 2.3126(10); **S–Si** 2.0999(13), 2.0929(13), 2.0923 (12), 2.1007(13), 2.0979(12), 2.0989(13); IR, UV–Vis, TG-DSC, TG-FTIR, EPR, ac/dc magn. stud., EA	[28]
12		{(3-AP)₂Co[SSi(OtBu)₃]₂·2CH₃OH}; blue crystals; Single crystal structure: triclinic, *P*-1, *a, b, c* [Å] = 9.556(9), 13.484(7), 20.611(14), α, β, γ [°] = 99.29(5), 101.10(6), 108.21(6); Bond lengths [Å]: **Co–S** 2.294(3), 2.2956 (18); **S–Si** 2.0883(18), 2.079(3); IR, UV–Vis, TG-DSC, TG-FTIR, EPR, ac/dc magn. stud., EA	[28]
13		{(4-AP)₂Co[SSi(OtBu)₃]₂·2CH₃OH}; blue crystals; Single crystal structure: triclinic, *P*-1, *a, b, c* [Å] = 9.825(3), 15.238(4), 18.819(5), α, β, γ [°] = 108.65(2), 96.17(2), 108.46(2); Bond lengths [Å]: **Co–S** 2.3101, 2.3127; **S–Si** 2.0843(8), 2.0888(9); IR, UV–Vis, TG-DSC, TG-FTIR, EPR, ac/dc magn. stud., EA	[28]
14	R₁ = 2-Mepy; 2-Etim; 2-Etpy; 3,5-dMepy R₂ = NH₃; H₂O	{(NH₃)(2-Etpy)[Co{SSi(OtBu)₃}₂]}; blue crystals; Single crystal structure: triclinic, *P*-1, *a, b, c* [Å] = 9.6939(4), 13.7249(6), 16.1266(6), α, β, γ [°] = 78.605(4), 88.106(3), 81.830(4); Bond lengths [Å]: **Co–S** 2.2967(6), 2.2968(6); **S–Si** 2.0787(7), 2.0899(7)	[164]
15		{(NH₃)(3,4-dMepy)Co{SSi(OtBu)₃}₂}; blue crystals; Single crystal structure: monoclinic, *P*2₁/*c*, *a, b, c* [Å] = 10.0221(3), 29.4417(9), 16.9752(7); α, β, γ [°] = 90, 123.326(2), 90; Bond lengths [Å]: **Co–S** 2.2753(16), 2.2966(15); **S–Si** 2.069(2), 2.087(2); IR, UV–Vis, EA	[163]
16		[(H₂O)(2-Mepy)Co{SSi(OtBu)₃}₂]; blue crystals; Single crystal structure: triclinic, *P*-1, *a, b, c* [Å] = 9.483(2), 13.333(3), 18.332(4), α, β, γ [°] = 110.70(3), 100.88(3), 93.59(3); Bond lengths [Å]: **Co–S** 2.3101(15), 2.3121 (17); **S–Si** 2.0939(17), 2.0858(19); UV–Vis, EA	[158]
17		[(H₂O)(Etim)Co{SSi(OtBu)₃}₂]; blue crystals; Single crystal structure: triclinic, *P*-1, *a, b, c* [Å] = 9.0474(3), 12.8885(5), 18.5665(7), α, β, γ [°] = 82.923(7), 77.056(3), 78.090; Bond lengths [Å]: **Co–S** 2.3013(5), 2.2780 (5); **S–Si** 2.0907(7), 2.0864(6); IR, EA	[168]

Table XIV (*continued*)

No	Formula	Available data, comments	Ref.
18		[(him)Co{SSi(O*t*Bu)₃}₂]; blue crystals; Single crystal structure: triclinic, *P*-1, *a*, *b*, *c* [Å] = 9.2498(4), 14.3000 (9), 16.0164(11), α, β, γ [°] = 95.190(5), 96.805(4), 107.336(4); Bond lengths [Å]: **Co–S** 2.2724(5), 2.3028(5); **S–Si** 2.0810(7), 2.0794(6); {[(hypy)Co{SSi(O*t*Bu)₃}₂]·CH₃OH}; dark-blue crystals; Single crystal structure: monoclinic, *P*2₁/*c*, *a*, *b*, *c* [Å] = 9.827(3); 15.797(3), 28.607(2), α, β, γ [°] = 90, 105.790(3), 90; Bond lengths [Å]: **Co–S** 2.2647(5), 2.3043(6); **S–Si** 2.0878(6), 2.0962(6); IR, UV–Vis, EA	[165]
19			[166]
20		[(dmpda)Co{SSi(O*t*Bu)₃}₂]; blue crystals; Single crystal structure: triclinic, *P*-1, *a*, *b*, *c* [Å] = 9.3248(3), 13.7854(5), 17.3992(7), α, β, γ [°] = 69.407(3), 74.593(3), 82.950(3); Bond lengths [Å]: **Co–S** 2.2755(7), 2.2832(7), **S–Si** 2.0832(9), 2.0817(9); IR, UV–Vis, EA	[167]
21		{[(2-Meim)Co{SSi(O*t*Bu)₃}₂(CH₃OH)]-[(2-Meim)Co{SSi(O*t*Bu)₃}₂]·CH₃OH}; blue plates; Single crystal structure: monoclinic, *P*2₁/*n*, *a*, *b*, *c* [Å] = 18.443(4), 26.388(5), 18.847(4), α, β, γ [°] = 90, 115.98(3), 90; Bond lengths [Å]: **Co–S** 2.2879(14), 2.2902(11), 2.2887(12), 2.2926(11); **S–Si** 2.0781(15), 2.0887(14); 2.0967(14); 2.0816(14); IR, UV–Vis, EPR, EA	[27]
22		[(py)Co{SSi(O*t*Bu)₃}₂]; pink-violet crystals; Single crystal structure: monoclinic, *P*2₁/*c*, *a*, *b*, *c* [Å] = 8.719(2), 25.412(5), 18.804(4), α, β, γ [°] = 90, 96.44(3), 90; Bond lengths [Å]: **Co–S** 2.2650(12), 2.2718(12); **S–Si** 2.0707(16), 2.0713(16); UV–Vis, EA	[160]
23		[(2,5-dMepy)Co{SSi(O*t*Bu)₃}₂]; pink-violet crystals; Single crystal structure: triclinic, *P*-1, *a*, *b*, *c* [Å] = 8.7119 (4), 15.1562(7), 16.3029(11), α, β, γ [°] = 98.930(5), 99.469(5), 102.953(4); Bond lengths [Å]: **Co–S** 2.3076(6), 2.2894(7); **S–Si** 2.0837(8), 2.0768(8); IR, UV–Vis, EA	[163]
24	R = py; 2-Mepy; 3-Mepy; 4-Mepy; 3,5-dMepy; 2,5-dMepy	[(3-Mepy)Co{SSi(O*t*Bu)₃}₂]; pink-violet crystals; Single crystal structure: monoclinic, *P*2₁/*c*, *a*, *b*, *c* [Å] = 8.5964(2), 25.2844(5), 18.6162(4); α, β, γ [°] = 90, 96.073(2), 90; Bond lengths [Å]: **Co–S** 2.2773(7), 2.2818(7); **S–Si** 2.0766(10), 2.0812(10); IR, UV–Vis, EA	[162]
25		[(μ-pyr)(Co{SSi(O*t*Bu)₃}₂)₂]; brown crystals; Single crystal structure: triclinic, *P*-1, *a*, *b*, *c* [Å] = 9.6820(3), 12.0489(4), 16.6252(7), α, β, γ [°] = 69.039(4), 80.961(3), 79.394(3); Bond lengths [Å]: **Co–S** 2.2832(5), 2.2760(5), **S–Si** 2.0803(7), 2.0845(7); IR, UV–Vis, EA	[169]
26		[(μ-4,4′-bipy)(Co{SSi(O*t*Bu)₃}₂)₂];**violet crystals**; Single crystal structure: monoclinic, *C*2/*c*, *a*, *b*, *c* [Å] = 27.1645(4), 23.8988(12), 13.9710(8); α, β, γ [°] = 90, 116.223(3), 90; Bond lengths [Å]: **Co–S** 2.2852 (15), 2.2659(15); **S–Si** 2.071(2), 2.071(2);**brown crystals**; Single crystal structure: Monoclinic, *P*2₁/*c*, *a*, *b*, *c* [Å] = 9.405(2), 15.947(3), 27.978(4); α, β, γ [°] = 90, 103.044(15), 90; Bond lengths [Å]: **Co–S** 2.2804(18), 2.2848(18); **S–Si** 2.072(2), 2.080(2); IR, UV–Vis, EA	[169]
27		[(μ-bpe)(Co{SSi(O*t*Bu)₃}₂)₂]; pink-violet crystals; Single crystal structure: triclinic, *P*-1, *a*, *b*, *c* [Å] = 10.0771 (4), 12.1055(5), 17.1374(6), α, β, γ [°] = 107.131(4), 91.363(3), 95.439(4); Bond lengths [Å]: **Co–S** 2.2916(9), 2.2948(10); **S–Si** 2.0846(13), 2.0817(13); IR, EA	[170]
28	R = pyr; 4,4′-bipy; bpey; bpea; bpe; azpy	[(μ-azpy)(Co{SSi(O*t*Bu)₃}₂)₂]·2CHCl₃; deep-red crystals; Single crystal structure: triclinic, *P*-1, *a*, *b*, *c* [Å] = 9.8911(6), 11.9655(8), 21.6409(14), α, β, γ [°] = 76.717(6), 85.354(5), 76.288(5); Bond lengths [Å]: **Co–S** 2.2917(14), 2.3087(13); **S–Si** 2.0900(17), 2.0944(17); IR, TGA, DSC, luminescence, EA	[171]
29		[(μ-bbi)Co{SSi(O*t*Bu)₃}₂]₂·3CH₃OH; blue crystals; Single crystal structure: triclinic, *P*-1, *a*, *b*, *c* [Å] = 11.947 (7), 15.360(14), 15.347(17), α, β, γ [°] = 90.85(8), 112.01(7), 92.77(6); Bond lengths [Å]: **Co–S** 2.299(3), 2.300 (3), **S–Si** 2.089(3), 2.077(3); IR, TG, magn. susc., EA	[172]

Table XIV (*continued*)

No	Formula	Available data, comments	Ref.
30		[(μ-3AMP)(Co{SSi(OtBu)₃}₂)₂]; blue crystals; Single crystal structure: triclinic, *P*-1, *a*, *b*, *c* [Å] = 9.825(3), 15.238(4), 18.819(5), α, β, γ [°] = 108.65(2), 96.17(2), 108.46(2); Bond lengths [Å]: **Co–S** 2.3101(10), 2.3127 (7); **S–Si** 2.0843(8), 2.0888(9); IR, UV–Vis, TG-DSC, TG-FTIR, EPR, *ac* and *dc* magnetic studies, EA	[28]
31		[(μ-4,4′-bipy)Co{μ-SSi(OtBu)₃}{SSi(OtBu)₃}]ₙ; IR, UV–Vis, EA	[169]
32		[(bda)₂Co{SSi(OtBu)₃}₂]ₙ; blue powder; IR, EA	[167]
33		[(pda)₂Co{SSi(OtBu)₃}₂CH₃OH]ₙ; blue crystals; Single crystal structure: monoclinic, *P*2₁/*c*, *a*, *b*, *c* [Å] = 15.5290(7), 9.5600(5), 29.9519(15), α, β, γ [°] = 90, 109.376(4), 90; Bond lengths [Å]: **Co–S** 2.2830(13), 2.2996(14); **S–Si** 2.094(2), 2.0790(18); IR, TG, TG-DSC, TG-IR, EA	[167]
34		[(hda)₂Co{SSi(OtBu)₃}₂CH₃OH]ₙ; blue crystals; Single crystal structure: triclinic, *P*-1, *a*, *b*, *c* [Å] = 15.6922 (13), 17.9585(16), 18.5573(17), α, β, γ [°] = 88.539(7), 68.954(8), 68.860(8); Bond lengths [Å]: **Co–S** 2.2845 (17), 2.2951(17), 2.313(5), 2.2997(14); **S–Si** 2.103(2), 2.077(2), 2.093(5), 2.0837(18); FT, TG, TG-DSC, TG-IR, EA	[167]
35		[(μ-api)Co{SSi(OtBu)₃}₂]ₙ; blue crystals; Single crystal structure: monoclinic, *P*2₁/*a*, *a*, *b*, *c* [Å] = 9.592(3), 33.010(8), 14.296(4), α, β, γ [°] = 90, 103.94(2), 90; Bond lengths [Å]: **Co–S** 2.2884(14), 2.3042(13); **S–Si** 2.084(2), 2.0813(17); IR, TG, TG-FTIR, magn. susc., EA	[172]
36		[(μ-4-AMP)Co{SSi(OtBu)₃}₂]ₙ; blue crystals; Single crystal structure: orthorhombic, *Pca*2₁, *a*, *b*, *c* [Å] = 27.991 (3), 9.623(3), 16.419(3), α, β, γ [°] = 90, 90, 90; Bond lengths [Å]: **Co–S** 2.291(2), 2.310(3); **S–Si** 2.068(3), 2.073(3); IR, UV–Vis, TG-DSC, TG-FTIR, EPR, EA	[28]

bridging silanethiolate ligands. The terminal silanethiolate anions and ammonia molecules complete the coordination sphere of each metal ion. The saturation of the hexane solution of [{(NH₃)Co(μ-SSi-(OtBu)₃)(SSi(OtBu)₃)}₂] with gaseous ammonia in the presence of air led to the oxidation of Co(II) and formation of the ionic Co(III) species, featuring the complex cation: [(NH₃)₄Co{SSi(OtBu)₃}₂]SSi(OtBu)₃ (Table XIV-4) [157]. Dissolution of the dimer in acetonitrile resulted in the formation of mononuclear [(NH₃)₂Co{SSi(OtBu)₃}₂]·MeCN (Table XIV-5) [158]. A similar tetrahedral complex with SSi(Odipp)₃⁻ ligands was later described (Table XIV-7, Fig. 29b) [159]. The replacement of ammonia with non-coordinating trimethylamine resulted in the formation of mononuclear, ionic, aqua-ligated (HNEt₃)[(H₂O)Co {SSi(OtBu)₃}₃] (Table XIV-6). Both ions are held together by N–H···S hydrogen bonding [158].

The dimer [(NH₃)Co(μ-SSi(OtBu)₃)(SSi(OtBu)₃)}₂] served as a convenient precursor of a large series of heteroleptic mononunclear Co(II) tri-*tert*-butoxysilanethiolates with diverse N-donor ligands. The complexes exhibited distorted tetrahedral or trigonal bipyrimidal geometries on Co(II) ions and CoN₂S₂, CoNOS₂ and CoNO₂S₂ cores. The first group of tetrahedral complexes was synthesized by Becker and co-workers [160] and the studies were continued by Pladzyk [161–163]. The complexes were obtained

following the same synthetic procedure: to the hexane solution of [{(NH₃)Co(μ-SSi(OtBu)₃)(SSi(OtBu)₃)}₂] the appropriate organic N-donor ligand was added yielding compounds with the general formula [(L)₂Co{SSi(OtBu)₃}₂], where L = py, 3-Mepy, 4-Mepy, 3,4-dMepy, Meim, pyrr, morph (*e.g.* Fig. 30a, Table XIV-8–10) [160–163].

The use of aminopyridines 2-AP, 3-AP and 4-AP as co-ligands leads to three mononuclear Co(II) silanethiolates with a tetrahedral CoN₂S₂ environment at the cobalt atom (Table XIV-11–13) [28]. All complexes were obtained as blue crystals by the simple reaction of [{(NH₃)Co(μ-SSi(OtBu)₃)(SSi(OtBu)₃)}₂] with a respective amine in a 1:4 M ratio using toluene and methanol as solvent. The asymmetric unit of [(2-AP)₂Co{SSi(tBuO)₃}₂]₃·2H₂O·CH₃OH is composed of three complex molecules that crystallized together with two water and one methanol molecule, while both [(3-AP)₂Co{SSi(OtBu)₃}₂]· 2CH₃OH and [(4-AP)₂Co{SSi(OtBu)₃}₂]·2CH₃OH crystallize as methanol solvates. Hydrogen bonding interactions, present in the structures of the complexes, lead to the formation of a 1D polymeric chain- and 2D net spatial-structures, respectively. For all complexes, the *ac* and dc magnetic studies with EPR spectroscopy reveal paramagnetic high–spin Co(II) ions with a considerable contribution of the ZFS effect in a low temperature range [28].
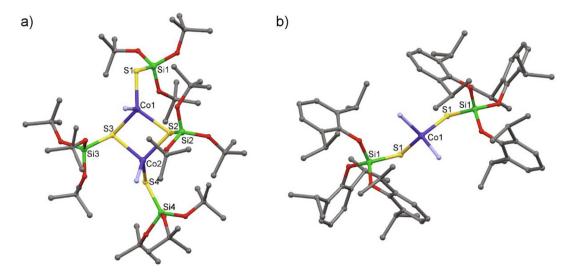
Fig. 29. Molecular structures of ammonia ligated Co(II) silanethiolates without hydrogen atoms: a) [(NH₃)Co(μ-SSi(OtBu)₃)(SSi(OtBu)₃)}₂] [157]; b) [(NH₃)₂Co{SSi(Odipp)₃}₂]·CH₂Cl₂ [159].
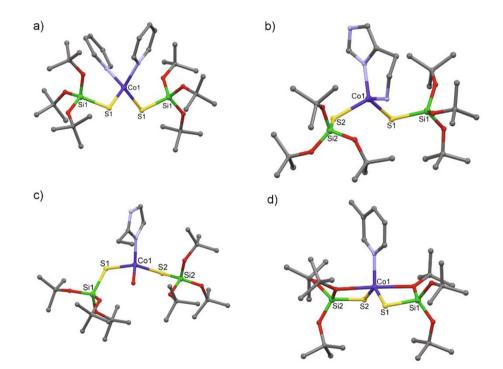
Fig. 30. Molecular structures of mononucleat Co(II) tri-*tert*-butoxysilanethiolates; H atoms are omitted for clarity.: a) [(py)₂Co{SSi(OtBu)₃}₂] [160]; b) [(him)Co{SSi(OtBu)₃}₂] [165]; c) [(2-Etim)(H₂O)Co{SSi(OtBu)₃}₂] [168]; d) [(3-Mepy)Co{SSi(OtBu)₃}₂] [162].

The use of 2-Etpy and 3,4-dMepy led to two complexes of the general formula [(NH₃)(L)Co{SSi(OtBu)₃}₂] with two different nitrogen ligands within the tetrahedral Co(II) coordination sphere [163,164]. The complexes were obtained using a molar ratio 1:2 of [{(NH₃)Co(μ-SSi(OtBu)₃)(SSi(OtBu)₃)}₂] and the N-donor ligand, respectively (Table XIV-14,15). These compounds are unstable at room temperature due to the fast elimination of ammonia and formation of penta-coordinated complexes with the formula [(L)Co{SSi(OtBu)₃}₂]. Interestingly, the pink-violet crystals of [(L)Co{SSi(OtBu)₃}₂] in ammonia atmosphere quickly turn into blue

tetrahedral ammonia complexes again, indicating the reversible character of the process [163].

In search of the spectroscopic models of alcohol dehydrogenase initiated by Becker in 2002 [158] several tetrahedral Co(II) tri-*tert*-butoxysilanethiolates were obtained with the use of chelating N,N- and N,O-donor ligands like histamine (him) (Fig. 30b) [165], 2-(2′-hydroxyethyl)pyridine (hypy) [166] and dmpda [167] (*e.g.* Table XIV-16–20) as well as various imidazole-based ligands (*e.g.* Table XIV-21) [27]. Within these studies two Co(II) tri-*tert*-butoxysilanethiolates [(H₂O)(L)Co{SSi(OtBu)₃}₂] (L = 2-Mepy, 2-
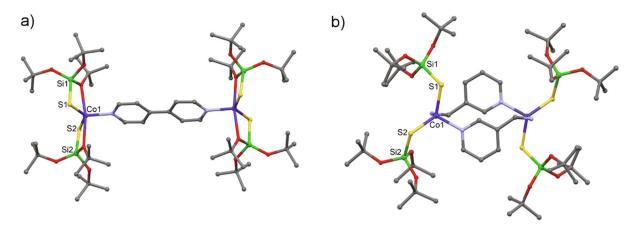
Fig. 31. Molecular structures of dinuclear Co(II) tri-*tert*-butoxysilanethiolates without hydrogen atoms: a) [(μ-4,4′-bipy)(Co{SSi(O*t*Bu)$_3$}$_2$)$_2$] [169]; b) [{(μ-3-AMP)Co{SSi-(O*t*Bu)$_3$}$_2$}$_2$] [28].
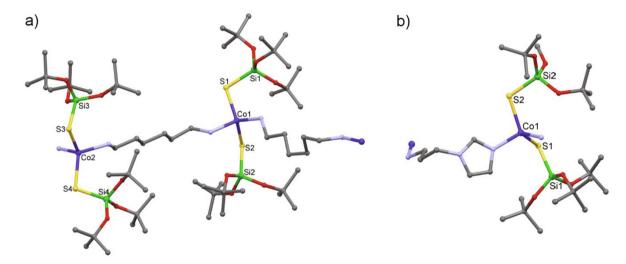
Fig. 32. Molecular structures of polynuclear Co(II) tri-*tert*-butoxysilanethiolates without hydrogen atoms: a) [Co{SSi(O*t*Bu)$_3$}$_2$(pda)$_2$CH$_3$OH]$_n$ [167]; b) [Co{SSi(O*t*Bu)$_3$}$_2$(μ-api)]$_n$ [172].
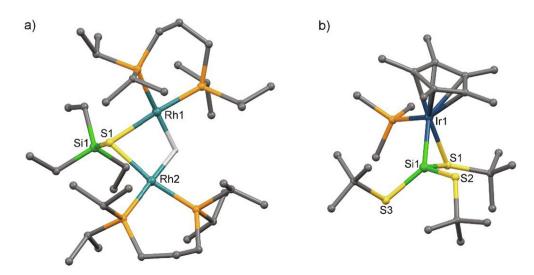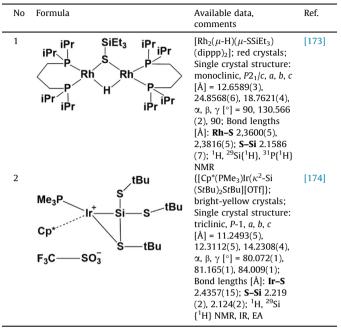
Fig. 33. Molecular structures of ruthenium and iridium silanethiolates; hydrogen atoms are omitted for clarity: a) [Rh$_2$(μ-H)(μ-SSiEt$_3$)(dippp)$_2$] [173]; b) [Cp*(PMe$_3$)Ir(κ^2-Si-(S*t*Bu)$_2$S*t*Bu][OTf] [174].

Table XV
Formulas and general characteristics of the Group 9 silanethiolates described in chapter **3.6.2.**

No	Formula	Available data, comments	Ref.
1		[Rh$_2$(μ-H)(μ-SSiEt$_3$) (dippp)$_2$]; red crystals; Single crystal structure: monoclinic, $P2_1/c$, a, b, c [Å] = 12.6589(3), 24.8568(6), 18.7621(4), α, β, γ [°] = 90, 130.566 (2), 90; Bond lengths [Å]: **Rh–S** 2,3600(5), 2,3816(5); **S–Si** 2.1586 (7); ^{1}H, ^{29}Si{^{1}H}, ^{31}P{^{1}H} NMR	[173]
2		{[Cp*(PMe$_3$)Ir(κ^2-Si (StBu)$_2$StBu][OTf]}; bright-yellow crystals; Single crystal structure: triclinic, P-1, a, b, c [Å] = 11.2493(5), 12.3112(5), 14.2308(4), α, β, γ [°] = 80.072(1), 81.165(1), 84.009(1); Bond lengths [Å]: **Ir–S** 2.4357(15); **S–Si** 2.219 (2), 2.124(2); ^{1}H, ^{29}Si {^{1}H} NMR, IR, EA	[174]

Etim) with tetrahedral CoNOS$_2$ cores and water molecules bonded to the cobalt atom were obtained (Fig. 30c, Table XIV-16, 17) [158,168]. For the overall discussion of the results of these studies see the review by Dołęga [22].

The use of py, 2-Mepy, 3-Mepy, 4-Mepy, 2,5-dMepy and 3,5-dMepy as co-ligands allowed the isolation of pink-violet crystals of penta-coordinated Co(II) compounds of the general formula [(L)Co{SSi(OtBu)$_3$}$_2$] exhibiting a CoNO$_2$S$_2$ core. The Co(II) ions in these complexes approach highly distorted trigonal bipyramidal geometries being coordinated by one N-donor ligand and two TBST residues acting as O,S-chelating ligands (e.g. Fig. 30d, Table XIV-22–24). The usual method of their synthesis employed slow diffusion of the vapors of pyridine derivatives into the hexane solution of the substrate: [(NH$_3$)Co(μ-SSi(OtBu)$_3$)(SSi(OtBu)$_3$)}$_2$] [160,162,163].

Several dinuclear Co(II) tri-$tert$-butoxysilanethiolate complexes were obtained in the reaction of [(NH$_3$)Co(μ-SSi(OtBu)$_3$)(SSi-(OtBu)$_3$)}] with bidentate N,N'-donor ligands. These complexes of the general formula: [(μ-L)(Co{SSi(OtBu)$_3$}$_2$)$_2$], where L = pyr, qx, 4,4'-bipy, bpe and azpy, are all characterized by two pentacoordinated Co(II) ions with trigonal-bypiramidal geometry of CoNO$_2$S$_2$ coordination cores and two TBST residues coordinating to Co(II) in O,S-chelating manner; the metal ions are linked by the nitrogen spacer ligand (e.g. Table XIV-25–28) [169–171]. Interestingly the reaction with 4,4'-bipy led to two products that crystallize from the same reaction mixture; brown and violet crystals were polymorphs of [(μ-4,4'-bipy)(Co{SSi(OtBu)$_3$}$_2$)$_2$] (Fig. 31a) which differed only in the dihedral angle of the pyridyl rings within the 4,4'-bipy bridging molecules [169]. Among bimetallic Co(II) tri-$tert$-butoxysilanethiolates there are also examples of complexes with tetrahedral CoN$_2$S$_2$ cores doubly bridged by bbi [172] or 3-AMP (Fig. 31b, Table XIV-29,30) [28]. The first compound: [{(μ-bbi)Co{SSi(OtBu)$_3$}$_2$}$_2$]·3CH$_3$OH crystallizes with methanol molecules engaged in the formation of a net of hydrogen bonding interactions which, together with the additional weak C–H···O and C–H···π interactions, allow the molecules to be arranged as a chain of dimers [172]. On the contrary the complex {[(μ-3-AMP)-Co{SSi(OtBu)$_3$}$_2$]$_2$} crystallizes without any solvent (Fig. 31b) [28].

Reaction of [{(NH$_3$)Co(μ-SSi(OtBu)$_3$)(SSi(OtBu)$_3$)}$_2$] with 4,4'-bipy carried out in hexane most probably produced the first Co (II) silanethiolate coordination polymer in the form of a green powder. The compound was characterized with IR-, UV–Vis spectroscopy and elemental analysis to give the tentative formula [(μ-4,4'-bipy)Co{μ-SSi(OtBu)$_3$}{SSi(OtBu)$_3$}]$_n$ (Table XIV-31) [169]. Attempts to produce polymeric complexes were continued with the use of aliphatic diamines, such as pda and hda [167]. In two obtained 1D coordination polymers: [(pda)$_2$Co{SSi(OtBu)$_3$}$_2$·CH$_3$-OH]$_n$ and [(hda)$_2$Co{SSi(OtBu)$_3$}$_2$·CH$_3$OH]$_n$ (Fig. 32a, Table XIV-32,33) the pda and hda molecules link the Co(II) ions, while bulky silanethiolate anions (tBuO)$_3$SiS$^-$ serve as terminal ligands. The polymeric chains adopt different topologies: in the crystals of the pda-based polymer 3D channels are formed via hydrogen bonding interactions with the solvent, while complex [(hda)$_2$Co{SSi-(OtBu)$_3$}$_2$·CH$_3$OH]$_n$ forms infinite, folded chains with no H-bond interactions between them [167]. In 2017 and 2020 similar 1D coordination polymers were obtained in the reactions of api and 4AMP with [{(NH$_3$)Co(μ-SSi(OtBu)$_3$)(SSi(OtBu)$_3$)}$_2$] carried out in methanol (4:1 M ratio): [(μ-api)Co{SSi(OtBu)$_3$}$_2$]$_n$ and [(μ-4-AMP)-Co{SSi(OtBu)$_3$}$_2$]$_n$ (Fig. 32b, Table XIV-34,35) [28,172].

3.6.2. Rh and Ir silanethiolates

There is only one rhodium silanethiolate reported so far and it was obtained within the research project exploring ways of defluorination of SF$_6$ and RSF$_5$ organyl compounds to sulfide species under mild conditions. Hence, during the reaction of SF$_6$ at the rhodium complex [{Rh(μ-H)(dippp)}$_2$] in the presence of Et$_3$SiH red crystals of the dinuclear complex [Rh$_2$(μ-H)(μ-SSiEt$_3$)(dippp)$_2$] are formed along with FSiEt$_3$ and H$_2$ (Fig. 33a, Table XV-1) [173]. The reaction of the complex with HCl leads to the formation of the chloride compound [{Rh(μ-Cl)(dippp)}$_2$], H$_2$S, H$_2$ and ClSiEt$_3$. The same complex was also identified as one of the products during the activation of CF$_3$SF$_5$ in the presence of Et$_3$SiH which allowed to the cleavage of both: S–F and CS bonds. The molecular structure of the complex revealed two Rh atoms adopting distorted square-planar geometry being coordinated by 1,3-bis(diisopropyl phosphanyl)propane in a chelating manner and the bridging hydride and silanethiolato residues. The Rh–S distance of 2.9162 (2) Å is shorter than the sum of the covalent radii, while the S–Si distance (2.1586(7) Å) is close to the average S–Si bond length (2.19 Å) [173].

In 2002 the only known iridium silylthiolate complex was reported [174]. The yellow powder - product of the reaction between CH$_2$Cl$_2$ solution of {[Cp*(PMe$_3$)Ir(Me)][OTf]} with (tBuS)$_3$-SiH - gives, after recrystallization from a CH$_2$Cl$_2$/pentane mixture at 238 K bright yellow crystals of [Cp*(PMe$_3$)Ir(κ^2-Si(StBu)$_2$StBu] [OTf] (Fig. 33b, Table XV-2). The activation of Si–H bonds usually leads to silyl iridium derivatives with a complete migration of the thiolato group from silicon to iridium, but in this case it was not observed. The compound consists of a cationic iridium complex and a TfO$^-$ counter ion. The structure of the cationic part of the compound involves a dative interaction between one of the $tert$-butylthiolato groups at the silicon atom and the iridium center. As a result, a three-membered IrSiS ring forms. Ir–S bond length (2.4357(15) Å) is almost the same as d_{cov} of Ir and S (2.46 Å), whereas the S–Si bond that resides in the ring is significantly longer than the average S–Si bond length and thus longer than the other S–Si bonds present in the complex (Fig. 33b, Table XV-2) [174].

Table XVI
Formulas and general characteristics of the nickel silanethiolates described in chapter 3.7.1.

No	Formula	Available data, comments	Ref.
1		[(tmeda)Ni(SSiPh$_3$)$_2$]·2CH$_2$Cl$_2$; yellow crystals; Single crystal structure: monoclinic, $C2/c$, a, b, c [Å] = 35.806(6), 11.0410(8), 27.789(5), α, β, γ [°] = 90, 122.860(7), 90; Bond lengths [Å]: **Ni–S** 2.271(2), 2.276(2); **S–Si** 2.100(2), 2.110(2); ^{1}H NMR, IR, UV–Vis, EA	[124]
2		[(dppe)Ni(SSiMe$_3$)$_2$]; purple crystals; Single crystal structure: monoclinic, $P2_1/c$, a, b, c [Å] = 10.309(6), 27.50(2), 13.133(8), α, β, γ [°] = 90, 110.341(7), 90; Bond lengths [Å]: **Ni–S** 2.250(1), 2.231(1); **S–Si** 2.136(2), 2.115(2); ^{1}H NMR, IR, EA	[7]
3		[(dppe)Ni(SSiMe$_2$tBu)$_2$]; dark-purple crystals; Single crystal structure: monoclinic, $P2_1/c$, a, b, c [Å] = 10.802(2), 26.287(4), 14.132(2), α, β, γ [°] = 90, 92.561(3), 90; Bond lengths [Å]: **Ni–S** 2.253(2), 2.246(2); **S–Si** 2.127(2), 2.131(2); ^{1}H NMR, IR, EA	[7]
4		[Ni(μ-Br)(μ-SSitBu$_3$)]$_{12}$(C$_6$H$_{14}$)$_n$; red crystals; Single crystal structure: hexagonal, $P6_3mc$, a, c [Å] = 26.128(16), 24.69(2), α, β, γ [°] = 90, 90, 120; Bond lengths [Å]: **Ni–S** 2.229(5), 2.350(7), 2.247(6), 2.277(6), 2.275(6), 2.230(5); **S–Si** 2.225(10), 2.235(7), 2.287(10); ^{1}H NMR, IR, EA	[129,153]
5		[{Ni(μ-SSitBu$_3$)}$_5$(μ$_5$-S)]; red rod-like crystals; Single crystal structure: monoclinic, $P2_1/n$, a, b, c [Å] = 14.193(8), 16.493(10), 36.54(2), α, β, γ [°] = 90, 98.564(11), 90; Bond lengths [Å]: **Ni–S** 2.180(4), 2.185(4), 2.186(4), 2.188(4), 2.190(4), 2.197(4), 2.198(4), 2.198(4), 2.198(4), 2.202(4); **S–Si** 2.195(5), 2.216(6), 2.199(5), 2.203(6), 2.219(6); ^{1}H NMR	[153]
6		[(py)Ni{SSi(OtBu)$_3$}$_2$]; violet crystals; Single crystal structure: tetragonal, $I4$, a, b, c [Å] = 29.900(4), 29.900(4), 8.8450(18), α, β, γ [°] = 90, 90, 90; Bond lengths [Å]: **Ni–S** 2.302(8), 2.311(8); **S–Si** 2.075(2), 2.071(2); IR, UV–Vis, EA	[175]
7		[(2-Mepy)$_2$Ni{SSi(OtBu)$_3$}$_2$]; violet crystals; Single crystal structure: triclinic, P-1, a, b, c [Å] = 9.1388(6), 9.4625(6), 14.6865(11), α, β, γ [°] = 77.324(6), 75.767(6), 62.410(7); Bond lengths [Å]: **Ni–S** 2.253(2); **S–Si** 2.075(2); IR, UV–Vis, EA	[175]
8		{[(3,5-dMepy)$_2$(H$_2$O)Ni{SSi(OtBu)$_3$}$_2$](bz)}; dark-violet crystals; Single crystal structure: orthorhombic, $Pbca$, a, b, c [Å] = 16.1204(4), 20.5424(4), 31.5906(11), α, β, γ [°] = 90, 90, 90; Bond lengths [Å]: **Ni–S** 2.385(4), 2.420(4); **S–Si** 2.068(2), 2.050(2); IR, EA	[175]
9		{[(NH$_3$)Ni(Odipp)]$_2$·CHCl$_3$}; deep-violet crystals; Single crystal structure: monoclinic, $P2_1/c$, a, b, c [Å] = 14.3971(7), 17.3487(12), 16.9667(10), α, β, γ [°] = 90, 97.240(5), 90; Bond lengths [Å]: **Ni–S** 2.2623(7); **S–Si** 2.0771(9); IR, UV–Vis, magn. susc., EA	[159]

Table XVI (*continued*)

No	Formula	Available data, comments	Ref.
10		[(μ-prda)$_2$Ni{SSi(OtBu)$_3$}$_2$]; blue crystals; Single crystal structure: monoclinic, $P2_1/n$, a, b, c [Å] = 13.7931(7), 12.4749(6), 25.3305(12), α, β, γ [°] = 90, 94.231(4), 90; Bond lengths [Å]: **Ni–S** 2.5070(19), 2.5741(19); **S–Si** 2.064(3), 2.055(3); IR, UV–Vis, HFEPR, EA	[176]
11		[(μ-bda)$_2$Ni{SSi(OtBu)$_3$}$_2$(CHCl$_3$)]$_n$; deep-violet powder; IR, UV–Vis, TG, TG-FTIR, EA	[176]
12		[(μ-pda)$_2$Ni{SSi(OtBu)$_3$}$_2$(CHCl$_3$)]$_n$; deep-violet powder; IR, EA	[176]
13		[(μ-hda)$_2$Ni{SSi(OtBu)$_3$}$_2$]$_n$; deep-violet crystals; Single crystal structure: triclinic, P-1, a, b, c [Å] = 8.7740(6), 9.3769(9), 14.3325(13), α, β, γ [°] = 99.828(8), 102.707(7), 104.192(7); Bond lengths [Å]: **Ni–S** 2.2472(15); **S–Si** 2.085(2); IR, UV–Vis, TG, TG-FTIR, EA	[176]
14		[(μ-hpda)$_4$Ni{SSi(OtBu)$_3$}$_2$]$_n$; blue crystals; Single crystal structure: triclinic, P-1, a, b, c [Å] = 9.6544(4), 10.2058(4), 14.2556(5), α, β, γ [°] = 101.887(3), 99.904(3), 109.865(3); Bond lengths [Å]: **Ni–S** 2.5045(5), **S–Si** 2.0579(8); IR, UV–Vis, HF EPR, EA	[176]
15		[(μ-api)Ni{SSi(OtBu)$_3$}$_2$]$_n$; blue crystals; Single crystal structure: monoclinic, $P2_1/c$, a, b, c [Å] = 14.3711(16), 11.9655(8), 9.5370(11); α, β, γ [°] = 90, 103.618(9), 90; Bond lengths [Å]: **Ni–S** 2.2651(10), 2.2905(11); **S–Si** 2.0870(15), 2.0840(15); IR, TG, TG-FTIR, magn. susc., EA	[172]
16		[(H$_2$O)$_6$(NH$_3$)$_4$Ni$_6$(μ-O)$_6${SSi(OtBu)$_3$}$_6$]; green crystals; Single crystal structure: triclinic, P-1, a, b, c [Å] = 15.5475(6), 16.1036(8), 25.7393(12), α, β, γ [°] = 77.544(4), 74.867(4), 82.644(4); Bond lengths [Å]: **Ni–S** 2.4557(14); 2.4501(13), 2.4443(16), 2.4560(17), 2.4730(16), 2.4253(14); **S–Si** 2.072(2), 2.073(2), 2.0749(12), 2.068(2), 2.066(2), 2.071(2); IR, magn. susc., EA	[177]

3.7. Group 10 elements

3.7.1. Nickel silanethiolates

The development of new synthetic strategies towards metal-sulfido clusters include the synthesis of Ni(II) silanethiolate complexes and investigations of their reactivity as potential precursors towards heterometallic sulfido clusters. As a part of this research the tetrahedral Ni(II) silanethiolate complex, [(tmeda)Ni(SSiPh$_3$)$_2$]·2CH$_2$Cl$_2$ was obtained in the reaction of triphenylsilanethiol with a solution of [Ni(NPh$_2$)]$_2$ in toluene in the presence of tmeda (Table XVI-1) [124]. Similar Ni(II) complexes: [(dppe)Ni(SSiMe$_3$)$_2$] and [(dppe)Ni(SSiMe$_2$$t$Bu)$_2$] were reported in 2004 (Table XVI-

2,3) [7]. Purple crystals of the trimethylsilanethiolate complex were obtained from a reaction of an Et$_2$O solution of LiSSiMe$_3$, prepared *in situ* from cyclotrisilthiane and methyllithium with a solution of [(dppe)NiCl$_2$]. Dark-purple crystals of the *tert*-butyldimethylsilanethiolate compound were synthesized using the same Ni(II) precursor and a solution of [{(tmeda)LiSSiMe$_2$$t$Bu}$_2$] dissolved in THF. Molecules of both complexes exhibit a distorted square planar geometry at Ni(II). The reactivity of the complexes was investigated by a reaction with [(Cp)TiCl$_3$]. Compound [(dppe)Ni(SSiMe$_3$)] was found to react with the titanium complex in toluene at RT with the clean formation of the heterobimetallic complex [(Cp)TiCl(μ-S)$_2$Ni(dppe)] in 66% yield. In turn, the reaction
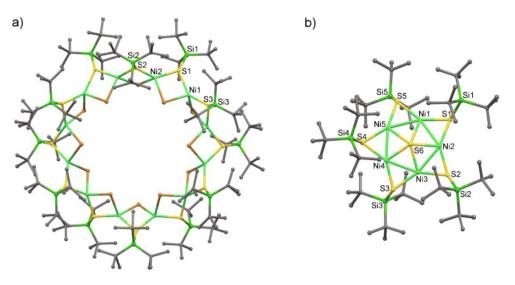
Fig. 34. Molecular structures of Ni(II) tri-*tert*-butylsilanethiolate complexes; H atoms and solvent molecules omitted: a) [{Ni(μ-Br)(μ-SSi*t*Bu$_3$)}$_{12}$] (hexane)$_n$; b) [{Ni(μ-SSi*t*Bu$_3$)}$_5$(μ_5-S)] [129,153].
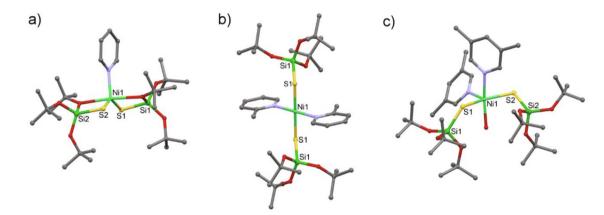
Fig. 35. Molecular structures of mononuclear Ni(II) tri-*tert*-butoxysilanethiolates; H atoms and solvent molecules omitted: a) [(py)Ni{SSi(O*t*Bu)$_3$}$_2$]; b) [(2-Mepy)$_2$Ni{SSi-(O*t*Bu)$_3$}$_2$]; c) [(3,5-dMePy)$_2$(H$_2$O)Ni{SSi(O*t*Bu)$_3$}$_2$]·bz [175].

of [(dppe)Ni(SSiMe$_2$*t*Bu)] with (Cp)TiCl$_3$ gives the same complex along with different, unidentified products [7]. The S–Si bond lengths in all three compounds mentioned above are slightly shorter in comparison with the average S–Si bond distance

(2.19 Å), whereas Ni–S distances are longer than the sum of covalent radii of Ni and S atoms (2.13 Å).

A Ni-based cyclic oligomer, realized *via* the aggregation of [(*t*Bu$_3$SiS)NiBr] units was reported by Sydora and co-workers
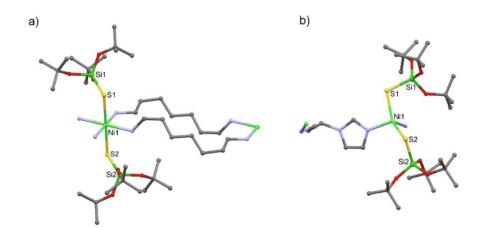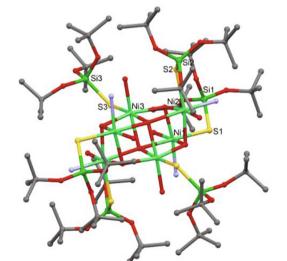
Fig. 36. Molecular structures of Ni(II) tri-*tert*-butoksysilanethiolates with 1D polymeric structures; H atoms omitted for clarity: a) [(μ-hpda)$_4$Ni{SSi(O*t*Bu)$_3$}$_2$]$_n$ [176]; b) [(μ-api)Ni{SSi(O*t*Bu)$_3$}$_2$]$_n$ [172].

[129,153]. The twelve-membered wheel [Ni(μ-Br)(μ-SSitBu$_3$)]$_{12}$ (hexane)$_n$ was synthesized in the reaction of NiBr$_2$ with NaSSitBu$_3$ in THF. The thermolysis at 361 K led to the formation of a red–purple solid, which, after washing with Et$_2$O gave crystals of dimeric [{Ni(μ-SSitBu$_3$)(SSitBu$_3$)}$_2$], while further extraction of the green residue with hexane led to red crystals of [Ni(μ-Br)(μ-SSitBu$_3$)]$_{12}$(hexane)$_n$, isolated with 17% yield (Table XVI-4). The wheel is similar to the cobalt analogue described in chapter 3.6.1.1 with the structure based on edge-sharing tetrahedra (Fig. 34a). Interestingly, when the thermolysis is carried out at higher temperature (403 K), the red rods of [{Ni(μ-SSitBu$_3$)}$_5$(μ_5-S)] are isolated in 75% yield (Table XVI-5) [153]. The obtained complex contains mixed-valence Ni(II)$_2$Ni(I)$_3$ and has the form of a symmetric star (Fig. 34b). Both compounds have Ni–S bonds a bit longer than average Ni–S bond lengths (2.13 Å). The S–Si distances are, in case of the wheel, slightly longer, whereas in the symmetric star they are close to the sum of the covalent radii of Si and S (2.19 Å) (Table XVI-4,5).

Among tri-*tert*-butoxysilanethiolate Ni(II) complexes, there are several examples of mononuclear or polynuclear ones. In contrast to Co(II) derivatives described in chapter 3.6.1, only one probable dinuclear Ni(II) complex was obtained. All of the complexes were synthesized at atmospheric conditions and in the majority they are quite stable. A considerable number of mononuclear heteroleptic Ni(II) tri-*tert*-butoxysilanethiolates was described over the last ten years. The studies were essentially devoted to the search of Ni(II) complexes with S-thiolate and N-donor ligands that may serve as a biomimetic model for the active site of nickel-containing metalloproteins. The first three complexes: [(py)Ni{SSi-(OtBu)$_3$}$_2$], [(2-Mepy)$_2$Ni{SSi(OtBu)$_3$}$_2$] and [(3,5-dMepy)$_2$(H$_2$O)Ni-{SSi(OtBu)$_3$}$_2$]·bz (Fig. 35a-c, Table XVI-6–9) were obtained from a reaction of pyridine and its derivatives 2-Mepy and 3,5-dMepy with NiCl$_2$ and TBST in water in 4:1:2 M ratio. [(py)Ni{SSi-(OtBu)$_3$}$_2$], obtained as violet crystals show the typical transition metal tri-*tert*-butoxysilanethiolate unit with two S,O-chelating TBST residues and one molecule of pyridine (Fig. 35a, Table XVI-6). In [(2-Mepy)$_2$Ni{SSi(OtBu)$_3$}$_2$] the NiN$_2$S$_2$ core adopts a square-planar geometry (Fig. 35b, Table XVI-7), while [(3,5-dMepy)$_2$(H$_2$O)Ni{SSi(OtBu)$_3$}$_2$]·bz contains penta-coordinated Ni(II) with distorted tetragonal pyramidal NiN$_2$OS$_2$ environment (Fig. 35c, Table XVI-8). In contrast to the previous two compounds, the last complex is unstable under atmospheric conditions. The

Ni–S bond distances in the mononuclear complexes are significantly elongated, while the S–Si bond distances are shorter than the average bond lengths of Ni–S and S–Si bonds (2.13 Å and 2.19 Å, respectively) [175]. One more example of a square planar silanethiolate Ni(II) complex: *trans*-[{(NH$_3$)Ni(Odipp)}$_2$]·CHCl$_3$ (Table XVI-9) was described in 2014, where magnetic studies confirmed the diamagnetic property of the complex [159].
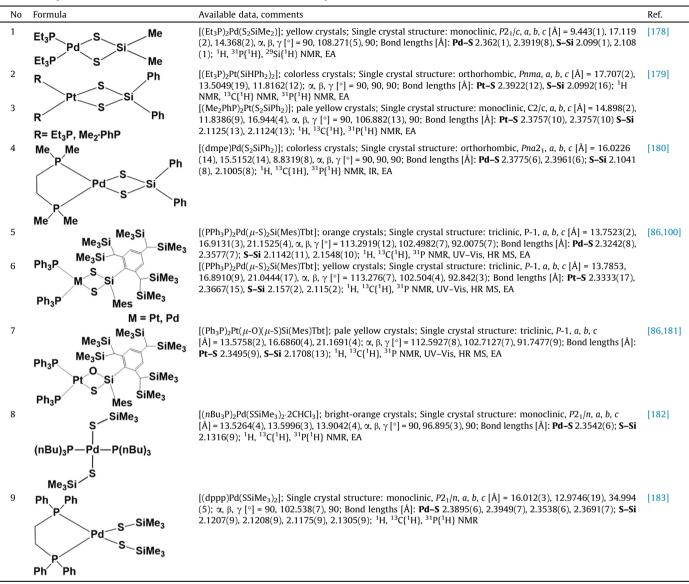
In 2016 an attempt to prepare a counterpart of the Co(II) dimer [{(NH$_3$)Co(μ-SSi(OtBu)$_3$)(SSi(OtBu)$_3$)}$_2$] was undertaken and the reaction of NiCl$_2$·6H$_2$O in water with tri-*tert*-butoxysilanethiol and an excess of NH$_3$ was investigated. The green precipitate was recrystallized from hexane and IR spectra and elemental analysis indicated the formation of [(H$_2$O)(NH$_3$)Ni{SSi(OtBu)$_3$}$_2$] [176]. The complex was further applied as a Ni(II) substrate in reactions with several diamines of variable length of the spacer chain (C$_3$H$_6$ to C$_7$H$_{14}$): prda, bda, pda, hda, hpda (Table XVI-10–14). The use of the shortest diamine prda (1,3-diaminopropane) gives blue crystals of [(μ-prda)$_2$Ni{SSi(OtBu)$_3$}$_2$], in which the Ni(II) ions are coordinated by two molecules of chelating diamine and two S-donor TBST residues adopting the distorted octahedral NiN$_4$S$_2$ core (Table XVI-10). High-field HF EPR spectra allowed to determine its spin Hamiltonian parameters g, D, and E. Reactions of [(H$_2$O)-(NH$_3$)Ni{SSi(OtBu)$_3$}$_2$] with longer diamines like hda or hpda lead to 1-D coordination polymers: doubly-bridged [(μ-hda)$_2$Ni{SSi-(OtBu)$_3$}$_2$]$_n$ and even quadruply-bridged [(μ-hpda)$_4$Ni{SSi-(OtBu)$_3$}$_2$]$_n$, respectively (Fig. 36a, Table XVI-13,14). In [(μ-hda)$_2$Ni{SSi(OtBu)$_3$}$_2$]$_n$ nickel(II) adopted a square-planar NiN$_2$S$_2$ core, while the [(μ-hpda)$_4$Ni{SSi(OtBu)$_3$}$_2$]$_n$ displayed a distorted *trans*-octahedral NiN$_4$S$_2$ coordination center; in both cases, the TBST anions coordinate to Ni(II) as S-terminal ligands. Compounds were stable under atmospheric conditions, however blue crystals of [(μ-hpda)$_4$Ni{SSi(OtBu)$_3$}$_2$]$_n$ turned deep-violet under heating, which hints to a change of the composition and/or geometry [176].

The first example of a Ni(II) silanethiolate with tetrahedral geometry was reported in 2017 [172]. The reaction of NiCl$_2$·6H$_2$O with api, TBST and an excess of ammonia solution resulted in a blue solid which, on recrystallization from methanol, gave blue crystals of polynuclear [(μ-api)Ni{SSi(OtBu)$_3$}$_2$]$_n$. Ni(II) ions in [(μ-api)Ni{SSi(OtBu)$_3$}$_2$]$_n$ are coordinated terminally by two S atoms from the TBST residues and two N atoms from two api molecules acting as bridges between neighboring metal centers (Table XVI-15, Fig. 36b). The resulted 1D polymeric chain is strongly folded due to the presence of N–H⋯O hydrogen bonds as well as C–H⋯π interactions within the structure. The complex is isostructural with its Co(II) analogue. The magnetic analysis points to the presence of weak magnetic coupling between Ni(II) ions from neighboring chains [172].

With the use of TBST a different supramolecular arrangement of Ni(II) ions was also achieved. Dicubane shaped [(H$_2$O)$_6$(NH$_3$)$_4$Ni$_6$-(μ-O)$_6${SSi(OtBu)$_3$}$_6$] was isolated as green crystals from the reaction of NiCl$_2$·6H$_2$O with two equivalents of TBST and an excess of ammonia in water and subsequent recrystallization from hexane. The hexanuclear complex, which may be described as a face-sharing double cubane, contains Ni(II) centers with different coordination motifs NiO$_5$S and NiO$_4$NS (Table XVI-16, Fig. 37). The Ni–Ni distances are in the range 3.062–3.262 Å. The magnetic susceptibility studies showed strong antiferromagnetic interactions between the six Ni(II) ions which led to a zero total spin ground state [177].

3.7.2. Palladium and platinum silanethiolates

The few known Pd and Pt silanethiolates were usually investigated towards their potential application as cluster precursors. The first example of a Pd(II) silanedithiolate was obtained in the reaction between Pd(OAc)$_2$ and *cyclo*-(SSiMe$_2$)$_3$ in the presence of PEt$_3$ [178]. Thereby, yellow crystals of [(Et$_3$P)$_2$Pd(S$_2$SiMe$_2$)], were

Fig. 37. Molecular structure of Ni(II) cluster [(H$_2$O)$_6$(NH$_3$)$_4$Ni$_6$(μ-O)$_6${SSi(OtBu)$_3$}$_6$] without hydrogen atoms [177].

Table XVII
Formulas and general characteristics of the nickel silanethiolates described in chapter 3.7.2.

No	Formula	Available data, comments	Ref.
1	Et₃P–Pd(S₂SiMe₂)	[(Et₃P)₂Pd(S₂SiMe₂)]; yellow crystals; Single crystal structure: monoclinic, $P2_1/c$, a, b, c [Å] = 9.443(1), 17.119(2), 14.368(2), α, β, γ [°] = 90, 108.271(5), 90; Bond lengths [Å]: **Pd–S** 2.362(1), 2.3919(8), **S–Si** 2.099(1), 2.108(1); ¹H, ³¹P{¹H}, ²⁹Si{¹H} NMR, EA	[178]
2	R–Pt(SiHPh₂)₂	[(Et₃P)₂Pt(SiHPh₂)₂]; colorless crystals; Single crystal structure: orthorhombic, *Pnma*, a, b, c [Å] = 17.707(2), 13.5049(19), 11.8162(12); α, β, γ [°] = 90, 90, 90; Bond lengths [Å]: **Pt–S** 2.3922(12), **S–Si** 2.0992(16); ¹H NMR, ¹³C{¹H} NMR, ³¹P{¹H} NMR, EA	[179]
3	R= Et₃P, Me₂·PhP	[(Me₂PhP)₂Pt(S₂SiPh₂)]; pale yellow crystals; Single crystal structure: monoclinic, C2/c, a, b, c [Å] = 14.898(2), 11.8386(9), 16.944(4), α, β, γ [°] = 90, 106.882(13), 90; Bond lengths [Å]: **Pt–S** 2.3757(10), 2.3757(10) **S–Si** 2.1125(13), 2.1124(13); ¹H, ¹³C{¹H}, ³¹P{¹H} NMR, EA	
4	(dmpe)Pd(S₂SiPh₂)	[(dmpe)Pd(S₂SiPh₂)]; colorless crystals; Single crystal structure: orthorhombic, *Pna2₁*, a, b, c [Å] = 16.0226(14), 15.5152(14), 8.8319(8), α, β, γ [°] = 90, 90, 90; Bond lengths [Å]: **Pd–S** 2.3775(6), 2.3961(6); **S–Si** 2.1041(8), 2.1005(8); ¹H, ¹³C{1H}, ³¹P{¹H} NMR, IR, EA	[180]
5		[(PPh₃P)₂Pd(μ-S)₂Si(Mes)Tbt]; orange crystals; Single crystal structure: triclinic, P-1, a, b, c [Å] = 13.7523(2), 16.9131(3), 21.1525(4), α, β, γ [°] = 113.2919(12), 102.4982(7), 92.0075(7); Bond lengths [Å]: **Pd–S** 2.3242(8), 2.3577(7); **S–Si** 2.1142(11), 2.1548(10); ¹H, ¹³C{¹H}, ³¹P NMR, UV–Vis, HR MS, EA	[86,100]
6	M = Pt, Pd	[(PPh₃P)₂Pd(μ-S)₂Si(Mes)Tbt]; yellow crystals; Single crystal structure: triclinic, P-1, a, b, c [Å] = 13.7853, 16.8910(9), 21.0444(17), α, β, γ [°] = 113.276(7), 102.504(4), 92.842(3); Bond lengths [Å]: **Pt–S** 2.3333(17), 2.3667(15), **S–Si** 2.157(2), 2.115(2); ¹H, ¹³C{¹H}, ³¹P NMR, UV–Vis, HR MS, EA	
7		[(Ph₃P)₂Pt(μ-O)(μ-S)Si(Mes)Tbt]; pale yellow crystals; Single crystal structure: triclinic, *P*-1, a, b, c [Å] = 13.5758(2), 16.6860(4), 21.1691(4); α, β, γ [°] = 112.5927(8), 102.7127(7), 91.7477(9); Bond lengths [Å]: **Pt–S** 2.3495(9), **S–Si** 2.1708(13); ¹H, ¹³C{¹H}, ³¹P NMR, UV–Vis, HR MS, EA	[86,181]
8	(nBu)₃P–Pd–P(nBu)₃	[(nBu₃P)₂Pd(SSiMe₃)₂·2CHCl₃]; bright-orange crystals; Single crystal structure: monoclinic, $P2_1/n$, a, b, c [Å] = 13.5264(4), 13.5996(3), 13.9042(4), α, β, γ [°] = 90, 96.895(3), 90; Bond lengths [Å]: **Pd–S** 2.3542(6); **S–Si** 2.1316(9); ¹H, ¹³C{¹H}, ³¹P{¹H} NMR, EA	[182]
9	(dppp)Pd(SSiMe₃)₂	[(dppp)Pd(SSiMe₃)₂]; Single crystal structure: monoclinic, $P2_1/n$, a, b, c [Å] = 16.012(3), 12.9746(19), 34.994(5); α, β, γ [°] = 90, 102.538(7), 90; Bond lengths [Å]: **Pd–S** 2.3895(6), 2.3949(7), 2.3538(6), 2.3691(7); **S–Si** 2.1207(9), 2.1208(9), 2.1175(9), 2.1305(9); ¹H, ¹³C{¹H}, ³¹P{¹H} NMR	[183]

Fig. 38. Molecular structures of Pd(II) and Pt(II) complexes with Tbt protected S–Si bonds; H-atoms are omitted for clarity: a) [(Ph₃P)₂Pd(μ-S)₂Si(Mes)Tbt] [86,100]; b) [(Ph₃P)₂Pt(PPh₃)₂(μ-O)(μ-S)Si(Mes)Tbt] [86,181].

collected with 88% yield, showing a planar complex with Pd(II) ions coordinated by a $Me_2SiS_2^{2-}$ chelating ligand and two phosphane molecules (Table XVII-1). The reactivity of the resulted complex was investigated in reaction with (Cp)TiCl$_3$ in toluene and as a result, yellow plates of the binuclear heterometallic complex [(Cp)TiCl(μ-S)$_2$Pd(PEt$_3$)$_2$] were obtained with good yield. The reaction with Cp$_2$TiCl$_2$ did not give any isolable product, while with TiCl$_4$(THF)$_2$ a yellow powder of [TiCl$_2$(S)(μ-S)$_2$Pd$_2$(PEt$_3$)$_4$] was formed with 84% yield. X-ray analysis revealed its heterometallic cluster structure with a TiPd$_2$ triangular core capped by two μ_3-sulfido ligands [178].

The bis(silyl)platinium(II) complex [(Et$_3$P)$_2$Pt(SiHPh$_2$)$_2$] was used as a substrate in reactions with organic isothiocyanates. As a result, the diphenylsilanedithiolato Pt(II) complexes of [(Et$_3$P)$_2$-Pt(SiHPh$_2$)$_2$] and [(Me$_2$PhP)$_2$Pt(S$_2$SiPh$_2$)] were obtained (Table XVII-2,3) [179]. The first of them was synthesized with the use of the Pt(II) substrate and PhNCS mixed in the 1:1 M ratio in THF. Recrystallization of the primary solid from an ether/CH$_2$Cl$_2$ mixture gave colorless crystals of the product. The use of p-tolylNCS in a similar reaction resulted in crystals of the same compound. The other complex was obtained from a mixture of dithiocarbonimidato derivative and unidentified oily materials, obtained from a reaction of [(Et$_3$P)$_2$Pt(SiHPh$_2$)$_2$] with p-tolylNCS and iPrNCS in a 1:1 M ratio in THF. A similar reaction was employed to prepare the diphenyl-silanedithiolato Pd(II) complex [(dmpe)Pd(S$_2$SiPh$_2$)] out of the bis(silyl) palladium(II) complex [(dmpe)Pd(SiHPh$_2$)$_2$] and isopropyl isothiocyanate at RT. The colorless solid obtained in THF was recrystallized from an ether/CH$_2$Cl$_2$ mixture (Table XVII-4) [180].

Two mononuclear Pd(II) and Pt(II) complexes were synthesized during studies on silanethiolates kinetically stabilized by large substituents at silicon, especially Tbt. The syntheses involved the reaction of a THF solution of the dilithium salt of silanedithiol, Tbt(Mes)Si(SLi)$_2$, generated in situ by the reaction of the corresponding silanedithiol with 2 equivalents of butyllithium, and a THF solution of cis-[(Ph$_3$P)$_2$PdCl$_2$] or cis-[(Ph$_3$P)$_2$PtCl$_2$] [86,100]. Orange crystals of [(Ph$_3$P)$_2$Pd(μ-S)$_2$Si(Mes)Tbt] or yellow crystals of the platinum analogue, [(PPh$_3$P)$_2$Pt(μ-S)$_2$Si(Mes)Tbt] are obtained via recrystallization from hexane/benzene or hexane, respectively. The X-ray analysis revealed the presence of folded, four-membered SiS$_2$Pd or SiS$_2$Pt rings, while the SiS$_2$Pd ring in [(Et$_3$P)$_2$Pd(S$_2$SiMe$_2$)], mentioned above (Table XVII-1), is almost planar. This is probably the result of steric repulsion between the bulky Tbt group and the triphenylphosphane moiety (Table XVII-5,6, Fig. 38a). Both compounds are air- and moisture resistant. Similar procedures were described for the synthesis of the Pt complex of the stable hydroxysilanethiol Tbt(Mes)Si(OH)(SH) (Table XVII-7, Fig. 38b) [86,181].

The first trans-palladium trimetylsilanethiolate complex [(nBu$_3$-P)$_2$Pd(SSiMe$_3$)$_2$]·2CHCl$_3$ was reported in 2010 as a result of a metathesis reaction of trans-[(nBu$_3$P)$_2$PdCl$_2$] and LiSSiMe$_3$ in THF at 273 K and recrystallization of the oily product from Et$_2$O/CHCl$_3$ at 193 K [182]. The Pd(II) atom in the complex display a slightly distorted square-planar geometry and retains the trans configuration of the substituens. (Table XVII-8). Similar reaction between [(dppp)Pd(OAc)$_2$] and LiSSiMe$_3$ yielded [(dppp)Pd(SSiMe$_3$)$_2$] (Table XVII-9) [183]. The reactivity of this square-planar complex was investigated in the reaction with [(MeCN)$_2$Mn(OTf)$_2$] in THF at RT, which gives the Mn-Pd-sulfide cluster, [MnOTf(THF)$_2$(μ_3-S)$_2$Pd$_2$(dppp)$_2$]OTf in 45% yield [183]. In both complexes the Pd–S bond lengths are longer than the average Pd–S bond distance, while the S–Si bond distance is slightly shorter or close to d$_{cov}$.

3.8. Group 11 elements (coinage metals)

All coinage metals usually form similar complexes with bulky silanethiolate ligands. Therefore we will discuss the elements

together and group them by similar coordination numbers, geometries and nuclearities.

3.8.1. Mononuclear silanethiolates of coinage metals

In general, it should be noted that the bonding between sulfur and the metal atom seems to become more ionic with increasing number of bonded ligands as observed by Chojnacki for the silanethiolates of the copper group [104]. He provided an explanation of this phenomenon with the use of B3LYP/6–31$^+$G(d) DFT calculations and NBO analysis indicating a greater population of the $\sigma^*_{S—M}$ orbital by lone pairs of the ligands [104]. Among group 11 silanethiolates C.N. = 2 is the most common and silver silanethiolates are probably the least stable and therefore less common with respect to Cu(I) and Au(I) compounds.

3.8.1.1. Complexes with C.N. = 2.
The first example of a group 11 silanethiolate was the Au(I) complex [Ph$_3$PAuSSi(SiMe$_3$)$_3$] reported by Arnold and co-workers [184]. It was synthesized from HSSi-(SiMe$_3$)$_3$ and [Ph$_3$PAuN(SiMe$_3$)$_2$] dissolved in ether, however, the composition was established by mass spectrometric and NMR spectroscopic investigations only and no structural data were available. The confirmation of the molecular structure of this first complex came over 20 years later in the work of Schnepf and co-workers (Table XVIII-1, Fig. 39a) [42]. Thus, the first fully characterized molecular gold(I) silanethiolate, [Ph$_3$PAuSSiPh$_3$] was synthesized and reported 1996 by Schmidbaur and co-workers [185] and was obtained in the reaction of triphenylsilanethiol with [Ph$_3$-PAu(acac)] in dichloromethane at RT. Thereby, silanethiol displaced the weaker acid acetylacetone and the product [Ph$_3$PAuSSiPh$_3$] was obtained as a colorless, light- and air-stable solid in moderate yield (Table XVIII-3, Fig. 39b). The atom of gold in both [Ph$_3$PAuSSi(SiMe$_3$)$_3$] and [(Ph$_3$PAuSSiPh$_3$] is linearly coordinated by S- and P-ligands and no aurophilic Au-Au contacts were observed [42,185]. It was initially emphasized [185] that whereas the Au—S and Au—P bond lengths were in the normal range, the angle at the sulfur atom (95,0(1)°) is significantly smaller than the values found for phosphanegold alkyl and aryl thiolates [e.g. [186]]. This is however a typical value, found later for many other silanethiolate complexes and in our opinion can be connected with the more ionic character of the S—Si bond compared to the S—C bond. In 2000 very similar examples of triphenylphosphanegold (I) silanethiolates were reported and all of them were characterized, showing small Au—S—Si angles in the range 96.30–97.95° [187]. The complexes were obtained by the reactions of [Ph$_3$PAuCl] with triethylammonium salts of three alkoxysilanethiols (RO)$_3$-SiSH, R = iPr, sBu, tBu. An example is presented in Fig. 39c and Table XVIII-4 [187]. In 2018 Schnepf and co-workers described the syntheses and structures of a variety of well-defined [R$_3$PAuSSi(SiMe$_3$)$_3$] precursors that contained a phosphane or a phosphite group (Table XVIII-15,16, Fig. 39d). The compounds were not only fully characterized but also further used for the synthesis of metalloid gold clusters [188].

A series of monomeric copper(I) silanechalcogenolates, namely [tBu$_3$PCuESiPh$_3$] (E = O, S, Se), was prepared from the reaction of [tBu$_3$Cu(CH$_3$CN)$_3$]BF$_4$ with [{Ph$_3$SiELi(THF)$_2$}$_2$] in acetonitrile. The compounds, that were meant to serve as building blocks to heterobimetallic complexes or as chemical vapor deposition precursors to copper chalcogenolates CuE, were colorless, crystalline, thermally labile solids [189]. The Cu atoms have a typical, linear or nearly linear, coordination geometry in all complexes. Interestingly for us, the authors interpreted the X-ray diffraction results of the complex [tBu$_3$PCuOSiPh$_3$] as having a linear Cu–O–Si angle, in contrast to the highly bent S and Se analogues. However, since the ellipsoid of the oxygen atom is large and the Cu—O distance is abnormally short (1.769(4) Å); the same is true about Si—O, in our opinion a disorder of the O atom over two equally occupied

Table XVIII

Formulas and general characteristics of the Cu, Ag, Au silanethiolates described in chapter 3.8.1.1.

No	Formula	Available data, comments	Ref.
1	Ph₃P—Au—S—Si(SiMe₃)₃	[Ph₃PAuSSi(SiMe₃)₃]; colorless crystals; Single crystal structure: monoclinic, $P2_1/c$, a, b, c [Å] = 9.5782(5), 11.2017(6), 31.6530(17), α, β, γ [°] = 90, 97.7190(10), 90; Bond lengths [Å] = **Au−S**, 2.2923(10), **S−Si**, 2.1481(15); ^{1}H, ^{13}C{^{1}H}, ^{31}P{^{1}H} NMR, IR, MS, EA	[42,184]
2	[CuSSiMe₃] and [BuCuSSiMe₃]Li	[CuSSiMe₃] and [BuCuSSiMe₃]Li; The complexes were assumed to form in ethereal or THF solutions (yellow to brown). They were not isolated and their presence was not confirmed by any spectroscopic method.	[193]
3	Ph₃P—Au—S—SiPh₃	[Ph₃PAuSSiPh₃]; colorless crystals; Single crystal structure: monoclinic, $P2_1/n$, a, b, c [Å] = 14.747(1), 9.285(1), 22.843(2), α, β, γ [°] = 90, 91.55(1), 90; Bond lengths [Å] = **Au−S**, 2.304(2), **S−Si**, 2.105(3); ^{13}C{^{1}H}, ^{31}P{^{1}H} NMR, MS, EA	[185]
4	Ph₃P—Au—S—Si(OiPr)₃	[Ph₃PAuSSi(OiPr)₃]; colorless crystals; Single crystal structure: triclinic, P-1, a, b, c [Å] = 9.306(2), 13.324(3), 13.554(3), α, β, γ [°] = 119.22(3), 90.66(3), 96.42(3); Bond lengths [Å] = **Au−S**, 2.302(2), **S−Si**, 2.104(3); ^{1}H NMR, EA	[187]
5	(tBu)₃P—Cu—S—SiPh₃	[tBu₃PCuSSiPh₃]; colorless crystals; Single crystal structure: monoclinic, $P2_1/c$, a, b, c [Å] = 10.4907(8), 13.2600(10), 21.230(2), α, β, γ [°] = 90, 97.2200(10), 90; Bond lengths [Å] = **Cu−S** 2.1578(11), 2.439(1), **S−Si** 2.0916(14); ^{1}H, ^{13}C, ^{31}P NMR, EA	[189]
6	Ph₃Si—S—Cu—S—SiPh₃ N⁺[Et]₄	{[Et₄N][Cu(SSiPh₃)₂]}; colorless crystals; Single crystal structure: triclinic, P-1, a, b, c [Å] = 9.448(3), 9.582(3), 12.742(4), α, β, γ [°] = 94.349(4), 94.349(4), 117.022(4); Bond lengths [Å] = **Cu−S** 2.148(1), **S−Si** 2.094(1); ^{1}H NMR; MS	[194]
7		{[Na(diglyme)₂][Cu{SSi(Odipp)₃}₂]}; colorless crystals; Single crystal structure: monoclinic, $C2/c$, a, b, c [Å] = 12.8389(5), 21.8925(6), 32.0980(8), α, β, γ [°] = 90, 96.751(3), 90; Bond lengths [Å] = **Cu−S** 2.455(2), 2.470(2), **S−Si** 2.095(3) Å; 2.096(3); IR	[51]
8		[(IPR)CuSSiMe₃]; colorless crystals; Single crystal structure: monoclinic, $C2/c$, a, b, c [Å] = 28.986(15), 12.887(7), 19.067(9), α, β, γ [°] = 90, 92.619(12), 90; Bond lengths [Å] = **Cu−S** 2.133(1), **S−Si** 2.105(2); ^{1}H, ^{13}C{^{1}H} NMR, EA	[197]
9		[(IPR)AgSSiMe₃]; colorless blocks; Single crystal structure: triclinic, P-1, a, b, c [Å] = 10.196(2), 12.625(3), 16.038(5), α, β, γ [°] = 67.516(13), 79.534(12), 71.104(9); Bond lengths [Å] = **Ag−S** 2.431(1), **S−Si** 2.093(3); ^{1}H, ^{13}C{^{1}H} NMR, EA	[198]
10		[(IMes)CuSSiiPr₃]; colorless blocks; Single crystal structure: monoclinic, $P2_1/c$, a, b, c [Å] = 19.4065(18), 10.8938(10), 15.2754(14), α, β, γ [°] = 90, 104.834(1), 90; Bond lengths [Å] = **Cu−S** 2.1336(4), **S−Si** 2.1207(5); ^{1}H, ^{13}C, ^{29}Si NMR, EA	[200]
11		[(IPR*)Cu(SSiMe₃)]; colorless powder; ^{1}H, ^{13}C{^{1}H} NMR, EA	[199]

Table XVIII (*continued*)

No	Formula	Available data, comments	Ref.
12		[Na(EtOH)$_4$][Ag{SSi(Odipp)$_3$}$_2$]; colorless crystals; Single crystal structure: monoclinic, $I2/a$, a, b, c [Å] = 20.792(2), 11.4774(19), 33.0058(4), α, β, γ [°] = 90, 104.499(9), 90; Bond lengths [Å] = **Ag**−**S** 2.3569 (7), **S**−**Si** 2.0722(10); ^{1}H, ^{13}C{^{1}H}, ^{29}Si NMR, IR, EA	[52]
13		[{PhC(NtBu)$_2$}Si(=S → CuCl)N(SiMe$_3$)$_2$]; colorless crystals; Single crystal structure: orthrhombic, *Pbca*, a, b, c [Å] = 17.7574(18), 16.0785(17), 19.521(2), α, β, γ [°] = 90, 90, 90; Bond lengths [Å] = **Cu**−**S** 2.1260(18), **S**−**Si** 2.039(2); ^{1}H, ^{13}C{^{1}H}, ^{29}Si{^{1}H} NMR, EA	[202]
14	[(IPR)AuSSiMe$_3$]	[(IPR)AuSSiMe$_3$]; colorless, rapidly desolvating crystals; ^{1}H, ^{13}C{^{1}H}, ^{29}Si NMR, EA	[201]
15		[(MeO)$_3$PAuSSi(SiMe$_3$)$_3$]; colorless, crystals; Single crystal structure: monoclinic, $P2_1/c$, a, b, c [Å] = 15.1647(9), 8.6620(5), 19.3969(12), α, β, γ [°] = 90, 96.6940(10), 90; Bond lengths [Å] = **Au**−**S** 2.2921 (8), **S**−**Si** 2.165(1); ^{1}H, ^{13}C{^{1}H}, ^{29}Si, ^{31}P{^{1}H} NMR	[188]
16		[nPr$_3$PAuSSi(SiMe$_3$)$_3$]; colorless, crystals; Single crystal structure: monoclinic, $P2_1/n$, a, b, c [Å] = 14.7402 (8), 14.3037(7), 15.5747(8), α, β, γ [°] = 90, 112.127(2), 90; Bond lengths [Å] = **Au**−**S** 2.300(1), **S**−**Si** 2.152 (1); ^{1}H, ^{13}C{^{1}H}, ^{29}Si, ^{31}P{^{1}H} NMR, EA	[188]
17		[(CAAC^{Cy})CuSSiMe$_3$]; colorless needles; ^{1}H, ^{13}C{^{1}H}, ^{29}Si, NMR, EA	[10]

Fig. 39. Molecular structures of the selected heteroligand silanethiolate complexes of Au(I) of C.N. = 2 without hydrogen atoms: a) [Ph$_3$PAuSSi(SiMe$_3$)$_3$] [42,184]; b) [Ph$_3$PAuSSiPh$_3$] [185]; c) [Ph$_3$PAuSSi(OiPr)$_3$] [187]; d) [nPr$_3$PAuSSi(SiMe$_3$)$_3$] [188].

positions should be considered as well *e.g.* [190]. For [tBu$_3$-PCuSSiPh$_3$] see Table XVIII-5 [189]. A detailed theoretical analysis of the bonding in dicoordinate copper(I) chalcogenides with the use of DFT calculations followed in 2007 [191]. The bond analyses revealed that the dominant interaction within the Cu–E bond is

Pauli repulsion and a reduction in Pauli repulsion favors a bent arrangement adopted by these complexes. Moreover, the bending increases the covalency of the Cu–E bond (E = O, S, Se) thus all monomeric copper(I) chalcogenides tend to adopt a bent ground state geometry [191,192]. It was established that the energy profile
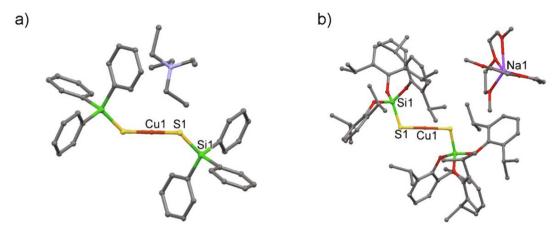
Fig. 40. Molecular structures of the known homoleptic silanethiolate complexes of Cu(I) without hydrogen atoms: a) (Et$_4$N)[Cu(SSiPh$_3$)$_2$] [194]; b) [Na(diglyme)$_2$][Cu{SSi-(Odipp)$_3$}$_2$] [51].
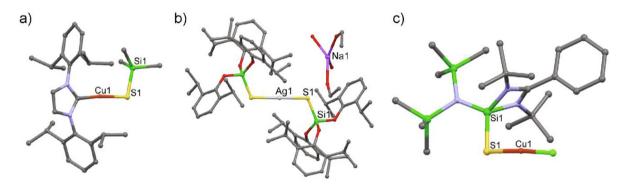
Fig. 41. Molecular structures of silanethiolate complexes of Cu(I) (heteroleptic) and Ag(I) (homoleptic) with C.N. = 2; H atoms are omitted for clarity: a) [(IPR)CuSSiMe$_3$] [197]; b) [Na(EtOH)$_4$][Ag(TDST)$_2$] [52]; c) [{PhC(NtBu)$_2$}Si(=S → CuCl)N(SiMe$_3$)$_2$] [202].

for thermal decomposition is quite independent of the nature of the phosphane ligand and the silyl group and is very similar for oxides, sulfides, and selenides [192].

In 1996 the Cu(I) complex: [BuCuSSiMe$_3$]Li was prepared from RLi and CuSSiMe$_3$, which was formed *in situ* from CuI and LiSSiMe$_3$ (Table XVIII-2). The trimethylsilanothiolate Cu(I) complex was tested along with other cuprates as a reagent for the selective carbon–carbon bond formation and its reactivity was described as excellent. The complexes that could be the first examples of linear anionic copper(I) silanethiolates, were neither isolated nor characterized in solution by any spectroscopic methods [193].

The first structurally characterized, homoleptic, linear Cu(I) silanethiolate was reported in 2010 in a large publication of Holm's research group devoted to the modelling of the structure of the active site of carbon monoxide dehydrogenase [194]. Most of the Cu(I) silanethiolates described in this paper belong to the group of trigonal complexes and are described in 3.8.1.2. The only homoleptic Cu(I) silanethiolate was obtained by ligand exchange between Ph$_3$SiSH and [Cu(S-1-Ad)$_2$]$^-$. Like the other examples of mononuclear homoleptic two-coordinate Cu(I) thiolates [*e.g.* [195]] the centrosymmetric anion of the complex {(Et$_4$N)[Cu-(SSiPh$_3$)$_2$]} is characterized by a linear coordination and very short Cu—S bonds (Table XVIII-6, Fig. 40a) [194].

In 2012 an attempt to prepare mixed ligand (thiolate)(silanethiolate) Cu(I) complex was described but such mononuclear heteroleptic species [Cu(SR)(SSiPh$_3$)]$^-$ could be generated in solution only in mixtures with the homoleptic bis(thiolate) or bis(silanethiolate) anions, from which they were not separable [196].

A second instance of a homoleptic silanethiolate Cu(I) anion comes from our work published in 2014 (Table XVIII-7, Fig. 40b) [51]. The linear Cu(I) complex {[Na(diglyme)$_2$][Cu{SSi(Odipp)$_3$}$_2$]} was obtained from copper(I) chloride and the sodium salt of TDST in hexane with very low yield. Its short Cu—S bonds indicate high degree of covalency. Apart from the covalent interaction with the ligand there is an additional anagostic interaction CH$\cdots$Cu between the ligand and the metal ion stabilizing the conformation of the complex [51].

The low temperature synthetic strategy for copper trimethylsilylchalcogenolates, elaborated within Corrigan's research group and described in more detail in 3.8.1.3 was utilized to prepare a series of thermally stable N-heterocyclic copper–chalcogenolate complexes of the general formula [(IPR)CuESiMe$_3$], where IPR = 1,3-bis-(2,6-diisopropylphenyl)imidazolin-2-ylidene and E = S, Se, Te [197]. The idea to apply N-heterocyclic carbene ligands instead of phosphanes that were originally utilized to prepare copper silanechalcogenolates with C.N. = 3 and 4, (see chapter 3.8.1.3) [11,12] allowed to create thermally stable compounds with much higher melting points (over 150° difference) in comparison to the phosphane complexes. The synthesis utilized (IPR)CuOAc and a usual precursor of the silanechalcogenolate: E(SiMe$_3$)$_2$, E = S, Se, Te. The data for [(IPR)CuSSiMe$_3$] are shown in Table XVIII-8 and the molecular structure of the compound is illustrated in Fig. 41a. As soon as obtained, [(IPR)CuSSiMe$_3$] was successfully applied as a precursor to heterometallic copper–mercury sulfide cluster [197]. The same reactions and isostructural products were observed for silver(I) compounds (Table XVIII-9), however, [(IPR)
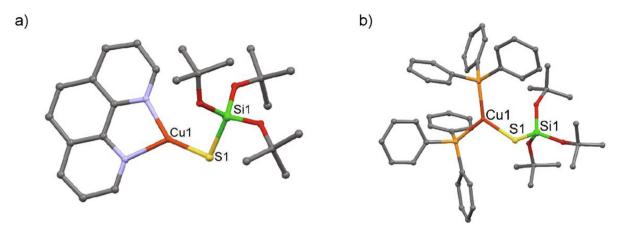
Fig. 42. Molecular structures of the trigonal, heteroligand silanethiolate complexes of Cu(I) without hydrogen atoms: a) [(1,10-phen)CuSSi(OtBu)$_3$] [203]; b) [(Ph$_3$P)$_2$CuSSi(OtBu)$_3$] [204].

AgSSiMe$_3$] was less stable in solution compared to [(IPR)CuSSiMe$_3$] [198]. Moreover, similar investigations were employed in the parallel work of Hillhouse and co-workers [9]. The reaction between equimolar quantities of [(IPR)CuCl] and S(SiMe$_3$)$_2$ in THF produced [(IPR)Cu(SSiMe$_3$)] in very good yield. Treatment of [(IPR)Cu-(SSiMe$_3$)] with [(IPR)Cu(NCMe)][BF$_4$] led to the dicopper cluster [{(IPR)Cu}$_2$(μ-SSiMe$_3$)][BF$_4$] (see 3.8.2.1), which underwent a subsequent reaction with (IPR)CuF to afford the tricopper sulfide cluster [{(IPR)Cu}$_3$(μ_3-S)][BF$_4$] in high yield [9]. A similar synthetic route was described for a different carbene [(IPR*)CuSSiMe$_3$] (Table XVIII-11) [199], whereas a different procedure and carbene were used to obtain [(IMes)Cu(SSiiPr$_3$)] (Table XVIII-10) [200]. The latter was synthesized from [(IMes)CuCl] and triisopropylsilanethiol deprotonated with nBuLi in dry THF at 273 K. The reaction initiated at lowered temperature was continued overnight at RT [200]. In 2017 the NHC-stabilized gold trimethylsilylchalcogenolates [(IPR)AuESiMe$_3$] were prepared by salt metathesis of [(IPR)-AuCl] with Li[ESiMe$_3$] (E = S, Se, Te) in THF. Repeated crystallization attempts produced fragile and easily weathering crystals unsuitable for diffraction analysis. Their molecular structures were thus confirmed by 1D and 2D NMR spectroscopy and elemental analysis (Table XVIII-14) [201]. Within a recent communication new types of carbene-stabilized copper(I) trimethylsilylchalcogenolates [(CAAC^{Cy})CuESiMe$_3$] (E = S, Se, Table XVIII-17) are described as efficient precursors to a series of phosphorescent homo- and heterometallic copper(I) − chalcogenide clusters stabilized by cyclic (alkyl)(amino)carbene ligands [10].

Not earlier than in 2017 the formation and structure of the first, and so far unique, linear homoleptic silanethiolate of silver(I) was reported [52]. The synthesis utilized a double replacement reaction between the sodium salt of TDST and silver nitrate, both dissolved/suspended in EtOH. The low nuclearity of [Na(EtOH)$_4$][Ag-{SSi(Odipp)$_3$}$_2$] was imposed not only by very large substituents but also by the synthetic method; the use of the thiol instead of its salt as well as application of the less polar solvent led to polynuclear compounds described in 3.8.2.1. The anion resembles [Cu{SSi-(Odipp)$_3$}$_2$]$^-$ - being thus obviously a linear complex with short Ag–S bonds, stabilized by anagostic CH···Ag interactions (Fig. 41b, Table XVIII-12) [52].

Unique monomeric copper(I) compounds featuring the Si=S—Cu group were reported by Parvin and co-workers [202]. Silylene-S-thione [PhC(NtBu)$_2$Si(=S)N(SiMe$_3$)$_2$] and silylene-Se-selone [PhC(NtBu)$_2$Si(=Se)N(SiMe$_3$)$_2$] were prepared from the silylene [PhC(NtBu)$_2$SiN(SiMe$_3$)$_2$] and reacted with CuCl and CuBr to yield the Cu complexes [{PhC(NtBu)$_2$}Si(=S→CuX)N(SiMe$_3$)$_2$] and [{PhC(NtBu)$_2$}Si(=Se→CuX)N(SiMe$_3$)$_2$] (X = Cl, Br). These complexes are also directly obtained from the reaction of sulfur and selenium with the silylene copper complexes [{PhC(NtBu)$_2$}Si{N(SiMe$_3$)$_2$}]$_2$-Cu$_2$X$_2$ (X = Cl, Br). Computational analysis confirmed the experimental result that the silicon−chalcogen double bonds in all the complexes are elongated in comparison to those in the Si chalcogenones. NBO analysis showed a significant donor − acceptor interaction between a lone pair of the S atom and an empty s orbital at Cu. Complex [{PhC(NtBu)$_2$}Si(=S→CuCl)N(SiMe$_3$)$_2$] is presented in Fig. 41c and Table XVIII-13. Despite the elongation mentioned above the S=Si bond is extremely short and obviously has a double bond character (Table XVIII-13) [202].

3.8.1.2. Complexes with C.N. = 3. The first instance of a mononuclear copper(I) silanethiolate that featured C.N. = 3: [(1,10-Phen)CuSSi-(OtBu)$_3$] (Fig. 42a, Table XIX-1) was realized by the monodentate coordination of the silanethiolate and the bidentate coordination mode of the phenanthroline ligand. [(1,10-phen)CuSSi(OtBu)$_3$] was obtained by splitting tetrameric [Cu{SSi(OtBu)$_3$}$_4$] with 1,10-phenanthroline in benzene and is the first example of a mononuclear group 11 silanethiolate at all [203]. The bulky tri-$tert$-butoxysilane substituent occupied the position nearly perpendicular to the SCuNN plane, thus one hemisphere of the complex could be considered as "open" for additional interactions. However, in the crystal structure, no intramolecular interactions of copper(I) was observed apart from π···π stacking between the coordinated phenanthrolines [203]. The same reaction was applied in 1993 to produce the heteroligand Cu(I) silanethiolate with triphenylphosphane co-ligands [(Ph$_3$P)$_2$CuSSi-(OtBu)$_3$]. Again, C.N. = 3 was observed but the spatial requirement of PPh$_3$ resulted in a more uniform and complete spacefilling around the copper atom (Fig. 42b, Table XIX-2) [204]. The isomorphous silver(I) complex [(Ph$_3$P)$_2$AgSSi(OtBu)$_3$], prepared by the reaction of tri-$tert$-butoxysilanethiol, triphenylphosphane and silver nitrate in the presence of sodium acetate in a CH$_3$Cl/H$_2$O mixture is also known (Table XIX-3) [205].

Basically two types of trigonal Cu(I) silanethiolates were structurally characterized in 2010 by Holm and co-workers during their search for a model compound of the active site of carbon monoxide dehydrogenase (CODH) [194]. These were heterometal and heteroligand W/Cu complexes, synthesized with the intention to further use them to synthesize complexes with one W−S−Cu bridge and a CuS$_3$ unit. These two types of compounds are exemplified by (Et$_4$N)$_2$[WO(bdt)(μ_2-S)$_2$Cu(SSiiPr$_3$)] and (Et$_4$N)$_2$[Cu(mnt)(SSiPh$_3$)] (Table XIX-4,5 and Fig. 43a,b) and the authors emphasized that their complexes showed a structural relation to the active site of carbon monoxide dehydrogenase (CODH) [194].

Table XIX
Formulas and general characteristics of the Cu, Ag, Au silanethiolates described in chapter 3.8.1.2.

No	Formula	Available data, comments	Ref.
1		[(1,10-Phen)CuSSi(OtBu)₃]; dark red crystals; Single crystal structure: triclinic, P-1 , a, b, c [Å] = 9.412(3), 17.710(6), 9.395 (3), α, β, γ [°] = 90.42(3), 118.32(2), 102.90 (3); Bond lengths [Å]: Cu—S, 2.140 (1), S—Si, 2.086(1)	[203]
2		[(Ph₃P)₂CuSSi(OtBu)₃]; colorless crystals, Single crystal structure: triclinic, P-1 , a, b, c [Å] = 12.772(1), 18.475(2), 10.259 (1), α, β, γ [°] = 93.38(1), 106.302(7), 90.128 (9); Bond lengths [Å]: Cu—S, 2.250 (1), S—Si, 2.074(1)	[204]
3		[(Ph₃P)₂AgSSi(OtBu)₃]; colorless needles, Single crystal structure: triclinic, P-1 , a, b, c [Å] = 10.259(3), 12.946(2) 18.626 (2), α, β, γ [°] = 90.19(1), 94.11(2), 106.58 (2); Bond lengths [Å]: Ag—S, 2.250 (1), S—Si, 2.074(1)	[205]
4		(Et₄N)₂[WO(bdt)(μ₂-S)₂CuSSiiPr₃]; pink needles; Single crystal structure: monoclinic, P2₁/c, a, b, c [Å] = 14.551 (5), 15.531(5), 17.680(5), α, β, γ [°] = 90, 91.693(5), 90; Bond lengths [Å] = Cu—S 2.170 (3), S—Si 2.080(4); ¹H NMR, UV–Vis, IR, MS, EA	[194]
5		(Et₄N)₂[Cu(mnt)(SSiPh₃)]; yellow-orange crystals; Single crystal structure: monoclinic, P2₁, a, b, c [Å] = 9.024(5), 24.784(5), 9.108 (5), α, β, γ [°] = 90 106.965(5), 90; Bond lengths [Å] = Cu—S 2.184 (1), S—Si, 2.061(1); ¹H NMR, UV–Vis, IR, EA	[194]

Table XIX (*continued*)

No	Formula	Available data, comments	Ref.
6		[(iPr₃P)₂Cu(μ-SSiMe₃)(InMe₃)]; dark green crystals; Single crystal structure: orthorhombic, Pna2₁, a, b, c [Å] = 16.9964(4), 11.4766(3), 52.602 (2), α, β, γ [°] = 90, 90, 90; Bond lengths [Å] = Cu—S 2.338(3), S—Si 2.109(4); ¹H, ¹³C, ³¹P{¹H}, ²⁹Si NMR	[206]

The concept of stabilizing copper trimethylsilylchalcogenolates at low temperatures described in more detail in chapter 3.8.1.3 [11,12] was employed for the preparation of [(iPr₃P)₂CuESiMe₃] E = S, Se [206]. The complexes generated *in situ* were reacted with InMe₃ with the purpose to cleave the E–SiMe₃ bond, and to generate [(iPr₃P)nCu–E–InMe₂] as a precursor to indium rings or clusters. However, the reaction did not proceed as expected, and instead of cleavage, the formation of a simple Lewis acid–base adduct was observed (*e.g.* Table XIX-6). Hence, within the reactions the [(R₃P)₂CuESiMe₃] molecules act as electron pair donors towards the Lewis acidic InMe₃ [206].

3.8.1.3. Complexes with C.N. = 4. Copper trimethylsilanechalcogenolates with C.N. = 4 were communicated and then systematically described by Corrigan and co-workers [11,12]. Instead of using bulky substituents at the chalcogen atom, these relatively simple compounds were obtained by restricting the number of vacant coordination sites at the metal atom. Thus the syntheses began with the treatment of CuOAc with four equivalents of Et₃P or nPr₃P followed by the addition of {(CH₃)₃Si}E, E = S, Se, Te. The reactions were carried out at temperatures as low as 228 K, to give products of the general formula [(R₃P)₃CuESiMe₃] (see Table XX-1,2 for examples), which were oils at RT and white solids below 268 K and could be recrystallized from cold diethyl ether. Although relatively stable as pure liquids under inert atmosphere, the complexes underwent rapid condensation reactions to form copper chalcogenide clusters in solution. The molecular structure of tetrahedral [(nPr₃P)ₕCuSSiMe₃] is illustrated in Fig. 44a The Cu—S bond lengths are clearly elongated in comparison to the complexes of lower coordination number [11,12]. The products of the clustering reactions will be presented in chapter 3.8.2.3. Three years later similar synthetic effort was undertaken, in which (Me₃Si)₂S was replaced with the cyclotrisilathiane (Me₂SiS)₃; it allowed the isolation of thermally stable copper and silver complexes containing the S(SiMe₂S)₂²⁻ ligand [207]. The description of these dimers is given in chapter 3.8.2.1. In 2007 Borecki and Corrigan broadened the approach to include not only trimethylsilanethiolates and copper but also trimethylsilylselenolates/tellurolates and silver [208]. With the use of E(SiMe₃)₂, E = S, Se, Te, PEt₂Ph, PEtPh₂, and CuOAc/AcOAg seven tetrahedral complexes of Cu(I) and four Ag(I) counterparts were synthesized and fully characterized. Thanks to the large number of obtained compounds important observations could be made. The complexes were all thermally unstable with respect to the formation of binary metal chalcogenides. The copper trimethylsilylselenolates and -tellurolates were less stable than the silanethiolates. An evident downfield shift was observed in the ¹H and ¹³C{¹H}
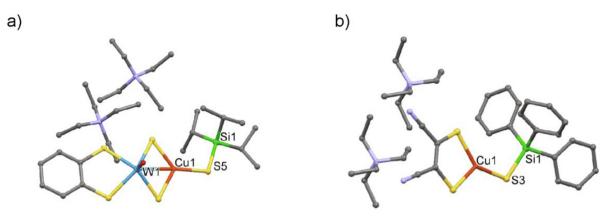
Fig. 43. Molecular structures of the trigonal Cu(I) complexes with silanethiolate co-ligands; hydrogen atoms are omitted: a) $(Et_4N)_2[WO(bdt)(_{\mu2}-S)_2Cu(SSiiPr_3)]$ [194]; b) $(Et_4N)_2[Cu(mnt)(SSiPh_3)]$ [194].

NMR spectra for the $SiMe_3$ signals on going from S to Se and to Te. At very low temperatures all $^{31}P\{^1H\}$ NMR spectra displayed only one broad resonance illustrating fluxional processes undergoing in solution. For selenium and tellurium derivatives $^{77}Se\{^1H\}$ and $^{125}Te\{^1H\}$ NMR spectra were measured. It was also proven that the complexes may serve as precursors of heterometallic clusters (see chapter 3.8.2.2). The data for $[(EtPh_2P)_3CuSSiMe_3]$ are listed and illustrated in Table XX-3 and Fig. 44b [208].

A different synthetic procedure was utilized to obtain [(triphos)Cu(SSiiPr$_3$)] featuring C.N. = 4 forced by the tripodal phosphane ligand (Table XX-4, Fig. 44c) [200]. The complex was obtained from [(triphos)CuCl] and triisopropylsilanethiol deprotonated with nBuLi in dry THF. The RT NMR spectra for [(triphos)Cu(SSiiPr$_3$)] revealed broadened signals, which were attributed to fluxional binding/dissociation of the triphos arms – in spite of the chelating nature of the ligand. The Cu−S bond length in [(triphos)Cu(SSiiPr$_3$)] is notably shorter (2.2670(4) Å) than the corresponding bond lengths in the related compounds (Table XX-4) [200].

3.8.2. Polynuclear complexes of group 11 elements

The tendency of the S−Si bond to undergo hydrolysis makes the polynuclear complexes bridged or terminated by silanethiolato ligands rare species compared to the organic thiolate complexes. Below we describe the several known examples arranged according to their nuclearity.

3.8.2.1. Dimers and trimers.

The first example of a dimeric complex bridged by silanethiolate ligand comes from Chojnacki and co-workers [19]. The complex formed in the reaction of [{Ph$_3$PAg-(acac)}$_2$] with the silanethiol (o-MeC$_6$H$_4$)$_3$SiSH in toluene. The bimetallic central Ag_2S_2 ring of [{Ph$_3$PAgSSi(o-MeC$_6$H$_4$)$_3$}$_2$] is rare even among neutral organic thiolates. The molecule possesses a center of symmetry in the middle of the Ag_2S_2 ring, where two different Ag–S bond lengths are found, which are longer than the bonds of the mononuclear thiolates. Both Ag–P bonds are in the ring plane, whereas the silanethiolate groups protruded above and below the plane (Fig. 45a, Table XXI-1). Detailed NMR studies in the solid state confirmed that one more dimeric complex [{Ph$_3$-PAgSSiiPr$_3$}$_2$] was isolated within the study [19].

Trimethylsilylchalcogenolates were introduced as terminal ligands in a series of dinuclear tris(phosphane)copper(I)-(trimethylsilyl)chalcogenolates (E = S, Se, Te) [209]. The complexes were prepared from the reaction of 2 equiv of $E(SiMe_3)_2$ and already triply-bridged dimers [(X-Cu)$_2$(μ-Ph$_2$PC≡CPPh$_2$-κ^2P)$_3$] (X = Cl, OAc) in THF. The molecule of [(Me$_3$SiSCu)$_2$(μ-Ph$_2$PC≡CPPh$_2$-κ^2P)$_3$], presented as a typical example in Fig. 45b and Table XXI-2, consists of two pseudo-tetrahedral copper centres, each bonded to one sulfur and three phosphorus atoms. The two Cu centres are linked by three helical diphosphane ligands, with a Cu⋯Cu distance of ∼ 6.5 Å. The two trimethylsilylanethiolate ligands are bonded terminally representing potential reactive sites for further reactions and formation of supramolecular structures. Although unstable in solution, the complexes were stable in the solid state under inert atmosphere at low temperatures [209].

Treatment of Cu(OAc) with cyclotrisilathiane in the presence of PEt$_3$ at room temperature generated the silylthiolate-bridged dimer [(Et$_3$P)$_3$Cu$_2${(SSiMe$_2$)$_2$S}] (Table XXI-3) [125,207]. The synthesis of the silver(I) congener was also described (Table XXI-4) [125,207]. Within [(Et$_3$P)$_3$Cu$_2${(SSiMe$_2$)$_2$S}], whose structure is shown in Fig. 45c the silanedithiolate ligand bridges two Cu atoms, one of which is three-coordinate and the other four-coordinate. Because of these different coordination geometries, the Cu—S bond lengths are unequal (Table XXI-3). Although the molecular structure in the solid state was unsymmetrical, within solution only one sharp singlet (at RT) from the methyl protons of the silanedithiolato ligand was observed indicating a rapid ring inversion as well as a fast exchange of the PEt$_3$ ligands between the two Cu centres. Interestingly [(Et$_3$P)$_3$Cu$_2${(SSiMe$_2$)$_2$S}] did not show any signs of decomposition in C_6D_6 at RT over 48 h when monitored by ^1H NMR spectroscopy, however, it did react with metal halides under mild conditions to afford mixed-metal clusters in high yields [207].

Novel dimeric Cu(I) complexes [{CH{C(Me)N(2,6-iPr$_2$C$_6$H$_3$)}$_2$Si-(=S)OCu}$_2$] (E = S, Se) with intermolecular association based on the unprecedented Si=E–Cu–O–Si coordination mode were reported in 2013. They were obtained by the rapid reactions of thio/selenosilanoic acid–base adducts CH{C(Me)N(2,6-iPr$_2$C$_6$-H$_3$)}$_2$Si(=E)OH(dmap) with the metalorganic substrate [(MesCu)$_4$] in THF at 253 K. The molecule of [{CH{C(Me)N(2,6-iPr$_2$C$_6$H$_3$)}$_2$Si-(=S)OCu}$_2$] possesses C_2 symmetry and consists of a planar eight-membered $Si_2O_2S_2Cu_2$ ring with two *trans*-oriented β-diketiminato ligands. The coordination geometry of the Cu centres is linear and short Cu⋯Cu distance of 2.8135(7) Å suggested a weak cuprophilic interaction within the molecule. Both Cu—S and S—Si bonds were extremely short (Fig. 46a, Table XXI-5) [210].

As mentioned in chapter 3.8.1.1 mononuclear copper silanethiolate [(IPR)Cu(SSiMe$_3$)] reacted with [(IPR)Cu(NCMe)][BF$_4$] yielding the dicopper cluster [{(IPR)Cu}$_2$(μ-SSiMe$_3$)][BF$_4$] featuring a bridging silanethiolate ligand [9]. The crystal structure of the dimer revealed two Cu(I) centers with an approximately linear geometry connected *via* a bent Cu−S−Cu unit. Though short in general, the Cu−S bond distances are slightly longer (by ∼0.02 Å) than those in [(IPR)Cu(SSiMe$_3$)] in agreement with the increased coordination number at the sulfur atom (Table XXI-6, Fig. 46b). Further reaction

Table XX
Formulas and general characteristics of the Cu, Ag, Au silanethiolates described in chapter 3.8.1.3.

No	Formula	Available data, comments	Ref.
1	Et$_3$P, Et$_3$P—Cu—S—SiMe$_3$, PEt$_3$	[(Et$_3$P)$_3$CuSSiMe$_3$]; colorless blocks; Single crystal structure: monoclinic, P2$_1$/n, a, b, c [Å] = 11.9276(4), 13.9813(5), 18.2051 (5), α, β, γ [°] = 90, 97.5700(19), 90; Bond lengths [Å]: **Cu—S**, 2.4022(5), **S—Si**, 2.0812(6); ^{1}H, ^{31}P{^{1}H}, ^{77}Se{^{1}H}, ^{13}C{^{1}H}, ^{29}Si {^{1}H} NMR, EA	[12]
2	Pr$_3$P, Pr$_3$P—Cu—S—SiMe$_3$, PPr$_3$	[(nPr$_3$P)$_3$CuSSiMe$_3$]; colorless blocks; Single crystal structure: triclinic, P-1, a, b, c [Å] = 10.9010(8), 11.1233(7), 17.3734 (11), α, β, γ [°] = 92.8890(34), 97.3160(38), 105.1135 (26); Bond lengths [Å]: **Cu—S**, 2.3970(10), **S—Si**, 2.0776(13); ^{1}H, ^{13}C{^{1}H}, ^{31}P{^{1}H}, ^{77}Se {^{1}H}, ^{29}Si{^{1}H} NMR, EA	[12]
3	Et, Ph, Ph, P, Ph, Et—P—Cu—S—SiMe$_3$, Ph, P, Ph, Et	[(EtPh$_2$P)$_3$CuSSiMe$_3$]; colorless needles, Single crystal structure: monoclinic, P2$_1$/n, a, b, c [Å] = 14.6360(5), 23.7333(3), 17.3278 (5), α, β, γ [°] = 90, 97.851(1), 90; Bond lengths [Å]: **Cu—S**, 2.371(1), **S—Si**, 2.105 (2); ^{1}H, ^{13}C{^{1}H}, ^{29}Si {^{1}H}, ^{31}P{^{1}H} NMR, also Ag as well as Se, Te analogs of Cu and Ag were obtained; ^{77}Se {^{1}H}, and ^{125}Te{^{1}H} NMR measured for Se and Te analogs	[208]
4	Ph, Ph, Ph, P, Me—P—Cu—S—Si(iPr)$_3$, Ph, P, Ph, Ph	[(triphos)CuSSi/Pr$_3$]; colorless blocks; Single crystal structure: monoclinic, P2$_1$/n, a, b, c [Å] = 14.5029(10), 16.1500(11), 22.0822 (15), α, β, γ [°] = 90, 93.455(1), 90; Bond lengths [Å] = **Cu—S** 2.2670(4), **S—Si** 2.1019 (5); ^{1}H, ^{31}P NMR, EA	[200]

of the dimer with [(IPR)CuF] underwent with the formation of unsupported μ_3-S tricopper [{(IPR)Cu}$_3$(μ_3-S)][BF$_4$] in high yield [9].

The final examples of silanethiolate dimers in this chapter come from the publication of Corrigan and co-workers [198]. Thereby, the carbene complex [(IPR2-bimy)CuOAc] (IPR2-bimy − 1,3-di-isopropylbenzimidazolin-2-ylidene) was reacted with E(SiMe$_3$)$_2$ at 200 K and in this way complexes [{(IPR2-bimy)CuESiMe$_3$}$_2$] (E = S, Se) were obtained as colorless crystals. Both of the Cu complexes (sulfur and selenium derivative) exist as [(IPR2-bimy)$_2$Cu$_2$(μ-ESiMe$_3$)$_2$] dimers in the solid state, with a "hinged butterfly shaped" E$_2$Cu$_2$ central ring". The smaller size of the ancil-

lary carbene IPR2-bimy compared to IPR provided an access to the additional coordination sites around the Cu atom and enabled the dimerization. Additionally [(IPR2-bimy)$_2$Cu$_2$(μ-SSiMe$_3$)$_2$] (Table XXI-7, Fig. 46c) showed relatively high thermal stability [198].

In 2017 we described a series of unique Ag(I) silanethiolate trimers. Cyclic e.g. [{AgSSi(Odipp)$_3$}$_3$] and unusual open (linear) e.g. [(EtOH)Ag$_3$(NO$_3$){μ-SSi(Odipp)$_3$}$_2$] trinuclear systems were characterized, which were stabilized by additional Ag(I)···π coordination of the phenyl substituents of the (dippO)$_3$SiS$^-$ ligand (Table XXI-8,9, Fig. 47a,b) [52]. The reactions of silanethiol TDST with AgNO$_3$ in ether reproducibly produced trinuclear, molecular [{Ag{SSi-(Odipp)$_3$}$_3$] stabilized by Ag(I)···π interactions, while the reactions of the sodium salts of TDST with silver salts in more polar solvents led to anionic complexes with the conformation reinforced by CH···Ag interactions [52].

3.8.2.2. Tetramers. The formation of tetramers has been observed in the case of many different ligands and seems to be a typical arrangement for coinage metal silanethiolates. The first tetrameric group 11 silanethiolate [{AgSSi(OtBu)$_3$}$_4$] was described 1985 (Fig. 48a, Table XXII-1) [211]. It was obtained by the reaction of both TBST or its sodium salt with AgNO$_3$ in water/benzene. The central unit of the molecule is a nearly plane eight-membered ring made from alternating Ag and S atoms with threefold bonded sulfur and two-coordinated silver atoms. The deviations of the S—Ag—S bonds from linear arrangement resulted from shifts of the silver atoms toward the center of the ring. The authors initially ascribed this effect to the existence of direct Ag···Ag argentophilic interactions [211]. However, detailed NMR studies performed and described few years later practically excluded such possibility. The ^{109}Ag spectra at 9.4 T and at 2.1 T were single lines without fine structure and no proof of any {Ag, Ag}-coupling could be deduced from them. The Ag signal in [{AgSSi(OtBu)$_3$}$_4$] was shifted to higher frequency by δ = (725.8 ± 1.5) ppm relative to the resonance of the Ag$^+$ ion in aqueous solution [212]. The copper tetramer [{CuSSi-(OtBu)$_3$}$_4$] was obtained from TBST and copper(II) acetate or CuCl or Cu$_2$O five years later. Its molecular structure very similar to its silver congener. However, in the copper compound the ring is centrosymmetric (Table XXII-2) [13]. It is worth to mention here that a whole series of Au tetramers with metal ions coordinated by organic thiolates (also Se and Te organic derivatives) with tris (trimethylsilyl)methyl groups at the chalcogen atom were reported by Bonasia and co-workers in 1993 [184]. The series of TBST stabilized tetramers finished in 1994 with the description of the molecular structure of [{AuSSi(OtBu)$_3$}$_4$], advertised in the title of the paper as the first example of an Au$_4$S$_4$ ring system, which we now know not to be the exact information taking into account the one year earlier paper of Arnold's group [184,213]. However, it was the first example of a structurally characterized silanethiolate of gold (Table XXII-3). There is a structural difference between the Au tetramer and the Cu/Ag compounds - in [{CuSSi(OtBu)$_3$}$_4$] and [{AgSSi(OtBu)$_3$}$_4$] the central M$_4$S$_4$ rings are almost planar, while in case of [{AuSSi(OtBu)$_3$}$_4$] the core is folded as illustrated in Fig. 48b. The folding was attributed to the observed conformation of the silyl substituents; for the Cu and Ag silanethiolates, the (tBuO)$_3$Si groups are in a staggered conformation, whereas in [{AuSSi(OtBu)$_3$}$_4$] they adopted an eclipsed conformation [213].

The next tetrameric Cu(I) complex [(CuSSiPh$_3$)$_4$] was prepared by the transfer of the silanethiolato ligand from iron(II) to copper (I) (Table XXII-4) [124]. Apparently, the soft silanethiolato ligand "preferred" the softer Cu(I) center. The centrosymmetric molecule consists of an eight-membered Cu$_4$S$_4$ ring. The planar arrangement of the four copper atoms resembled the geometry of [{CuSSi-(OtBu)$_3$}$_4$]. The two triphenylsilyl groups of adjacent silanethiolato ligands were situated above the Cu$_4$S$_4$ plane, and the other two
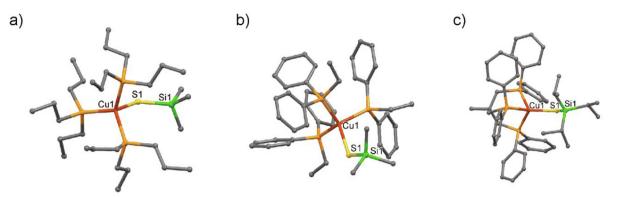
Fig. 44. Molecular structures of the tetrahedral complexes of Cu(I) with phosphane and silanethiolate ligands without hydrogen atoms: a) [(nPr$_3$P)$_3$CuSSiMe$_3$] [11,12]; b) [(EtPh$_2$P)$_3$CuSSiMe$_3$] [208]; c) [(triphos)Cu(SSiPr$_3$)] [200].
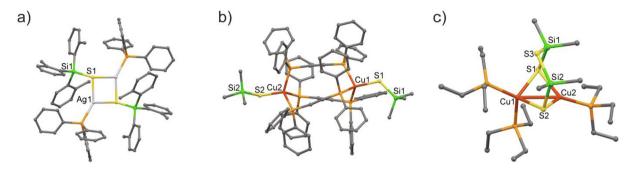
Fig. 45. Molecular structures of the dinuclear complexes of Ag(I) and Cu(I) with phosphane and silanethiolate ligands; H atoms are omitted for clarity: a) [{Ph$_3$PAgSSi(o-MeC$_6$H$_4$)$_3$}$_2$] [19]; b) [(Me$_3$SiSCu)$_2$(μ-Ph$_2$PC≡CPPh$_2$-κ^2P)$_3$] [209]; c) [(Et$_3$P)$_3$Cu$_2${(SSiMe$_2$)$_2$S}] [125,207].

groups are below the Cu$_4$S$_4$ plane (Fig. 48c) [124]. The same researchers described another tetranuclear Cu(I) silanethiolate [{Cu(SSiMe$_2$$t$Bu)}$_4$] in 2004 [7], which was synthesized by the reaction of the lithium salt of the silanethiol with [Cu(CH$_3$CN)$_4$](PF$_6$) in acetonitrile. Though the core of the complex was typical, the conformation of the ligands was different from its predecessors. Three silanethiolato substituents were directed to one side of the Cu$_4$S$_4$ ring, while the fourth substituent was oriented toward the opposite side. Moreover, the Cu$_4$S$_4$ ring is folded and the two-coordinate copper atoms adopt a geometry distorted from linear (Fig. 49a, Table XXII-5). In the solid-state structure the authors noticed that the tetramers displayed intermolecular Cu–S interactions connecting the tetramers with the formation of octamers; the aggregation was facilitated by the special orientations of the silanethiolato substituents relative to the Cu$_4$S$_4$ core [7]. This feature definitely distinguished [{Cu(SSiMe$_2$$t$Bu)}$_4$] from the related silanethiolato complexes described above; similar aggregation was earlier observed for silver thiolates [214]. We suggest that the singular conformation must be additionally connected with the less steric hindrance as another copper(I) tetramer incorporating bulkier tBu$_2$PhSiS$^-$ ligands "returns" to the centrosymmetric arrangement of ligands around the ring. [{Cu(SSiMe$_2$$t$Bu)}$_4$] was synthesized out of tBu$_2$PhSiSNa and CuCl in THF. It crystallizes in the tetragonal I-4 space group. The S–Cu–S angles deviate only slightly from linearity and the intermetallic distances within the ring are of similar length (Fig. 49b, Table XXII-6) [14]. One more example of a Cu(I) tetramer comes from the publication of Schnepf and co-workers [42]. Complex [{CuSSi(SiMe$_3$)$_3$}$_4$] was obtained from [(THF)$_2$LiSSi-(SiMe$_3$)$_3$]$_2$ and (tht)CuCl in toluene. The metal atoms were arranged in the form of a usual planar four-membered ring with Cu–Cu–Cu angles of almost 90° and the ligands adopted the alternate conformation above or below the Cu$_4$ plane. However, instead

of the square planar arrangement, a rectangular one was formed with two strongly different Cu$\cdots$Cu contacts of 2.73 pm and 3.16 Å (Fig. 49c, Table XXII-7). The authors suggested that the tendency to form square planar or rectangular arrangements could be due to packing effects. The structure of a similar silver tetramer [{AgSSi(SiMe$_3$)$_3$}$_4$] was also described [42].

In summary to this chapter we would like to mention that the bonding in cyclic M$_n$(SMe)$_n$ (n = 2 – 6) complexes (M = Cu, Ag, Au) was investigated with the use of DFT methods by Howell [215]. He was able to conclude that although the bonds were primarily σ in nature, there also existed a set of 2n metal-localised orbitals with a spatial distribution suitable for M–M orbital overlap for each M$_n$(SR)$_n$ complex (nonetheless the net M–M bonding was zero) [215]. The weak intermetallic ligation may therefore be responsible for the contractions of some of the M$\cdots$M distances in the complexes presented here.

Interestingly, no silanethiolate complexes of nuclearity higher than 4 are known for group 11 metals. Though silanethiolate complexes were utilized as precursors to homo- and heterometallic sulfido-clusters of coinage metals they were not present in the final products. [e.g. [9,11,201,208]] The genuine silanethiolate stabilized cluster of Cu, Ag or Au is yet to be synthesized.
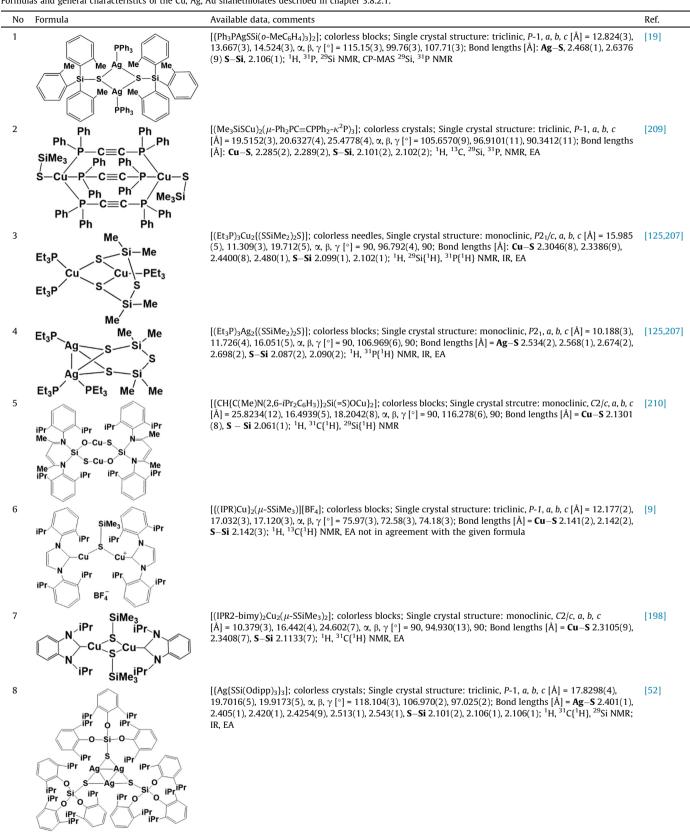
3.9. Group 12 elements

For zinc group elements we return to the separate mode of description of their silanethiolate complexes. The differences in the typical coordination geometries of zinc and cadmium ions were discussed in the earlier review paper [22]. In general zinc as a smaller cation (r = 1.18 Å) usually forms complexes with C.N. = 4 or 5 while cadmium (r = 1.36 Å) often expands its coordination number to six. Mercury(II) is an "extremely" soft Pearson

Table XXI

Formulas and general characteristics of the Cu, Ag, Au silanethiolates described in chapter 3.8.2.1.

No	Formula	Available data, comments	Ref.
1		[{Ph$_3$PAgSSi(o-MeC$_6$H$_4$)$_3$}$_2$]; colorless blocks; Single crystal structure: triclinic, P-1, a, b, c [Å] = 12.824(3), 13.667(3), 14.524(3), α, β, γ [°] = 115.15(3), 99.76(3), 107.71(3); Bond lengths [Å]: **Ag–S**, 2.468(1), 2.6376(9) **S–Si**, 2.106(1); ^{1}H, ^{31}P, ^{29}Si NMR, CP-MAS ^{29}Si, ^{31}P NMR	[19]
2		[(Me$_3$SiSCu)$_2$(μ-Ph$_2$PC≡CPPh$_2$-κ^{2}P)$_3$]; colorless crystals; Single crystal structure: triclinic, P-1, a, b, c [Å] = 19.5152(3), 20.6327(4), 25.4778(4), α, β, γ [°] = 105.6570(9), 96.9101(11), 90.3412(11); Bond lengths [Å]: **Cu–S**, 2.285(2), 2.289(2), **S–Si**, 2.101(2), 2.102(2); ^{1}H, ^{13}C, ^{29}Si, ^{31}P, NMR, EA	[209]
3		[(Et$_3$P)$_3$Cu$_2${(SSiMe$_2$)$_2$S}]; colorless needles, Single crystal structure: monoclinic, P2$_1$/c, a, b, c [Å] = 15.985(5), 11.309(3), 19.712(5), α, β, γ [°] = 90, 96.792(4), 90; Bond lengths [Å]: **Cu–S** 2.3046(8), 2.3386(9), 2.4400(8), 2.480(1), **S–Si** 2.099(1), 2.102(1); ^{1}H, ^{29}Si{^{1}H}, ^{31}P{^{1}H} NMR, IR, EA	[125,207]
4		[(Et$_3$P)$_3$Ag$_2${(SSiMe$_2$)$_2$S}]; colorless blocks; Single crystal structure: monoclinic, P2$_1$, a, b, c [Å] = 10.188(3), 11.726(4), 16.051(5), α, β, γ [°] = 90, 106.969(6), 90; Bond lengths [Å] = **Ag–S** 2.534(2), 2.568(1), 2.674(2), 2.698(2), **S–Si** 2.087(2), 2.090(2); ^{1}H, ^{31}P{^{1}H} NMR, IR, EA	[125,207]
5		[{CH{C(Me)N(2,6-iPr$_2$C$_6$H$_3$)}$_2$Si(=S)OCu}$_2$]; colorless blocks; Single crystal strcutre: monoclinic, C2/c, a, b, c [Å] = 25.8234(12), 16.4939(5), 18.2042(8), α, β, γ [°] = 90, 116.278(6), 90; Bond lengths [Å] = **Cu–S** 2.1301(8), **S – Si** 2.061(1); ^{1}H, ^{31}C{^{1}H}, ^{29}Si{^{1}H} NMR	[210]
6		[{(IPR)Cu}$_2$(μ-SSiMe$_3$)][BF$_4$]; colorless blocks; Single crystal structure: triclinic, P-1, a, b, c [Å] = 12.177(2), 17.032(3), 17.120(3), α, β, γ [°] = 75.97(3), 72.58(3), 74.18(3); Bond lengths [Å] = **Cu–S** 2.141(2), 2.142(2), **S–Si** 2.142(3); ^{1}H, ^{13}C{^{1}H} NMR, EA not in agreement with the given formula	[9]
7		[(IPR2-bimy)$_2$Cu$_2$(μ-SSiMe$_3$)$_2$]; colorless blocks; Single crystal structure: monoclinic, C2/c, a, b, c [Å] = 10.379(3), 16.442(4), 24.602(7), α, β, γ [°] = 90, 94.930(13), 90; Bond lengths [Å] = **Cu–S** 2.3105(9), 2.3408(7), **S–Si** 2.1133(7); ^{1}H, ^{31}C{^{1}H} NMR, EA	[198]
8		[{Ag{SSi(Odipp)$_3$}$_3$]; colorless crystals; Single crystal structure: triclinic, P-1, a, b, c [Å] = 17.8298(4), 19.7016(5), 19.9173(5), α, β, γ [°] = 118.104(3), 106.970(2), 97.025(2); Bond lengths [Å] = **Ag–S** 2.401(1), 2.405(1), 2.420(1), 2.4254(9), 2.513(1), 2.543(1), **S–Si** 2.101(2), 2.106(1), 2.106(1); ^{1}H, ^{31}C{^{1}H}, ^{29}Si NMR; IR, EA	[52]

Table XXI (*continued*)

No	Formula	Available data, comments	Ref.
9		[(EtOH)Ag$_3$(NO$_3$){μ-SSi(Odipp)$_3$}$_2$]; colorless crystals; Single crystal structure: monoclinic, $P2_1/n$, *a, b, c* [Å] = 17.3627(4), 19.6399(3), 22.8264(6), α, β, γ [°] = 90, 104.436(2), 90; Bond lengths [Å] = **Ag–S** 2.372(2), 2.381(2), 2.385(2), **S–Si** 2.099(3), 2.102(3); ^{1}H, ^{31}C{^{1}H} NMR, EA	[52]

Fig. 46. Molecular structures without hydrogen atoms of the dinuclear complexes of Cu(I) bearing SiS functionality and further stabilized by 1,3-diketimines at silicon or carbene ligands at copper: a) [{CH{C(Me)N(2,6-iPr$_2$C$_6$H$_3$)}$_2$Si(=S)OCu}$_2$] [210]; b) [{(IPR)Cu}$_2$(μ-SSiMe$_3$)][BF$_4$] (anionic part not shown) [9]; c) [{(IPR2-bimy)CuSSiMe$_3$}$_2$] [198].
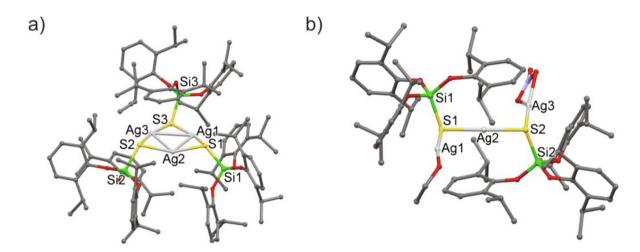
Fig. 47. Molecular structures withour hydrogen atoms of the trinuclear Ag(I) complexes with the (dippO)$_3$SiSi$^-$ ligand: a) [{Ag{SSi(Odipp)$_3$}$_3$]; b) [(EtOH)Ag$_3$(NO$_3$){μ-SSi-(Odipp)$_3$}$_2$] [52].
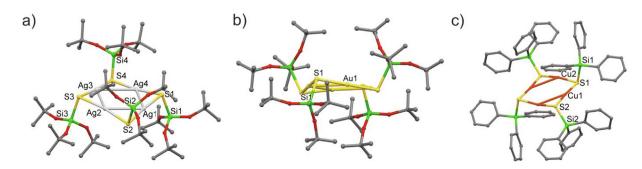
Fig. 48. Molecular structures of the homoleptic, tetranuclear complexes of Cu(I), Ag(I) and Au(I) with silanethiolate ligands; hydrogen atoms are omitted: a) [{AgSSi(OtBu)$_3$}$_4$] [211]; b) [{AuSSi(OtBu)$_3$}$_4$] [213]; c) [(CuSSiPh$_3$)$_4$] [124].

A. Pladzyk, D. Kowalkowska-Zedler, A. Ciborska et al.

Table XXII
Formulas and general characteristics of the Cu, Ag, Au silanethiolates described in chapter 3.8.2.2.

No	Formula	Available data, comments	Ref.
1	[{AgSSi(OtBu)₃}₄] structure	[{AgSSi(OtBu)₃}₄]; colorless plates; Single crystal structure: triclinic, $P\text{-}1$, a, b, c [Å] = 17.697(25), 20.128(17), 12.668(6), α, β, γ [°] = 119.63(6), 82.22(7), 95.08(9); Bond lengths [Å]: **Ag–S**, 2.377(4), 2.377(5), 2.382(4), 2.383(4), 2.384(4), 2.384(5), 2.385(4), 2.388(5), **S–Si**, 2.112(6), 2.114(5), 2.119(4), 2.132(5); ¹³C, ²⁹Si NMR; MS, EA	[211]
2	[{CuSSi(OtBu)₃}₄] structure	[{CuSSi(OtBu)₃}₄]; colorless crystals; Single crystal structure: monoclinic, $C2/c$, a, b, c [Å] = 24.787(15), 24.721(27), 12.714(7), α, β, γ [°] = 90, 100.99(4), 90; Bond lengths [Å]: **Cu–S**, 2.160(4), 2.170(4), 2.172(4), 2.175(4), **S–Si**, 2.126(4), 2.138(3); ¹H, ¹³C, ²⁹Si NMR, IR, UV, EA	[13]
3	[{AuSSi(OtBu)₃}₄] structure	[{AuSSi(OtBu)₃}₄]; colorless blocks, Single crystal structure: orthorhombic, $Fddd$, a, b, c [Å] = 32.42(2), 35.33(2), 13.309(7), α, β, γ [°] = 90, 90, 90; Bond lengths [Å]: **Au–S** 2.284(4), 2.296(4), **S–Si** 2.169(7); ¹H, ¹³C, ²⁹Si NMR, IR, UV	[213]
4	[(CuSSiPh₃)₄] structure	[(CuSSiPh₃)₄]; colorless crystals; Single crystal structure: triclinic, $P\text{-}1$, a, b, c [Å] = 12.308(5), 13.154(2), 11.090(4), α, β, γ [°] = 98.06(2), 109.63(2), 96.91(2); Bond lengths [Å] = **Cu–S** 2.160(1), 2.168(1), 2.168(1), **S–Si** 2.142(2), 2.153(2); ¹H NMR, IR, UV–Vis, EA	[124]
5	[{Cu(SSiMe₂tBu)}₄] structure	[{Cu(SSiMe₂tBu)}₄]; colorless crystals; Single crystal structure: triclinic, $P\text{-}1$, a, b, c [Å] = 11.404(4), 13.672(5), 14.338(5), α, β, γ [°] = 66.80(1), 77.46(2), 86.71(2); Bond lengths [Å] = **Cu–S** 2.148(1), 2.151(2), 2.157(1), 2.168(2), 2.171(1), 2.178(1), 2.180(2), 2.181(1), **S–Si**, 2.152(2), 2.158(2), 2.160(2), 2.178(2); ¹H NMR, IR, EA	[7]
6	[{Cu(SSiPhtBu₂)}₄] structure	[{Cu(SSiPhtBu₂)}₄]; colorless blocks; Single crystal structure: tetragonal, $I\text{-}4$, a, b, c [Å] = 20.106(2), 20.106(2), 7.7980(8), α, β, γ [°] = 90, 90, 90; Bond lengths [Å] = **Cu–S** 2.158(1), 2.161(1), **S–Si** 2.173(1); ¹H, ¹³C, ²⁹Si NMR, EA	[14]
7	[{CuSSi(SiMe₃)₃}₄] structure	[{CuSSi(SiMe₃)₃}₄]; colorless needles; Single crystal structure: monoclinic, $C2/c$, a, b, c [Å] = 51.236(3), 24.4910(17), 13.7908(10), α, β, γ [°] = 90, 101.892(3), 90; Bond lengths [Å] = **Cu–S** 2.147(1), 2.150(1), 2.152(1), 2.152(1), 2.157(1), 2.162(1), 2.163(1), 2.163(1), **S–Si**, 2.189(2), 2.193(2), 2.202(2), 2.204(2); ¹H, ³¹C{1H}, ²⁹Si NMR	[42]

acid [32] and thiophilic element, which often forms linear or tetrahedral complexes.

Two major motives to prepare zinc and cadmium silanethiolates may be indicated:

- the first incentive is so-called bio-mimetic chemistry – zinc is a constituent of many enzymes whereas the toxicity of cadmium is often ascribed to its ability to falsely replace zinc in zinc proteins. Bulky silanethiolates allowed not only the syntheses of well-defined molecular thiolates of both zinc and cadmium but also the research on their coordination preferences and spectroscopic features. A certain number of zinc and cadmium and also cobalt tri-*tert*-butoxysilanethiolates were synthesized to model the structural and spectroscopic features of alcohol dehydrogenase and we ask the interested reader to refer to the review published in 2010 [22].
- zinc and cadmium sulfides are valuable semiconductors and zinc sulfide is a luminescent material – silanethiolates were considered as possible precursors to various forms of the sulfide materials, *e.g.* [216–218], and their luminescences was investigated, *e.g.* [170,219].

The coordination geometry and properties of mercury compounds are quite peculiar and a very limited number of silanethiolate compounds of mercury are known.

3.9.1. Silanethiolates of zinc

First mention of zinc silanethiolates dates back to 1977, when the preparation of complexes of the general formula EtZnSEPh₃ (M = Si, Ge) was described by Galiulina and co-workers in a very brief communication [220]. The metalorganic compounds were prepared by treating Ph₃MSH with Et₂Zn and they were described as white, crystalline solids soluble in aromatic solvents and insoluble in hexane.

A relatively large number of tri-*tert*-butoxysilanethiolates of zinc were obtained and their molecular structures were characterized by X-ray diffraction. This was possible thanks to the peculiar properties of tri-*tert*-butoxysilanethiol. TBST is resistant to hydrolysis while the presence of oxygen atoms allows the formation of additional intra- and intermolecular interactions and facilitates crystallization of the assembling complexes. Typically the C.N. of zinc in these complexes is 4 or 5 and the first two complexes reported in 1996 by Becker et al. were four- or five-coordinated with chelating *tert*-butoxy- groups: [(2,2'-bipy)Zn{SSi(OtBu)₃}₂] and [(MeCN)Zn{SSi(OtBu)₃}₂] (Table XXIII-1,2, Fig. 50a,b). The authors described the syntheses of the homoleptic zinc silanethiolate [Zn{SSi(tBuO)₃}₂] which is a viscous, colorless oil at RT (Table XXIII-3) and several other heteroleptic zinc silanethiolates with nitrogen co-ligands. Quite surprisingly these compounds are obtained in water in spite of the hydrophobicity of both TBST and the resulting products [4]. As indicated in the introduction to this chapter, the structure and spectroscopic properties of most of the zinc tri-*tert*-butoxysilanethiolates that were synthesized to model the structural and spectroscopic features of alcohol dehydrogenase were reviewed in 2010 [22]. Several distinct examples of coordination geometries and ligands are given in Table XXIII-4–7 and in Fig. 51c-f [26,27,168,221]. The structural studies were followed by the attempts to apply the complexes in the dehydrogenation of alcohols [166].

The syntheses of reactive zinc chalcogen complexes bonded to a trimethylsilyl functionality as precursors to the formation of zinc-chalcogen (Zn-E) materials was offered in 2005 by DeGroot and Corrigan [222]. They prepared a series of [(N,N'-tmeda)Zn-(ESiMe₃)₂] as well as [(3,5-dMepy)₂Zn(ESiMe₃)₂] complexes (E = S,
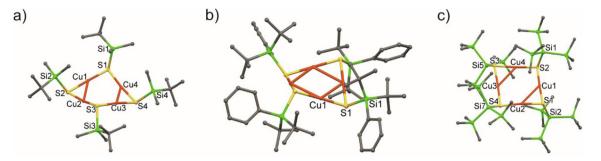
Fig. 49. Molecular structures of the homoleptic, tetranuclear complexes of Cu(I) with silanethiolate ligands; hydrogen atoms are omitted: a) [{Cu(SSiMe$_2t$Bu)}$_4$] [7]; b) [{Cu(SSiPhtBu$_2$)}$_4$] [14]; c) [{CuSSi(SiMe$_3$)$_3$}$_4$] [42].

Se, Te) (see Table XXIII-8 and Fig. 51a for an example) *via* the reaction of Zn(OAc)$_2$ with an appropriate nitrogen donor ligand in tetrahydrofuran or CHCl$_3$ followed by the addition of E(SiMe$_3$)$_2$ at low temperatures. Metal-chalcogen bonds formed with the generation and elimination of AcOSiMe$_3$ and the complexes were obtained in high yield. All complexes are monomeric and feature tetrahedral coordination as illustrated in Fig. 51a. Since the compounds could be stored under inert atmosphere for extended periods they were announced as convenient precursors for the generation of metal-sulfide nanoclusters [222]. The anticipated ternary, chalcogenide clusters were realized within the same year. For example, the reaction of cadmium acetate with [(3,5-dMepy)$_2$Zn(ESiMe$_3$)$_2$], PhSSiMe$_3$, and PnPr$_3$ afforded the larger nanocluster [Zn$_{2.3}$Cd$_{14.7}$S$_4$(-SPh)$_{26}$(PnPr$_3$)$_2$] [223]. Several years later the same precursors were used to prepare structurally defined ternary Zn−Mn sulfide clusters [224]. Thermolysis experiments of [(N,N'-tmeda)Zn(ESiMe$_3$)$_2$] and [(3,5-dMepy)$_2$Zn(ESiMe$_3$)$_2$] in the solid state as well as in solution reveal that below 473 K nanocrystalline ZnS and ZnSe materials are produced with surfaces protected by coordinated TMEDA/3,5-lutidine ligands. Beside this, solid state thermolysis above 523 K resulted in the formation of hexagonal ZnS, *via* the liberation of TMEDA or 3,5-lutidine and S(SiMe$_3$)$_2$ [225].

Metathesis reaction of ZnCl$_2$ with NaSSitBu$_3$ [14] or the quite new synthetic approach, which utilized the reaction of sulfur with [Zn(SitBu$_3$)$_2$] [226], both in THF, yielded the supersilylthiolate complexes [{ZnCl(SSitBu$_3$)(THF)}$_2$] [14] and homoleptic [{Zn-(SSitBu$_3$)$_2$}$_2$] [226] respectively (*e.g.* Table XXIII-9, Fig. 51b). Contrary to the mononuclear compounds described earlier in this chapter these complexes featured dinuclear Zn$_2$S$_2$ folded rings with two bridging and two terminal silanethiolate ligands (Fig. 51b). Similar for other bridging silanethiolate complexes it can be observed that the bridging mode of sulfur leads to an elongation of the S−Si bond in comparison to terminal silanethiolates, which implicates both its weakening and readiness for the formation of the sulfide. A unique homoleptic Zn silanethiolate [[(iPr$_3$SiS)Zn(μ-SSiiPr$_3$)$_2$Zn(μ-SSiiPr$_3$)$_2$Zn(SSiiPr$_3$)] was obtained as a result of the equally unique recipe, which employed the reaction of diethylzinc with triisopropylsilanethiol in hexane [227]. XRD studies revealed that the molecular complex is a *spiro* compound that consists of two Zn$_2$S$_2$ rings sharing one common central zinc atom. The two terminal Zn ions are three-coordinate and possess a single non-bridging silanethiolate ligand and a bridging silanethiolate ligand to the central Zn ion – connector of the two rings (Fig. 51c and Table XXIII-10). The tetrahedral coordination of the central Zn atom imposes almost perpendicular, mutual orientation of both Zn$_2$S$_2$ rings [227].

Taking the advantage of the peculiar properties of TBST, several dinuclear complexes as well as 1-D coordination polymers of Zn (also Co/Ni/Cd – see chapters 3.6.1.2/3.7.1/3.9.2 respectively) were synthesized within our research group mainly by Pladzyk and co-workers [*e.g.* [170,219,228]]. Zn(acac)$_2$ proved to be a very efficient starting Zn precursor for most of the syntheses. The complexes

contained the (tBuO)$_3$SiS$^-$ residue coordinated to Zn(II) as terminal ligand whereas metal ions were bridged by various pyridine, imidazole and pyrazine double donors. Typically, the Zn atoms adopt C.N. = 4 with chelating (tBuO)$_3$SiS$^-$ and NOS$_2$ donor set of atoms in dimers and tetrahedral geometry with the N$_2$S$_2$ donor set of atoms in dimers and CPs. The compounds were often thermally stable up to approximately 470 – 520 K and a lot of them display luminescent properties - *e.g.* blue emissions [228]. Examples are given in Fig. 52a,b and Table XXIII-11,12.

Several new molecular Zn complexes with unique donor sets were prepared with the use of Zn acetate and Zn acetylacetonate and new bulky silanethiol TDST (Table XXIII-13–15, Fig. 53a,b). The new silanethiol obviously formed σ M−S bonds with metal cations but, compared to TBST, the additional intramolecular interactions between the TDST and metal cations were changed from M···O to M···π, especially for soft metal cation like silver and cadmium (chapter 3.8.2.2. and 3.9.2.) [5,52]. This was due to the well-known fact that the oxygen atom would donate one of its lone pairs of electrons *via* resonance into the π system of benzene, increasing the electron density within the ring. So far we have observed the coordination between the oxygen and metal cation in the complexes with (dippO)$_3$SiS$^-$ only once in a non-solvated sodium salt (Table I-19 [20]). Accordingly, in heteroleptic complexes, apart from intramolecular hydrogen bonds XH···O, which were also typical for complexes of TBST, *e.g.* Fig. 50c, Fig. 53b, XH···π interactions were sometimes observed, *e.g.* in Co(II) and Ni(II) complexes described by Dołęga and co-workers (see also chapter 3.6.1.2 and 3.7.1) [5,159]. When zinc acetate was reacted with a limited amount of TDST in methanol an unprecedented tetrameric zinc complex was isolated (Table XXIII-15) [5].

In recent years two trigonal silanethiolate zinc complexes were characterized [42,218]. Planar arrangements are unusual for three coordinated zinc(II) compounds with monodentate ligands – the unique example of an organic thiolate is [(Et$_4$N)Zn(SAd)$_3$] [229]. The first of the trigonal Zn silanethiolates was an adduct of (THF)$_2$-LiSSi(SiMe$_3$)$_3$ and [Zn(SSi(SiMe$_3$)$_3$)$_2$] obtained in the reaction of ZnCl$_2$ and LiSSi(SiMe$_3$)$_3$ carried out at low temperature in THF. The coordination of the solvated lithium cation to [Zn(SSi-(SiMe$_3$)$_3$)$_3$]$^-$ gave a neutral molecule, which is well-soluble in pentane (Fig. 54a, Table XXIII-16) [42]. In 2020 the homoleptic, trigonal trimethylsilylchalcogenolato zincates [Zn(ESiMe$_3$)$_3$]$^-$ (E = S, Se) were not only fully characterized but also investigated as potential precursors towards heterometallic sulfide materials (Fig. 54b, Table XXIII-17). The complexes were prepared with the use of ZnCl$_2$ and the well-known precursor: E(SiMe$_3$)$_2$ [218].

3.9.2. Silanethiolates of cadmium

The dimeric, homoleptic cadmium silanethiolate [{Cd{SSi(OtBu)$_3$}$_2$}$_2$], which was the first characterized silanethiolate of cadmium, was initially synthesized from tri-*tert*-butoxysilanethiol and cadmium acetate in the biphasic system

Table XXIII
Formulas and general characteristics of the Zn silanethiolates described in chapter 3.9.1.

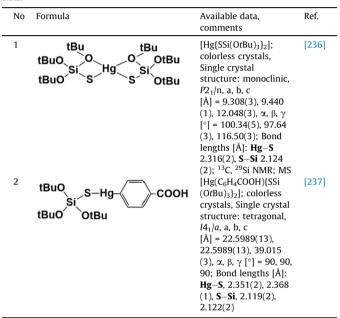| No	Formula	Available data, comments	Ref.
1		[(2,2′-bipy)Zn{SSi(OtBu)$_3$}$_2$]; colorless crystals; Single crystal structure: triclinic, *P*-1, *a*, *b*, *c* [Å] = 9.588(2), 14.569(3), 16.498(3), α, β, γ [°] = 107.57(3), 95.21(3), 99.84(3); Bond lengths [Å] = **Zn–S**, 2.247(2), 2.296(2) **S–Si**, 2.090(2), 2.092(2); IR, EA	[4]
2		[(MeCN)Zn{SSi(OtBu)$_3$}$_2$]; colorless crystals; Single crystal structure: orthorhombic, *Fdd2*, *a*, *b*, *c* [Å] = 17.845 (4), 45.811(9), 9.059(2), α, β, γ [°] = 90, 90, 90; Bond lengths [Å] = **Zn–S**, 2.2491(8), **S–Si**, 2.0680(11); IR, EA	[4]
3		[Zn{SSi(OtBu)$_3$}$_2$]; colorless oil; ^{1}H, ^{13}C, ^{29}Si NMR, IR, MS, EA	[4]
4		[(2-Etim)(H$_2$O)Zn{SSi(OtBu)$_3$}$_2$]; colorless crystals; Single crystal structure: triclinic, *P*-1, *a*, *b*, *c* [Å] = 9.0648 (3), 12.8755(4), 18.6199(6), α, β, γ [°] = 83.064(3), 76.828(3), 78.183(3); Bond lengths [Å] = **Zn–S**, 2.3070(4), 2.2759(5), **S–Si**, 2.0871(7), 2.0923(6); IR, EA	[168]
5		[(2-Meim)(MeOH)Zn{SSi(OtBu)$_3$}$_2$][(2-Meim)Zn{SSi(OtBu)$_3$}$_2$]·MeOH; colorless crystals; Single crystal structure: monoclinic, *P*2$_1$/*n*, *a*, *b*, *c* [Å] = 18.5515(3), 26.4480(5), 18.7446(3), α, β, γ [°] = 90, 115.206(2), 90; Bond lengths [Å] = **Zn–S**, 2.2708(7), 2.2792(8), 2.2831(9), 2.2851(6), **S–Si**, 2.082(1), 2.083(1), 2.091(1), 2.0990(9); ^{1}H, ^{13}C{^{1}H} NMR, IR, EA	[26]
6		[(2-*i*Prim)Zn(acac){SSi(OtBu)$_3$}]; colorless crystals; Single crystal structure: monoclinic, *P*2$_1$/*c*, *a*, *b*, *c* [Å] = 8.6401(19), 22.7749(14), 15.4304(19), α, β, γ [°] = 90, 90.035(19), 90; Bond lengths [Å] = **Zn–S**, 2.2602 (7), **S–Si**, 2.1033(9); IR, EA	[221]
7		[{(tBuO)$_3$SSi}Zn(2-Etim)$_3$][(tBuO)$_3$SSi}; colorless crystals; Single crystal structure: monoclinic, *P*2$_1$/*c*, *a*, *b*, *c* [Å] = 21.5198(3), 20.4036(2), 31.1289(3), α, β, γ [°] = 90, 130.435(1), 90; Bond lengths [Å] = **Zn–S** 2.256(1), 2.268(1), **S–Si**^{free} 2.069(1), 2.070(1), **S–Si**^{bonded} 2.081(2), 2.098(1); IR, EA	[27]
8		[(3,5-dMepy)$_2$Zn(SSiMe$_3$)$_2$]; colorless crystals; Single crystal structure: monoclinic, *P*2$_1$/*n*, *a*, *b*, *c* [Å] = 9.9388 (2), 17.7413(4), 15.1322(4), α, β, γ [°] = 90, 94.8760(11), 90; Bond lengths [Å] = **Zn–S** 2.2721(9), 2.744(9) **S–Si** 2.098(1), 2.114(1); ^{1}H, ^{13}C[^{1}H}, ^{29}Si NMR	[222]
9		[{Zn(SSi*t*Bu$_3$)$_2$}$_2$]; colorless crystals; Single crystal structure: monoclinic, *C2/c*, *a*, *b*, *c* [Å] = 24.5151(10), 13.3594(8), 38.3603(16), α, β, γ [°] = 90, 92.103(3), 90; Bond lengths [Å] = **Zn–S**^{b} 2.309(1), 2.325(1), 2.346 (1), 2.349(1), **Zn–S**^{t} 2.186(1), 2.196(1), **S–Si**^{b} 2.166(2), 2.202(2), **S–Si**^{t} 2.144(2), 2.147(2); ^{1}H, ^{13}C, ^{29}Si NMR; IR, EA	[226]
10		[[(*i*Pr$_3$SiS)Zn(μ-SSi*i*Pr$_3$)$_2$Zn(μ-SSi*i*Pr$_3$)$_2$Zn(SSi*i*Pr$_3$)]; colorless crystals; Single crystal structure: monoclinic, *P*2$_1$/*c*, *a*, *b*, *c* [Å] = 15.179(7), 13.746(6), 36.180(16), α, β, γ [°] = 90, 101.564(7), 90; Bond lengths [Å] = **Zn–S**^{b} 2.302(1), 2.314(1), 2.318(1), 2.333(1), 2.355(1), 2.376(1), 2.382(1), 2.391(1), **Zn–S**^{t} 2.189(1), 2.190(1), **S–Si**^{b} 2.171(1), 2.175(1), 2.182(1), 2.196(1), **S–Si**^{t} 2.131(2), 2.131(2)	[227]

Table XXIII (*continued*)

No	Formula	Available data, comments	Ref.
11		{[{Zn{SSi(O*t*Bu)$_3$}$_2$(μ-bpea)}$_n$](MeCN)}$_n$; colorless crystals; Monoclinic, *P*2$_1$/*n*, *a*, *b*, *c* [Å] = 10.588(2), 16.170 (3), 28.531(6), α, β, γ [°] = 90, 99.16(3), 90; Bond lengths [Å] = **Zn−S** 2.283(2), 2.287(2), **S−Si** 2.080(2), 2.083 (3); IR, EA	[228]
12		[{Zn{SSi(O*t*Bu)$_3$}$_2$(μ-pyr)}]; colorless crystals; monoclinic, *P*2$_1$/*c*, *a*, *b*, *c* [Å] = 8.6084(3), 23.5912(8), 18.7859 (8) α, β, γ [°] = 90, 104.541(4), 90; Bond lengths [Å] = **Zn−S** 2.2276(9), 2.2577(9), **S−Si** 2.084(1), 2.093(1); IR, EA	[170]
13		[(EtOH)Zn(acac){SSi(Odipp)$_3$}]; colorless crystals; Single crystal structure: triclinic, *P*-1, *a*, *b*, *c* [Å] = 11.4794 (6), 12.4070(6), 18.2427(9), α, β, γ [°] = 72.017(5), 84.044(4), 87.136(4); Bond lengths [Å] = **Zn−S**, 2.222(2), **S−Si**, 2.074(2); EA	[159]
14		[(MeOH)$_2$Zn{SSi(Odipp)$_3$}$_2$]; colorless crystals; Single crystal structure: triclinic, *P*-1, *a*, *b*, *c* [Å] = 16.0638(9), 24.0988(13), 27.5030(15), α, β, γ [°] = 109.787(2), 105.457(2), 98.688(2); Bond lengths [Å] = **Zn−S**, 2.2671 (7), 2.2684(7), 2.2693(8), 2.2729(8), **S−Si**, 2.0662(7), 2.0677(7), 2.0688(7), 2.0698(7) ^{1}H, ^{13}C NMR; IR; EA	[5]
15		[((MeOH)Zn(μ-MeCOO){SSi(Odipp)$_3$})$_4$]; colorless crystals; Single crystal structure: monoclinic, *P*2$_1$/*c*, *a*, *b*, *c* [Å] = 28.187(6), 39.831(8), 19.793(4), α, β, γ [°] = 90, 93.85(3), 90; Bond lengths [Å] = **Zn−S**, 2.243(2), 2.244 (1), 2.244(1), 2.250(1), **S−Si**, 2.064(2), 2.064(2), 2.065(2), 2.067(2); IR	[5]
16		(THF)$_2$[LiZn{SSi(SiMe$_3$)$_3$}$_3$]; colorless crystals; Single crystal structure: monoclinic, *P*2$_1$/*c*, *a*, *b*, *c* [Å] = 20.8591 (11), 28.2563(15), 23.8860(12), α, β, γ [°] = 90, 114.507(1), 90; Bond lengths [Å] = **Zn−S**, 2.2293(7), 2.234(1), 2.3094(7), 2.323(1), 2.241(1), 2.2419(8), **S−Si**, 2.143(1), 2.146(1), 2.147(1), 2.160(1), 2.1533(9), 2.160(1); ^{1}H, ^{13}C{^{1}H}, ^{29}Si NMR	[42]
17		{(Ph$_4$P)Zn(SSiMe$_3$)$_3$}; colorless, crystals; Single crystal structure: monoclinic, *P*2$_1$/*n*, *a*, *b*, *c* [Å] = 11.687(2), 18.890(4), 18.770(4), α, β, γ [°] = 90, 98.27(3), 90; Bond lengths [Å] = **Zn−S**, 2.2534(7), 2.2536(8), 2.2543(7), **S−Si**, 2.1055(9), 2.1174(7), 2.1242(8); ^{1}H, ^{13}C, ^{29}Si NMR; EA	[218]

Fig. 50. Molecular structures of typical molecular tri-*tert*-butoxysilanethiolate complexes of Zn(II) withour hydrogen atoms: a) [(2,2′-bipy)Zn{SSi(*t*BuO)$_3$}$_2$] [4]; b) [(MeCN)Zn{SSi(*t*BuO)$_3$}$_2$] [4]; c) [(2-Etim)(H$_2$O)Zn{SSi(*t*BuO)$_3$}$_2$] [168]; d) [(2-Meim)(MeOH)Zn{SSi(*t*BuO)$_3$}$_2$] [(2-Meim)Zn{SSi(*t*BuO)$_3$}$_2$]·MeOH [26]; e) [(2-*i*Prim)Zn(acac){SSi(*t*BuO)$_3$}] [221]; f) [(2-Etim)$_3$ZnSSi(*t*BuO)$_3$]{SSi(*t*BuO)$_3$} [27].
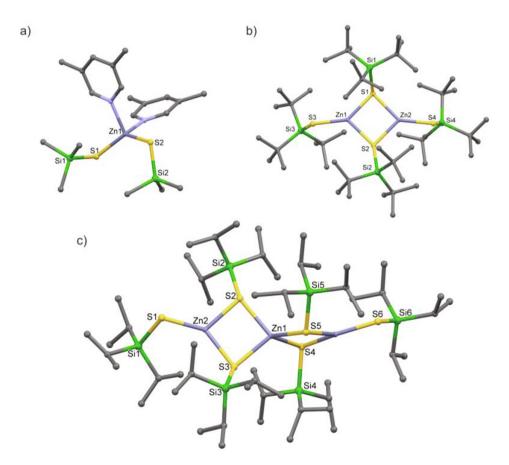
Fig. 51. Molecular structures of molecular trialkylsilanethiolate complexes of Zn(II) of growing nuclearity; hydrogen atoms are omitted: a) [(3,5-dMepy)$_2$Zn(SSiMe$_3$)$_2$] [222]; b) [{Zn(SSi*t*Bu$_3$)$_2$}$_2$] [226]; c) [[(iPr$_3$SiS)Zn(μ-SSiiPr$_3$)$_2$Zn(μ-SSiiPr$_3$)$_2$Zn(SSiiPr$_3$)] [227].

water/benzene. The Cd$_2$S$_2$ central ring is folded; *pseudo*-trigonal coordination CdS$_3$ is completed with at least two coordinative Cd—O bonds with the *tert*-butoxy substituents of the silanethiol

(Fig. 55a, Table XXIV-1) [230] Though according to the mass spectra the dimeric molecule is not preserved in the gas phase [230] it was confirmed to exist in solution – at least within ben-
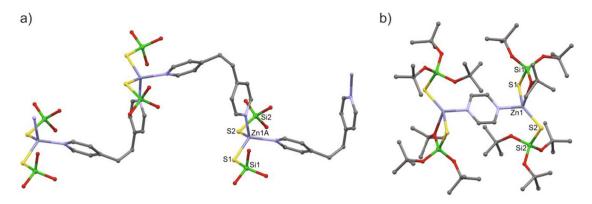
Fig. 52. Molecular structures without hydrogen atoms of polynuclear silanethiolate complexes of Zn(II) with metal centres bridged by heteroligands: a) [{Zn{SSi(OtBu)₃}₂(μ-bpea)}ₙ] (MeCN)ₙ tBuO groups are omitted [228]; b) [{Zn{SSi(OtBu)₃}₂(μ-pyr)] [170].
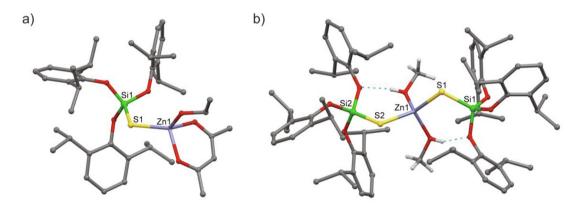
Fig. 53. Molecular structures of heteroleptic complexes of Zn(II) with bulky (dippO)₃SiS⁻ ligand; hydrogen atoms are omitted: a) [(EtOH)Zn(acac){SSi(Odipp)₃}] [159]; b) [(MeOH)₂Zn{SSi(Odipp)₃}₂] [5].
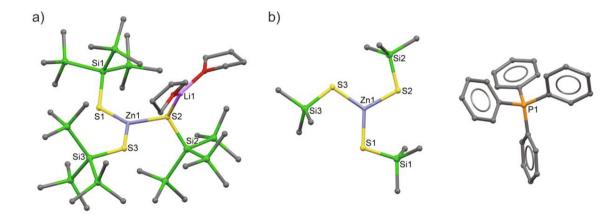
Fig. 54. Molecular structures of trigonal, silanethiolate complexes of Zn(II) without hydrogen atoms: a) (THF)₂[LiZn{SSi(SiMe₃)₃}₃] [42]; b) (Ph₄P)[Zn(SSiMe₃)₃] [218].

zene solutions [231]. The reactions with nucleophiles: 1,10-phen, 2,2′-bipy and other N-donor ligands produced molecular complexes with C.N. = 4 and C.N. = 5 (Fig. 55b, Table XXIV-2,3) [e.g. [26,230,232]]. Tri-*tert*-butoxysilanethiolate complexes of cadmium were studied in detail by XRD and ¹¹³Cd NMR as models for the Cd-substituted active site of alcohol dehydrogenase [22,166]. Molecular, mixed ligand tri-*tert*-butoxysilanethiolates/thiocarbamates were considered as CVD precursors for the formation of semiconducting thin films of CdS (*e.g.* Fig. 56a, Table XXIV-4) [21,217]. Moreover optical properties and thermal

stability were investigated in detail for a variety of 1-D polymers and a dimer with terminal silanethiolate ligands and bridging N-donors (*e.g.* dimer Fig. 56b, Table_XXIV-9, polymers Fig. 57a,b, Table XXIV-5,6) [170–172,219,228,233].

With the use of TDST a pseudo-trigonal cadmium silanethiolate complex is easily obtained from cadmium acetate, silanethiol within a MeOH/tol mixture of solvents in the form of colourless crystals. The coordination sphere of cadmium – formally CdOS₂ - is completed by π-donating phenyl rings of the aryloxysilanethiolate ligands (Fig. 58a, Table XXIV-8) [5].

Fig. 55. Molecular structures of tri-*tert*-butoxysilanethiolate complexes of Cd(II) without hydrogen atoms: a) [{Cd{SSi(*t*BuO)₃}₂}₂] [230]; b) [(N-Meim)₂Cd{SSi(*t*BuO)₃}₂] [232].

Table XXIV
Formulas and general characteristics of the Cd silanethiolates described in chapter 3.9.2.

No	Formula	Available data, comments	Ref.
1		[{Cd(SSi(O*t*Bu)₃)₂}₂]; colorless crystals, Single crystal structure: monoclinic, $P2_1/n$, a, b, c [Å] = 15.664(3), 33.321(8), 14.267(3), α, β, γ [°] = 90, 104.14(2), 90; Bond lengths [Å]: **Cd–S**[b] 2.541(2), 2.547(2), 2.574(2), 2.576(2), **Cd–S**[t] 2.407(2), 2.409(2), **S – Si**[b] 2.116(4), 2.119(4), **S–Si**[t] 2.074(5), 2.076(5); ¹H, ¹³C, ²⁹Si NMR; UV, MS, EA	[230]
2		[(N-Meim)₂Cd{SSi(O*t*Bu)₃}₂]; colorless crystals, Single crystal structure: monoclinic, C2, a, b, c [Å] = 16.0333(8), 9.0116(5), 15.9506(12), α, β, γ [°] = 90, 113.962(6), 90; Bond lengths [Å]: **Cd–S**, 2.491(2), **S–Si**, 2.040(2); ¹¹³Cd NMR; CP MAS ¹³C, ²⁹Si, ¹¹³Cd NMR; IR, EA	[232]
3		[(im)Cd{SSi(O*t*Bu)₃}₂]·MeOH; colorless plates, Single crystal structure: orthorhombic, $Pna2_1$, a, b, c [Å] = 17.5326(7), 8.6735(3), 26.7413(10), α, β, γ [°] = 90, 90, 90; Bond lengths [Å]: **Cd–S**, 2.451(1), 2.478(1), **S–Si**, 2.083(2), 2.097(2); ¹H, ¹³C, ¹¹³Cd NMR; CP MAS ¹³C, ²⁹Si, ¹¹³Cd NMR; IR, EA	[26]
4		[Cd{μ-SSi(O*t*Bu)₃}(S₂CNEt₂)]₂; colorless crystals; Single crystal structure: triclinic, P-1, *a, b, c* [Å] = 10.6730(14), 10.7200(16), 12.452(2) α, β, γ [°] = 65.199(15), 73.677(13), 78.583(12); Bond lengths [Å] = **Cd–S** 2.5716(9), **S–Si** 2.122(1); ¹H NMR, UV–Vis, IR, MS, AFM, XPS, EA	[21]
5		[{Cd{SSi(O*t*Bu)₃}₂(μ-bpea)}ₙ](MeCN)ₙ; colorless crystals; Single crystal structure: monoclinic, C2/c, *a, b, c* [Å] = 17.5369(5), 14.4176(3), 22.6213(6), α, β, γ [°] = 90, 97.639(2), 90; Bond lengths [Å] = **Cd–S** 2.4605(4), **S–Si** 2.0824(5); IR, luminescence, TG, EA	[228]

Table XXIV (*continued*)

No	Formula	Available data, comments	Ref.
6		[{Cd{SSi(OtBu)₃}₂(μ-C₇H₁₈N₂)}ₙ]; colorless crystals; Single crystal structure: triclinic, *P*-1, *a, b, c* [Å] = 10.2109(3), 13.5526(5), 15.4806(5), α, β, γ [°] = 89.220(3), 81.646(3), 83.857(3); Bond lengths [Å] = **Cd−S** 2.4430(8), 2.4980(7); **S−Si** 2.074(1), 2.097(1); IR, TG, EA	[233]
7		[(py)₂Cd{S₂(μ-O){Si(Odipp)₃}₂}]; colorless crystals; Single crystal structure: monoclinic, *C*2/*c*, *a, b, c* [Å] = 28.2952(18), 25.6156(9), 21.1582(13), α, β, γ [°] = 90, 124.333(9), 90; Bond lengths [Å] = **Cd−S** 2.4469 (12), 2.4505(11); **S−Si** 2.0718(14), 2.0751(12); ¹H, ¹³C, ²⁹Si NMR, IR	[190]
8		[(MeOH)Cd{SSi(OtBu)₃}₂]·MeOH; colorless crystals; Single crystal structure: monoclinic, *P*2₁/*c*, *a, b, c* [Å] = 17.0361(8), 20.7953(9), 21.8995(10), α, β, γ [°] = 90, 104.873(5), 90; Bond lengths [Å] = **Cd−S** 2.4271 (6), 2.4299(6); **S−Si** 2.084(1), 2.087(1); ¹H, ¹³C, ¹¹³Cd NMR, IR, EA	[5]
9		[{(μ-tmbiim)Cd{SSi(OtBu)₃}₂}₂]; colorless crystals; Single crystal structure: triclinic, *P*-1, *a, b, c* [Å] = 13.3522 (5), 18.3127(7), 20.4152(6), α, β, γ [°] = 85.869(3), 74.089(3), 74.772(3); Bond lengths [Å] = **Cd−S** 2.470(2), 2.482(1), 2.482(1), 2.482(2); **S−Si** 2.061(2), 2.087(2), 2.091(2), 2.092(2); ¹H, ¹³C NMR, IR, EA	[219]

Fig. 56. Molecular structures of binuclear, silanethiolate complexes of Cd(II) without hydrogen atoms: a) with the bridging (*t*BuO)₃SiS⁻ [Cd{μ-SSi(O*t*Bu)₃}(S₂CNEt₂)]₂ [21]; b) with the terminal (*t*BuO)₃SiS⁻ [[{Cd{SSi(O*t*Bu)₃}₂(μ-tmbiim)}₂] [219].

Partial hydrolysis of tetrakis(2,6-diisopropylphenoxy)-cyclodi-silthiane allows the formation of potentially bridging or chelating bis(2,6-diisopropylphenoxy)disiloxane-1,3-dithiol. This is a substance quite sensitive to hydrolysis although it may be isolated as colorless crystals and used for the preparation of metal complexes [190]. So far two such complexes were synthesized: heteroleptic, mononuclear Cd complex (Fig. 58b, Table XXIV-7)

[190] and unstable, trinuclear silver anion described by Ciborska and co-workers [52]. In both compounds the double donor ligand shows a chelating binding mode [52,190].

We did not find any structural information on cadmium silan-ethiolates other than alkoxy and aryloxy derivatives but simple silanethiolates and silaneselenolates of cadmium: [{Cd(ESiMe₃)₂}-ₙ] were reported as unstable, polymeric compounds, difficult to
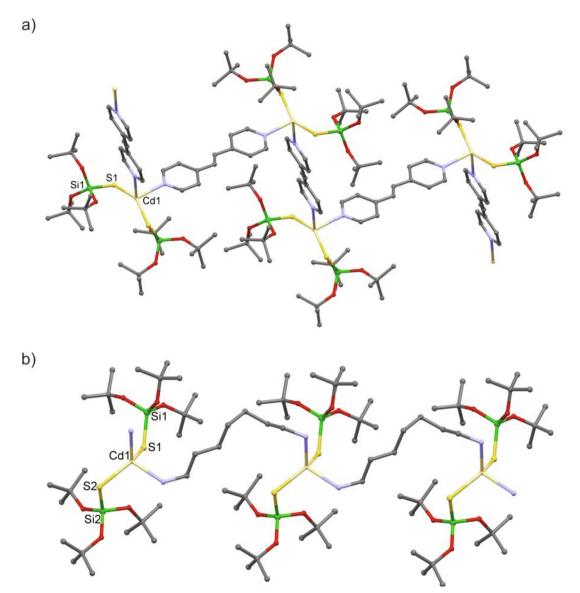
Fig. 57. Molecular structures of Cd(II) CP with the terminal $(tBuO)_3SiS^-$ ligands; hydrogen atoms are omitted: a) $[\{Cd\{SSi(OtBu)_3\}_2(\mu\text{-bpea})\}_n]$ $(MeCN)_n$ [228]; b) $[\{Cd\{SSi(OtBu)_3\}_2(\mu\text{-}C_7H_{18}N_2)\}_n]$ [233].
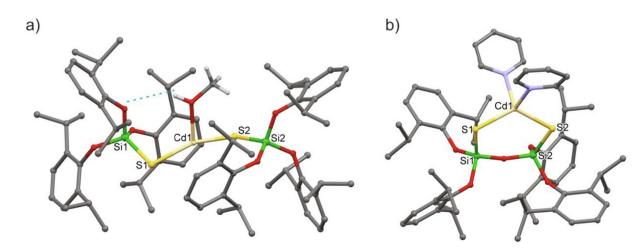
Fig. 58. Molecular structures of heteroleptic Cd(II) silanethiolate complexes with bulky silanethiolate ligands: $(dippO)_3SiS^-$ and $\{(dippO)_3Si\}_2(\mu\text{-O})S_2^{2-}$; hydrogen atoms are omitted: a) $[(MeOH)Cd\{SSi(OtBu)_3\}_2]\cdot MeOH$ [5]; b) $[(py)_2Cd\{S_2(\mu\text{-O})\{Si(Odipp)_3\}_2\}]$ [190].
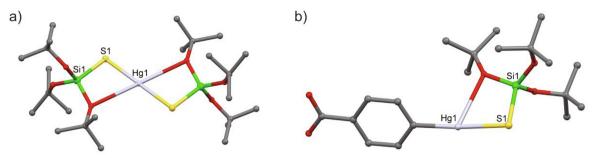
Fig. 59. Molecular structures of Hg(II) tri-*tert*-butoxysilanethiolate complexes without hydrogen atoms: a) [Hg{SSi(O*t*Bu)$_3$}$_2$] [236]; b) [Hg(C$_6$H$_4$COOH){SSi(O*t*Bu)$_3$}$_2$] [237].

Table XXV
Formulas and general characteristics of the Hg silanethiolates described in chapter 3.9.2.

No	Formula	Available data, comments	Ref.
1		[Hg{SSi(O*t*Bu)$_3$}$_2$]; colorless crystals, Single crystal structure: monoclinic, *P*2$_1$/n, a, b, c [Å] = 9.308(3), 9.440(1), 12.048(3), α, β, γ [°] = 100.34(5), 97.64(3), 116.50(3); Bond lengths [Å]: **Hg**–**S** 2.316(2), **S**–**Si** 2.124(2); ^{13}C, ^{29}Si NMR; MS	[236]
2		[Hg(C$_6$H$_4$COOH){SSi(O*t*Bu)$_3$}$_2$]; colorless crystals, Single crystal structure: tetragonal, *I*4$_1$/*a*, a, b, c [Å] = 22.5989(13), 22.5989(13), 39.015(3), α, β, γ [°] = 90, 90, 90; Bond lengths [Å]: **Hg**–**S**, 2.351(2), 2.368(1), **S**–**Si**, 2.119(2), 2.122(2)	[237]

Table XXVI
Formulas and general characteristics of the Gd and Dy silanethiolates described in chapter 3.10.

No	Formula	Available data, comments	Ref.
1		[{MeCp$_2$M(μ-SSiPh$_3$)}$_2$]·tol (M = Dy, Gd):**Gd**: colorless blocks, Single crystal structure: Monoclinic, *P*2$_1$/n; a, b, c [Å] = 9.7437(2), 18.8921(6), 15.4871(5); α, β, γ [°] = 90, 96.694(2), 90; Bond lengths [Å] = **Gd**–**S** 2.622(7), 2.707(14), **S**–**Si** 2.124(2); EA, μ, magn. susc.**Dy**: yellow crystalline blocks, Single crystal structure: monoclinic, *P*2$_1$/n; a, b, c [Å] = 9.7223(19), 18.864(4), 15.410(3); α, β, γ [°] = 90, 96.55(3), 90; Bond lengths [Å] = **Dy**–**S** 2.599(15), 2.693(10), **S**–**Si** 2. 123(3); EA, μ, magn. susc.	[238]

Fig. 60. Molecular structure of [{MeCp$_2$Gd(μ-SSiPh$_3$)}$_2$]·tol (solvent molecule and hydrogen atoms are removed for clarity) [238].

3.9.3. Silanethiolates of mercury

Though the synthesis of silanethiolates of mercury was reported as early as 1971 in a preliminary communication [235], very few well-characterized examples are described in the literature. Within this first report (C$_2$H$_5$)$_3$SiEHgSi(C$_2$H$_5$)$_3$ (E = S, Se) were obtained by the following reaction: (Et$_3$Si)$_2$Hg + 1/8E$_8$ → Et$_3$SiSHgSiEt$_3$ and iso-lated from the reaction mixtures after crystallization from pentane at 200 K. Cryoscopic molecular weight measurements showed that these compounds were monomeric in benzene solution. All obtained complexes underwent slow decomposition in hexane solution at RT [235].

In the mid-eighties the homoleptic silanethiolate of mercury was synthesized from HgO and TBST and structurally characterized (Fig. 59a, Table XXV-1). The monomeric molecule features a linear coordination typical of Hg(II), extended however by two O atoms of the butoxy groups (Fig. 59a) [236]. Another, and final so far, linear silanethiolate: 4-(tri-*tert*-butoxysilylthiomercurio)benzoic acid (Fig. 59b, Table XXV-2) was described in 2003 [237].

3.10. Lanthanide silanethiolates

According to the HSAB concept lanthanides act as hard acids while thiolates are soft bases which means that complexes with Ln–S bonds are difficult to obtain and unstable. Indeed, it is con-firmed by the number of structurally characterized lanthanide silanethiolate complexes: there are only two of them described

purify, showing spontaneous decomposition to CdE [234]. Mononuclear [(3,5-dMepy)$_2$Cd(SeSiMe$_3$)$_2$] was generated *in situ* as a precursor to heterometallic clusters [223].

until now with the general formula $[\{MeCp_2Ln(\mu\text{-}SSiPh_3)\}_2]$ (Ln = Gd, Dy). They were synthesized by Tuna and co-workers in search of lanthanide-containing SMM (Fig. 60, Table XXVI). Dinuclear complexes with metal ions bridged by thiolate residues were obtained in the reaction of two equiv. of lithium triphenylsilanethiolate with MeCp₃Ln using standard Schlenk technique [238].

4. Summary

In this review we have described the syntheses, structures and other properties of metal complexes with silanethiolate ligands. Silanethiolates are soft S-donor ligands and thus willingly bind to metal ions that are intermediate to soft Lewis acids. The reactivity of the silicon-sulfur bond, which is prone to nucleophilic attack and oxidation, usually requires that the complexes are synthesized in non-aqueous solvents under an inert gas atmosphere. The main precursors to silanethiolate ligands are: silanethiols and their salts with alkali metals, silyl sulfides and sometimes silanides. Most of the silanethiolate complexes reported in the literature are molecular species of low nuclearity. In contrast to organic thiols silanethiols rarely serve as bridging ligands in polynuclear metal complexes. This feature is often connected with the presence of large substituents at the silicon atom, which serve as a kinetic protection of the silicon-sulfur bond. Though silanethiolate 1-D coordination polymers are known, the silicon-sulfur anions serve as terminal ligands in these compounds. Moreover, a bridging mode further weakens the silicon-sulfur bond and therefore silanethiolate complexes are often considered in material and cluster synthesis as precursors to metal sulfides of various nuclearity and form. The formation of predefined clusters and precipitation of metal chalcogenide nanoparticles from organic solution with the use of silyl derivatives of chalcogenides still captures the attention of researchers and the knowledge is accumulating [239].

Another application of silanethiolate complexes is the construction of molecular model compounds featuring metal centers that mimic those present at the active sites of metalloproteins. The increased acidity of the silanethiols in comparison with the organic thiols offers a variety of simple synthetic methods to obtain a metal silanethiolate and a choice of substituents allows to achieve specific coordination environments. Silicon-sulfur complexes are therefore either present within the final structures with a predefined geometry or serve as coupling intermediates, which lose their silyl group in the course of the reaction as described in the review.

Declaration of Competing Interest

The authors declare that they have no known competing financial interests or personal relationships that could have appeared to influence the work reported in this paper.

References

[1] A. Haas, Angew. Chem. Int. Ed. Engl. 4 (1965) 1014–1023, https://doi.org/10.1002/anie.196510141.
[2] D.A. Armitage, in: Z. Rappoport (Ed.), The Chemistry of Functional GroupsThe Chemistry of Organic Silicon Compounds, John Wiley & Sons, Ltd, Chichester, UK, 1998, pp. 1869–1894, https://doi.org/10.1002/0470857250.ch31.
[3] M. Simon, F. Breher, Dalton Trans. 46 (2017) 7976–7997, https://doi.org/10.1039/C7DT02085F.
[4] B. Becker, K. Radacki, W. Wojnowski, J. Organomet. Chem. 521 (1996) 39–49, https://doi.org/10.1016/0022-328X(96)06233-X.
[5] A. Jabłońska, J. Bender, D. Gudat, Ł. Ponikiewski, A. Dołęga, Polyhedron 115 (2016) 219–227, https://doi.org/10.1016/j.poly.2016.05.022.
[6] Y.R. Luo, Comprehensive Handbook of Chemical Bond Energies, CRC Press, Boca Raton, FL (2007), https://doi.org/10.1201/9781420007282.
[7] T. Komuro, T. Matsuo, H. Kawaguchi, K. Tatsumi, Dalton Trans. (2004) 1618–1625, https://doi.org/10.1039/B316567A.
[8] C.B. Khadka, D.G. Macdonald, Y. Lan, A.K. Powell, D. Fenske, J.F. Corrigan, Inorg. Chem. 49 (2010) 7289–7297, https://doi.org/10.1021/ic902346u.
[9] J. Zhai, M.D. Hopkins, G.L. Hillhouse, Organometallics 34 (2015) 4637–4640, https://doi.org/10.1021/acs.organomet.5b00421.
[10] A.M. Polgar, A. Zhang, F. Mack, F. Weigend, S. Lebedkin, M.J. Stillman, J.F. Corrigan, Inorg. Chem. 58 (2019) 3338–3348, https://doi.org/10.1021/acs.inorgchem.8b03399.
[11] D.T.T. Tran, N.J. Taylor, J.F. Corrigan, Angew. Chem. Int. Ed. Engl. 39 (2000) 935–937, https://doi.org/10.1002/(SICI)1521-3773(20000303)39:5<935::AID-ANIE935>3.0.CO;2-I.
[12] D. T. T. Tran, J. F. Corrigan, Organometallics, 19 (2000) 5202-5208. https://doi.org/0.1021/om000624d
[13] B. Becker, W. Wojnowski, K. Peters, E.-M. Peters, H.G. Von Schnering, Polyhedron 9 (1990) 1659–1666, https://doi.org/10.1016/S0277-5387(00)83968-6.
[14] T.I. Kückmann, M. Hermsen, M. Bolte, M. Wagner, H.-W. Lerner, Inorg. Chem. 44 (2005) 3449–3458, https://doi.org/10.1021/ic048710j.
[15] A. Pladzyk, N. Daca, Ł. Ponikiewski, Z. Anorg, Allg. Chem. 638 (2012) 1497–1500, https://doi.org/10.1002/zaac.201200203.
[16] W. Wojnowski, A. Herman, Z. Anorg, Allg. Chem. 425 (1976) 91–96, https://doi.org/10.1002/zaac.19764250111.
[17] B. Thapa, H.B. Schlegel, J. Phys. Chem. A 120 (2016) 5726–5735, https://doi.org/10.1021/acs.jpca.6b05040.
[18] J. Chojnacki, Polyhedron 27 (2008) 969–976, https://doi.org/10.1016/j.poly.2007.11.041.
[19] J. Chojnacki, B. Becker, A. Konitz, M.J. Potrzebowski, W. Wojnowski, J. Chem. Soc., Dalton Trans. (1999) 3063–3068, https://doi.org/10.1039/A903694F.
[20] A. Dołęga, W. Marynowski, K. Baranowska, M. Śmiechowski, J. Stangret, Inorg. Chem. 51 (2012) 836–843, https://doi.org/10.1021/ic2013073.
[21] A. Kropidłowska, J. Chojnacki, A. Fahmi, B. Becker, Dalton Trans. (2008) 6825–6831, https://doi.org/10.1039/B806248J.
[22] A. Dołęga, Coord. Chem. Rev. 254 (2010) 916–937, https://doi.org/10.1016/j.ccr.2009.12.039].
[23] B. Xi, R.H. Holm, Inorg. Chem. 50 (2011) 6280–6288, https://doi.org/10.1021/ic200641k.
[24] D.J. Meininger, J.D. Caranto, H.D. Arman, Z.J. Tonzetich, Inorg. Chem. 52 (2013) 12468–12476, https://doi.org/10.1021/ic401467k.
[25] I. Kovács, F. Bélanger-Gariépy, A. Shaver, Inorg. Chem. 42 (2003) 2988–2991, https://doi.org/10.1021/ic030049g.
[26] A. Dołęga, K. Baranowska, D. Gudat, A. Herman, J. Stangret, A. Konitz, M. Śmiechowski, S. Godlewska, Eur. J. Inorg. Chem. (2009) 3644–3660, https://doi.org/10.1002/ejic.200900106.
[27] A. Dołęga, A. Pladzyk, K. Baranowska, J. Jezierska, Inorg. Chim. Acta 362 (2009) 5085–5096, https://doi.org/10.1016/j.ica.2009.08.028.
[28] D. Kowalkowska-Zedler, A. Dołęga, N. Nedelko, R. Łyszczek, P. Aleshkevych, I. Demchenko, J. Łuczak, A. Ślawska-Waniewska, A. Pladzyk, Dalton Trans. 49 (2020) 697–710, https://doi.org/10.1039/C9DT03722E.
[29] P. Pyykkö, S. Riedel, M. Patzschke, Chem. Eur. J. 11 (2005) 3511–3520, https://doi.org/10.1002/chem.200401299.
[30] P. Pyykkö, M. Atsumi, Chem. Eur. J. 15 (2009) 186–197, https://doi.org/10.1002/chem.200800987.
[31] P. Pyykkö, M. Atsumi, Chem. Eur. J. 15 (2009) 12770–12779, https://doi.org/10.1002/chem.200901472.
[32] R.G. Pearson, Inorg. Chem. 27 (1988) 734–740, https://doi.org/10.1021/ic00277a030.
[33] K. Baranowska, J. Chojnacki, W. Wojnowski, I. Krossing, Acta Crystallogr Sect. E: Struct. Rep. Online 58 (2002) m569–m570, https://doi.org/10.1107/S1600536802016987.
[34] R. Piękoś, W. Wojnowski, Z. Anorg. Allg. Chem. 318 (1962) 212-216. https://doi.org/10.1002/zaac.19623180310
[35] E. Jesionka, A. Ciborska, J. Chojnacki, W. Wojnowski, Acta Crystallogr Sect. C: Cryst. Struct. Commun. 61 (2005) m321–m323, https://doi.org/10.1107/S0108270105015076.
[36] M. Kloskowska, J. Chojnacki, W. Wojnowski, B. Becker, Acta Crystallogr Sect. C: Cryst. Struct. Commun. 62 (2006) m541–m544, https://doi.org/10.1107/S0108270106041746.
[37] G.A. Kraus, B. Andersh, Tetrahedron Lett. 32 (1991) 2189–2192, https://doi.org/10.1016/S0040-4039(00)79676-6.
[38] M. Niemeyer, P.P. Power, Inorg. Chem. 35 (1996) 7264–7272, https://doi.org/10.1021/ic960570t.
[39] S. Spirk, F. Belaj, N. Hurkes, R. Pietschnig, Chem. Commun. 48 (2012) 8398–8400, https://doi.org/10.1039/C2CC33883A.
[40] Y. Li, H. Zhu, D.M. Andrada, G. Frenking, H.W. Roesky, Chem. Commun. 50 (2014) 4628–4630, https://doi.org/10.1039/C4CC00912F.
[41] G. Gutekunst, A.G. Brook, J. Organomet. Chem. 225 (1982) 1–3, https://doi.org/10.1016/S0022-328X(00)86805-9.
[42] M. Kotsch, C. Gienger, C. Schrenk, A. Schnepf, Z Anorg, Allg. Chem. 642 (2016) 670–675, https://doi.org/10.1002/zaac.201600137.
[43] C. Kayser, R. Fischer, J. Baumgartner, C. Marschner, Organometallics 21 (2002) 1023–1030, https://doi.org/10.1021/om010815w.
[44] W. Wojnowski, K. Peters, E.-M. Peters, H.G. von Schnering, Z. Kristallogr, Cryst. Mater. 174 (1986) 297–303, https://doi.org/10.1524/zkri.1986.174.14.297.
[45] S. Chadwick, U. Englich, K. Ruhlandt-Senge, Organometallics 16 (1997) 5792–5803, https://doi.org/10.1021/om9707230.

[46] D.J. Rose, Y.D. Chang, Q. Chen, P.B. Kettler, J. Zubieta, Inorg. Chem. 34 (1995) 3973–3980, https://doi.org/10.1021/ic00119a019.
[47] P.J. Bonasia, V. Christou, J. Arnold, J. Am. Chem. Soc. 115 (1993) 6777–6781, https://doi.org/10.1021/ja00068a039.
[48] T.I. Kückmann, F. Schödel, I. Sänger, M. Bolte, M. Wagner, H.-W. Lerner, Eur. J. Inorg. Chem. (2010) 468–475, https://doi.org/10.1002/ejic.200900806.
[49] M. Kloskowska, J. Chojnacki, W. Wojnowski, B. Becker, Acta Crystallogr, Sect. E: Struct. Rep. Online 62 (2006) m2476–m2478, https://doi.org/10.1107/S1600536806035070.
[50] J. Chojnacki, A. Ciborska, W. Wojnowski, Acta Crystallogr Sect. C: Cryst. Struct. Commun. 64 (2008) m240–m242, https://doi.org/10.1107/S0108270108015242.
[51] S. Godlewska, K. Baranowska, A. Dołęga, Inorg. Chem. Commun. 40 (2014) 69–72, https://doi.org/10.1016/j.inoche.2013.11.017.
[52] A. Ciborska, Z. Hnatejko, K. Kazimierczuk, A. Mielcarek, A. Wiśniewska, A. Dołęga, Dalton Trans. 46 (2017) 11097–11107, https://doi.org/10.1039/c7dt00740j.
[53] E. Jesionka, K. Baranowska, W. Wojnowski, Phosphorus, Sulfur, Silicon Relat. Elem. 184 (2009) 1426–1439, https://doi.org/10.1080/10426500902947674.
[54] S.-H. Zhang, H.-W. Xi, K.H. Lim, C.-W. So, Organometallics 30 (2011) 3686–3689, https://doi.org/10.1021/om200285u.
[55] C.W. So, H.W. Roesky, J. Magull, R.B. Oswald, Angew. Chem. Int. Ed. Engl. 46 (2006) 3948–3950, https://doi.org/10.1002/anie.200600647.
[56] J.L. Brown, A.C. Montgomery, C.A. Samaan, M.T. Janicke, B.L. Scott, A.J. Gaunt, Dalton Trans. 45 (2016) 9841–9852.
[57] E. Jesionka, J. Chojnacki, W. Wojnowski, Acta Crystallogr Sect. E: Struct. Rep. Online 62 (2006) m1982–m1984, https://doi.org/10.1107/S1600536806028054.
[58] A.L. Rheingold, M. Hampden-Smith, CSD HABPOS Communication (2015).
[59] W. Wojnowski, K. Peters, E.-M. Peters, H.G. von Schnering, Z. Anorg, Allg. Chem. 531 (1985) 147–152, https://doi.org/10.1002/zaac.19855311220.
[60] M. Taghiof, M.J. Heeg, M. Bailey, D.G. Dick, R. Kumar, D.G. Hendershot, H. Rahbarnoohi, J.P. Oliver, Organometallics 14 (1995) 2903–2917, https://doi.org/10.1021/om00006a040.
[61] V. Jancik, H.W. Roesky, Inorg. Chem. 44 (2005) 5556–5558, https://doi.org/10.1021/ic050693q.
[62] O.T. Beachley Jr., D.B. Rosenblum, M.R. Churchill, C.H. Lake, L.M. Toomey, Organometallics 15 (1996) 3653–3658, https://doi.org/10.1021/om960284p.
[63] J. Chojnacki, A. Schnepf, W. Wojnowski, Z. Kristallogr.-New Cryst. Struct. 216 (2001) 208-210. https://doi.org/10.1524/ncrs.2001.216.14.208
[64] K. Baranowska, J. Chojnacki, W. Wojnowski, E. Wurster, Acta Crystallogr Sect. E: Struct. Rep. Online 58 (2002) m728–m729, https://doi.org/10.1107/S160053680202055X.
[65] Y. Xiong, S. Yao, R. Muller, M. Kaupp, M. Driess, Angew. Chem. Int. Ed. Engl. 54 (2015) 10254–10257, https://doi.org/10.1002/anie.201504489.
[66] J. Guschlbauer, T. Vollgraff, J. Sundermeyer, Inorg. Chem. 58 (2019) 15385–15392, https://doi.org/10.1021/acs.inorgchem.9b02453.
[67] H. Rahbarnoohi, M. Taghiof, M.J. Heeg, D.G. Dick, J.P. Oliver, Inorg. Chem. 33 (1994) 6307–6314, https://doi.org/10.1021/ic00104a047.
[68] O. Kluge, M. Puidokait, R. Biedermann, H. Krautscheid, Z. Anorg, Allg. Chem. 633 (2007) 2138–2140, https://doi.org/10.1002/zaac.200700373.
[69] G. Ossig, A. Meller, C. Brönneke, O. Müller, M. Schäfer, R. Herbst-Irmer, Organometallics 16 (1997) 2116–2120, https://doi.org/10.1021/om961087t.
[70] R. Lehnert, M. Höppner, H. Kelling, Z. Anorg, Allg. Chem. 591 (1990) 209–213, https://doi.org/10.1002/zaac.19905910125.
[71] U. Herzog, U. Böhme, E. Brendler, G. Rheinwald, J. Organomet. Chem. 630 (2001) 139–148, https://doi.org/10.1016/S0022-328X(01)01010-5.
[72] U. Herzog, G. Rheinwald, Organometallics 20 (2001) 5369–5374, https://doi.org/10.1021/om0105573.
[73] U. Herzog, H. Borrmann, J. Organomet. Chem. 675 (2003) 42–47, https://doi.org/10.1016/S0022-328X(03)00226-2.
[74] T.J. Boyle, L.J. Tribby, L.A.M. Ottley, S.M. Han, Eur. J. Inorg. Chem. (2009) 5550–5560, https://doi.org/10.1002/ejic.200900556.
[75] J.D. Epping, S. Yao, M. Karni, Y. Apeloig, M. Driess, J. Am. Chem. Soc. 132 (2010) 5443–5455, https://doi.org/10.1021/ja1004812.
[76] K. Peters, E.-M. Peters, H.G. von Schnering, W. Wojnowski, S. Tamulewicz, Z. Kristallogr.-New Cryst. Struct. 213 (1998) 347–348, https://doi.org/10.1524/ncrs.1998.213.14.361.
[77] M. Kloskowska, A. Konitz, W. Wojnowski, B. Becker, Z. Anorg, Allg. Chem. 632 (2006) 2424–2428, https://doi.org/10.1002/zaac.200600221.
[78] W. Wojnowski, M. Wojnowski, K. Peters, E.-M. Peters, H.G. Von Schnering, Z. Anorg, Allg. Chem. 535 (1986) 56–62, https://doi.org/10.1002/zaac.19865350408.
[79] K. Peters, E.-M. Peters, H.G. von Schnering, W. Wojnowski, S. Tamulewicz, K. Radacki, Z. Kristallogr.-New, Cryst. Struct. 212 (1997) 341–342, https://doi.org/10.1524/ncrs.1997.212.jg.341.
[80] J. Chojnacki, M. Kloskowska, U. Wójtowicz, W. Wojnowski, Acta Crystallogr Sect. C: Cryst. Struct. Commun. 63 (2007) m349–m351, https://doi.org/10.1107/S0108270107029629.
[81] U. Herzog, G. Rheinwald, J. Organomet. Chem. 648 (2002) 220–225, https://doi.org/10.1016/S0022-328X(01)01450-4.
[82] K. Peters, E.-M. Peters, H. G. von Schnering, W. Wojnowski, S. Tamulewicz, K. Radacki, Z. Kristallogr.-New Cryst. Struct. 212 (1997b) 343-344. https://doi.org/10.1524/ncrs.1997.212.1.343
[83] K. Peters, E.-M. Peters, H. G. von Schnering, W. Wojnowski, S. Tamulewicz, K. Radacki, Z. Kristallogr.-New Cryst. Struct. 212 (1997c) 347-348. https://doi.org/10.1524/ncrs.1997.212.1.347
[84] K. Peters, E.-M. Peters, H. G. von Schnering, W. Wojnowski, S. Tamulewicz, K. Radacki, Z. Kristallogr.-New Cryst. Struct. 212 (1997d) 345-346. https://doi.org/10.1524/ncrs.1997.212.1.345
[85] N. Tokitoh, H. Suzuki, R. Okazaki, K. Ogawa, J. Am. Chem. Soc. 115 (1993) 10428–10429, https://doi.org/10.1021/ja00075a096.
[86] T. Tanabe, Y. Mizuhata, N. Takeda, N. Tokitoh, J. Organomet. Chem. 694 (2009) 353–365. https://doi.org/j.jorganchem.2008.11.001
[87] T. Sasamori, E. Mieda, N. Takeda, N. Tokitoh, Chem. Lett. 33 (2004) 104–105, https://doi.org/10.1246/cl.2004.104.
[88] D.M. Giolando, T.B. Rauchfuss, G.M. Clark, Inorg. Chem. 26 (1987) 3082–3083, https://doi.org/10.1021/ic00266a002.
[89] A. Ziółkowska, N. Szynkiewicz, J. Pikies, Ł. Ponikiewski, Inorg. Chem. 59 (2020) 11305–11315, https://doi.org/10.1021/acs.inorgchem.0c00824.
[90] J. Albertsen, R. Steudel, J. Organomet. Chem. 424 (1992) 153–158, https://doi.org/10.1016/0022-328X(92)83145-8.
[91] L.J. Procopio, P.J. Carroll, D.H. Berry, Organometallics 12 (1993) 3087–3093, https://doi.org/10.1021/om00032a035.
[92] N. Choi, S. Sugi, S. Morino, W. Ando, Phosphorus, Sulfur Silicon Relat. Elem. 93 (1994) 465–466, https://doi.org/10.1080/10426509408021906.
[93] N. Choi, S. Sugi, W. Ando, Chem. Lett. (1994) 1395–1398, https://doi.org/10.1246/cl.1994.1395.
[94] N. Choi, S. Morino, S. Sugi, W. Ando, Bull. Chem. Soc. Jpn. 69 (1996) 1613–1620, https://doi.org/10.1246/bcsj.69.1613.
[95] Z.K. Sweeney, J.L. Polse, R.A. Andersen, R.G. Bergman, M.G. Kubinec, J. Am. Chem. Soc. 119 (1997) 4543–4544, https://doi.org/10.1021/ja970168t.
[96] Z.K. Sweeney, J.L. Polse, R.G. Bergman, R.A. Andersen, Organometallics 18 (1999) 5502–5510, https://doi.org/10.1021/om9907876.
[97] J. Pinkas, R. Gyepes, P. Štěpnička, J. Kubišta, M. Horáček, K. Mach, Inorg. Chem. Commun. 7 (2004) 1135–1138, https://doi.org/10.1016/j.inoche.2004.08.012.
[98] D.P. Krut'ko, M.V. Borzov, L.G. Kuz'mina, A.V. Churakov, D.A. Lemenovskii, O. A. Reutov, Inorg. Chim. Acta 280 (1998) 257–263, https://doi.org/10.1016/S0020-1693(98)00175-3.
[99] N. Takeda, T. Tanabe, N. Tokitoh, Bull. Chem. Soc. Jpn. 79 (2006) 1573–1579, https://doi.org/10.1246/bcsj.79.1573.
[100] T. Tanabe, N. Takeda, N. Tokitoh, Eur. J. Inorg. Chem. (2007) 1225–1228, https://doi.org/10.1002/ejic.200601226.
[101] F. Preuss, H. Noichl, J. Kaub, Z. Naturforsch. 41 B (1986) 1085-1092. https://doi.org/10.1515/znb-1986-0905
[102] F. Preuss, H. Noichl, Z. Naturforsch. 42 B (1987) 121-129. https://doi.org/10.1515/znb-1987-0201
[103] F. Preuss, M. Steidel, R. Exner, Z. Naturforsch. 45 B (1990) 1618-1624. https://doi.org/10.1515/znb-1990-1204
[104] J. Chojnacki, J. Mol. Struct: THEOCHEM 862 (2008) 112–117, https://doi.org/10.1016/j.theochem.2008.05.006.
[105] C.R. Lucas, Can. J. Chem. 61 (1983) 1096–1099, https://doi.org/10.1139/v83-194.
[106] C.R. Lucas, Can. J. Chem. 64 (1986) 1758–1763, https://doi.org/10.1139/v86-290.
[107] D.H. Berry, J. Chey, H.S. Zipin, P.J. Carroll, Polyhedron 10 (1991) 1189–1201, https://doi.org/10.1016/S0277-5387(00)86095-7.
[108] S.-B. Yu, Polyhedron 16 (1992) 2115–2117, https://doi.org/10.1016/S0277-5387(00)83169-1.
[109] P. Hong, N.H. Damrauer, P.J. Carroll, D.H. Berry, Organometallics 12 (1993) 3698–3704, https://doi.org/10.1021/om00033a048.
[110] A. Ciborska, K. Baranowska, W. Wojnowski, Acta Crystallogr. Sect E Struct Rep Online E63 (2007), https://doi.org/10.1107/S1600536807055614 m2972.
[111] A. Ciborska, K. Baranowska, W. Wojnowski, Acta Crystallogr Sect E Struct Rep Online E63 (2009), https://doi.org/10.1107/S1600536809021680 m763.
[112] T. Muraoka, T. Nakamura, A. Nakamura, K. Ueno, Organometallics 29 (2010) 6624–6626, https://doi.org/10.1021/om100875h.
[113] Y. Ishiguro, T. Kudo, T. Muraoka, K. Ueno, Organometallics 33 (2014) 2704–2712, https://doi.org/10.1021/om401084f.
[114] T. Muraoka, S. Tanabe, K. Ueno, Organometallics 38 (2019) 735–738, https://doi.org/10.1021/acs.organomet.8b00877.
[115] A. Kropidłowska, J. Chojnacki, B. Becker, Inorg. Chem. Commun. 9 (2006) 383–387, https://doi.org/10.1016/j.inoche.2005.12.017.
[116] A. Kropidłowska, J. Chojnacki, B. Becker, Polyhedron 25 (2006) 2142–2148, https://doi.org/10.1016/j.poly.2005.12.030.
[117] A. Kropidłowska, J. Chojnacki, B. Becker, Inorg. Chim. Acta 360 (2007) 2363–2367, https://doi.org/10.1016/j.ica.2006.11.025.
[118] A. Kropidłowska, J. Chojnacki, B. Becker, J. Inorg. Biochem. 101 (2007) 578–584, https://doi.org/10.1016/j.jinorgbio.2006.11.023.
[119] A. Kropidłowska, M. Strankowski, M. Gazda, B. Becker, J. Therm. Anal. Calor. 88 (2007) 463–470, https://doi.org/10.1007/s10973-007-8088-6.
[120] T.I. Kückmann, F. Schödel, I. Sänger, M. Bolte, M. Wagner, H.-W. Lerner, Organometallics 27 (2008) 3272–3278, https://doi.org/10.1021/om800211k.
[121] S. Yao, Y. Xiong, M. Driess, Chem. Eur. J. 18 (2012) 11356–11361, https://doi.org/10.1002/chem.201201335.
[122] C.A. Smith, F. Tuna, M. Bodensteiner, M. Helliwell, D. Collisona, R.A. Layfield, Dalton Trans. 42 (2013) 71–74, https://doi.org/10.1039/c2dt32362e.
[123] R.N. Mukherjee, A.J. Abrahamson, G.S. Patterson, T.D.P. Stack, R.H. Holm, Inorg. Chem. 27 (1988) 2137–2144, https://doi.org/10.1021/ic00285a026.

[124] T. Komuro, H. Kawaguchi, K. Tatsumi, Inorg. Chem. 41 (2002) 5083–5090, https://doi.org/10.1021/ic025715c.

[125] T. Komuro, T. Matsuo, H. Kawaguchi, K. Tatsumi, Inorg. Chem. 42 (2003) 5340–5347, https://doi.org/10.1021/ic0343253.

[126] J.B. Gordon, A.C. Vilbert, I.M. DiMucci, S.N. MacMillan, K.M. Lancaster, P. Moënne-Loccoz, D.P. Goldberg, J. Am. Chem. Soc. 141 (2019) 17533–17547, https://doi.org/10.1021/jacs.9b05274.

[127] I. Kovács, C. Pearson, A. Shaver, J. Organomet. Chem. 596 (2000) 193–203, https://doi.org/10.1016/S0022-328X(99)00678-6.

[128] J. Vela, J.M. Smith, Y. Yu, N.A. Ketterer, C.J. Flaschenriem, R.J. Lachicotte, P.L. Holland, J. Am. Chem. Soc. 127 (2005) 7857–7870, https://doi.org/10.1021/ja042672l.

[129] O.L. Sydora, T.P. Henry, P.T. Wolczanski, E.B. Lobkovsky, E. Rumberger, D.N. Hendrickson, Inorg. Chem. 45 (2006) 609–626, https://doi.org/10.1021/ic051289u.

[130] T.I. Kückmann, F. Dornhaus, M. Bolte, H.-W. Lerner, M.C. Holthausen, M. Wagner, Eur. J. Inorg. Chem. (2007) 1989–2003, https://doi.org/10.1002/ejic.200601207.

[131] K. Fukumoto, A. Sakai, T. Oya, H. Nakazawa, Chem. Commun. 48 (2012) 3809–3811, https://doi.org/10.1039/c2cc17163e.

[132] K. Fukumoto, A. Sakai, K. Hayasaka, H. Nakazawa, Organometallics 32 (2013) 2889–2892, https://doi.org/10.1021/om400304v.

[133] D.J. Meininger, N. Muzquiz, H.D. Arman, Z.J. Tonzetich, Dalton Trans. 44 (2015) 9486–9495, https://doi.org/10.1039/c5dt01122a.

[134] J.A. Weigel, R.H. Holm, J. Am. Chem. Soc. 113 (1991) 4184–4191, https://doi.org/10.1021/ja00011a020.

[135] B.R. Crane, L.M. Siegel, E.D. Getzoff, Science 270 (1995) 59–67, https://doi.org/10.1126/science.270.5233.59.

[136] L. Cai, J.A. Weigel, R.H. Holm, J. Am. Chem. Soc. 115 (1993) 9289–9290, https://doi.org/10.1021/ja00073a055.

[137] L. Cai, R.H. Holm, J. Am. Chem. Soc. 116 (1994) 7177–7188, https://doi.org/10.1021/ja00095a021.

[138] C. Zhou, L. Cai, R.H. Holm, Inorg. Chem. 35 (1996) 2767–2772, https://doi.org/10.1021/ic951493p.

[139] C. Zhou, R.H. Holm, Inorg. Chem. 42 (2003) 11–21, https://doi.org/10.1021/ic020464t.

[140] L. Deng, A. Majumdar, W. Lo, R.H. Holm, Inorg. Chem. 49 (2010) 11118–11126, https://doi.org/10.1021/ic101702b.

[141] B.M. Hoffman, D. Lukoyanov, Z.-Y. Yang, D.R. Dean, L.C. Seefeldt, Chem. Rev. 114 (2014) 4041–4062, https://doi.org/10.1021/cr400641x.

[142] O.L. Sydora, P.T. Wolczanski, E.B. Lobkovsky, Angew. Chem. Int. Ed. Engl. 42 (2003) 2685–2687, https://doi.org/10.1002/anie.200351143.

[143] H.-C. Liang, P.A. Shapley, Organometallics 15 (1996) 1331–1333, https://doi.org/10.1021/om950696i.

[144] I. Kovács, A.-M. Lebuis, A. Shaver, Organometallics 20 (2001) 35–41, https://doi.org/10.1021/om000497l.

[145] M. Ochiai, H. Hashimoto, H. Tobita, Organometallics 31 (2012) 527–530, https://doi.org/10.1021/om2010854.

[146] H. Xie, Z. Lin, Organometallics 33 (2014) 892-89. https://doi.org/10.1021/om401020g

[147] T. Stahl, H.F.T. Klare, M. Oestreich, J. Am. Chem. Soc. 135 (2013) 1248–1251, https://doi.org/10.1021/ja311398j.

[148] T. Stahl, P. Hrobárik, C.D.F. Königs, Y. Ohki, K. Tatsumi, S. Kemper, M. Kaupp, H.F.T. Klare, M. Oestreich, Chem. Sci. 6 (2015) 4324–4334, https://doi.org/10.1039/c5sc01035g.

[149] S. Webbolt, M.S. Maji, E. Irran, M. Oestreich, Chem. Eur. J. 23 (2017) 6213–6219, https://doi.org/10.1002/chem.201700304.

[150] S. Bähr, M. Oestreich, Chem. Eur. J. 24 (2018) 5613–5622, https://doi.org/10.1002/chem.201705899.

[151] F. Cecconi, C.A. Ghilardi, S. Midollini, A. Orlandini, P. Zanello, Polyhedron 5 (1986) 2021–2031, https://doi.org/10.1016/S0277-5387(00)87133-8.

[152] D.M. Jenkins, J.C. Peters, J. Am. Chem. Soc. 127 (2005) 7148–7165, https://doi.org/10.1021/ja045310m.

[153] O.L. Sydora, P.T. Wolczanski, E.B. Lobkovsky, E. Rumberger, D.N. Hendrickson, Chem. Commun. (2004) 650–651, https://doi.org/10.1039/B311212H.

[154] J.B. Gordon, A.C. Vilbert, M.A. Siegler, K.M. Lancaster, P. Moënne-Loccoz, D.P. Goldberg, J. Am. Chem. Soc. 141 (2019) 3641–3653, https://doi.org/10.1021/jacs.8b13134.

[155] B. Becker, K. Radacki, A. Konitz, W. Wojnowski, Z. Anorg, Allg. Chem. 621 (1995) 904–908, https://doi.org/10.1002/zaac.19956210533.

[156] A. Kropidłowska, J. Chojnacki, J. Gołaszewska, B. Becker, Acta Crystallogr, Sect E Struct Rep Online E 62 (2006) m2260–m2262, https://doi.org/10.1107/S1600536806032673.

[157] B. Becker, A. Zalewska, A. Konitz, W. Wojnowski, Z. Anorg, Allg. Chem. 627 (2001) 271–279, https://doi.org/10.1002/1521-3749(200102)627:2<271::AID-ZAAC271>3.0.CO;2-G.

[158] B. Becker, A. Pladzyk, A. Konitz, W. Wojnowski, Appl. Organomet. Chem. 16 (2002) 517–524, https://doi.org/10.1002/aoc.332.

[159] A. Dołęga, A. Jabłońska, A. Pladzyk, Ł. Ponikiewski, W. Ferenc, J. Sarzyński, A. Herman, Dalton Trans. 43 (2014) 12766–12775, https://doi.org/10.1039/C4DT01079E.

[160] B. Becker, A. Zalewska, A. Konitz, W. Wojnowski, Polyhedron 20 (2001) 2567–2576, https://doi.org/10.1016/S0277-5387(01)00855-5.

[161] A. Pladzyk, K. Baranowska, Acta Crystallogr, Sect. E: Struct. Rep. Online E 62 (2006) m2602–m2604, https://doi.org/10.1107/S1600536806036750.

[162] A. Pladzyk, K. Baranowska, P. Hapter, Transition Met. Chem. 35 (2010) 373–379, https://doi.org/10.1007/s11243-010-9337-2.

[163] A. Pladzyk, J. Olszewska, K. Baranowska, A.M. Dziurzyńska, Transition Met. Chem. 35 (2010) 821–827, https://doi.org/10.1007/s11243-010-9399-1.

[164] A. Pladzyk, K. Baranowska, Acta Crystallogr., Sect. E: Struct. Rep. Online E 63 (2007) m1594. https://doi.org/10.1107/S1600536807025421

[165] A. Dołęga, K. Baranowska, A. Pladzyk, K. Majcher, Acta Cryst. C 64 (2008) m259–m263, https://doi.org/10.1107/S0108270108017265.

[166] A. Pladzyk, K. Baranowska, D. Gudat, S. Godlewska, M. Wieczerzak, J. Chojnacki, M. Bulman, K. Januszewicz, A. Dołęga, Polyhedron 30 (2011) 1191–1200, https://doi.org/10.1016/j.poly.2011.01.026.

[167] A. Pladzyk, K. Baranowska, J. Mol. Struct. 1058 (2014) 252–258, https://doi.org/10.1016/j.molstruc.2013.11.020.

[168] A. Dołęga, A. Pladzyk, K. Baranowska, M. Wieczerzak, Inorg. Chem. Commun. 11 (2008) 847–850, https://doi.org/10.1016/j.inoche.2008.04.014.

[169] A. Pladzyk, K. Baranowska, Z. Anorg, Allg. Chem. 635 (2009) 1638–1644, https://doi.org/10.1002/zaac.200900093.

[170] A. Pladzyk, Z. Hnatejko, K. Baranowska, Polyhedron 79 (2014) 116–123, https://doi.org/10.1016/j.poly.2014.04.049.

[171] A. Pladzyk, Ł. Ponikiewski, A. Dołęga, K. Słowy, A. Sokołowska, K. Dziubińska, Z. Hnatejko, Chem. Asian J. 10 (2015) 2388–2396, https://doi.org/10.1002/asia.201500652.

[172] D. Kowalkowska, A. Dołęga, N. Nedelko, Z. Hnatejko, Ł. Ponikiewski, A. Matracka, A. Ślawska-Waniewska, A. Strągowska, K. Słowy, M. Gazda, A. Pladzyk, CrystEngComm 19 (2017) 3506–3518, https://doi.org/10.1039/C7CE00555E.

[173] L. Zámostná, T. Braun, B. Braun, Angew. Chem. Int. Ed. Engl. 53 (2014) 2745–2749, https://doi.org/10.1002/anie.201308254.

[174] S.R. Klei, T. Don Tilley, R.G. Bergman, Organometallics 21 (2002) 3376–3387, https://doi.org/10.1021/om020191+.

[175] Ł. Ponikiewski, A. Pladzyk, W. Wojnowski, B. Becker, Polyhedron 30 (2011) 2400–2405, https://doi.org/10.1016/j.poly.2011.06.028.

[176] A. Pladzyk, A. Ożarowski, Ł. Ponikiewski, Inorg. Chim. Acta 440 (2016) 84–93, https://doi.org/10.1016/j.ica.2015.10.034.

[177] A. Pladzyk, Ł. Ponikiewski, Y. Lan, A.K. Powell, Inorg. Chem. Commun. 20 (2012) 66–69, https://doi.org/10.1016/j.inoche.2012.02.018.

[178] T. Komuro, T. Matsuo, H. Kawaguchi, K. Tatsumi, Chem. Commun. (2002) 988–989, https://doi.org/10.1039/B201702D.

[179] K.-E. Lee, X. Chang, Y.-J. Kim, H.S. Huh, S.W. Lee, Organometallics 27 (2008) 5566–5570, https://doi.org/10.1021/om8006079.

[180] Y.-J. Kim, H.-T. Jeon, K.-E. Lee, S.W. Lee, J. Organomet. Chem. 695 (2010) 2258–2263, https://doi.org/10.1016/j.jorganchem.2010.06.013.

[181] T. Tanabe, Y. Mizuhata, N. Takeda, N. Tokitoh, Organometallics 27 (2008) 2156–2158, https://doi.org/10.1021/om800210g.

[182] T. Niebel, D.G. Macdonald, C.B. Khadka, J.F. Corrigan, Z. Anorg, Allg. Chem. 636 (2010) 1095–1099, https://doi.org/10.1002/zaac.200900393.

[183] K.N.W. Rozic, M.A. Fard, B.K. Najafabadi, J.F. Corrigan, Z. Anorg, Allg. Chem. 643 (2017) 973–979, https://doi.org/10.1002/zaac.201700179.

[184] P.J. Bonasia, D.E. Gindelberger, J. Arnold, Inorg. Chem. 32 (1993) 5126–5131, https://doi.org/10.1021/ic00075a031.

[185] A. Bauer, W. Schneider, K. Angermaier, A. Schier, H. Schmidbaur, Inorg, Chim. Acta 251 (1996) 249–253, https://doi.org/10.1016/S0020-1693(96)05277-2.

[186] M. Nakamoto, W. Hiller, H. Schmidbaur, Chem. Ber. 126 (1993) 605–610, https://doi.org/10.1002/cber.19931260310.

[187] J. Chojnacki, B. Becker, A. Konitz, W. Wojnowski, Z. Anorg, Allg. Chem. 626 (2000) 2173–2177, https://doi.org/10.1002/1521-3749(200010)626:10<2173::AID-ZAAC2173>3.0.CO;2-T.

[188] S. Kenzler, M. Kotsch, A. Schnepf, Eur. J. Inorg. Chem. (2018) 3840–3848, https://doi.org/10.1002/ejic.201800595.

[189] I. Medina, H. Jacobsen, J.T. Mague, M.J. Fink, Inorg. Chem. 45 (2006) 8844–8846, https://doi.org/10.1021/ic061579q.

[190] A. Ciborska, E. Conterosito, M. Milanesio, K. Kazimierczuk, K. Rzymowska, K. Brzozowski, A. Dołęga, Eur. J. Inorg. Chem. 19 (2015) 3059–3065, https://doi.org/10.1002/ejic.201500457.

[191] H. Jacobsen, M.J. Fink, Inorg. Chim. Acta 360 (2007) 3511–3517, https://doi.org/10.1016/j.ica.2007.04.041.

[192] H. Jacobsen, M.J. Fink, Eur. J. Inorg. Chem. (2007) 5294–5299, https://doi.org/10.1002/ejic.200700743.

[193] S.H. Bertz, M. Eriksson, G. Miao, J.P. Snyder, J. Am. Chem. Soc. 118 (1996) 10906–10907, https://doi.org/10.1021/ja962559y.

[194] S. Groysman, A. Majumdar, S.-L. Zheng, R.H. Holm, Inorg. Chem. 49 (2010) 1082–1089, https://doi.org/10.1021/ic902066m.

[195] K. Fujisawa, S. Imai, N. Kitajima, Y. Moro-oka, Inorg. Chem. 37 (1998) 168–169, https://doi.org/10.1021/ic971317b.

[196] S.J. Ferrara, J.T. Mague, J.P. Donahue, Inorg. Chem. 51 (2012) 6567–6576, https://doi.org/10.1021/ic300124n.

[197] M.A. Fard, F. Weigend, J.F. Corrigan, Chem. Commun. 51 (2015) 8361–8364, https://doi.org/10.1039/c5cc00940e.

[198] M.A. Fard, T.I. Levchenko, C. Cadogan, W.J. Humenny, J.F. Corrigan, Chem. Eur. J. 22 (2016) 4543–4550, https://doi.org/10.1002/chem.201503320.

[199] J. Zhai, A.S. Filatov, G.L. Hillhouse, M.D. Hopkins, Chem. Sci. 7 (2016) 589–595, https://doi.org/10.1039/c5sc03258j.

[200] S.J. Ferrara, B. Wang, E. Haas, K. Wright LeBlanc, J.T. Mague, J.P. Donahue, Inorg. Chem. 55 (2016) 9173–9177, https://doi.org/10.1021/acs.inorgchem.5b02811.

[201] A.M. Polgar, F. Weigend, A. Zhang, M.J. Stillman, J.F. Corrigan, J. Am. Chem. Soc. 139 (2017) 14045–14048, https://doi.org/10.1021/jacs.7b09025.

[202] N. Parvin, S. Pal, S. Khan, S. Das, S.K. Pati, H.W. Roesky, Inorg. Chem. 56 (2017) 1706–1712, https://doi.org/10.1021/acs.inorgchem.6b02833.

[203] B. Becker, W. Wojnowski, K. Peters, E.-M. Peters, H.G. Von Schnering, Polyhedron 11 (1992) 613–616, https://doi.org/10.1016/S0277-5387(00)83316-1.

[204] B. Becker, W. Wojnowski, K. Peters, E.-M. Peters, H.G. Von Schnering, Inorg. Chim. Acta 214 (1993) 9–11, https://doi.org/10.1016/S0020-1693(00)87517-9.

[205] B. Becker, J. Chojnacki, A. Konitz, W. Wojnowski, Z. Kristallogr.-New Cryst. Struct. 213 (1998) 697-698. https://doi.org/10.1524/ncrs.1998.213.14.737

[206] R. Biedermann, D. Oliver Kluge, H. Krautscheid Fuhrmann, Eur. J. Inorg. Chem. (2013) 4727–4731, https://doi.org/10.1002/ejic.201300768.

[207] T. Komuro, T. Matsuo, H. Kawaguchi, K. Tatsumi, Angew. Chem. Int. Ed. Engl. 42 (2003) 465–468, https://doi.org/10.1002/anie.200390141.

[208] A. Borecki, J.F. Corrigan, Inorg. Chem. 46 (2007) 2478–2484, https://doi.org/10.1021/ic0618910.

[209] A.I. Wallbank, J.F. Corrigan, Can. J. Chem. 80 (2002) 1592–1599, https://doi.org/10.1139/v02-032.

[210] G. Tan, Y. Xiong, S. Inoue, B. Blom, J.D. Epping, M. Driess, Chem. Commun. 49 (2013) 5595–5597, https://doi.org/10.1039/c3cc41965g.

[211] W. Wojnowski, M. Wojnowski, K. Peters, E.-M. Peters, H.G. Von Schnering, Z. Anorg. Allg. Chem. 530 (1985) 79–88, https://doi.org/10.1002/zaac.19855301109.

[212] A. Schwenk, U. Piantini, W. Wojnowski, Z. Naturforsch. 46a (1991) 939-946. https://doi.org/10.1515/zna-1991-1103

[213] W. Wojnowski, J. Saßmannshausen, E.M. Peters, K. Peters, H.G. Von Schnering, Z. Anorg. Allg. Chem. 620 (1994) 1417–1421, https://doi.org/10.1002/zaac.19946200816.

[214] E. Block, M. Gernon, H. Kang, G. Ofori-Okai, J. Zubieta, Inorg. Chem. 28 (1989) 1263–1271, https://doi.org/10.1021/ic00306a013.

[215] J.A.S. Howell, Polyhedron 25 (2006) 2993–3005, https://doi.org/10.1016/j.poly.2006.05.014.

[216] A. Kropidłowska, A. Rotaru, M. Strankowski, B. Becker, E. Segal, J. Therm. Anal. Calor. 91 (2008) 903–909, https://doi.org/10.1007/s10973-007-8553-2.

[217] A. Rotaru, A. Mietlarek-Kropidłowska, C. Constantinescu, N. Scariooreanu, M. Dumitru, M. Strankowski, P. Rotaru, V. Ion, C. Vasiliu, B. Becker, M. Dinescu, Appl. Surf. Sci. 255 (2009) 6786–6789, https://doi.org/10.1016/j.apsusc.2009.02.062.

[218] J. Guschlbauer, T. Vollgraff, J. Sundermeyer, Dalton Trans. 49 (2020) 2517–2526, https://doi.org/10.1039/C9DT04144C.

[219] P. Maślewski, K. Kazimierczuk, Z. Hnatejko, A. Dołęga, Inorg. Chim. Acta 459 (2017) 22–28, https://doi.org/10.1016/j.ica.2017.01.014.

[220] R.F. Galiullina, Yu.N. Krasnov, T.R. Shnol, Zhurnal Obshchei Khimii 47 (1977) 1667.

[221] A. Dołęga, A. Farmas, K. Baranowska, A. Herman, Inorg. Chem. Commun. 12 (2009) 823–827, https://doi.org/10.1016/j.inoche.2009.06.025.

[222] M.W. DeGroot, J.F. Corrigan, Organometallics 24 (2005) 3378–3385, https://doi.org/10.1021/om050088v.

[223] M.W. DeGroot, N.J. Taylor, J.F. Corrigan, Inorg. Chem. 44 (2005) 5447–5458, https://doi.org/10.1021/ic0481576.

[224] C.B. Khadka, A. Eichhöfer, F. Weigend, J.F. Corrigan, Inorg. Chem. 51 (2012) 2747–2756, https://doi.org/10.1021/ic200307g.

[225] M.W. DeGroot, C.B. Khadka, H. Rösner J. F. Corrigan,, J. Clust. Sci. 17 (2006) 97–110, https://doi.org/10.1007/s10876-005-0044-7.

[226] F. Meyer-Wegner, M. Bolte, H.-W. Lerner, Inorg. Chem. Commun. 29 (2013) 134–137, https://doi.org/10.1016/j.inoche.2012.11.033.

[227] I.E. Medina-Ramírez, M.J. Fink, J.P. Donahue, Acta Crystallogr. Sect. C 65 (2009) m475–m477, https://doi.org/10.1107/S0108270109045570.

[228] A. Pladzyk, Ł. Ponikiewski, N. Stanulewicz, Z. Hnatejko, Optical Mat. 36 (2013) 554–561, https://doi.org/10.1016/j.optmat.2013.10.034.

[229] Y. Matsunaga, K. Fujisawa, N. Ibi, N. Amir, Y. Miyashita, K. Okamoto, Bull. Chem. Soc. Jpn. 78 (2005) 1285–1287, https://doi.org/10.1246/bcsj.78.1285.

[230] W. Wojnowski, B. Becker, L. Walz, K. Peters, E.-M. Peters, H.G. Von Schnering, Polyhedron 11 (1992) 607–612, https://doi.org/10.1016/S0277-5387(00)83315-X.

[231] A. Dołęga, M. Walewski, Magn. Reson. Chem. 45 (2007) 410–415, https://doi.org/10.1002/mrc.1983.

[232] A. Dołęga, K. Baranowska, J. Gajda, S. Kaźmierski, M. Potrzebowski, Inorg. Chim. Acta 360 (2007) 2973–2982, https://doi.org/10.1016/j.ica.2007.02.046.

[233] A. Pladzyk, K. Baranowska, K. Dziubińska, Ł. Ponikiewski, Polyhedron 50 (2013) 121–130, https://doi.org/10.1016/j.poly.2012.10.035.

[234] J.R. Babcock, R.W. Zehner, L.R. Sita, Chem. Mater. 10 (1998) 2027–2029, https://doi.org/10.1021/cm980202i.

[235] E.N. Gladyshev, N.S. Vyazankin, V.S. Andreevichev, A. Klimov, G.A. Razuvaev, J. Organomet. Chem. 28 (1971) C42–C44, https://doi.org/10.1016/S0022-328X(00)88008-0.

[236] W. Wojnowski, M. Wojnowski, H.G. Von Schnering, M. Noltemeyer, Z. Anorg. Allg. Chem. 531 (1985) 153–157, https://doi.org/10.1002/zaac.19855311221.

[237] J. Chojnacki, A. Wałaszewska, E. Baum, W. Wojnowski, Acta Crystallogr, Sect E Struct Rep Online 59 (2003) m125–m127, https://doi.org/10.1107/S1600536803004045.

[238] F. Tuna, C.A. Smith, M. Bodensteiner, L. Ungur, L.F. Chibotaru, E.J.L. McInnes, R. E.P. Winpenny, D. Collison, R.A. Layfield, Angew. Chem. Int. Ed. Engl. 51 (2012) 6976–6980, https://doi.org/10.1002/anie.201202497.

[239] J. Guschlbauer, T. Vollgraff, X. Xie, F. Weigend, J. Sundermeyer, Inorg. Chem. 59 (2020) 17565–17572, https://doi.org/10.1021/acs.inorgchem.0c02808.